Dissertation zur Erlangung des Doktorgrades der Fakultät für Chemie und Pharmazie der Ludwig-Maximilians-Universität München

Purification, characterization and lyophilization of adeno associated virus vectors

Ruth Katharina Rieser

aus

Weingarten, Deutschland

2022

Erklärung

Diese Dissertation wurde im Sinne von § 7 der Promotionsordnung vom 28. November 2011 von Herrn Prof. Dr. Gerhard Winter betreut.

Eidesstattliche Versicherung

Diese Dissertation wurde eigenständig und ohne unerlaubte Hilfe erarbeitet.

München, 21.03.2022

_____

Ruth Rieser

Dissertation eingereicht am 23.03.2022

1. Gutachter: Prof. Dr. Gerhard Winter

2. Gutachter: Prof. Dr. Stylianos Michalakis

Mündliche Prüfung am 02.05.2022

To my family

Acknowledgements

I would like to express my sincere gratitude to my supervisor Prof. Dr. Gerhard Winter who gave me the opportunity to work on this fascinating and challenging project. I am grateful for all the advice, ideas, patience and also criticism that helped immensely to expand my scientific mindset. Thank you also for the great work atmosphere you created and for the opportunity to share our results with scientists at conferences around the world.

Secondly, I want to thank Prof. Dr. Stylianos Michalakis for being such an excellent co-supervisor of this thesis, for your support all around the AAV production and material, advice to shape the project and the valuable discussions on the challenges we faced throughout this project. Also, thank you for being a co-referee of my thesis.

Furthermore, I like to thank Dr. Tim Menzen for his advice, support, and ideas in the analytical field, as well as for the fruitful discussions about evaluation and results of the experiments. Another thanks you belongs to Coriolis Pharma who gave me the opportunity to do AUC measurements of my samples. In this regard, I would like to thank Dr. Klaus Richter for carrying out and evaluating these experiments.

Many thanks are expressed to my students Anna-Lena Friesenhahn, Sophie Gabriel, Isabella Jakob, who did their "Wahlpflichtpraktikum" on my project and Greta Faccioli, who conducted her master thesis under my supervision.

A further big thank you goes to Johanna Koch and Kerstin Skokann, both of whom have always diligently provided AAV supplies and have always been there to help and advise me in cell culture and qPCR data analysis. I would also like to thank Jacqueline Bogedein and Sabrina Babutzka for their support in cell culture and many other experiments.

I am thankful to my colleagues from AK Winter, AK Frieß and AK Merkel at the LMU for a good time together and for the numerous social activities. I want to thank my lab mate Simon Eisele for his advice in the lab, his open ear and helping hand.

I would especially like to thank Nicole Härdter, Sebastian Groël and Alice Hirschmann for the many fun lunches, coffee breaks and for the Heidelberger Melonenschnaps in both good and bad times!

Finally, I would like to sincerely thank my family and friends for their constant support, encouragement, and endless patience. Foremost, I would like to thank my parents, my brother, my sisters, and Oliver for being supportive all along.

Tabel of Content

Chapter I Detection of critical quality attributes of AAV formulation

I.1 Introduction

Vectors based on recombinant adeno-associated viruses (rAAV) have emerged as the leading gene delivery system due to their safety and long-term gene expression (1, 2). AAV gene therapy has successfully been proven as a strategy for various monogenetic diseases and is with Luxturna® and Zolgensma® already on the market (3). AAV can attach itself and enter the target cell, transfer to the nucleus, and express the transgene in a stable manner over a sustained period of time. Currently, there are over 190 ongoing clinical trials utilizing different AAV serotypes to target various genetic diseases, including hemophilia (AAV2 and AAV8), congenital heart failure (AAV1 and AAV6), cystic fibrosis (AAV2), rheumatoid arthritis (AAV2), and Batten disease (AAVrh.10) (3). Final preparation, formulation, and characterization of AAV drug substance are fundamental to support preclinical and clinical applications. Characterization of AAV preparations includes the determination of identity, potency, purity, stability, and safety of a rAAV batch (4, 5).

For the characterization, feasible, time and cost-efficient methods are needed to get a reliable information on critical quality attributes (CQA) of AAV drug products. Due to the complex nature of AAV, the development of analytical methods is extremely challenging, and some well-established methods from protein analytics are unsuitable for AAV. The main reason is the large size and molecular weight of AAV. Another challenge is the vector DNA inside the capsid, which is negatively charged and therefore requires some effort to analytically characterize this component of the AAV vector.

As one part of characterization, the identity of the AAV product must be demonstrated. In particular, identity of the capsid serotype as well as the target vector genome (vg) need to be confirmed. Identity of the vg can be deduced by product-specific PCR methods. The identity of capsid proteins (cp) can be demonstrated by serotype-specific ELISA or differential scanning fluorimetry (DSF). The latter is a relatively easy method to determine identity of a given serotype via identification of the characteristic melting temperature (T_m). Those and other methods will be discussed in I.3.1.

Traditionally, concentration of AAV vectors is measured by quantification of the amount of vg in the sample with qPCR. However, this vector genome titer underestimates the total amount of capsid in the sample, because in most cases only a fraction of the capsids contains a vg, whereas the remaining fraction consists of empty capsids only. The current

method of choice for determination of the number of capsids is the serotype specific ELISA. However, alternative methods for fast and easy determination of vg and cp titer are available, as well as different options to quantify the infectious titer of an AAV sample. These methods will be discussed in I.3.2.

Many possible impurities could be contained in a particular AAV preparation due to the production and purification process of AAV. Host cell proteins, host cell DNA, and empty AAV are examples that might occur in the AAV sample and can lead to immune reactions (6, 7). Thus, the purity of AAV must be controlled, for example by SDS-PAGE, qPCR, ELISA, TEM, AUC, or chromatography methods, depending on the type of impurity (7-9). This is explained in more detail in I.3.3.

Controlling the physical and chemical stability of AAV is necessary because it was shown previously that for example deamidation results in less infectious AAV (10). Appropriate analytical methods to determine the stability are discussed in 0.

As for all drug products (DP), safety must be taken into consideration, therefore a short overview on methods to assess safety is given in 0.

Finally, the objectives of this work lead from the challenges in analytical characterization and purification of AAV to the formulation and freeze-drying of AAV suspensions with a stable lyophilized AAV formulation as the desired endpoint.

I.2 Recombinant adeno-associated viral vectors

AAV was first detected in 1965 under the electron microscope (EM) as a contamination of adenovirus preparations (11-13) and has been used for gene transfer since the mid-1980s. It can be considered the most commonly used vector (14). AAV belong to the family of *Parvoviridae* and have a linear single-stranded DNA genome of about 4.7 kilobases (kb) (max. 5,2 kb) (15, 16). The genome encodes replication (*rep*), capsid (*cap*) flanked by inverted terminal repeats (ITR). The ITR are flanking the coding area and consist of a palindromic sequence building a hairpin structure (17). The *cap* gene encodes the structural viral proteins (VP 1-3), a chaperone AAP which facilitates capsid assembly by providing a scaffolding function within the nucleus (18, 19) and the membrane-associated accessory protein (MAAP), which acts as AAV egress factor (20) The rep gene encodes the proteins which are regulating the replication (21).

The capsid is icosahedral and consists of the three different viral proteins (VP1, VP2, VP3, with a molecular weight of 87, 73, and 62 kDa, respectively), all back splice versions of the *cap* gene (22). In the 60-mer capsid the ratio of VP1:VP2:VP3 is 1:1:10 (11, 12, 23).

The AAV particle has a total molecular weight of around 5100 kDa and a diameter of 25 – 28 nm (24). With approx. 3750 kDa, the protein part makes up 74% of the molecular weight of the whole virus, leaving 26% for the DNA (approx. 1350 kDa). The isoelectric point (IEP) of the AAV depends on the presence or absence of the vg. AAV containing vg have an IEP of around 5.9, while empty capsids have an IEP of 6.3 (25, 26).

As all members of the genus of Dependoparvoviruses AAV needs another virus for a productive infection cycle, a so-called helper virus. Examples of helper virus are adenovirus, herpes simplex virus (HSV), Cytomegalovirus (CMV), as well as human Papillomaviruses (HPV) (13, 27-30).

For gene therapy only recombinant AAV (rAAV) are used, which have their *rep* and *cap* genes replaced by a given gene expression cassette. Due to the lack of *rep*, rAAV are not able to integrate into the host genome and, after infection, their genome persists in the host cell nucleus primarily in episomal form as linear and circular monomers and linear and circular concatemers (31, 32). These episomal forms can be associated with histones in chromatin-like structures and support sustained transgene expression (33).

Hundreds of naturally occurring AAV serotypes and numerous engineered AAV variants have been identified or generated and differ in their tissue tropsim (34). From this group AAV2 is the most intensively studied one and many of the findings on the biology of the virus are based on this serotype. Up to 80% of the human adult population have antibodies to one or more serotypes of AAV (35, 36). Nevertheless, AAV has not been linked to any disease and is therefore considered nonpathogenic.

I.3 Critical quality attributes of AAV vectors

CQA for therapeutical products are defined as: “A CQA is a physical, chemical, biological, or microbiological property or characteristic that should be within an appropriate limit, range, or distribution to ensure the desired product quality.” (37)

For all biopharmaceuticals as well as rAAV samples, quality control of identity, potency, purity, stability and safety is required. More detailed characterization of the effect of changes in production process parameters or cleaning methods on CQA will improve process understanding and enable process optimization, ultimately ensuring highest product quality in rAAV production. (38).

Given the increasing number of engineered capsids as well as new vg, it is necessary to ensure the identity of both parts of the rAAV. Concerning the capsid structure, not only the serotype is of interest but also the post-translational modifications (PTM), as it has been

shown in previous studies that a variation in the PTM coming from different production cell lines may result in functional differences of the rAAV (39-41).

Another CQA is the AAV vector concentration in the sample. This refers either to infectious, capsid or vg concentration. For clinical trials the vg titer is typically used for dosing. Yet, for safety concerns the capsid titer is also of interest because to date the impact of the empty capsids on immune reactions remains unclear (42). Therefore, also the ratio of vg/cp should be considered a CQA for rAAV because a high number of empty capsids can lead to a stronger immune reaction in the patient.

For the CQA of purity not only empty capsids are of interest. There are also other impurities like residual helper viruses, nucleic acids, proteins, residual benzonase or affinity ligands that can contribute to immuno- or genotoxic effects (7, 25).

One stability indicating attribute of biopharmaceuticals is the number of aggregates and it was shown that AAV capsids are prone to aggregation (6). Aggregate formations highly affects the stability of AAV vector formulations. It was shown that dimers (d ~ 35nm), small oligomers (d < 100 nm), and large subvisible aggregates (d > 100 nm) are present in AAV vector formulations (43-45). Trigger for aggregation of AAV2 can be high capsid concentrations, free DNA or low ionic strength (< 150 mM) (6).

In a nutshell, a clear understanding of the origin and risks associated with the vector manufacturing process and product-related impurities in rAAV vectors is necessary to ensure and control the identity, purity, potency, stability, and safety of the product.

I.3.1 Identity of vector plasmid and AAV capsid

Today, a myriad of serotypes and engineered AAV vectors are available and a huge number of interesting genes for gene therapy. To distinguish the capsid variants and genes analytics for identity must be performed to ensure that the correct combination of both is present.

I.3.1.1 Vector plasmid identification methods

The vector plasmid contains the origin, antibiotic resistance genes, ITR, promotor and transgenes. Before encapsulating the gene of interest into the AAV capsid, the identity of the transgene and the ITR must be controlled by genome sequencing or analytical restriction analysis. The latter needs less work and results in reliable results, as well. When it comes to the identity of the transgene, Sanger sequencing is working well, but as it was shown the sequencing of the ITR is quite challenging (46): The ITR create a hairpin structure which is hard to decode by conventional sequencing analysis. If the genome is already encapsulated, alternatively, the size of the AAV genome can be checked by AUC,

because AUC works based on mass differences and bigger vector genome has a higher total mass.

I.3.1.2 AAV capsid identification methods

The icosahedral capsid is a 60-mer composed of 5 VP1, 5 VP2 and 50 VP3. VP3, the smallest of the three proteins, contributes most to capsid structure and tissue tropism because of its abundance. VP2 is necessary for capsid assembly, as was shown in studies in insect cells (47). However, viruses composed only of VP3 have been produced recently (48).VP1/2 N termini of AAV harbor a conserved catalytic phospholipase A2 (PLA2) domain. The PLA2 domain has been described as necessary for endosomal escape (49, 50) and the basic regions contribute to viral infectivity by possibly allowing nuclear import of capsids (51-53).

Among the different serotypes, there are some highly conserved regions on the capsid but also some variable ones. Of the many naturally occurring serotypes, 1-13 are the best characterized and are commonly used in preclinical studies, and some are already in clinical development. Many more mutated and engineered variants are generated. Hence, the identity of the capsid must be controlled for the crude lysate as well as DP. This can be done with specific antibodies and Western blot analysis (54) or by determination of the melting point of the capsid (3, 55, 56).

I.3.1.2.1 Western/dot blot analysis with specific antibodies

For Western or dot blot analysis a specific antibody that recognizes an antigen on the capsid must be available. In both assays a selective, reversible, and non-covalent binding of the antibody and the denatured (Western blot) or native (dot blot) antigen must be created. The building of antigen-antibody-complexes can be detected for example by bioluminescence reactions.

For dot blot analysis 1 µL of the AAV suspension of 10^9 cp fully assembled capsids is spotted directly onto a PVDF membrane. For AAV2 and AAV3 intact capsids can be detected by the conformation specific monoclonal A20 antibody (54, 57). This cross-reactivity originates from the sequence homology of the AAV serotypes 2 and 3. Similar cross interactions were shown for the ADK1a antibody that reacts with AAV1, AAV6, and AAV12 (58, 59).

For Western blot analysis, a previous denaturation of AAV capsid and separation of VPs on a SDS-PAGE must be performed. The individual VPs are then electrophoretically transferred (aka "blotted") onto a PVDF membrane and incubated with monoclonal antibodies. The monoclonal B1 antibody that bind denatured VP1, VP2 and VP3 can be used to confirm the presence of AAV capsid proteins, because it binds to an epitope in the C terminus present in all three viral capsid proteins and conserved in all serotypes except AAV4 (60). The Western blot also provides information about the stoichiometry of the VPs as well as their molecular weight. This is especially informative if some engineered variants with additional amino acids or complete deletion of one VP are used.

I.3.1.2.2 Capsid unfolding temperature detection by fluorescence and changes in heat capacity

The T_m of the capsids is a serotype specific characteristic (55). T_m is the temperature where half of the protein is unfolded, allowing the SYPRO Orange dye to bind to the hydrophobic regions of the protein, exposed during unfolding (3). Therefore, it is possible to determine the capsid identity by T_m, independent of the genome.

The differential scanning fluorimetry (DSF) measurement can be run on a thermocycler instrument, with temperatures ranging from 30°C to 99°C and ramping at 0.5°C – 1°C per minute (3, 22). The measurement of T_m can also be done label free, using the intrinsic fluorescence of the tryptophan, tyrosine, and phenylalanine residues (56). Advantages of this method are the smaller sample volume of 10 µL as well as the lower virus titer of $3*10^{11}$ AAV. For comparison: The measurement using SYPRO Orange requires samples of 45 µL and a titer of $1 – 5*10^{12}$ (55). Lastly, iDSF allows the measurement of samples containing detergents like Tween 20 or poloxamer 188, commonly used in AAV formulations (4). Further information and a discussion about the measurement of capsid unfolding by intrinsic fluorescence can be found in Chapter II.

Differential scanning calorimetry (DSC) is an analysis technique used to characterize the stability of a protein or other biomolecule in its native form, without the need for extrinsic or intrinsic fluorophores. This is done by measuring the heat capacity change associated with thermally induced processes, such as the molecule's thermal denaturation triggered by heating at a constant rate (61, 62). With DSC it is also possible to determine the capsid unfolding (22, 63) as well as the DNA ejection from the filled capsid and finally the melting of the genome DNA at around 95°C (64). The melting signals of empty and filled capsids differ and allows therefore for differentiation of full and empty capsid. Another point for

distinction of full and empty capsids is the DNA melting peak occurring at around 95°C because this melting peak is missing for empty capsids. However, getting a reliable ratio of full and empty capsids using this method is quite challenging because the melting peaks of full and empty capsids are overlapping and therefore no ratio can be derived from the peak areas. In addition, the required amount of capsid for this measurement is quite high with around 10^{13} cp/mL and 325 µL.

I.3.1.2.3 Conclusion

Western or dot blot analysis are widely used methods in AAV research because both assays work with low titer samples, do not require special equipment, only the special antibodies, and are commonly used in laboratories. Nevertheless, they are time consuming and, depending on serotype and antibody, not 100% serotype specific. In contrast, most AAV serotypes can easily be distinguished via the capsid unfolding temperature, except the couple of AAV9 and AAVrh10. These methods require a little more AAV material, but the measurement is easy, reproducible, and takes only 1 h. What is more, the measurement using a fluorescent dye can be performed with qPCR equipment, which is anyway often available in labs working with AAV, neither requiring extra equipment. Finally, the capsid unfolding temperature might be of additional use in evaluating lot-to-lot product consistency (34).

I.3.2 Potency – quantification of AAV vectors

For an accurate quantification of AAV vectors, differentiation between the vg titer, capsid amount and vector functionality should be considered: If the quantification of AAV vectors relies on the capsid amount, the capsid titer is measured without differentiation between vg containing capsids and empty capsids. The vg titer refers to the number of encapsulated vg only. Finally, the vector functionality means the transduction activity or infectivity of AAV vectors. The number of infective particles is usually lower compared to the vg titer, as not all full AAV vectors in a sample are able to transduce cells.

I.3.2.1 Capsid titer

The total capsid content can be as important as the vector genome titer. Yet, until today there is no harmonized method to assay the total capsid amount. The number of capsids can be determined using techniques, such as enzyme linked immunosorbent assay (ELISA) (57), dot blot and western blot analysis (60), UV spectrometry (65), dynamic and static

light scattering (DLS + SLS) (64), as well as multiangle light scattering (MALS) (64), SDS-PAGE (66), (cryo-) electron microscopy (EM), or TEM and flow virometry (67).

I.3.2.1.1 ELISA

The conventional sandwich ELISA uses a microtiter plate coated with monoclonal antibodies to capture only intact, assembled AAV capsids. The biotin/ streptavidin peroxidase color reaction of the detecting antibody allows for the photometrical determination of the precise titer of intact AAV capsids. ELISA methods are serotype specific: antibodies need to bind to capsid proteins. A method to quantify AAV2 capsid protein was originally described using an A-20 antibody-based ELISA (57), but more recently ELISA detection for most AAV serotypes has been developed and is commercially available, e.g. AAV1-3, AAV5, AAV6, AAV8, AAV9 and AAVrh10.

Calibration can be done with reference standard material (RSM) for AAV2 (68) and AAV8 (69) or with an internal calibration sample, characterized previously characterized by electron microscopy and protein content tests on purified capsid preparations: Protein content is equated to capsid titers by assuming that a capsid is made up of 60 subunits having a uniform stoichiometry of structural proteins (VP1:VP2:VP3 = 1:1:10); one particle is estimated to have a molecular weight around 6.5×10^{-9} ng. Depending on where the sample is situated on the calibration curve, the coefficient of variation (CV) can vary between 3 and 67% (57).

The ELISA allows reliable detection for various steps in the production process and does not require highly purified material. This method can be performed with only a few microliters of sample containing $10^7 – 10^9$ cp/mL. Some matrix effects can occur, due to high levels of salt, surfactant or iodixanol in the sample (57). In addition, the ELISA assay does not provide much flexibility because of the serotype specific antibodies and the turnaround time of four up to five hours.

I.3.2.1.2 Dot and western blot

Non-denatured AAV capsid (dot blot) and denatured AAV (Western blot) can be used to quantify the number of fully assembled capsids. This is done by using RSM or internal generated calibration standards and a serotype specific antibody for labeling. As already discussed in I.3.1.2.1 this method requires only 1 µL sample volume and the required sample concentration of 10^8- 10^9 cp/mL is usually available for DP. For Western blot densitometric analysis of protein bands is possible. However, structural protein ratios of VP1:VP2:VP3 have been observed to fluctuate between 1:1:8 and 1:1:20 (70). This

fluctuation leads to two-fold to three-fold change in the total capsid number, because the capsid titer is calculated based on the amount of VP3. One exception must be made for crude lysates: In these samples free VP occurs , which can shift the ratio between the three VP much more (71). Special diligence should also be paid to AAV that were produced in systems of baculovirus production, because it has been discovered that the VP ratio is dependent on the production system (58, 72, 73).

I.3.2.1.3 SDS-PAGE

SDS-PAGE is used to analyze the size of proteins. As a separation medium for this type of electrophoresis, a polyacrylamide-based discontinuous gel and a sensitive protein staining, usually Coomassie blue or silver stain, is utilized (74). SDS, an anionic surfactant, covers the intrinsic charges of the protein, allowing for the analysis and differentiation of the different capsid proteins VP1 (87 kDa) VP2 (73 kDa) VP3 (62 kDa) (11, 12, 23). SDS-PAGE can also be used to determine the purity of AAV samples (75-77), as it detects smaller proteins (in this case contaminations, like cell host debris, protein, genomic DNA, serum protein, helper DNA, or helper virus), as well (26). The reason why it is important to control the impurity level is their potential immunogenicity: even though AAV themselves also have an immunogenicity, a higher amount of impurities implies a stronger immunogenicity (78). In addition, with SDS-PAGE we can calculate the capsid amount in the sample, using the following equation after calibration with BSA (8):

$$cp = \frac{VP3\ [g]}{4.9868 \times 10^{-18} g}$$

The denominator, 4. 9868 × 10^{-18} g, is the mass of VP3 in one capsid. Because each capsid contains 50 VP3 subunits, total VP3 of one capsid equals approximately 3 MDa (66). Dividing the amount of VP3 (in g) by 4.9868*10^{-18} g will yield the number of viral particles. The required sample volume for this method ranges from 4 µL up to 20 µL depending on the AAV concentration. The AAV amount in the sample volume should be higher than 10^{10} cp to use silver staining (see Chapter III).

Classical SDS-PAGE can be exchanged for capillary electrophorese or chip-based – SDS-PAGE: Both methods take around 2 hours, including sample preparation and running time. They are equipped with an automatic detection system and detection limit is comparable to Coomassie Blue staining. The systems eliminate handling of SDS-PAGE slab gels, staining, and imaging steps for a more efficient workflow and results are achieved rapidly, with the automated analysis. Disadvantages are the upper detection limit of 270 kDa, not

allowing for the detection of native AAV, and observed matrix effects due to high salt amounts and surfactant in the sample, requiring buffer exchange from time-to-time that can lead to a loss of AAV. Finally, these measurements need special equipment which is not regularly available in all labs.

I.3.2.1.4 UV spectrometry

For highly purified material, a spectrophotometric method to determine the number of capsids and the number of vg from the A260/A280 ratio, taking only 30 minutes, has been established (65). This method requires the denaturation of particles prior to analysis, because of significant light scattering from intact particles (cf.I.3.2.2.5).

Although this method is sensitive to impurities and to buffer, it is probably the simplest method available to measure AAV concentrations and a well-established one to measure the concentration of protein samples (71). However, this method is problematic for AAV vectors purified by iodixanol gradient centrifugation , because iodixanol can interfere with the determination of optical density at the relevant wavelengths (79). To solve this problem, an extra purification steps can be added to remove the iodixanol.

Capsid protein concentrations are derived as the product of vg per mL and capsids per vg, using 3.74 MDa as the molecular mass of empty capsid particles (80). The MW of the vg can be calculated form the sequence or can be measured with a multiangle light scattering (MALS) detector. The ratio between full and empty AAV can be calculated by the following equation (65):

$$cp/vg = MW_{DNA} * \frac{1.76*10^{-6}(1.8-\frac{A_{260}}{A_{280}})}{\frac{A_{260}}{A_{280}}-0{,}59}$$

I.3.2.1.5 Static light scattering – SLS

In SLS the average molecular particle weight and size of a sample are quantified by measuring the time-steady intensity of light, scattered by its solutes due to Rayleigh scattering. To improve the accuracy of SLS, measurements are combined with DLS. Through the combination, determination of capsid titer, molecular weight, and the presence of aggregates is possible, while the sample can be recovered after measurement, if necessary (44). The measurements are performed as batch measurements, using 1 to 30 µL sample containing a minimum of $6*10^{10}$ cp/mL and can be performed in less than 5 minutes, because no sample preparation is required. Using a plate reader instrument, high throughput is feasible by using 384- or 1536-well plates (43, 44, 81).

Major challenges for accuracy and precision of SLS/DLS measurements are the high sensitivity to the refractive index, as well as the viscosity of the sample (43, 44, 81). Reliability is particularly poor due to the difference in refractive index in samples containing empty and full capsids side by side, leading to errors of up to 33%, since in the case of a mixture the refractive index can only be estimated and is required for particle number calculation by SLS. However, it is of course possible to make two measurements with the two different RI, so one can at least estimate the smallest and the largest possible titer as it is done by Stunner (Unchained Labs, Boston, MA, USA) (38). The same is true for the viscosity, especially for samples containing iodixanol. In these samples the amount of iodixanol can differ from preparation to preparation, thus the viscosity must be adjusted carefully from batch to batch to get reliable data.

Stunner also uses SLS/DLS measurements for vg and cp titer determination. In addition, Stunner combines SLS/DLS with UV spectrometry and can therefore gather information about aggregation, full-empty-ratio and other impurities like free DNA or proteins. Measurement with Stunner only require 2 µL of sample with 10^{12} cp/mL and take 2 minutes, including data analysis. Measurement is fully automated and up to 96 samples can be measured in one plate. The UV spectrum holds additional information about iodixanol content, yet, if the sample contains iodixanol, a full-empty-ratio cannot be determined by this method because of the high UV absorption of iodixanol. Nevertheless, based on the information about the iodixanol amount, the viscosity can be corrected to produce reliable data from the SLS measurements (82).

I.3.2.1.6 Multiangle light scattering – MALS

MALS is an alternative to determine cp titer, full empty ratio and aggregates: MALS detectors are now commonly used for in-line measurements with UV detector and/ or differential refractive index (dRI), after sample separation via SEC (83-85), AF4 (86-89), or AEX (90, 91). But batch mode measurements are possible, too. Capsid and vg titers can be calculated by measuring MW for individual species. Furthermore, it is also possible to determine the percentage and size of aggregates when a separation device is used before the MALS (89, 92-94).

For the calculation of the vg or capsid titer, the refractive index, as well as the extinction coefficient of the capsid and the genome DNA, must be known. The refractive index is mostly constant for different serotypes and engineered variants, but the extinction coefficient varies widely and must be calculated for every capsid and genome DNA.

Importantly, this analysis method assumes that the sample is either full or empty, whereas it is not possible to account for partly filled or overfilled particles (64).

The detection limit of the MALS depends on the LOD of the UV and RI detector and on the sample itself: Full capsids have a higher extinction coefficient and can be detected at lower concentration., while in general, in-process controls (IPC) or DP with an injected capsid amount >10^{11}cp are measurable. With the following equations the respective particle number can be calculated (NA is Avogadro's number, MW_{cp} is the molecular weight (g/mol) of the capsid, MW_{vg} is the molecular weight of the genome calculated from the sequence) (64):

Total capsids: $$C_{total} = \frac{(Conc_{cp}\left[\frac{mg}{mL}\right] \times NA)}{MW_{cp}[\frac{g}{mol}]}$$

Full capsids: $$C_{full} = \frac{(Conc_{DNA}\left[\frac{mg}{mL}\right] \times NA)}{MW_{vg}}$$

Empty capsid: $$C_{empty} = C_{total} - C_{full}$$

With AEX a full empty separation can be achieved by using an UV detector. The relative area of the full capsid peak is higher than the empty capsid peak if the same capsid amount of the two species is in the sample. This results in a substantial overestimation of full capsids, due to the higher extinction coefficient (65). One option to correct this overestimation is to calculate a correction factor as demonstrated by some papers (95, 96). However, this correction factor must be calculated for each AAV construct separately, while a MALS detector can be used in-line to calculate the capsid amount of both peaks without overestimation of the full capsid peak. In addition, MALS also provides insights about the relative size of empty and full capsid peaks in harvests and lysates (93).

I.3.2.1.7 *Virus particle counting*

Particle counters such as nanoparticle tracking analysis (NTA) are primarily used in protein formulation for the analysis of subvisible particles. However, due to the small size of AAV, before measurement by NTA, labeling must be done to make the AAV visible. For NTA the AAV are labeled with small gold nanoparticles. The resulting gold-labeled virus particles scatter enough light to be visualized and tracked by the optical system, enabling the use of NTA to measure the size and concentration of AAV, as well as the aggregation state and formulation stability (97). Other optical systems like Virus Counter® (Sartorius

Stedim Biotech GmbH, Göttingen, Germany) require labeling of the AAV with a fluorescent dye, too. Particle counting has been successfully applied to a bride variety of virus samples at different purification steps and adds a 30 minutes labeling step to sample preparation (67). The fluorescence signal can be detected in the flow-through of 195 µL for $5*10^5$ to 10^9 cp/mL. It has been implemented for other viruses like lentiviruses, for which it is also possible to derive the full empty ratio of the virus suspension (98). At present, this technique is only available for AAV2 and AAV3, because only for those two serotypes a Virotag is commercially available (99, 100).

I.3.2.1.8 *Conclusion*

There are different methods for the quantification of the capsid titer, which can be divided into antibody-based, optical, and light scattering methods. While the antibody-based methods have a longer turnaround time, usually 4-5 hours, they have high specificity and quantify even unpurified in-process samples reliably. Recently developed antibody-based methods, such as BLI (101) and FV, promise rapid analysis with high throughput and marginal sample preparation, but FV in particular requires a fairly large sample volume for measurement. However, there is little published literature on BLI and FV with respect to rAAV or other viral vectors (38).

For the antibody-based methods, the main challenge is the need to have serotype-specific antibodies for the corresponding serotype. This is the case for the commonly used serotypes, but with the constantly increasing number of engineered capsids, new serotype-specific antibodies will always be a problem. As well as the provision of reference materials, as standardized reference materials are currently only available for rAAV2 and rAAV8 (69, 102).

Unlike antibody-based methods, optical and light scattering methods are easy to use and have high throughput, which is attractive for process development. Furthermore, some of these methods allow for the determination of additional CQA, such as the number of aggregates. However, it is not possible to measure unpurified samples with these methods because they lack specificity and robustness (38). Currently, there is limited experimental data overall for rAAV quantification to compare the accuracy and precision of all optical and light scattering methods. Chapter III does offer some new insights in this respect.

Each of the three method groups is already suitable for different applications, depending on sample purity and required analytical capacity. Nevertheless, the methods based on light

scattering or a combination of light scattering and UV spectrometry have the potential to become universal methods for at-line or in-line use during process development, where they are already regularly used in protein analysis.

I.3.2.2 Vector genome titer

The vg titer can be determined by quantifying the number of packaged vector genomes by several methods like: quantitative polymerase chain reaction (qPCR) (103), droplet digital PCR (ddPCR) (102), dot-blot hybridization (104, 105), Southern blotting (106), ultraviolet (UV) spectrophotometry (65), or DNA quantification using fluorescence dyes (107, 108).

I.3.2.2.1 PCR analyses

The common measured parameter of AAV concentration is the amount of vg by quantitative real-time Polymerase chain reaction (qRT-PCR) or digital droplet PCR (ddPCR). The qPCR is a nucleic acid amplification method, based on the principle of conventional polymerase chain reaction (PCR), moreover allowing for the quantification of recovered DNA. This method is often referred to as physical genome titration of AAV vectors and is the preferred and widely accepted method for the quantification. What is more, it is frequently used to determine clinical doses (109, 110).

I.3.2.2.2 Quantitative polymerase chain reaction – qPCR

Currently, qPCR is the most used quantitative assay for rAAV vector genome titration. This assay was also selected as the titration method for rAAV2 and rAAV8 RSM, as it has proven to be a robust and accurate method for determining rAAV genome titers (69, 103, 111-113). Quantification is performed based on the fluorescence signal, that increases in proportion to the amount of PCR products analyzed during a PCR cycle. For the quantification of the PCR product, only the phase of exponential increase of the fluorescence signal can be used, because only in this phase optimal reaction conditions prevail (112). Only a few µL of the sample are needed for the qPCR, containing $10^5 – 10^{10}$ vg/mL. The main benefits of qPCR under ideal conditions are that it is a simple and robust method and, therefore, can be used for a range of clinical applications requiring the detection or quantification of viruses. But as every method, qPCR has its limitations. The most significant disadvantages of qPCR are the labor intensity and the very sensitive experimental conditions. Other factors, such as PCR primers, reagents, equipment, and DNA standards can also significantly affect test results (109, 114).

DNA extraction prior to amplification is considered a crucial step for vg quantification, as this releases the DNA from the capsid and eliminates any PCR-inhibiting substances that were originally present in the matrix. For example, a sample derived from crude cell lysate must be appropriately diluted to obtain the correct vg titer by qPCR, because in the cell lysates and media inhibitory components are present (115). This is also relevant for samples that have been purified by hydrophobic interaction chromatography (HIC), as these samples contain high salt concentrations, that can interfere with qPCR. However, apart from the necessary dilutions, no further purification steps or buffer exchange steps are required. This is an advantage as every additional step can reduce the virus yield.

Another problem in vg titration, not to be underestimated, is the lack of harmonization of protocols and materials that can lead to significant differences between laboratories (4, 69, 113). The use of different forms of genome DNA alone as a calibration standard can significantly alter the quantification of vg concentration. These inter- and intra-laboratory variations may originate from the use of sequences as quantification standards that produce secondary structures, such as circular or supercoiled forms of genome DNA. This can lead to an overestimation of the AAV titer up to a factor of seven, compared with quantification based on a linear genome DNA standard (109, 116). Several attempts have been made to improve the variability of standard qPCR, for example by quantifying AAV2 ITR sequences in qPCR (117). This sequence is not only used in most rAAV vectors but also used as a common vector dosing unit against which laboratories should calibrate their measurements(114). Unfortunately, only two well-characterized reference standards for AAV2 and AAV8 are currently available for validating the method (69, 113, 118).

I.3.2.2.3 Digital droplet polymerase chain reaction – ddPCR

The ddPCR is an endpoint PCR approach with the capability of measuring the absolute number of DNA targets in a sample. It uses dilutions, PCR, and Poisson statistics. The concept that was first described by Sykes et al. in 1992 (119). The digital PCR can be performed as microfluidic/ chip based dPCR or emulsion (droplet) based ddPCR. Even at low copy numbers, targets are determined accurately and cost-efficiency can be significantly improved in combination with multiplexing (120). For absolute quantification, ddPCR does not require standard curves, avoiding the bias in amplification efficiency observed with qPCR (121-123). Furthermore, ddPCR is independent of reference materials and less sensitive to inhibitors of PCR reactions, thus simplifying both the performance of experiments and the comparability of data. ddPCR performs

significantly better than qPCR in terms of robustness and assay variance, which is particularly relevant to IPC or samples with high salinity (55, 102). Another accelerating effect of ddPCR is that it can be performed without prior DNA extraction (124). Limit of detection (LOD) and limit of quantification (LOQ) are comparable to qPCR, whereas the inter- and intra-laboratory-variability is lower (124-126).

However, the ddPCR titration method is not yet being used widely. Two reasons for this are the need for a special device and the labor intensity. Another downside is PCR inhibition when using primers near the hairpin of self-complimentary (sc)AAV vectors. A particular problem when performing ddPCR is the presence of aggregates: This is because aggregates can lead to distorted results since the distribution of virus particles in the droplets is not random in this case.

I.3.2.2.4 Vector DNA determination by membrane blotting

By blotting vector DNA on a membrane by using dot blot (71, 104, 127) or southern blot (106) the vg titer can be determined for low volumes and low vg titers. Independent of the method, the vector DNA must be extracted from the sample with phenol/chloroform and finally precipitated with ethanol before blotting. In doing so, some loss in DNA is possible. The extraction is followed by alkaline agarose gel electrophoresis and southern blot hybridization. The number of particles must be calculated from the specific, full-length of the virion DNA, hybridized with 32P-labeled probe DNA.

Dot blot assays have been extensively used to quantify rAAV vectors by hybridization, but this is a rather labor-intensive and time-consuming procedure because it requires sample processing to remove protein contaminants. Moreover, 5- to 10-fold inter- and intra-assay variations have been reported for dot blot analyses (127). AAV formulations containing magnesium ions have been reported to inhibit the interaction through DNA binding (128). These ions are more common in AAV samples nowadays, as full-empty separation by anion exchange chromatography (AEX) becomes customary practice (95).

I.3.2.2.5 UV spectrometry

Through the measurement of the optical density (OD) of AAV samples, it is possible to calculate the vg and the capsid titer of a sample. The sample must be highly purified as the measurement is affected by cellular proteins and DNA contamination. Furthermore, the MW of the vg must be known to correctly calculate the vg titer. Also 0.1% SDS must be added to the sample before heating to 75°C for 10 minutes, resulting in lysed AAV. Before

the absorbance measurement at 260 and 280nm, the sample must be slowly cooled down to room temperature. At all the UV assay takes 30 minutes and is therefore time- and cost efficient. To calculate vector genomes per milliliter the following equation is solved, using the value of the MW of DNA, and the measured absorbance (65):

$$vg/ml = \frac{4{,}47 \ * 10^{19} \ (A_{260} \ - 0{,}59 \ A_{280})}{MW_{DNA}}$$

The linear absorbance range is $5*10^{11}$ up to 10^{13} vg/mL and the required sample volume depends on the used spectrometer. As already mentioned, the measurement can be affected by residual protein impurities as well as by excipients that absorb in the UV range, like Tween 80 or iodixanol. To avoid AAV losses due to adsorption poloxamer 188 can be used instead of Tween 80, that does not show measurable absorbance at 260 and 280 nm.

I.3.2.2.6 Measurement of DNA amount by fluorescent dyes

Vg can also be calculated by measuring their DNA contents more directly: Cell Biolabs (San Diego, CA) has designed a commercial AAV titration kit (QuickTiter™ AAV Quantitation kit) based on quantifiable binding of DNA dye (CyQuant GR) to rAAV genome. Similarly, PicoGreen®, another DNA sensitive dye, has been used to measure AAV titer. However, only double-stranded DNA (dsDNA) can be labeled by PicoGreen® (107). Therefore, if used for quantification, the AAV capsid must be lysed first and the single-stranded genome annealed to dsDNA (65).

With PicoGreen®, the assay is linear in a range of 0.16 to 120 ng DNA, which corresponds to vg titers ranging almost 3 logs, from $3*10^{10}$ to $2.4*10^{13}$ vg/mL. For the measurement 2 µL of AAV suspension is diluted with 18 µL TE buffer with 0.1% SDS and lysed for 1 hour at 70°C.

The following formula is used to convert ng/mL to viral genome per mL (107):

$$rAAV \ vial \ genome \ \left(\frac{vg}{mL}\right) = \frac{rAAV \ genome \ conc. \left(\frac{ng}{mL}\right) * \ 1.82 * 10^{12} (\frac{bp}{ng})}{Length \ of \ AAV \ genome \ (\frac{bp}{vg})}$$

The quantification of the vg by PicoGreen® has also been tested in the most commonly used storage buffers for AAV: PBS (129, 130), PBS+5% sorbitol (131, 132) and PBS+135 mM NaCl (113). None of the storage buffers did interfere with the PicoGreen® titration assays.

Notably, both CyQuant GR and PicoGreen® are membrane permeable dyes belonging to the cyanine dye family. In recent years, several safe nucleic acid dyes have been developed, such as Gelgreen® and Gelred® from Biotium (Fremont, CA, USA), SYBR Safe and SYBR Gold from Thermo-Fisher Scientific (Waltham, MA, USA), and Diamond™ from Promega (Madison, WI, USA). These dyes are membrane impermeant, making them safer to use and more friendly to the environment (133).

For Gelgreen®, it was already shown that vg concentration can be determined (108). This dye needs to be diluted 1/10000 to end up in a linear measurement range of 0.16 ng to 50 ng DNA in 10 µL of a lysate sample, heated at to 95°C for 5 minutes. The LOQ of this assay is 0.39 ng DNA, which corresponds to a AAV titer of 10^{10} vg/mL in 10 µL of an AAV sample.

The following equation allows to convert encapsulated DNA (ng) to vg titer (vg/mL) (108):

$$AAV\ titer\ \left(\frac{vg}{mL}\right) = \frac{DNA\ mass\ (ng) * 10^{-9} g * 6.022 * 10^{23} mol^{-1}}{MW * volumen\ (\mu L) * 10^{-3} mL}$$

Both dye-based methods are simple, fast, and robust. The dyes are cheap, and the most labs are equipped with a fluorescence reader (PicoGreen®: excitation: 485 nm, emission: 535nm; Gelgreen®: excitation: 488 nm, emission: 528/20nm).

I.3.2.2.7 Conclusion

Preclinical and clinical dosing of rAAV DP is usually based on the number of genome copies, so the accuracy and precision of the vg titer is critical. The methods for determining the concentration of vg discussed here, can be divided into three groups: PCR-based, membrane blotting and spectrometry-based.

A clear advantage of the PCR-based methods is that they are already established in the field of AAV vector research. This is especially true for traditional qPCR. However, this method shows large inter- and intra-laboratory variations, as well as matrix effects for certain compounds in the sample. The ddPCR is less susceptible to these two problems, yet aggregates must be avoided at all costs during vg quantification.

Methods for determining vg concentration by membrane blotting are widely available, too, and require little laboratory equipment. However, they are all very labor- and time-intensive. In addition, like qPCR, these assays have a very high variation.

Both spectrometry and fluorimetry-based methods are very fast, compared to PCR-based methods. However, significantly higher titers are required, especially for UV spectrometry. These titers should not be a problem for DP, as the two gene therapeutics currently on the market are well above 10^{12} vg/mL. For IPC controls, on the other hand, both methods are not feasible, as both measurements are disturbed by residual DNA and proteins.

Another method for vg quantification that has received little attention so far could be DSC (64). DSC was introduced in chapter I.3.1.2.2. Because a clear melting peak for the DNA is visible in the thermogram, this could be calibrated and then used for quantification. However, right now very large volumes and concentrations of AAV samples are needed for such measurement. Nevertheless, it is a promising method for the future, as additional information on purity and possibly also on the ratio of full and empty capsids can be obtained at the same time.

I.3.2.3 Vector functionality: transduction and infection assays

The most important criterion for a functional gene therapy vector is the ability to infect and transduce specific cells. Not every genome containing capsid can infect cells, therefore it is well documented that the infectious genome titer can significantly differ from the vg titer (113, 134). This is also the reason why the Ph. Eur. (9.5.14) requires in-vitro and in-vivo activity data for genome vectors. Because of the different tropisms of the variety of AAV serotypes and engineered variants, the activity assay needs to be performed with relevant cell lines: For example, rAAV5 vectors infected HEK293 and HeLa cells very poorly (135),while it is very efficient at infecting retinal pigment epithelium (RPE) cells and retinal cells in human retinal organoids (136, 137). However, it is not always possible to culture the cells that are to be targeted in humans; thus, transduction of the desired cells is not tested as part of a routine assay. If it is not possible to cultivate the cell line to be transfected in the laboratory, the only possibility to prove the functionality of the AAV is an animal experiment. Such experiments are particularly costly and are therefore performed as late as possible in the development of new AAV vectors (71).

Another reason for a difference between the vg titer and the infectious titer can be fragmented genomes or damaged capsids. These genomes contribute to the vg titer in qPCR but are not able to infect cells.

There is a variety of activity tests: (end-point) dilution assays, serial dilution replication assays, fluorescent cell assays (single or multiple cells) (138), infectious center assays

(ICA) (139), infectivity titrations, replication center assays (140), and tissue-culture infected dose at 50% (TCID50) measurements (139, 141). All these assays involve the evaluation of transduction efficiency of the gene therapy vector and can be distinguished into two broad categories: transduction assays and infection assays.

I.3.2.3.1 Transduction assays

Theoretically, the best way to evaluate transduction efficiency is to add AAV to a non-complimenting cell line and to measure the expression of the transgene (71). This is a commonly used biological assay to test infectivity of AAV preparations and results in a titer of transducing units (TU). Prerequisites for transduction are entry of AAV vectors into the cells, translocation of vg into the nucleus and its conversion into double-stranded DNA, and, lastly, transcription of the transgene. However, it is not always possible to measure the transduction easily and directly.

The simplest way to determine the expression of genes is to measure the amount of proteins expressed. These assays are quite specific when marker genes such as GFP or lacZ are used (138). The number of GFP-expressing cells can be measured with fluorescence activated cell sorting (FACS) However, this is not possible for transgenes of clinical interest. Therefore, assays that detect the sequence of the transgene in the transduced target cells by qPCR are used (142-145).

Lately, Spark Therapeutics developed a commercial assay for the quantification of vector functionality. It measures the in-vitro potency of rAAV-RPE65 vectors (146). It uses a serial dilution of rAAV-RPE65 and tests the gene expression on modified HEK293 cells, constitutively expressing lecithin retinol acyltransferase. All cells are lysed after 72 hours, and the lysates are incubated with all-trans-retinol and cellular retinaldehyde-binding protein for 2 hours in the dark. Then, the amount of 11-cis-retinol is quantified by LC-MS because RPE65 is an enzyme that enzymatically converts all-trans-retinol to 11-cis-retinol (146).

Crucial for every transduction assay is the level of detectable expression, which depends on many biological properties of the capsid, transgene and promoter, as well as target cell line. For reporter genes like β-galactosidase, GFP, and luciferase under strong promoters, such as the cytomegalovirus (CMV) promoter, detection of transgene expression is relatively straightforward. For therapeutic transgenes with tissue-specific promoters, detection is very complex (71).

I.3.2.3.2 Infection assays

In contrast to the transduction assays, expression of the transgene is not essential for the infection assays because the aim of these assays is to control whether the transgene has entered the nucleus or not. One often used method to quantify infectiousness of AAV vectors, consists of infecting trans-complementing cells, such as HeRC32 cells (147) that have stably integrated AAV2 *rep* and *cap* genes (148). Determination of infectious units (IU) by intracellular amplification of the rAAV genome in rAAV preparations in the presence of wild-type AAV and adenovirus can be performed by various methods: $TCID_{50}$ and ICA.

In $TCID_{50,}$ qPCR is used for vg replication determination (113, 141). ICA-DNA hybridization, on the other hand, uses a probe of the rAAV gene cassette to detect cells in which vg replicate (140, 149). It can be expected that values obtained from this type of assay will be significantly higher compared to transduction assays because it does not rely on transgene expression.

I.3.2.3.3 Conclusion

AAV vector activity can be determined by two different assays: transduction or infectivity. In the transduction assay, the expression of a specific protein or product is measured. This assay is simplest when marker genes can be used, as the transduced cells can then be easily detected by color (138). Unfortunately, this detection capability is not available for transgenes of clinical interest, so the corresponding protein must be quantified by other analytical methods (142-145).

Compared to the measurement of transduction efficiency, the measurement of infectivity titer of AAV vectors is much more difficult and costly. The reasons are: (1) the vector is inherently incapable of replicating in transduced cells, so multiple helper virus genes as well as wild-type AAV must be replicated in cell culture to detect infectivity measured by replication of the AAV genome; (2) cytopathic effects (CPE) caused by infection with an AAV vector can be overridden by even stronger CPE of the helper viruses; and (3) is mainly relevant for AAV vectors that are not based on AAV2: Most available cell lines do not support efficient infection by vectors even when sufficient helper virus genes are present (7).

Notwithstanding these difficulties, infectivity can be used as a relative measure of the functional activity of AAV batches and provide further information about the stability of the vector. This is important, for example, in various upstream and downstream processes.

It is important to note that both infection and transduction titers can vary significantly depending on the combination of serotype and target cell line used for the assay. Other parameters, such as cell confluence or use of a helper virus, can result in significant differences in infectious titers and should be considered when batch-to-batch comparisons of vectors are made. Therefore, transduction activity assays were performed for all experiments discussed in Chapters V and IV. In each case, GFP expression is measured by the number of green-fluorescent cells. In Chapter V, the assay is used to compare the activity of batches of AAV with the same amount of AAV per cell for different upstream and downstream processes. The focus in Chapter VI is on constant GFP expression over storage time. Liquid and freeze-dried formulations are compared, after storage at 4°C and 25°C.

AAV capsids that contain the intended vector genome but have low replication or transduction pose similar risks as empty capsids: defective particles may release unnecessary viral antigen, impair transduction by infectious particles, and increase the risk of immunotoxicity. In addition, preparations of AAV vectors with lower infectivity require higher doses to be effective. Because the ratio of vg titer to infectious titer (vg/IU) is a key parameter for assessing vector quality, accurate titration of vg by free-ITR-PCR may allow better vector characterization (110).

I.3.3 Purity of AAV vectors

As with most biological products, it is necessary to perform quality control testing for AAV vector sterility, endotoxin content, mycoplasma, and adventitious virus detection (150). In addition, some tests specific to AAV production are required: host cell-, process- and product-related impurities, like DNA, RNA or protein impurities and vector-related impurities, like empty capsids and capsids encoding host-cell or helper DNA.

Accordingly, the production cell lines, either human cell lines (4, 148) or insect cell lines (151, 152), makes a difference in the type of possible contamination: remaining host cell proteins and nucleic acids lead to different risk levels of immunotoxicity and genotoxicity, as the overall risk of genotoxicity may be higher in transduced human cells because of the possibility of homologous recombination with genomic sequences. While the genotoxicity is lower if insect cells are used for AAV production, the risk of immunogenicity increases due to the possibility of unintended expression of polypeptides from insect cells in transduced tissue (7).

Therefore, quality control tests must be implemented to measure the level of process impurities, including residual host cells, residual production genome DNA, and other reagents added to the product as part of the manufacturing process. Useful methods to assess protein impurities in purified recombinant viral vectors, such as residual production cell protein and bovine serum albumin (BSA), include SDS-PAGE (discussed in I.3.2.1.3) and ELISA (discussed in I.3.2.1.1). Concerning DNA impurities, various qPCR methods are available and for other process-related impurities, like buffer ingredients, surfactants or affinity ligands, reverse phase chromatography (RP-HPLC), optionally combined with a charged aerosol detector, can be performed. These reagents may cause safety concerns, making it necessary to demonstrate the non-existence of these impurities at the end of the process.

Finally, the vg to capsid ratio is clearly another CQA for AAV samples because empty capsid can induce different effects which can lead to lower transduction efficiency and/ or immunogenicity. To determine the number of empty capsids in the sample, cryo electron microscopy (cryo-EM), analytical ultracentrifugation (AUC) or anion exchange chromatography (AEX) can be used.

I.3.3.1 Replication competent AAV

An AAV containing *rep* and *cap* flanked by ITR, and therefore able to replicate in the presence of a helper virus, is termed a helper virus-dependent replication-competent AAV (rcAAV), also known as "wild-type" or "pseudo-wild-type" AAV. The expression of AAV *rep* or *cap* from rcAAV present in an AAV vector investigational product increases the risk of immunotoxicity in vector-transduced tissues. There is evidence that rcAAV may contribute to the generation of CD8+ T cells which can recognize vector-transduced cells (153). These cells present peptides derived from the input capsid protein component of the vector inoculum through a cross-priming mechanism (153). Not all mechanisms are yet fully understood but the risk of immunotoxicity underscores the need to reduce rcAAV to the lowest achievable levels in AAV vector drugs.

Helper virus-dependent rcAAV closely resembles authentic AAV vectors, and thus cannot be separated by purification process steps. Rather, strategies are required to minimize rcAAV formation during vector generation in cell culture. The generation of rcAAV particles is highly dependent on the method used for AAV production, the triple

transfection method being more prone to generate rcAAV than productions relying on stable cell lines (154, 155).

To test the presence or absence of rcAAV forms, a sample of the vector stock should be amplified in a serial passage assay, typically on adenovirus infected HEK293 or HeLa cells. Thereafter, DNA is isolated from P2 cell population and analyzed for AAV replication intermediates (148). One problem of this method to test presence of rcAAV is the need of using wild-type AAV vectors as a control for the test, which are a risk for cross-contamination of rAAV stocks. Furthermore, with the increasing number of serotypes and mutants in use, it will be necessary to develop wild-type AAV standards for each serotype or mutant to ensure sufficient sensitivity of the test.

I.3.3.2 DNA impurities

During the production process, different types of DNA emerge that are required at a particular step to produce AAV. Accordingly, the foreign DNA in the final product can come from the production cells, from helper viruses, but also from the vector genome used itself. All this DNA is undesirable in the DP because it can be immunogenic. These DNA fragments can be free or enclosed in a capsid. The removal of foreign DNA enclosed in the capsid is much more difficult than the removal of free DNA fragments.

I.3.3.2.1 AAV-encapsulated DNA impurities

Although viral ITR in the vector genome functions as a signal for specific DNA encapsulation, it has been described that other DNA forms can be encapsulated nonspecifically (156-158). Encapsulated baculovirus DNA was one of six major product quality concerns identified during licensure assessment of Glybera (42).

When using triple transfection protocols, there is an increased risk of “cross-encapsulation” of DNA because high amounts of genome are used for this transfection. Indeed, AAV containing prokaryotic DNA and, in particular, the ampicillin resistance gene pose a significant problem, as this can lead to antibiotic allergies (156). One of the mechanisms that lead to undesired DNA packaging is the encapsulation of the backbone of pTransgene plasmid that contains the ITR-flanked vector genome by a reverse packaging process. Addressing this concern, it was demonstrated by Hauck et al. that, by including stuffer DNA to increase the size of the pTransgene above 5 kb, it is possible to reduce reverse packaging up to 7.6-fold (157).

To measure relevant specific nucleic acid impurities, the genome DNA can be quantified by qPCR with primers and probes specific for the ampicillin or kanamycin resistance gene common to all genomes used for rAAV vector generation. In the additional studies concerning purification strategies of AAV vectors in Chapter V, the amount of pTransgene backbone was determined by qPCR. Quantification of host cell DNA (HEK293 or Sf9) is possible by a TaqMan gene expression assay for 18S rRNA or by Alu sequence (a repetitive DNA sequence), as it is done in Chapter IV of this thesis. The amounts of these specific DNA impurities are indicated as amount in pg compared to vg (74). Furthermore, distinction can be made between encapsulated and naked DNA impurities, based on nuclease sensitivity. DNA fragments from host cells can account for 1-3% of the total AAV vectors (158).

Regardless of the cell lines used to produce the AAV, i.e., human or non-human origin, two possible risks are genotoxicity and immunotoxicity (7). As mentioned, the potential for homologous recombination with genomic sequences in transduced human cells is greater when human cell lines are used. Since these lead to AAV with residual human genomic DNA, which in turn leads to an increased genotoxicity risk. In contrast, when insect cells are used as production cell line, the risk of genotoxicity is likely to be reduced (7). However, the risk of immunotoxicity is increased, due to unintended expression of polypeptides from insect cells in transduced tissue. Lastly, both HEK293 and HeLa cells may have activating oncogenes present. This, of course, raises concerns because relevant amounts of these oncogenic DNA sequences can be conserved in viral vector preparations (159-161). In any case such impurities should be reduced to the lowest achievable levels.

I.3.3.2.2 Helper virus DNA

Helper viruses can occur as contaminant as whole virus or in the form of encapsulated DNA. Herpes simplex viruses, adenoviruses, or baculoviruses are commonly used for rAAV production, depending on the adopted strategy. Packaged helper DNA sequences can be determined and quantified by specific primers during qPCR, as already discussed in I.3.2.2.2. Packaged residual DNA impurities, derived from vector template and helper sequences, were reported to range from 1% to 8% of vg DNA in purified AAV samples (156, 157). A primary concern of residual helper DNA sequences packaged within AAV is the possibility of unintended expression of immunogenic peptides. In the DP no more than 0.1% of vg DNA is allowed to be residual helper DNA (162).

I.3.3.2.3 Free DNA/RNA impurities

In addition to the encapsulated DNA of host cells and helper viruses, the DNA may also be presented in free form. Therefore, it is also necessary to remove as much free DNA as possible from the DP. Despite numerous purification steps, it is possible that free DNA is found in the DP. Regardless of the cell line used for production, AAV products must be screened for the presence of DNA-related contaminants that originate from the host cell or helper components that are used part of AAV production. To quantify host cell DNA impurities, qPCR/ddPCR-based methods are used that target regions such as Alu repeats (163), 18SRNA (164) or other housekeeping genes within host cell genomic DNA. Primers for Alu repeats were also used in Chapter IV to quantify the amount of HEK cell DNA.
It has been shown that a large fraction of free DNA binds to the outside of the capsid and therefore co-elutes with the capsid when using size exclusion chromatography (SEC, for more information see I.3.4.2.2). During the SEC run, the presence of contaminated DNA can be measured by fluorimetry using Picogreen (93). However, quantitative comparisons should only be made with caution: even when assuming uniform staining and chromatography conditions, the intercalated dye may be displaced. For example, a high amount of salt (1M NaCl) can decrease Picogreen fluorescence, while divalent metal cations are known to enhance Picogreen fluorescence (93).

The concern that residual DNA impurities might express oncogenes led to the existing guidelines: residual DNA amount and size must be controlled; residual cell-substrate DNA should be ≤10 ng per dose, with a median DNA size of 200 bp or lower and residual plasmid DNA must be below 100 pg per 10^9 vg (165, 166).

I.3.3.3 Protein impurities

The only proteins that should be present in purified rAAV stocks are the capsid proteins (VP1, VP2, VP3). However, it is common for protein impurities to be co-purified with these vectors. In the case of AAV, the protein impurities can be of different origins: e.g., bovine serum contained in the culture medium or endogenous proteins from the producer cells (167). Depending on the serotype and the protein present, there may be significant interactions between the protein and the AAV. Human galectin-3 binding protein (hu-G3BP) has been shown to cause aggregation and precipitation in AAV6 and may even decrease the transduction efficiency of AAV6 (168).To determine the protein composition of the rAAV stocks, the most common method involves SDS-PAGE and sensitive protein

staining, usually silver stain (see I.3.2.1.3). In SDS-PAGE, the ratio of the capsid proteins VP1, VP2 and VP3 can be estimated, and the relative purity of the capsid can be controlled. This implies that the purity of the sample can only be assessed in comparison to a reference preparation. Unfortunately, for the moment only reference materials for AAV2 and AAV8 are available.

Alternatively, optical density measurement of rAAV stock at 260/280 nm and correlation of this value to vg can be used to estimate protein impurities (65, 74). There are also commercially available ELISA kits, for example Bio-Rad microassay (76), antibody affinity extraction, or LC-MS, that can be used to determine the protein content in the sample.

I.3.3.3.1 Empty capsids and other product-related impurities

Empty capsids consist of an identical AAV capsid shell as the full capsids. But unlike these they do not contain a nucleic acid molecule, so they are not therapeutically active. Empty capsids are the result of a very low encapsulation efficiency during production. In current standard production methods large amounts (50-90%) of AAV particles do not contain vector genomes (57, 65, 80, 103).

Whether empty capsids have a positive or negative effect on transduction efficiency is much debated: on the one hand, they may reduce transduction by competing for vector-binding sites on target cells, which in turn may lead to an increased need for vector dosing. On the other hand, empty capsids have also been reported to have a positive effect on transduction efficiency. Due to their immunological similarity, empty capsids may act as effective decoys to decrease neutralization of functional AAV vectors by pre-existing antibodies, thereby increasing transduction in target tissues after systemic administration (42, 169, 170).

In addition, capsids may be partially filled: Fragments of other nucleic acids contained in these capsids may pose a disproportionate risk for enhancing adaptive immune responses directed against the viral capsid antigen, if not removed. Furthermore, the ratio of empty capsids to genome-containing AAV particles may influence the outcome of in vivo gene transfer (4, 26).

There are several well-established methods for full-empty distinction of AAV products, including analytical ultracentrifugation (AUC), cryogenic electron microscopy (cryoTEM), and anion exchange chromatography (AEX). More recently, capillary electrophoresis isoelectric focusing (cIEF) (171), charge detection mass spectrometry (CDMS) (172), and

mass photometry (MP) detection (173) have also been used to distinguish between full and empty capsids. In addition to empty capsids, it is important to measure partially filled and aberrantly formed capsids, as well as the relative abundance of empty to full capsids.

I.3.3.3.2 Sedimentation-velocity analytical ultracentrifugation – SV-AUC

SV-AUC monitors sedimentation during centrifugation and links the sedimentation profiles of the AAV sample with the molecular weight and size of the particles. For detection UV extinction at 230 nm, 260 nm, or 280 nm, as well as Raleigh interference can be used. In a single experiment, information can be obtained on the relative content of full (100-120 Svedberg (S)), partially filled (80-95 S), and empty capsids (60-70 S), as well as on the number of aggregates and minor impurities (174-176). This makes AUC one of the few measurement methods that can detect partially filled capsids, at all. In addition to separating full and empty AAV by AUC, the 260 nm to 280 nm ratio can be used for determination of the full-empty ratio. For full AAV the ratio is about 1.4 and for empty AAV about 0.6.

The advantages of SV-AUC are the good reproducibility of the relative proportion of full and empty capsids and the quantification of partially filled capsids. However, this method also has its disadvantages: Quantification of aggregates is only possible when their content is higher than 3%, because the standard deviation for aggregate content is about 1% (177). To perform an SV-AUC experiment, 400 to 500 µL of sample volume and an AAV concentration higher than $1*10^{12}$ vg/mL are required, and it is not possible to recover the material after the measurement (174-176). AUC equipment is expensive, and scalability is difficult due to the limited throughput of seven samples within six hours. Nevertheless, it is often used as an orthogonal method to validate alternative methods that offer higher throughput but possibly poorer resolution, like AEX or cIEF (174, 178).

I.3.3.3.3 Transmission electron microscope – TEM

TEM is a well-established method providing visual information on AAV. This allows an image based morphological assessment of the capsid content (179, 180). An alternative to negative-staining TEM is cryogenic electron microscopy (cryo-EM) (181). The structural characterization relies on good contrast, which is typically achieved with heavy metal staining salts. The salt diffuses into the inside of empty AAV capsids and due to the electron dense staining material, the inside of the capsid appears dark (donut-like) in the TEM images. The higher the degree of filling of the capsid, the less space is available inside the capsid for the staining material and the brighter and more uniform, the core regions of the AAV appear. By counting the AAV particles, the titer of the AAV can be estimated. The

titer can be estimated separately for full and empty AAV (182). However, this estimation , is complicated by possible intermediate particles that appear neither empty nor full, as reported by Grimm et al. (183).

Using manual visual identification (123, 174, 184) by TEM is, along with AUC, de facto the reference method for determination of full to empty content ratio. Usually, TEM is used for purified samples because impurities can interfere with the accurate identification of AAV. Nevertheless, it was recently shown by Subramanian et al. that it is feasable to measure unpurified samples (181). Furthermore, it has been used for the identification of aggregates, deformed capsids, other particles such as host cell debris, and other contaminants (123).

The main advantages of electronic microscopy are that it can be used independently of the AAV serotype and only requires a small sample amount. On the downside, it is an imprecise and non-standardized method for titer measurements (4). Multiple thousands of capsids must be imaged and analyzed for statistical significance, with the capsid content of individual images varying by around 2% (174, 181). Moreover, it is not possible to detected over-filled capsids by TEM. Over-filled capsids are capsids that contain more DNA than the normal vector genome. Thus, unreliable results are common and poor agreement with orthogonal methods, such as AUC, has been reported (9, 80). Due to the low throughput and long turnaround time, it is difficult to use TEM as a routine analysis method. For the future, novel software solutions, that use deep learning algorithms for quantitative assessments, reveal potential for fully automatization of TEM image analysis (185).

I.3.3.3.4 Anion exchange chromatography - AEX

AEX is an established method in protein analytics. It uses charged functional groups with reversibly bound counter ions on a polymeric matrix. The species then can be separated, based on their different isoelectric points (IEP). The literature IEP of full AAV is 5.9, the IEP of empty AAV 6.3 (25, 186). AAV viral particles contain multiple sites to bind anion exchangers, therefore AEX is a widely used chromatography for purification and analytic. AEX can be used for purification of the AAV samples from empty capsids with fairly good results (26, 176, 187). This is also shown in Chapter IV. For example Poros HQ (26, 188), CIMmultus QA and PrimaS (93, 189), Q-Sepharose xl (26), or HiTrap Q (190) were used for full-empty separation of AAV1, 2, 4, 5, 6 and 8, successfully (95, 191-193).

Because the classical column materials used for protein purification (chromatographic resins) are of limited applicability for the size range of viruses, monoliths are an alternative

purification and analytic format for large macromolecular complexes (194). Significant overlap between empty and full capsid peaks in IEC chromatogram is commonly observed, which means that some full capsids must be sacrificed to achieve complete elimination of empty capsids, using this method. Until recently, the AEX had to be developed newly for every serotype. But lately, a robust AEX method to achieve complete separation of empty and full capsids for several serotypes was developed (189). For industrial scale chromatography, linear gradients are simpler and more robust, but separation performance can be significantly improved with step gradient chromatography (95).

What is more, AEX can be used for quantification of empty capsids in an AAV preparation, because empty capsids will elute earlier in the gradient (salt or pH), in respect to the full AAV (191). This can be important for future studies on stability and formulation screening because it is an easy, cheap, and time-efficient method (182). For detection, an UV-detector can be used, because from the ratio 260/280 nm, it is possible to confirm the ratio of full and empty AAV (194) (see I.3.3.3.2). A ratio ~1.438 indicates that the viruses are full and a ratio ~ 0.59 that they are empty (65). To derive the relative percentage of empty capsids, the different extinction coefficients must be considered - otherwise the empty capsids are underestimated because of the lower extinction coefficient (see I.3.2.1.6, Chapter IV). To reduce this difference to a minimum, the separation can be also monitored by intrinsic fluorescence, because DNA contributes only 0.2% of full capsid fluorescence (93, 195, 196). Using a fluorescence detector can also substantially lower the impact of free DNA, that occurs as impurity in the sample, and can enhance the sensitivity of AAV detection massively (93).

I.3.3.3.5 Capillary isoelectric focusing - cIEF

cIEF is another method to separate full and empty capsids on the basis of charge (171). cIEF is commonly applied in proteomics research due to the very high resolution power and has been reported to baseline separate components with a difference in their respective IEP of only 0.01 (197). The measurement can be done in less than one hour and results in good separation of full and empty capsids, as well as partially filled ones. In the application note of the PA 800 (SCIEX, Brea, CA, USA) 27 µL sample containing $3*10^{12}$ vg/mL AAV are used for the measurement. A good reproducibility was shown, with <5% RSD for the peak area and 2% RSD for the pI value. Thereby, it is possible to identify different AAV vectors based on their pI. The findings for the full-empty ratio in cIEF correlate well with orthogonal methods like AEX (171). Both methods work with UV detection, so a correction

factor is needed to prevent overestimation of full capsids (Chapter IV). Estimation of the vg titer is so far not possible, because the workflow is tedious and the process of calibration not yet established. But in future it should be possible to get this information from cIEF. A relatively large amount of sample is currently still needed to perform this analysis. The needed concentration of AAV in the sample is also in the upper range. These two factors are a clear disadvantage of this method, since for newer AAV constructs often only small amounts of sample with low titers are available at the beginning. If a FI detector were used instead of a UV detector, the AAV concentration in the sample could be about 10 times lower and still allow good detection. This improvement is also crucial because after this measurement the sample cannot be used for further analysis.

I.3.3.3.6 Charge detection mass spectrometry - CDMS

A mass spectrometry-based approach, such as CDMS, has recently been shown to be able to separate full, partially filled, and empty capsids (172, 198). CDMS measures the charge and mass-to-charge ratio of individual ions simultaneously, allowing direct determination of the mass of typically thousands of ions (199). This method has already been used for other viruses, like rice yellow mottle virus (RYMV) and tobacco mosaic virus (TMV), with RYMV being quite similar to AAV in size and shape (199).

CDMS, together with AUC, cIEF and MP is the only other method capable of resolving partially filled capsids. The turnaround time of CDMS is around 2 h, followed by a quick generation of a mass histogram from the CDMS data. However, the instrumentation is less mature and still in development, yet the technology has recently been commercialized by Megadalton Solutions Inc. (Bloomington, Indiana, USA), with a focus on improving the application to AAV (200).

Another problem for CDMS is the variation in mass distribution in each capsid due to the numerical changes of VP1-3, which depend on the expression system for AAV production (73). This heterogeneous mass distribution is a challenge to analyze by conventional mass spectrometry because each peak in the mass distribution would lead to several overlapping peaks in the mass-to-charge ratio spectrum. But some progress has been made in analyzing the m/z spectrum of AAV by Snijder et al. (201). Depending on the vg, a broad variety of partially filled capsids can be detected. Especially, for self-complementary vg, partially filled capsids were observed and there seems to be a preference for cleaving the genome near the hairpin that joins the two self-complementary segments. All in all, the results from CDMS correlate well with the data from cryo-EM (172).

I.3.3.3.7 Mass photometry -MP

MP measures the mass on the single particle level, by detecting the light scattered by the individual particles as they are bound on a glass surface. The measurement is neither affected by the particle's size nor its shape and can, therefore, quantify full and empty capsids easily (202, 203). The interferometric contrast of scattered and reflected light can be related to the mass of the particles through a calibration procedure applied both to proteins (204) and nucleic acids (205).

Refeyn Ltd. (Oxford, UK) demonstrated the ability of a mass photometer to measure the mass of empty capsids from AAV5, 6, 8, and DJ, with a mass precision of 2.7% (3.7 MDa ± 0.10 MDa). Before the measurement, a dilution of 2-10 µL of the sample in 10-18 µL of PBS is necessary and the capsid concentration in these 20 µL should be around 1-2*10^{11} cp/mL to have a good particle count rate during the 60 - 120 seconds measurement, while avoiding overloading the microscope coverslip (173, 206). Additionally, full-empty capsid ratio determination can be performed easily by MP, due to the difference in mass. Only the total capsid number or vg titer is not available for the moment. Besides this, the method is able to detect impurities if they have a mass above 40 kDa, including partially filled capsids, and calculate the percentage of the impurities in comparison to all detected particles (173).

I.3.3.3.8 Conclusion

When quantifying the full-empty quotient, a tradeoff between throughput and resolution must be made for each method. Among high-resolution methods, AUC remains the gold standard to quantify partially filled capsids, though it requires significant sample volumes. MP, CDMS, and capillary isoelectric focusing can achieve AUC resolution with a shorter turnaround time, but there is little literature on either method as they are still in development (38). The high resolution methods allow the quantification of partially filled capsids in process development, but the sample throughput is limited and the time required is expanded.

If it is only necessary to distinguish full and empty capsids, other methods are available with higher throughput compared to AUC. Of these, AEX is the most promising technology, as it is both more robust and more precise than other methods (38), and much more flexible in terms of detection capabilities of the species separated (193, 207). In addition, quantification of the capsid titer with AEX, either directly using a known extinction coefficient, or via a standard curve, is possible.

In general, there are two caveats for quantifying the content ratio using any of the methods presented here. First, results between orthogonal methods often do not correspond to each other, and in particular the accuracy of TEM with negative staining is often questionable (9, 38, 174). In low resolution methods, the contribution of partially filled capsids to the signals from empty and full capsids is usually not sufficiently clear. Moreover, the content ratio is a simplified ratio of a heterogeneous composition of capsids and therefore should not be given too much weight. Ultimately, the distinction between vectors with a complete, functional genome and a fragmented, nonfunctional genome of comparable size is the crucial point. Unfortunately, this important distinction is not currently possible with any of the methods. This is also the reason why the concentration of complete capsids, as estimated from the titer and content ratio of capsids, cannot be equated with the genome titer, nor with the number of transductable AAV (38).

I.3.4 Stability of AAV vectors

Stability is a very general term that can have different meanings to scientists and depends on their research focus. In the field of protein and AAV stability, four different types of stability must be considered: Conformational stability, colloidal stability, chemical stability, and interfacial stability. To each of these four stability types, different CQA can be assigned and studied, as will be discussed below. The goal here must be to find an AAV formulation that stabilizes the AAV well enough during storage that they are stable in this formulation for several months or even years.

I.3.4.1 Conformational stability

Conformational instability refers to a change in the higher order structure of AAV. There are two main pathways for conformational instability: denaturation or small changes in the capsids that lead to genome ejection. Conformational instability can not only affect the stability but also the transduction efficiency of AAV and the degradation products can be immunogenic, it is also a safety concern.

I.3.4.1.1 Denaturation

Denaturation is the loss of native structure of an AAV, either in the form of loss of secondary, tertiary or quaternary structures. Many factors can affect conformational stability, including temperature, pH, product concentration, ionic strength, and the type and concentration of denaturants. Adsorption to surfaces and shear stress during pumping,

filtration, filling, and processing can also lead to the unfolding of capsids and result in less infectious AAV or even force aggregation (208-212).

The conformational stability of biopharmaceuticals in a defined formulation can be studied by thermal or chemical denaturation to induce unfolding of the protein at a specific temperature or concentration of denaturant, and thus observe the changes in AAV conformation. Calorimetric methods such as DSC and spectroscopic methods such as fluorescence spectroscopy or circular dichroism (CD) are well established for characterizing the structure and conformational stability of biopharmaceuticals (186, 213). DSC has been established as one of the most important methods to study conformational stability of proteins (214, 215). Second, both the intrinsic and extrinsic fluorescence can be applied to study changes in the AAV conformation (3, 55, 56). With these techniques a serotype identification of AAV is also possible (see I.3.1.2.2 and Chapter II) and it was found that AAV2 is the least thermally stable serotype (3, 55, 56).

Venkatakrishanan et al. used 350 µL with an AAV concentration of 0.4 mg/mL ($4*10^{13}$ cp/mL) to investigate the structural changes of the AAV capsids due to low pH using CD (186). CD describes the differences in the absorption of left- and right-circularly polarized light by chiral molecules. The local chemical environment alters the respective absorption of light by intrinsic asymmetric peptide bonds and amino acid residues (216). Thus, in CD spectroscopy, changes in secondary structure are detected by far-UV CD at wavelengths from 180 to 240 nm and changes in tertiary structure are detected by near-UV CD at wavelengths from 260 to 320 nm (216). It was reported that a local unfolding of VP proteins occurred rather than the whole capsid degradation (217). And for the pH induced denaturation, reversibility was shown by adjusting pH again back to pH 7.4 (186).

I.3.4.1.2 Genome ejection

Depending on the formulation process and over storage, genome ejection can take place due to the fluidity of the capsid proteins at elevated temperatures (186). The loss of encapsulated DNA is relevant because it results in less transduction efficiency. A reduced transduction efficiency was shown in literature for example for lyophilization and storage (218) and is also discussed in Chapter VI.

Bee et al. developed an easy to perform method to determine the amount of free vector DNA in an AAV formulation (219). Before this, it was not possible to distinguish between encapsulated vector DNA and free vector DNA with the established qPCR methods. The

new method uses SYBR Gold to intercalate the free DNA, like it is done with the vector DNA in I.3.2.2.6. The measured fluorescence is then compared to the fluorescence count at 100% free vector DNA, generated by capsid rupture achieved by adding 0.1% poloxamer 188 and heating to 85°C for 20 minutes (218, 219).

Besides elevated temperatures, pH can force genome ejection, too, because Venkatakrishnan et al. found some structural changes of the α helices of VP1 in the capsid when lowering the pH from 7.5 to 4.0 (186). These changes may also result in the loss of the genome inside the capsid. Nevertheless, it was also shown, that setting pH back to 7.5, the structural changes are reversed. So, the partial unfolding of VP1 is reversible, nevertheless ejected genomes might not be encapsulated again and, in addition to the loss of encapsulated genomes, the unfolded regions are often prone to hydrophobic aggregation and if aggregation is irreversible, refolding is not possible anymore. In line with these finding, in a freeze-thaw study Croyle et al. showed that stability of AAV vectors can be improved by increasing pH from 4 up to 7.5 (210). However, an opposite pH trend was reported for the solubility of AAV2: the solubility increases from pH 10 to 4.5 (212). This implies that the pH stability is serotype specific. The pH range associated with the best stability should be usually established during (pre)-formulation development.

I.3.4.2 Colloidal stability

Colloidal stability is related to the weak net interactions between protein molecules in solution (220). Such net protein-protein interactions can be either attractive or repulsive and result from the sum of long-distance electrostatic interactions, short-distance attractive interactions, and interactions between hard spheres (209). In particular the weak protein-protein interactions are important for formulation development, because they impact aggregation, solubility, viscosity, phase separation, and crystallization behavior (209, 221, 222). For AAV, the factors solubility and viscosity are currently not yet an important issue, since the manufacturing possibilities are still limited and therefore only very few investigations of samples with high AAV titers were made. In contrast, aggregation plays a very important role in formulation development. Therefore, some methods for investigating aggregation are discussed here.

I.3.4.2.1 Aggregation

Another pathway to physical instability of AAV vectors is aggregation. As for all biopharmaceuticals, this is a key risk factor that limits the stability of AAV. Aggregates are a major concern with biologics because they can cause immunogenic reactions (6, 7, 208). It is known that immune responses can limit transgene expression after administration of AAV vectors (223, 224). Aggregation is caused by excessive attractive interactions like self-association or oligomerization of native proteins, (partially) unfolded intermediates, or largely unstructured proteins, which can be forced by extreme pH and suboptimal salt concentration in a liquid formulation (6, 225, 226). Furthermore, concentrated AAV stocks are prone to aggregate because there is an intrinsic tendency of AAV to aggregate, which can result in titer loss and inconsistencies in determining AAV concentration, for example when using ddPCR, particular for AAV2 (210-212, 227). Lastly, PEGylated AAV can aggregate by cross-linking the polymer with multiple viral capsids (228).

The efficient removal of residual vector surface host cell DNA by treatment with nucleases was reported to be an effective strategy to reduce aggregation (229). There are some appropriate analytical methods which are required to quantify soluble protein aggregates and subvisible particles. A combination of methods, such as, SEC, AF4-MALS, DLS, negative stain EM, or AUC can be used for accurate evaluation of aggregation of AAV capsids. Both, AUC and (cryo)-TEM, have already been discussed in I.3.3.3.1 and are therefore not included in the following sections.

For an injection, the European Pharmacopeia sets no limit for osmolality, but it is recommended to stay in the isohydric range of 280 – 320 mOsmol/kg (230). The impact of ionic strength on AAV aggregation was studied by Wright et al. (6). They found no correlation between osmolarity and AAV aggregation, whereas the relationship between low ionic strength and rising particle size is obvious. The inhibition of AAV aggregation by ionic excipients depends on their type and concentration. For example, a concentration of multi-charged excipients is effective at 180 – 220 mOsmol/kg to prevent aggregation of AAV, whereas 300 – 320 mOsmol/kg of NaCl is necessary for the same result.

I.3.4.2.2 Size exclusion chromatography – SEC

SEC is the gold standard for the analysis of soluble aggregates in formulations of biopharmaceuticals, but for AAV formulations SEC is of limited use due to the big size of AAV compared to proteins and antibodies. Recently some columns have been developed to measure AAV fragments, monomers, dimers and small soluble aggregates: for example

Superose 6 (Cytiva, Marlborough, MA, USA) (64), WTC-050S5 column (Wyatt Technology, Santa Barbara, CA, USA) (Chapter VI), Acquity UPLC protein BEH SEC, 450A, 2.5 µm (Waters Corporation, Eschborn, Germany) (45), TSKgel GSW4000swxl column (Tosoh Bioscience, Greisheim, Germany) (93). For detection, UV absorbance or FI can be used, each with its own advantages and disadvantages (93). While UV detection at 260 nm and 280 nm provides additional information about the full-empty ratio in the sample, the LOD is tenfold higher, compared with FI. Apart from aggregation SEC also allows for the detection of protein and DNA impurities (cf. I.3.3.2). On the downside, SEC will filter out bigger aggregates and particles. Not only can this result in an underestimated number of aggregates, but it also risks destroying the integrity of the column.

I.3.4.2.3 Asymmetrical flow field flow fractionation – AF4

To get a better overview of aggregates of different sizes in the AAV formulation, AF4 can be used. Especially the analysis of very large aggregates is possible by AF4 because no centrifugation or filtration is required before measurement. Separation in the channel is achieved through different diffusion coefficients of the particles in the sample, in contrast to the filtration principle in SEC. Frequently, AF4 is used in combination with a MALS detector. By this, it is possible to determine the total number of single, as well as aggregated AAV particles (see I.3.2.1.6). Deng et al. showed that only $1.08*10^{7}$ aggregated particles were eluted by SEC whereas AF4 detected $1.89*10^{14}$ particles (88). This means that a majority of aggregated particles were removed in the stationary phase of the SEC. This experiment underscores the value of AF4 for a correct analysis of AAV aggregates. However, there are some disadvantages of AF4 compared to SEC. In AF4, the sample is diluted to a greater extend, which results in a lower signal to noise ratio for the detection and especially the RI detector. To overcome this, a larger sample volume can be injected, or a two UV wavelength detector can be used instead of a RI detector. Because of robustness and simplicity SEC remains the first choice for monomer analysis of AAV, yet for aggregate analysis, AF4-MALS is nearly indispensable.

I.3.4.2.4 Dynamic light scattering - DLS

Light scattering-based techniques, such as DLS, are orthogonal analytical methods to directly assess the colloidal stability of proteins in solution in the respective formulations. The hydrodynamic radius of particles is measured based on the intensity fluctuation rate of laser light scattered by the particles or macromolecules over time due to Brownian motion, applying the Stokes-Einstein-Equation. The smaller the particles are, the faster will the

amount of scattered light change because smaller molecules have a higher diffusion speed than larger particles. The high sensitivity towards larger particles is useful to detect even trace amounts of aggregates.

Operated in batch mode, DLS is a non-destructive method with high throughput and often combined with SLS (44). No prior sample preparation is needed and the measurement take less than 5 minutes (43, 81). In highly purified samples, full capsids have a diameter around 26-27 nm, whereas empty capsids range around 32-33 nm (64). But the particle size distribution obtained from DLS is only semiquantitative and a particle number can only be achieved in combination with SLS (231-233). If a high polydispersity occurs, this can be due to inadequate salt amount or high viscosity of AAV formulations (6, 234). Limitations occurring from DLS/SLS are discussed in I.3.2.1.5 in more detail.

I.3.4.2.5 Submicron and subvisible particles detection methods

Besides aggregates with a defined number of monomeric units, like dimers and trimers, there are also bigger aggregates named oligomers, which contain a few monomeric units and these are generally submicron aggregates, depending on the size of the monomer (235). The size of submicron aggregates ranges from 100 nm up to 1 µm. Oligomers of these sizes can be detected by TEM, DLS/SLS, and AF4, which can also be used to detect the AAV monomers. But there are also methods that can only detect the oligomers, like nanoparticle tracking analysis (NTA), tunable resistive pulse sensing (TRPS), laser diffraction (LD), and resonant mass measurement (RMM). In particular NTA was already mentioned in I.3.2.1.7 for being able to detect the AAV monomers after labeling with gold nanoparticles. However, the common measurement range is from 30 nm up to 1 µm and is therefore perfect to detect AAV oligomers without labeling. For the measurement with NTA a sample volume > 200 µL containing 10^7 – 10^9 cp is injected into a sample chamber and illuminated by a laser beam. Thereby, the scattered light from the particles is detected with a dark field microscope and the Brownian motion is used to track hydrodynamic radius of the particles (236-239).

Recently, it was shown for TRPS that it is possible to detect particles and aggregates ranging from 40 nm up to 20 µm in exosome formulations (240), as well as the monomers of lentiviruses (236) and the vesicular stomatitis virus (241). To measure the particle size with TRPS 10^5-10^{11} viruses must be suspended in electrolytes and 40 µL sample volume is pipetted onto a flow cell and the particles are passed through the nanopore. In doing so, the magnitude of the signal is used to detect the particle size and the signal frequency is used

to calculate the concentration. All in all, one measurement takes around 10 minutes and automation is not possible so far. For impure samples the nanopore might be blocked by the impurities (237, 242, 243).

In addition to the submicron particles, the subvisible particles are also a well-known issue for biologicals (213, 240, 244). Particle of this group ranges from 1 µm up to 100 µm and can be detected by scanning electron microscopy (SEM), imaging flow cytometry (IFC), light microscopy, flow imaging microscopy (FIM), light obscuration (LO), or backgrounded membrane imaging (BMI) (235).

Recently, Halo Labs demonstrated that heat denatured AAV can be detected using their Aura device (245). The technique underlying Aura (Halo Labs, Burlingame, CA, USA) is BMI. Here, depending on the concentration of particles in the sample, up to 100 µL is added to a membrane filter well from which the background has previously been taken. After filtration, a picture of the membrane is taken and the background is subtracted from it. Thus, particles between 2 µm and 5 mm can be visualized and information about particle shape and morphology can be obtained. Besides BMI, also FIM can be used to detect subvisible particles. One instrument using this technique is FlowCam (FlowCam® 8100, Fluid Imaging Technologies, Inc., Scarborough, ME, USA). For one measurement 160 µL sample are needed and can detect aggregates in the range of 1 µm to 100 µm. For the moment there is very few literature about oligomers of AAV measured with one of the mentioned methods because the amount of needed sample for all these methods is rather large in the context of AAV formulation.

I.3.4.3 Interfacial stability

The interfacial stability of a protein and viral vector capsid proteins depends on the stress that occurs at the air-liquid, solid-liquid, or liquid-liquid interfaces. Such interfaces can be found, for example, between AAV capsid and primary packaging material, the air in the headspace of the container, or at the surface of silicone oil droplets. By shaking, stirring, or dropping, this surface area can be further increased. Many therapeutic proteins have been shown to be surface active and tend to accumulate at the interfaces mentioned above. This phenomenon has also been observed for AAV: They have a strong tendency to interact with the primary packaging agent or injection device, so that a significant loss of AAV after injection can be observed. In one study, up to 75% of vector loss occurred and a significant reduction in dose was reported due to surface adsorption of AAV vector when the product

was administered using an 1 mL syringe (246). In another preclinical study, AAV5 exhibited significant adsorption to glass and plastic surfaces (247). During adsorption, protein molecules may change their physical state and conformation (248, 249). There are several mechanisms of surface adsorption. The most important factors are intramolecular forces, hydrophobicity, and ionic and electrostatic interactions (250, 251). Misfolded proteins can reveal hydrophobic residues that facilitate protein aggregation through hydrophobic interactions (250, 252). These interactions then lead to the formation of small aggregates, which in turn may nucleate further AAV aggregation, ultimately generating visible particles in solution.

In most cases of therapeutic proteins, interfacial instability can be mitigated by the addition of an appropriate amount of nonionic surfactant, such as polysorbates. Therefore, these are nowadays included in most protein drugs on the market (248, 253). Comparable results have also been shown for AAV. The surfactant most frequently investigated in this context is poloxamer 188 (218, 254).

The interfacial stability of a protein is usually evaluated after application of mechanical stress, like shaking, stirring, vibration, freezing or dropping (220, 255, 256). For proteins, numerous studies are available in this area. For AAV, on the other hand, only a few studies are currently available (245, 254). Those studies currently focus primarily on adsorption to the packaging material or on freeze-thaw experiments, since AAV are currently stored below -60°C by default and are thus inevitably subjected to at least one FT cycle. In such studies, different formulations with and without surfactants and surfactant concentrations are usually tested.

For subsequent analysis, a variety of methods are available for proteins, such as: UV spectroscopy and chromatography to quantify the loss of soluble protein that occurs when protein adsorbs and remains at interfaces or when insoluble protein aggregates form. SEC, AF4, and light scattering are used to study the formation of small soluble aggregates. The presence of larger insoluble aggregates is investigated using techniques such as light obscuration, flow imaging microscopy, or others (257). In the field of AAV, these techniques are currently not widely used; instead, the vg titer is mainly determined using qPCR or ddPCR. Alternatively, the activity of AAV is directly determined using transduction or infection assays. However, due to the higher throughput and the possibility of automation, the methods already established for proteins will be used more and more in

the field of AAV analysis in the future. In Chapter III, capsid loss by filtration was investigated and loss of monomer recovery was determined by SEC. It was shown that with the aid of poloxamer 188 adsorption to both the syringe and the filter membrane can be reduced significantly. In addition, it was also shown that the choice of filter material has an influence on the amount of AAV adsorbed.

I.3.4.4 Chemical stability

The chemical stability of protein drugs is limited by chemical changes of the composing amino acids such as oxidation, deamidation, hydrolysis, disulfide exchange, and isomerization (258). The chemical degradation pathways have been well described in literature and the resulting chemical changes can also impact the physical properties of proteins such as electrostatics, hydrophobicity, secondary and/or tertiary structure, and the thermodynamic and kinetic unfolding/folding barriers (250, 251, 259). AAV capsid proteins can oxidate due to downstream process, storage, or by exogenous stresses. The oxidation as well as deamidation of AAV8 was reported in an LS-MS study (260) and acetylation was detected for AAV2 using CE/MS (261). Chemical changes of AAV capsid proteins could impact vector safety and efficacy.

One commonly occurring chemical alteration is oxidation which has been shown to impact safety and transduction efficiency (4). Mainly the amino acids Met, Tyr, Trp, His, and Cys are exposed to oxidation. Studies have shown that the main cause of damage of viral particles during long-term storage for 24 months at 5°C is free-radical oxidation (262-265). Damage to the viral capsid protein can result in the inability of viruses to recognize cellular receptors, thereby preventing cell transduction (266). By adding combinations of metal chelators and hydroxyl radical scavengers such as EDTA and histidine, it is possible to limit oxidation (6, 265).

One common analytical method to detect chemical changes of methionine residues in proteins is reverse phase (RP) chromatography that utilizes the differences in hydrophobicity to separate the degraded and non-degraded proteins (267). The coupling of RP chromatography with MS is a well-established analytical technique to detect chemical changes in proteins and identify specific amino acids that are susceptible to oxidation or deamidation (268). By performing an RP chromatography, the proteins normally undergo denaturation due to the combination of acidic pH values, high levels of organic solvents, and elevated temperatures. In contrast, hydrophobic interaction chromatography (HIC) is

able to separate proteins based on their hydrophobicity under non-denaturing conditions at neutral pH values and ambient temperature (269, 270). Therefore, the AAV capsid can be chromatographed in HIC as a whole, which is not possible in the RP due to the experimental conditions. To do so, hydrophobic interactions of the proteins with the column are triggered by high salt concentrations in the elution buffer and the applied gradient reduces the salt concentration until the proteins elute from the column.

Deamidation is another common chemical change within the capsid. It occurs when the amide group of an asparagine or glutamine side chain is cleaved off as the result of a nucleophilic attack. This leads to a succinimidyl intermediate (271) that, via hydrolysis, results in a mixture of aspartic acid and iso aspartic acid (or glutamic acid and isoglutamic acid) (272). Deamidation kinetics depend on the local flexibility of the peptide chain, overall protein structure, solvent accessibility, buffer identity, pH, and temperature (208, 273, 274). Deamidation of selected amino acids alters the stability, immune response, and in the case of AAV vectors also the transduction efficiency (250). It was recently reported that the deamidation of asparagine residues of AAV1, AAV3B, AAV4, AAV5, AAV7, AAV8, AAV9, and Rh32.33 serotypes results in a loss of activity (10).

Especially for deamidation, IEX is a valuable chromatographic method for the analysis of chemical degradation in protein formulations. Separation is achieved through differences in the respective charge-distribution on the VP surface and subsequent differences to the charged stationary phase (275, 276). As already discussed in I.3.3.3.5, isoelectric focusing is also a useful method to separate proteins based on differences in their charge (261).

Incorrect disulfide bond formation or exchange is a third common chemical degradation pathway for biotherapeutics. Disulfide formation is pH dependent, usually resulting from an increased pH value of the formulation (250). Free cysteine residues in proteins can be oxidized to form disulfide bond linkages or cause disulfide exchanges, causing protein aggregation or polymerization (277, 278). The AAV capsid protein contains five highly conserved cysteines that remain mostly buried within the capsid (279). So far, the impact of disulfide bonds on the function of the VP remains unclear (280).

Lastly, isomerization is a pH dependent formation that results either from Asn deamidation or Asp dehydration and leads to a succinimide intermediate (281). As described for the other deamidation processes, this succinimide intermediate results in a mixture of Asp and iso-Asp. For AAV5 isomerization has been reported under various stress conditions (263).

It is unclear whether chemical changes to the DNA also occur during storage, but it is reasonable to conclude that the DNA is largely protected from external influences by the AAV capsid. Free DNA, on the other hand, is certainly subject to chemical changes, but this is of little importance in the context of AAV DP formulation, since only DNA that is present in the AAV capsid can show its effect in the activity assay and thus also in the patient.

I.3.5 Safety

Next to the already discussed CQA of active pharmaceutical ingredients like identity, potency, purity, and stability the last CQA is the safety of the product. The applicable criteria result from the administration route of the product. Like most other biologicals, AAV must be injected to the body or the specific compartment of the body in order to take full effect.

Firstly, the formulation should be clear and colorless and should not contain any visible particles after USP 787. Additional safety testing for parenteral products includes sterility tests, as well as testing for the absence of microbial contaminations, mycoplasma, endotoxin, or adventitious viral agents. The absence of mycoplasma and adventitious viral agents must already be shown for the crude cell harvest, because this is the point where these contaminants would occur (282). The sterility and endotoxins testing must only be performed on the drug product. The allowed endotoxin amount depends on the route of administration of the product.

A special safety issue, only applicable to AAV DP, is the occurrence of rcAAV. Testing for rcAAV can be done with an infectious center assay and the required threshold is 1 rcAAV in 10^8 vg (283). But as already discussed in I.3.2.3.2 infection of cultured cells like HEK293T or HeLa often shows very low efficiency (282). Because this assay is very inaccurate and laborious, other more reliable analytical methods must be found to reliably detect rcAAV. For example, qPCR using appropriate primers and probes could be used (283).

I.4 Aim of the thesis

The aim of this thesis was to find new characterization methods for AAV serotypes, to enhance AAV vector stability, and to create a fast, easy, and serotype-independent purification process, with the final goal of improved storage stability of AAV vector formulations using lyophilization. Accordingly, the following chapters of the thesis build upon each other and reflect not only the research process but can also function as a guidance for better AAV DP development.

In Chapter II, a simple and rapid method for serotype identification based on intrinsic fluorescence is described. The only other method of serotype identification established for now is a dot or Western blot with specific antibodies for the corresponding serotype. In addition to the immense time required for these assays, the detection of multiple capsids by one antibody is considered problematic. To simplify this, it has already been shown with the help of SYPRO Orange dye that different AAV serotypes have different unfolding temperatures. The downside of SYPRO Orange is the relatively large sample size and concentration that is required. On top of this, measurements of samples containing surfactants are nearly impossible. Measuring the unfolding of the capsids using iDSF should reduce the sample amount and concentration, while at the same time allowing for measurement of samples containing surfactants. This is important because it has been shown several times that surfactants significantly reduce the adsorption of AAV to packaging materials and therefore should be included in formulations to achieve best possible stability.

The next crucial CQA to consider for AAV DP is the cp titer. Cp titer does not only provide a clear indication of the number of viral capsids, but in conjunction with the vg titer provides information on the ratio of full to empty capsids. The current standard method for the determination of the cp titer is an ELISA, which is, however, very labor and time intensive. Therefore, Chapter III compares different methods for the determination of the capsid titer with the goal of faster, yet still reliable, determination of the cp titer. The detection methods evaluated range from fluorescence and UV detectors, to light scattering analysis using MALS, DLS and/or SLS, UV spectrometry, as well as the well-established SDS-PAGE. Special attention is given to the additional information that can be obtained by the respective methods. In addition, the chapter deals with the positive effect of poloxamer 188 on adsorption to the primary packing that has already been demonstrated several times. However, adsorption does not only occur at the primary packing, but also

during the fill and finish process. Here adsorption to hoses and filters can occur. Therefore, the influence of poloxamer 188 and different membrane materials on AAV loss during sterile filtration is investigated in Chapter III, as well.

One of the main challenges for AAV DP production is purification. Classical purification of AAV is performed by ultracentrifugation in different layers of iodixanol or cesium chloride. This form of purification takes a lot of time and is also difficult to scale up. With the steadily increasing interest in AAV formulation, there is a growing need for faster, accurate, and scalable purification processes that meet the production requirements. For this purpose, different liquid chromatography-based purification strategies for AAV8 are tested and compared in Chapter IV, with a particular focus on virus yield and remaining impurities. Since a major advantage of ultracentrifugation purification is the easy application to all serotypes, the developed purification strategies are also tested with different variants of AAV2, AAV2.NN and AAV2.GL, manipulated variants of AAV2. The goal is to develop a strategy that can be used as universally as possible.

In a next step, Chapter V supplements the purification experiments with further studies of the purified samples. The analytical scope is extended towards the control of the residual pTransgene backbone, as well as new approaches for full-empty determination. The chapter closes with an evaluation of the impact of different purification strategies on capsid damage and transfection efficiency.

One of the main problems for the global application of the AAV DP is that its applicability is severely limited by storage conditions. Both gene therapeutics on the market are stored below -60°C because, according to current data, only at these low temperatures the stability of AAV can be guaranteed over a longer period. Since this form of storage not only requires a lot of energy, but also poses a problem for transport over long distances, Chapter VI aims at improved storage stability above -60°C by means of various excipients and freeze-drying. This is done by comparing the respective liquid and freeze-dried AAV formulations during storage over 4 weeks at 2-8°C and 25°C.

Finally, Chapter VII provides a summary of the presented results on the characterization, purification and lyophilization of AAV vector formulations, discusses the impact of the advancements this thesis provides for AAV DP, and gives an outlook on the future work on AAV vector formulations.

Chapter II Intrinsic differential scanning fluorimetry for fast and easy identification of AAV serotypes

This chapter is published as: Rieser, R., Penaud-Budloo, M., Bouzelha, M., Rossi, A., Menzen, T., Biel, M., Büning, H., Ayuso,E. Gerhard Winter & Michalakis, S. (2020). Intrinsic differential scanning fluorimetry for fast and easy identification of adeno-associated virus serotypes. *Journal of pharmaceutical sciences*, *109*(1), 854-862.

Author contributions:

M.P. and M.B. performed the SDS-PAGE, ELISA and SO-DSF experiments. R.R. performed all experiments with iDSF and evaluated the data. R.R., T.M., S.M. and G.W. conceived the presented idea and planned the experiments. R.R and S.M wrote the paper. G.W. conceptual guidance and corrected the manuscript. H.B., E.A, M.B. and S.M provided the AAV material.

Note from the authors:

The version included in this thesis is identical with the published article apart from minor changes. The reference, figure and table numbers were changed to fit into the coherent numbering of this document.

The published article can be accessed online via:

https://doi.org/10.1016/j.xphs.2019.10.031

II.1 Abstract

Recombinant adeno-associated virus (AAV) vectors have evolved as the most promising technology for gene therapy due to their good safety profile, high transduction efficacy, and long-term gene expression in non-dividing cells. AAV-based gene therapy holds great promise for treating genetic disorders like inherited blindness, muscular atrophy, or bleeding disorders. Multiple naturally occurring and engineered AAV serotypes exist, which differ in capsid sequence and as a consequence in cellular tropism. Individual AAV capsids differ in thermal stability and have a characteristic melting temperature (T_m), which enables serotype-specific discrimination of AAV vectors. Differential scanning fluorimetry (DSF)combined with a dye-like SYPRO Orange (SO-DSF), which binds to hydrophobic regions of unfolded proteins, has been successfully applied to determine the T_m of AAV capsids. Here, we present DSF measurement of intrinsic fluorescence signal (iDSF) as a simple alternative method for determination of AAV capsid T_m. The study demonstrates

that DSF measurement of intrinsic fluorescence signal is a simple, accurate, and rapid alternative to SO-DSF, which enables characterization of AAV capsid stability with excellent precision and without the need of SO or any other dye.

Keywords: adeno-associated virus AAV vector, high-throughput technology, intrinsic fluorescence, melting temperature, capsid thermal stability

Abbreviations: AAV - adeno-associated virus; Cp - capsid particle; DSF - differential scanning fluorimetry; SO-DSF - differential scanning fluorimetry with SYPRO Orange; iDSF - differential scanning fluorimetry with intrinsic fluorescence; IFS - intrinsic fluorescence signal; ITR - inverted terminal repeats; PBS - phosphate buffered solution; SEC - size exclusion chromatography; SO - SYPRO Orange; T_m - melting temperature; vg - vector genome.

II.2 Introduction

Gene therapy aims to treat a disease or improve patient conditions by genetic modification of patients cells (284). While the concept of gene therapy is not novel, major developments have been made during this past decade. An important reason for this is the availability of highly efficient and safe gene therapy vectors (285). Among the vectors used, recombinant adeno-associated virus (AAV) vectors have emerged as very promising option and have been already used in more than 190 clinical trials across different indications with very good safety characteristics (286-289). This is reflected in the recent marketing authorization of Luxturna® and Zolgensma®, AAV vector-based therapies for *RPE65*-linked retinal dystrophy and SMN1-linked spinal muscular atrophy, respectively. AAV are small, non-enveloped, non-pathogenic DNA viruses belonging to the *Dependoparvovirus* genus of *Parvoviridae*. They are dependent on the presence of helper viruses such as adeno-, papilloma- or herpes-viruses for replication and progeny production. Multiple naturally occurring AAV variants (so called serotypes) exist, which differ in their capsid amino acid sequence and, thus, show distinct anti-AAV antibody profiles. In addition, multiple engineered versions with synthetically or alternatively modified capsids exist. AAV particles consist of three structural viral proteins (VP1, VP2 and VP3) and an approx. 4.7 kb single-stranded DNA genome containing two genes, Rep and Cap, between two inverted terminal repeats (ITR). Rep encodes multiple non-structural Rep proteins, which are essential for viral genome replication and packaging. Cap contains an open reading frame (ORF) that produces the VP1, VP2 and VP3 proteins from distinct start codons in a ratio

of approx. 1:1:10. In addition, a second +1-frameshifted ORF produces the non-structural assembly-activating protein (AAP), which acts as a chaperone facilitating the assembly of the three VPs into the icosahedral capsid structure (19, 290). To construct recombinant AAV vectors for gene therapy the Rep and Cap genes are replaced with an expression cassette that contains the transgene cDNA of interest with an appropriate promoter and other regulatory components such as polyadenylation signals. For rAAV vector production the Rep and Cap genes as well as a minimal set of adenoviral genes are provided in trans from different plasmids that do not have ITRs.

Different AAV serotypes not only have distinct cellular tropism and transduction profiles, but also differ in their structural properties and stability. The latter feature is also reflected in the thermal stability and results in a serotype-specific melting temperature (T_m) of the capsids. Interestingly, T_m measurement allows for distinction of most AAV capsid pairs independently of the carried genome. So far, the established method for T_m measurement is based on differential scanning fluorimetry (DSF) with AAV samples treated with a fluorescent dye like SYPRO Orange, which binds to hydrophobic regions of unfolding proteins and enables monitoring of capsid unfolding in response to a temperature ramp (3, 55). The fluorescence of SYPRO Orange is quenched by solvent molecules and increases upon binding to the hydrophobic sites that are externalized during thermally induced protein unfolding (291).

We present a simple method with excellent precision, utilizing DSF without using SYPRO Orange. The DSF approach is based on the intrinsic fluorescence of tryptophan residues within the AAV capsid protein sequence, which are highly conserved across AAV serotypes and whose spectral properties are dependent on their local environment. Changes from hydrophobic to a hydrophilic environment lead to a red shift of the emission spectrum of tryptophan upon excitation in the UV range (292). With this easy measurement, it is possible to determine the T_m of different AAV serotypes within one hour, down to a concentration of around $2*10^{11}$ cp/mL with only 10 µL of sample volume.

II.3 Materials and methods

II.3.1 AAV production and purification

Recombinant AAV vectors were produced and purified based on previous studies in adherent HEK293 (293, 294) or Sf9 cells (295) and finally buffered in 1xPBS. Empty and

full particles from some AAV vectors were purified by two rounds of CsCl gradients as described previously in Ayuso et al.2010 (74).

When indicated, AAV vectors produced in HEK293 cells were purified by tangential flow filtration (TFF) using a 300 kDa mPES membrane from Repligen (Massachusetts, USA) and buffered in 1x PBS (10 mM Na_2PO_4, 1.8 mM KH_2PO_4, 4.27 mM KCl, and 137 mM NaCl, pH 7.4).

II.3.2 AAV particle quantification

II.3.2.1.1 Serotype-specific ELISA

For the capsid titer of AAV2 and AAV8 the quantitative and serotype specific ELISAs (Progen, Germany) were performed according to the manufacturer's instructions (57, 113)

II.3.2.1.2 SDS-PAGE densitometry

A serial dilution of an AAV internal control is prepared, typically five dilutions for a range of $1*10^{10}$ to $2*10^{11}$ particles per well. Dilutions of the recombinant AAV vectors to be analyzed are prepared in duplicate. Samples are loaded on a 10% Tris-Glycine gel (Life Technologies, USA) after addition of Laemmli 4X (Biorad, USA) and denaturation at 95°C. After electrophoresis in denaturing conditions, the gel is rinsed three times under agitation with deionized water. The Coomassie Blue staining is performed with Imperial Protein Stain solution (Thermo Scientific, Germany) for 1.5 hours with gentle shaking. The stained gel is washed once for 20 minutes and additional one to three times for 40 minutes with deionized water to obtain the clearest background for photography with the Luminescent Image Analyzer LAS-1000plus (Fujifilm). Quantification of the number of particles per mL is realized using the Icy open source image processing software based on the VP3 capsid protein signal in comparison to the AAV internal control. The standard curve is validated if the coefficient of determination r^2 is ≥ 0.95.

II.3.3 Vector genome titer determination by qPCR

The vector titer was measured by real-time PCR, carried out with the Step one Plus (Thermo Fisher scientific, Germany). AAV2 free ITR qPCR was realized as described in D'Costa et al. (114).

II.3.4 Determination of the thermal stability of AAV capsids by intrinsic differential scanning fluorimetry (iDSF)

A Prometheus NT.48 (NanoTemper Technologies GmbH, Munich, Germany) was used to measure the capsid melting temperatures. The system measures the intrinsic fluorescence

intensity at 330 and 350 nm after excitation at 280 nm. A minimum of three consecutive temperature upscans of the same sample (3*10 µL) from 30°C to 100°C in a linear ramp of 1°C/min were performed. The rate of changes in fluorescence with temperature was recorded and the thermal profile resulted in counts of fluorescence against temperature. The apparent AAV melting temperatures (T_m) were determined with the PR. ThermControl software V2.1 (NanoTemper Technologies, Munich, Germany) from the maximum of the 1st derivatives of the thermal unfolding curves (296, 297).

All samples were formulated in PBS (10 mM Na_2PO_4, 1.8 mM KH_2PO_4, 4.27 mM KCl, and 137 mM NaCl, pH 7.4) A negative control with only PBS was included in every run. The AAV samples were filled in standard iDSF-grade capillaries and the capillaries were sealed.

To survey the minimal concentration of AAV capsid that would provide measurable fluorescence using the intrinsic fluorescence signal (IFS), full and empty AAVrh10 were used ($1.2*10^{14}$ cp/mL and $1.1*10^{15}$ cp/mL, respectively). After serial ten to thousand-fold dilution of the AAV stocks in the formulation buffer, 3*10 µL of each dilution were used for triplet measurements with the DSF, as described above.

For the measurement with surfactants poloxamer 188 (BASF, Ludwigshafen, Germany, Lot. GNA19221BT), polysorbate 20 (Roth, Karlsruhe, Germany, Charge: 317259797) and 80 (Alfa Aesar, Massachusetts, USA, Lot.10200710) were added at the following concentrations: 0.5%, 0.1%, 0.01%, and 0.001%. The samples stayed at room temperature (RT) for around 30 minutes.

II.3.5 Determination of the thermal stability of AAV capsids by DSF using SYPRO Orange

The DSF method using SYPRO Orange was previously described in Pacouret et al. and Rayaprolu et al. (22, 55). SYPRO Orange 5000X (Thermo Fisher Scientific) was aliquoted (5–10 µL) and stored at −30°C for up to 18 months. For each new experiment, a 500 µL sample of SYPRO Orange 50X was prepared using PBS2+ (Corning) as a solvent. 96-well plates were loaded with 45 µL samples, supplemented with 5 µL SYPRO Orange 50X. PBS2+ and 0.25 mg/mL Lyzozyme (Sigma-Aldrich) solutions were used as negative and positive controls, respectively. Plates were sealed and centrifuged at 3,000 rpm for two minutes and subsequently loaded into the real-time PCR instrument (StepOnePlus Real-Time PCR System, Thermo Fisher Scientific). Samples were incubated at 25°C for two

minutes prior to undergo a temperature gradient (25°C to 99°C, ~2°C/10 min, step and hold mode with 0.4°C temperature increments), while monitoring the fluorescence of the SYPRO Orange dye using the ROX filter cube available on both qPCR systems. Fluorescence signals F were normalized between 0% and 100%, melting temperatures were defined as the temperature for which the numerical derivative dF/dT reached its maximum (55)

II.3.6 Size exclusion chromatography (SEC)

A Dionex Summit 2 system (Thermo Fisher, Dreieich, Germany) and an Acclaim 1000, 7.8 x 300 mm, 7 µm column (Thermo Fisher scientific, Dreieich, Germany) were used for the size exclusion chromatography. AAV elution was detected at 280 nm and 260 nm with a UV detector (Dionex UVD170U) and at excitations wavelength 280 nm and emission wavelength 330 nm with a fluorescence detector (Dionex RF2000). The running buffer consisted of 100 mM sodium phosphate and 200 mM sodium perchlorate at pH 7.4 with a flow rate of 0.3 mL/min. The chromatograms were integrated with Chromeleon V6.8 (Thermo Fisher, Dreieich, Germany).

II.4 Results

The Prometheus NT 48 system measures the intrinsic fluorescence signal (IFS) in proteins generated by tryptophan residues. During controlled heating from 30°C to 100°C, AAV capsid proteins denature. Tryptophan and to a lesser extent other aromatic residues get exposed and can contribute to a higher fluorescence signal, which allow for assessment of the T_m of AAV vectors.

AAV2 is the most studied AAV capsid and recombinant AAV vectors almost exclusively carry genomes with AAV2-derived ITR. Therefore, we first used iDSF to evaluate the suitability of IFS for determination of the T_m of AAV2 vectors. As depicted in Figure II.1, T_m of AAV2 is around 68°C and can be obtained with the fluorescence of the single wavelengths at 330 nm and 350 nm and also from the ratio 350/ 330 nm.

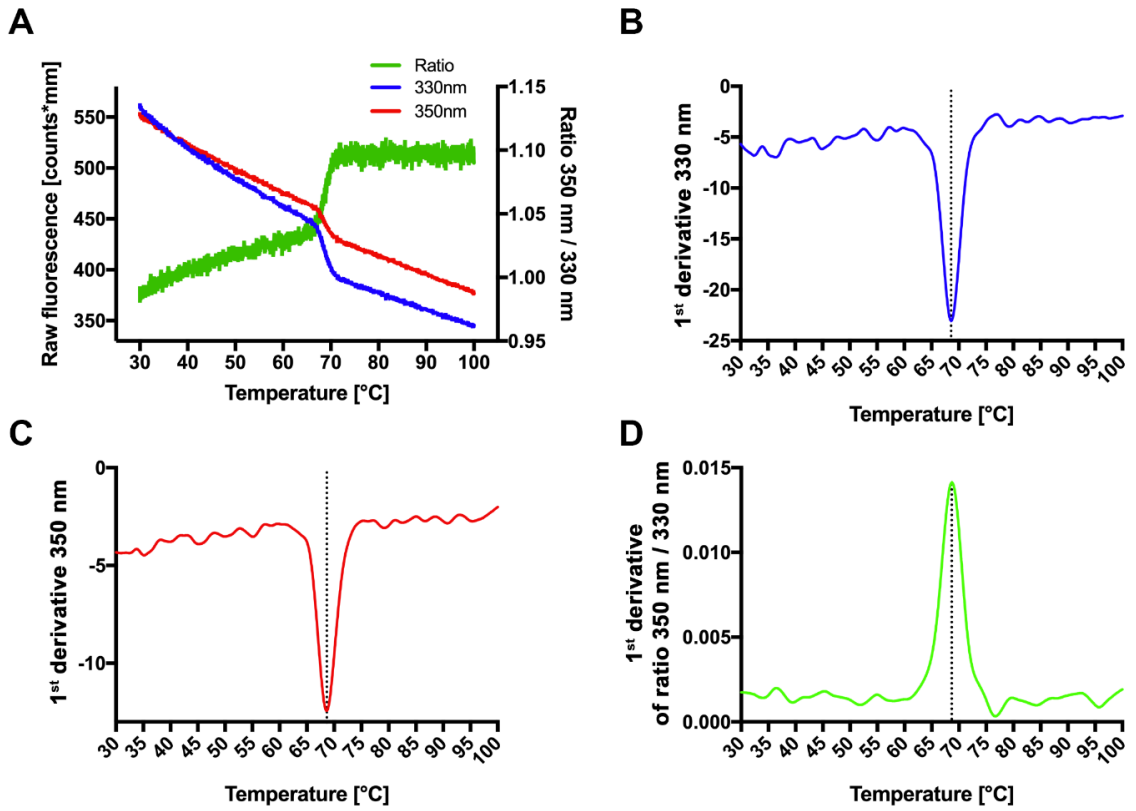

Figure II.1 DSF measurement of intrinsic fluorescence signal (iDSF) of AAV2. 10 µL of AAV2 vector at a concentration of $5*10^{11}$ vg/mL were heated at a rate of 1°C per minute from 30°C to 100°C. ISF was measured at 330 and 350 nm. (A) Graph showing the raw fluorescence (counts*mm) obtained at 330 nm (blue trace) or 350 nm (red trace). The ratio of the 350 nm / 330 nm signals is plotted in green. In all three evaluations a change of the signal was obtained at about 68°C. (B-D) First derivatives of the ISF obtained at 330 nm (B), 350 nm (C) and of the ration 350 / 330 nm. The peak is indicative of the Tm.

To test the ability of iDSF to discriminate between AAV serotypes, we next determined the T_m of various AAV capsids produced in HEK293 cells using triple-transfection. As shown in Figure II.2A, the resulting T_m varied substantially between different AAV serotypes and allowed distinction of almost all tested AAV. Only exceptions were the pairs AAV9/AAVrh10 and AAV3/AAV8, which under the tested conditions showed T_m values too similar to be distinguished (Figure II.2A).

We next tested the effect of different production processes on T_m. The production of AAV by different platforms (mammalian versus insect cells) was shown to result in a distinct glycosylation profile of the capsid (298), which might impact the melting behavior. However, as shown in Figure II.2B**,** no difference in T_m could be observed for AAV2 and AAV8 produced in HEK293 or Sf9 cell lines.

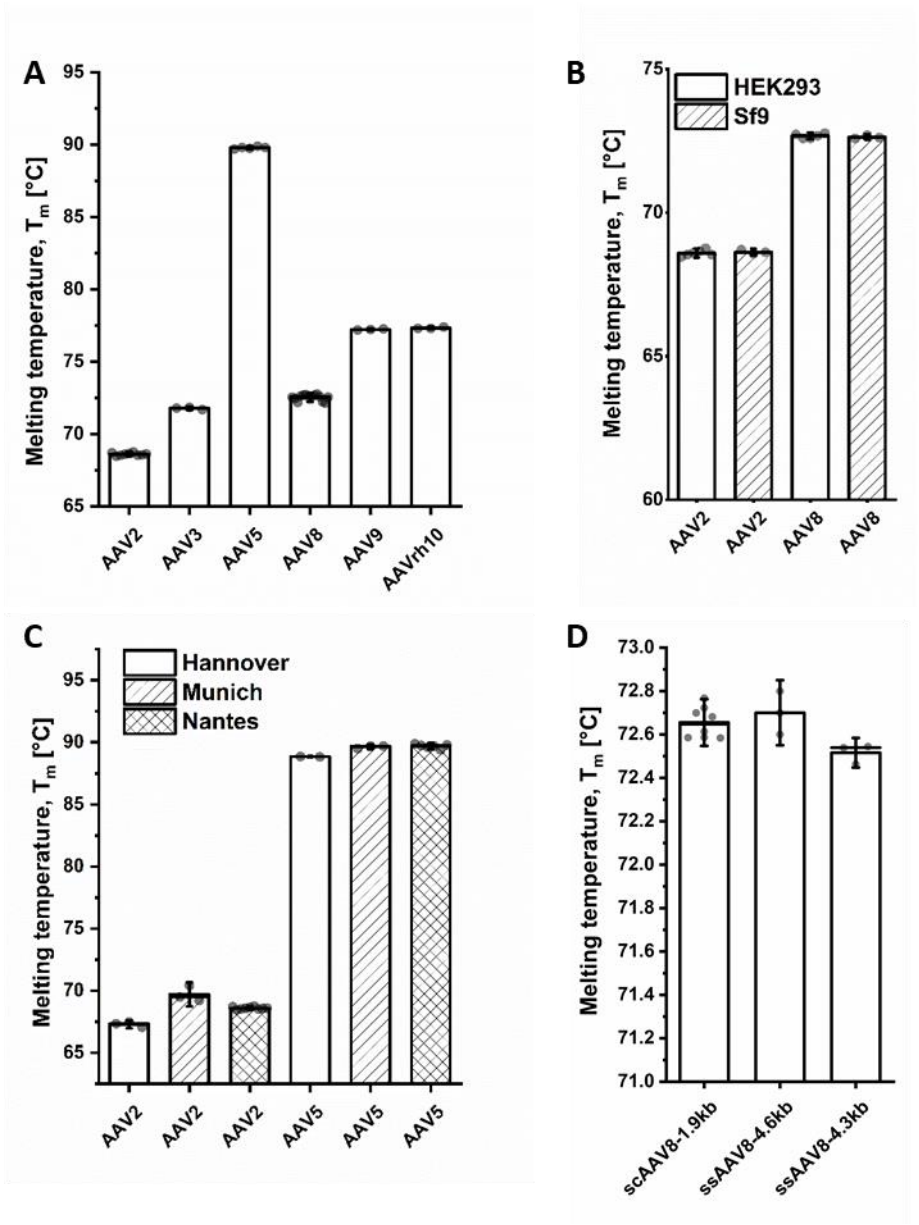

Figure II.2 T_m measurement of different AAV serotypes with iDSF. 10 µL of AAV were heated at a rate of 1°C per minute from 30°C to 100°C. ISF was measured at 330 and 350 nm. (A) shows the different melting temperatures of six different AAV serotypes at a concentration of $1*10^{12}$ cp/mL (B) shows AAV2 and AAV8 produced in two different cell lines (HEK293 and Sf9) at a concentration of $1*10^{12}$ cp/mL (C) shows T_m for AAV2 and AAV5 produced by three different laboratories (Hannover (blank), Munich (striped), Nantes (plaid)) at a concentration of AAV2: $5*10^{11}$ vg/mL and AAV5: $1*10^{12}$ vg/mL (D) AAV8 with three different genomes at a concentration of $1*10^{12}$ cp/mL.

To test for the robustness of the iDSF method, we next measured T_m in AAV2 and AAV5 preparations produced in three different laboratories. The most thermostable serotype AAV5 showed a very low standard deviation (SD) and resulted in very similar T_m independent of the producing laboratory (Figure II.2C). In contrast, for the serotype AAV2,

having the lowest T_m, SD was higher and the range of T_m values was more variable than for AAV5 (Figure II.2C). Finally, we evaluated the effect of the AAV genome on T_m by analyzing AAV8 capsids carrying genomes of different size and nature (single stranded (ss) or self-complementary (sc)). Previous DSF + SYPRO Orange (SO-DSF) studies suggested a minor effect of the genome on capsid stability (3, 55). Despite some variability, different AAV8 vectors carrying distinct genomes showed similar T_m (Figure II.2D).

Previous work showed that the SO-DSF method was able to discriminate AAV with distinct melting temperatures (AAV2 and AAV5) from each other when pre-incubated and measured as a mixture (22). To test if iDSF can be used to identify different AAV in a mixture as well, we incubated mixtures of AAV5 and AAV8 at room temperature for 30 minutes before running the iDSF temperature scan. A good baseline separation of the IFS was possible (Figure II.3). Mixing the two AAV serotypes at ratios up to 1:10 still resulted in clearly separated distinct signals at the expected T_m of each of the two capsids.

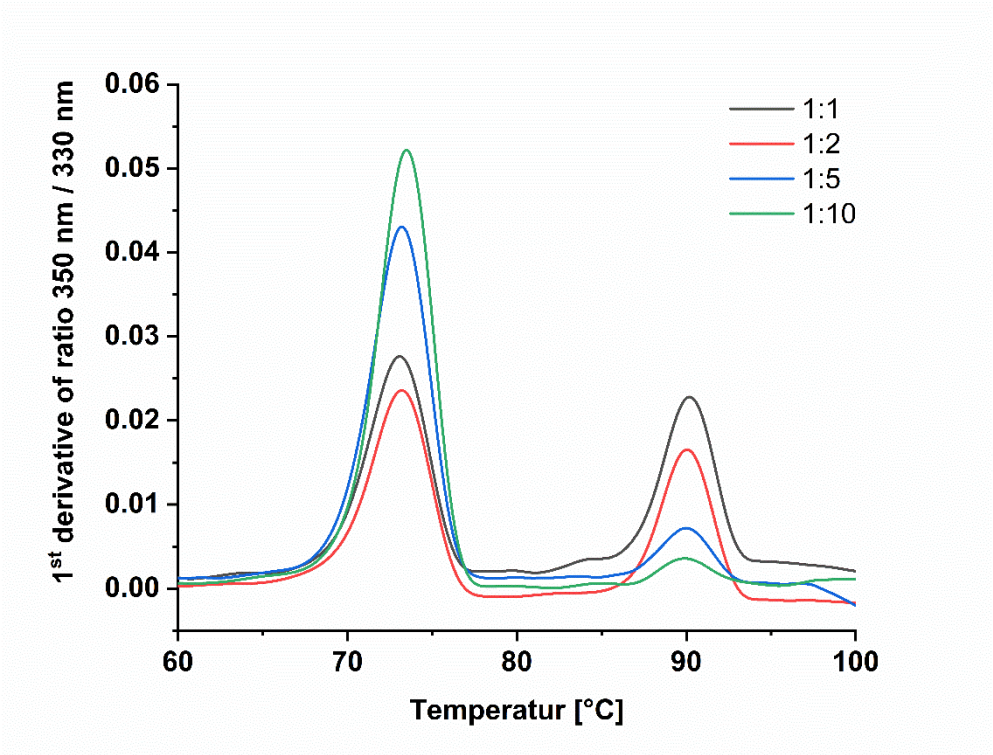

Figure II.3 iDSF measurement of AAV5 and AAV8 mixtures against the temperature. Graph shows 1st derivative of the ratio 350/330 nm of mixtures with different amounts of AAV5 (cp/mL determined by SDS-Page) and AAV8 (cp/mL determined by ELISA). Two distinct peaks at 90°C and 72°C with clearly separated baseline was observed in all ratios measured. Starting concentration was $1*10^{13}$ cp/mL of each vector.

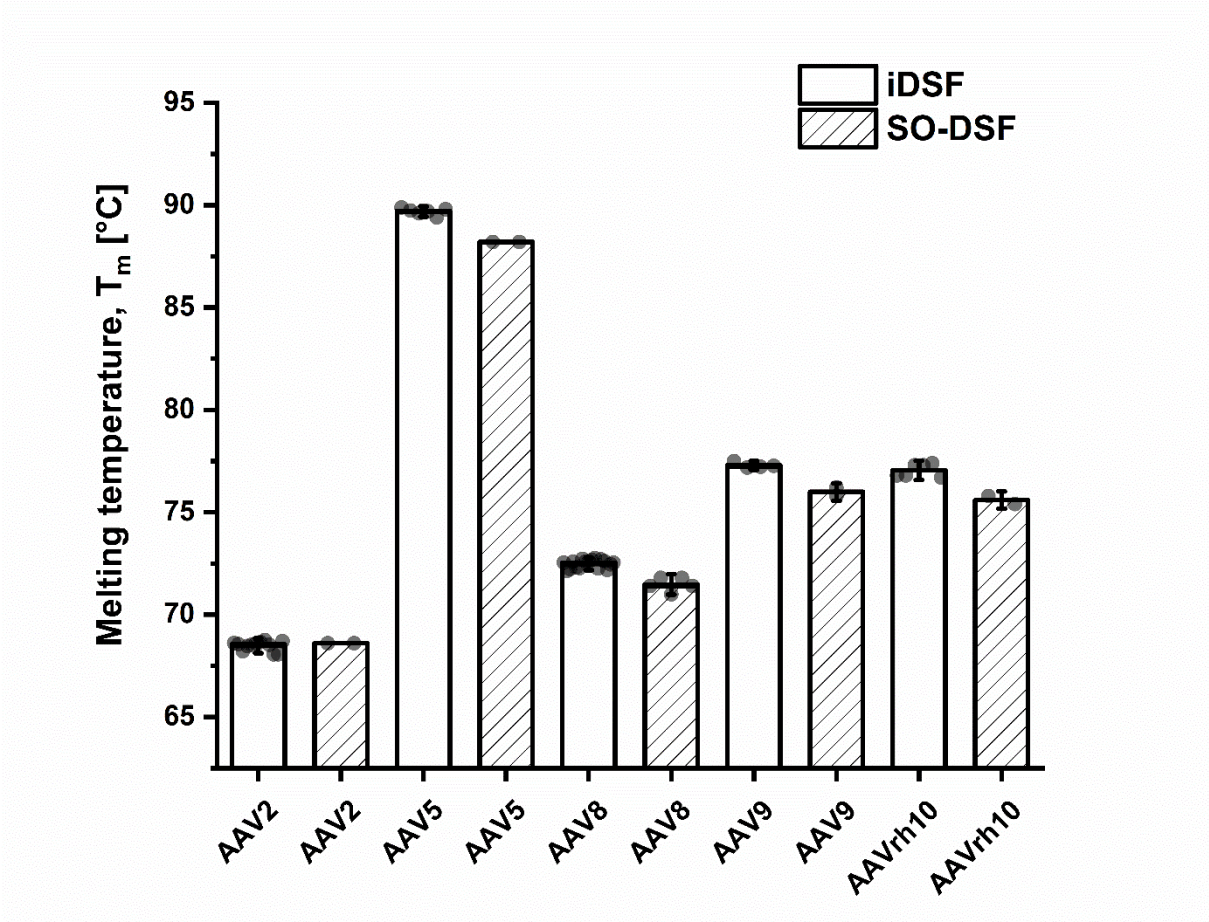

Figure II.4 Comparison of iDSF with SO-DSF for T_m measurements of AAV vectors T_m was measured for AAV2, AAV5, AAV8 – AAVrh10. The blank bars show T_m measured with iDSF at a concentration of $1*10^{12}$ cp/mL and plotted with SD of 3 technical replicates or more, the striped bars show T_m measured with SO-DSF with a heating rate of 0.4°C/min and n=2.

As mentioned above, SO-DSF was already introduced as a method for determination of T_m and for distinction between different AAV capsids (3, 22, 55). We therefore determined T_m of identical batches of different AAV serotypes with both methods, iDSF and SO-DSF. As shown in Figure II.4, both methods resulted in similar T_m values, confirming that both are equally well suited for distinction of the different serotypes. There was, however, a tendency for slightly higher T_m values with the iDSF method as compared to SO-DSF (Figure II.4).

Moreover, previous studies showed that SO-DSF measurement of T_m also informs about the concentration of the AAV sample, as there was a linear increase of the SO-DSF signal amplitude with increased particle concentration (55). The lowest detectable concentration of AAV particles by SO-DSF was shown to be 3.4 - $3.95*10^{11}$ cp/mL with a minimum test volume of 20 – 25 µL (3, 55). We, therefore, set out to determine the limit of detection of

iDSF with serial dilutions of an AAVrh10 sample. As shown in Figure II.5, measurement of T_m with iDSF is possible over a wide concentration range and quantifiable signals were obtained at a minimum titer of $2*10^{11}$ cp/mL and with a minimum volume of 10 µL. With increasing sample concentration, the IFS (fluorescence ratio amplitudes in Figure II.5A) increased, confirming that the IFS intensity – similar to SO-DSF – depends on sample concentration. AAVrh10 empty capsids showed a similar behavior and matching T_m value (Figure II.5B), suggesting that the packaged genome has little impact on the capsid's thermostability.

Intriguingly, closer inspection of the T_m values at different AAV concentrations revealed a shift of T_m towards higher values with increased AAV sample concentration (Figure II.5A-B). We therefore plotted the T_m values against AAV sample concentration and found a linear correlation between them (R^2: 0.99243) (Figure II.5C). Similar results were observed with all other tested AAV serotypes suggesting a generally lower T_m value obtained by iDSF at lower capsid concentrations.

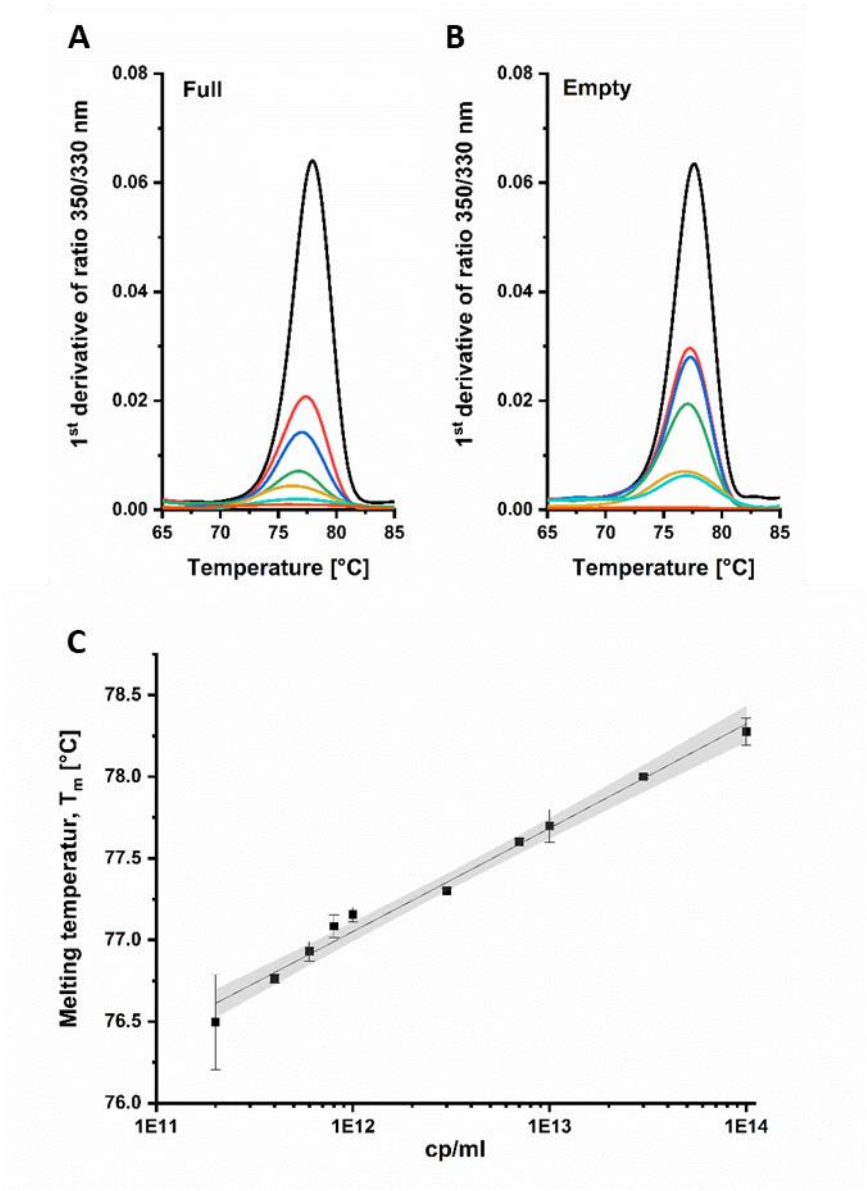

Figure II.5 iDSF measurement of T_m with a serial dilution of AAVrh10 *(*A) 1st derivative of the ratio 350/330 nm of the concentration series of AAVrh10 empty from $1*10^{13}$ – $1*10^{11}$ cp/mL (B) 1st derivative of the ratio 350/330 nm of the concentration series of AAVrh10 full (CAG-GFP) from $1*10^{13}$ – $1*10^{11}$ cp/mL. Color code for (A) and (B): black: $1*10^{13}$ cp/mL, red: $1*10^{12}$ cp/mL, blue: $8*10^{11}$ cp/mL, green: $6*10^{11}$ cp/mL, yellow: $4*10^{11}$ cp/mL, turquoise: $2*10^{11}$ cp/mL, orange:$1*10^{11}$ cp/mL (C) T_m plotted against concentration series of AAVrh10 empty from $1*10^{14}$ – $2*10^{11}$ cp/mL. Grey line: Nonlinear fit: y=13,29*ln(8,344*ln(x)), 95% Confidence Band Adj. R^2: 0,99243

The question arose, if it is possible to differentiate full and empty AAV samples by measuring T_m with iDSF.

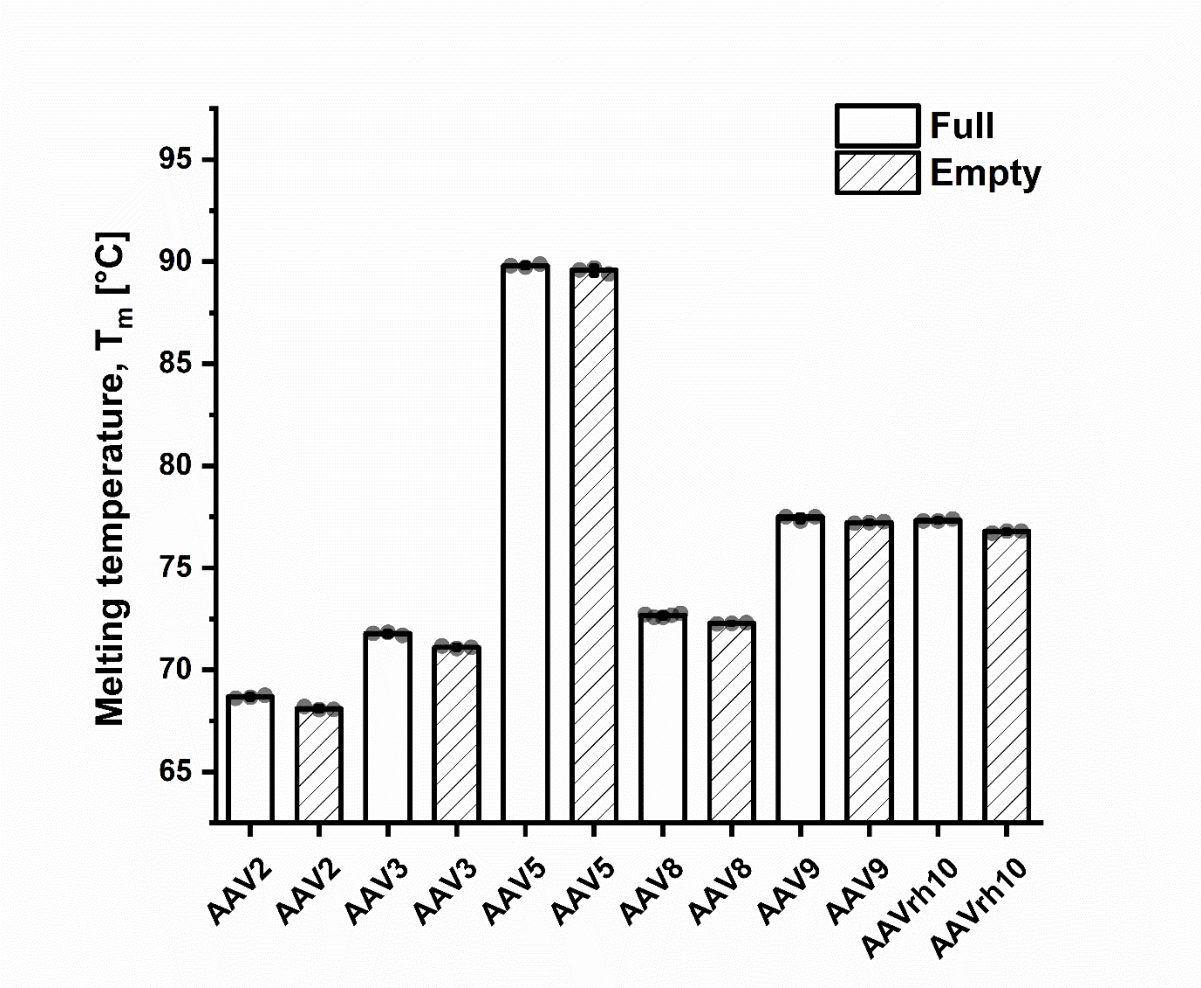

Figure II.6 Comparison of T_m of full (blank) and empty (striped) AAV measured by iDSF. Capsid titer for all samples was $1*10^{12}$cp/mL 3 technical replicates plotted with SD.

As shown in Figure II.5A-B, the fluorescence ratio plots for full and empty AAVrh10 were similar, but not identical. To follow up on this observation, we subsequently determined the T_m values of full and empty capsids of various serotypes. The main visible fluorescence measured by iDSF arises from the tryptophan residues exposed during unfolding of the capsid. In line with this, we found no gross differences between the T_m of full and empty capsids (Figure II.6). However, the T_m was consistently slightly higher for the full capsid than for the empty capsid. The T_m difference (T_m full - T_m empty) was lowest for AAV5 with only 0.2°C and highest for AAV3b with a 0.7°C (Figure II.6). While this difference in T_m between full and empty capsids is reliably quantifiable with iDSF, it is too small in

order to distinguish full from empty AAV species in mixed samples, e.g. in a non-purified or in process control samples.

iDSF relies predominately on the fluorescence of tryptophan residues within the AAV capsids and capsid structure-dependent changes in fluorescence intensity which occur during temperature-induced unfolding. Most tryptophan residues in the tested AAV capsids are conserved. In particular, AAV2 VP1 contains 15 tryptophans, which are all conserved in AAV3b, AAV8 and AAVrh10. In AAV5 and AAV9 VP1 most of those residues are conserved with only minor changes totaling 14 and 16 tryptophans, respectively. The N-terminal part of all VP1 proteins, except of AAV5 VP1, contains three tryptophans with two of them arranged as a doublet. To test for the contribution of these three tryptophans to the T_m values obtained with iDSF, we generated an AAV8 vector with VP2/3 only, lacking VP1 (delVP1). As shown in Supplemental Figure II.2, the T_m value was 0.3°C lower for AAV8delVP1 than for wildtype AAV8, suggesting that the N-terminal tryptophans contribute to a small extent to the T_m measured by iDSF.

SO-DSF is used as a high-throughput screening method for the analysis of AAV serotypes by measuring the melting temperature. Determination of T_m can be helpful to confirm the identity of the AAV capsid in final products (3, 55). As shown above, iDSF provides a facile alternative method for determining AAV T_m, which does not require pretreatment of the sample with fluorescent dyes likes SYPRO Orange. This makes iDSF an optimal candidate for in process control of AAV production, i.e. for monitoring the purification process. Since the standard heating rate of 1°C/min can be increased to 2°C/min, the analysis time could even be cut in half without compromising fidelity (Figure II.S1).

AAV used in this study were produced from HEK293 or Sf9 cells. As with many other cell-derived biotherapeutics AAV vectors, preparation scans contain a variety of impurities such as host cell proteins (HPC), proteins from any serum- or other animal-derived products in the cell culture media, nucleic acids from host cells or the transfection process (7). To test for the ability of iDSF to monitor the purification status of the AAV sample, we measured AAV with different purification status. As shown in Figure II.7, the sample highly purified by ultracentrifugation results in one sharp peak in the iDSF measurement, whereas the sample only rudimentary purified by a single tangential flow filtration (TFF) step showed an additional and clearly visible shoulder to the main peak at 65°C.

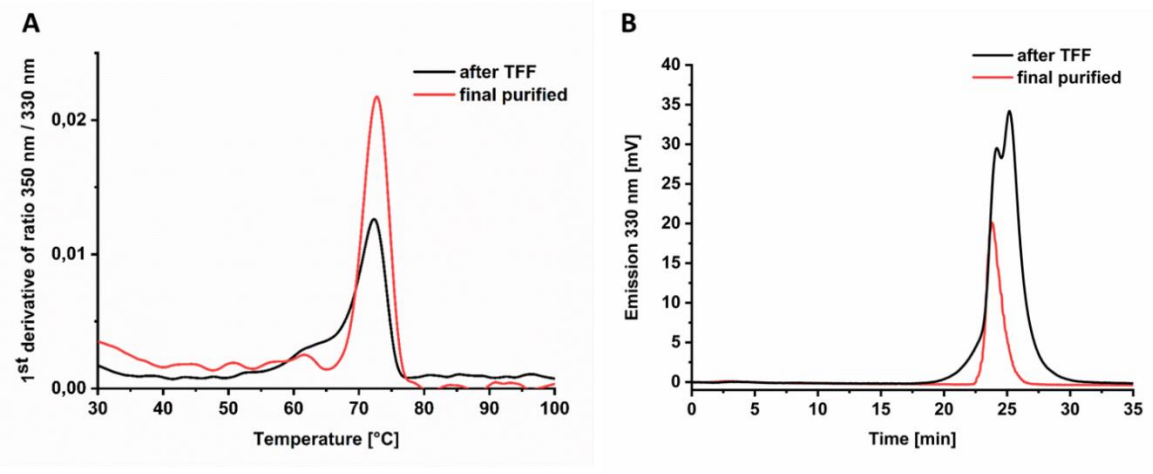

Figure II.7 AAV8 at different purification states measured with iDSF (A) and SEC (B). (A) The 1st derivative of the ratio 350/330 nm shows for the buffer exchanged product after TFF 300 kDa PES membrane (black line) one peak at 71°C and a shoulder. The red line shows the thermal unfolding of the final purified product via Iodixanol gradient and there no additional shoulder is detected. (B) The SEC- Chromatogramm shows two peaks for the buffer exchanged sample i.e. single TFF purification (black line). The fist peak contains the AAV and the second one some minor impurities. The final purified sample (red line) shows a single peak.

Nevertheless, the purity of the sample had no impact on the T_m of the serotype (Figure II.7A). The purification of the samples can also be evaluated by size exclusion chromatography (SEC) (Figure II.7B). In the SEC chromatogram two peaks were detected at an emission of 330 nm for the only TFF-purified sample likewise. In contrast, the iodixanol gradient purified sample showed only one peak containing the AAV at 24 minutes. The second peak at 26 min most probably represents process related impurities.

Typically, surfactants are utilized in AAV formulations to reduce the adsorption of AAV to the primary packaging or application devises such as syringes (299). However, the commonly applied polarity-sensitive dye SYPRO Orange shows bright fluorescence in the presence of micelles, which could conceal the signal of protein unfolding (215). We therefore tested the impact of commonly used surfactants on AAV T_m measurement with iDSF.

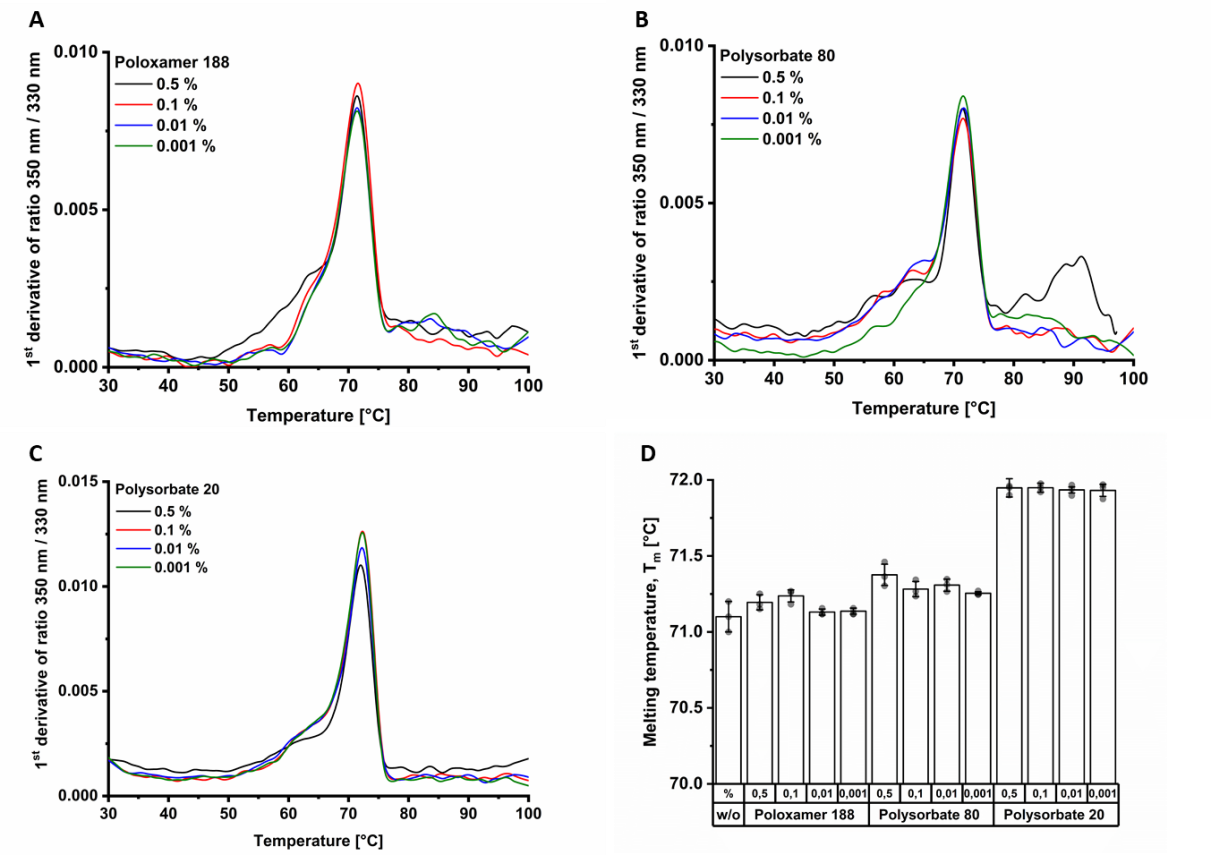

Figure II.8 T_m of AAV8 without (w/o) and with poloxamer 188 (A), polysorbate 80 (B) and 20 (C) in the formulation as measured by iDSF. (A-C) 1st derivative of the ratio 350/330 nm is plotted against the temperature [°C] and showed for all formulations a clearly defined melting peak for AAV8. All samples in the graph were only purified by TFF 300 kDa PES membrane. (D) The melting temperature is plotted against the amount of detergents using 3 technical replicates plotted with SD.

As shown in Figure II.8, the addition of a surfactant, i.e. poloxamer 188, polysorbate 20 or 80, did not impact the determination of T_m with iDSF as a clear peak for unfolding of the capsid was observed.

In the presence of polysorbate surfactants T_m was slightly shifting towards higher temperatures (Figure II.8D). Thermal shifts of T_m indicate stabilizing or destabilizing effects of excipients (300). The shift observed here, depending on the amount of surfactant, indicates a stabilizing effect. Furthermore, the T_m measurements indicate a difference between the surfactants. poloxamer 188 is normally used in formulations of AAV to reduce adsorption on the packaging material, but poloxamer 188 showed no significant shift in T_m when added to the formulation. In contrast to this, polysorbate 20 and polysorbate 80 showed a clear shift of T_m. For polysorbate 80, the shift in T_m seemed to be concentration dependent, because a slightly higher T_m is observed for 0.5% of polysorbate 80 than for

lower concentrations of polysorbate 80. The addition of polysorbate 20 resulting in the biggest shift of $T_{m,}$ independent of the concentration.

II.5 Discussion

In this study, a novel iDSF protocol was developed to determine T_m of AAV capsids as a method for serotype identification. The measurement of the IFS with iDSF is a simple, rapid (30-60 minutes), and high-throughput (48 samples/ 30-60 min) method for determination of AAV T_m with low costs and low material input (10 µL, $2*10^{11}$ cp/mL). Such low amount of material is easily attainable from the final product and from in process controls samples. Since iDSF measurements allow for the detection of process related impurities as well (see Figure II.6), the new method is a very attractive high throughput screening method for monitoring sample purity during the purification process and for analyzing batch-to-batch consistency.

Overall, iDSF measurements result in very reliable and accurate determination of T_m. As shown in this study, neither the production process, nor the source of the AAV samples had a strong impact on T_m. The comparison of AAV2 and AAV5 form the three different laboratories showed only minor differences for AAV5 and only a slightly higher variability for AAV2, which degrades at lower temperatures. However, AAV2 samples were matched according to the vector genome (vg) titer whereas for AAV5 capsid titers were available. The findings that vg titers can substantially vary between laboratories (114) and that the amount of cp/mL influences T_m (see Figure II.5), might explain the higher variability observed for AAV2. As for most techniques: the lower the value the higher the SD.

In comparison to SO-DSF, this new assay showed a slightly higher T_m for all serotypes. The reason for this slight difference is not known yet but could be related to different heating rates in the two experiments (1°C/min for iDSF and 0.4°C/min for SO-DSF). In support of this, we found that T_m measured by iDSF depends on the heating ramp: the higher heating rate the higher T_m (Figure II.S1). However, this phenomenon does not impact the ability of the method to distinguish between the different AAV serotypes. A clear determination of the serotype is still possible at higher heating rates. These differences could be controlled by fixing the heating ramp parameters and harmonizing the protocols.

Another factor, which influences the T_m measurement with iDSF and might explain the differences between the iDSF and SO-DSF T_m measurements, is the dependency of iDSF on the amount of the AAV capsid used. Whereas T_m in SO-DSF is independent of the AAV

concentration of the sample (22, 55) this is not the case for iDSF (as shown in Figure II.5). The structural stability (T_m) of AAV capsids increased with the capsid concentration. This result correlates well to the results of a stability study from Howard and Harvey (301). The authors found that the undiluted sample (2.1-5.9*10^{12} vg/mL) showed a higher transduction efficacy than 1:5 and 1:10 diluted sample after storage at 4°C over 7 weeks. Wright (6) also speaks about dilution stress by studying the impact of ionic strength on AAV aggregation. The stressing by dilution would fit good to our observations.

Given the dependency of iDSF on the concentration, valid comparison of T_m data from different AAV capsids require dilution of the test samples to a similar AAV capsid concentration. While this could complicate comparison of different AAV capsid samples if concentration vary substantially, it is common in the field that final products are concentrated in the range of 1*10^{12} – 1*10^{13} vg/mL.

In contrast to SO-DSF, iDSF allows for measuring the T_m in the presence of different surfactants. Unlike SYPRO Orange, which interacts with the surfactant and elevates the baseline, with iDSF the addition of polysorbate or poloxamer does not lead to a baseline shift (215). However, the addition of surfactant does shift T_m towards higher values. This can be explained either by a stabilizing effect of surfactants on AAV or a higher "real" concentration of (non-aggregated or non-adsorbed) AAV due to less aggregation and adsorption by the surfactant in the sample (302, 303). The latter is also the reason why AAV formulations commonly contain surfactant: to reduce adsorption effects to the packaging material.

While both SO-DSF and iDSF allow for quick and reliable determination of T_m and, thus, inform about the type of AAV capsid, they both have limitations. The most obvious issue is that AAV capsids with very similar level of thermostability, such as AAV3 and AAV8 or AAV9 and AAVrh10, cannot be distinguished by either method. This limitation could be overcome by measuring in different buffers in which the AAV serotypes exhibit different thermostability and allow to distinguish between the pairs (3). Other than that, discrimination of all other pairs of AAV capsid is easily possible. Moreover, mixtures of AAV5 and AAV8 can be precisely measured and discrimination between two serotypes in one sample is possible down to a concentration ratio of 1:10. Another limitation is the amount of AAV capsid needed for reliable measurement of T_m. As shown in our study, the lowest titer needed for iDSF is 2*10^{11} cp/mL in 10 µL. An improvement vis-à-vis SO-DSF

with a minimum amount of 3.4 - 3.95*10^{11} cp/mL in a minimum test volume of 20 – 25 µL (3, 55).

The effect of the empty capsids on clinical outcome is unclear and currently discussed in the field (42). There is a potential for increasing innate or adaptive immune responses to the vector. At the same time, very recent data showed that empty AAV capsids can actually enhance gene transfer by mitigating the problem of preexisting humoral immunity to AAV (42). Thus, methods for purification and for analytical distinction of full / empty AAV capsids are needed. When tested for its ability to discriminate between full and empty AAV, iDSF was able to detect a slight stabilizing in term of T_m of the vector DNA on the AAV capsids. For all serotypes the T_m for the DNA containing capsid was slightly higher (0.2-0.7°C). However, the differences were too small to clearly distinguish between full and empty AAV in a complex sample mixture. For this purpose, other analytical methods can be used such as anion-exchange-chromatography (26, 188), analytical ultracentrifugation (175, 176) and transmission- or cryo-electron microscopy (304).

In summary, DSF offers a rapid, cost effective and robust method for AAV serotype identification due to their unique thermal stability profiles in the commonly utilized formulation and storage buffers and detergents.

II.6 Acknowledgments

The authors want to thank Kerstin Skokann and Johanna Weiker for the production of the AAV.

We also want to thank Dennis Krieg for the technical support in the initial phase of this study.

This work was supported by the Deutsche Forschungsgemeinschaft (EXC114).

II.7 Supplement

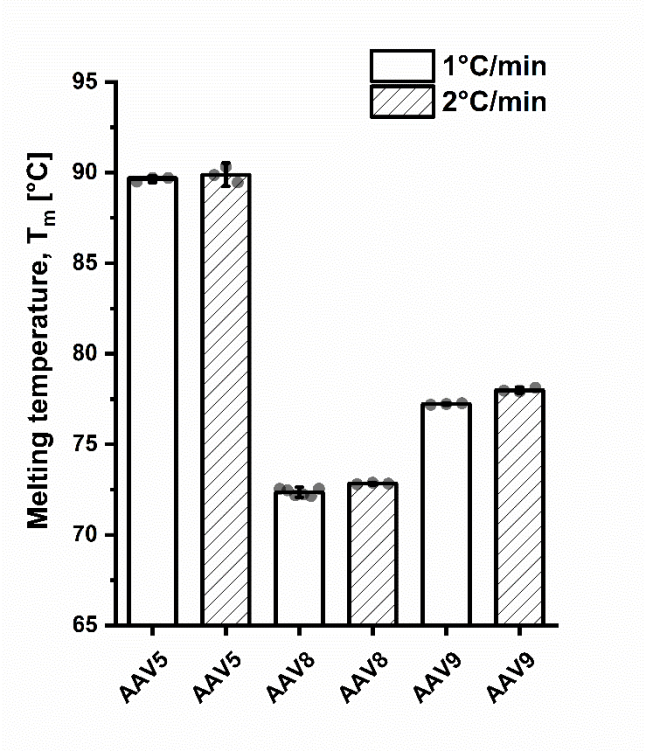

Figure II.S1 Effect of different heating rates on the iDSF measurent. T_m measured with iDSF at a heating rate of 1°C/min (blank bars) or at a heating rate of 2°C/min (striped bars). The concentration of all samples was $5*10^{11}$ vg/mL. 3 technical replicates were measured and plotted with SD.

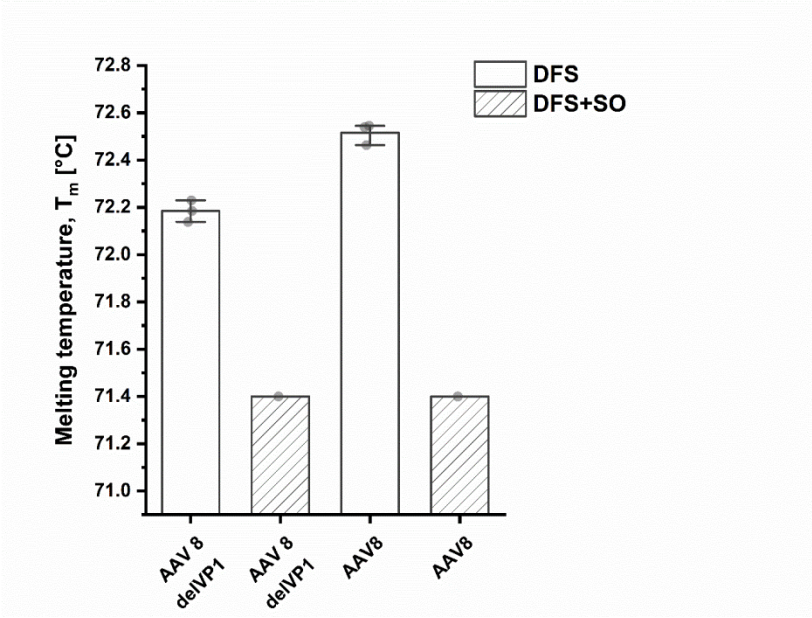

Figure II.S2 Comparison of T_m of AAV8 and AAV8 del VP1 as measured by iDSF. AAV8wt (CAG-hGFP) showed a higher T_m than AAV8 delVP1(CAG-hGFP) with a capsid titer of $1*10^{12}$cp/mL and 3 technical replicates plotted with SD.

Table II.S1. Multiple sequence alignment of viral protein VP1 sequences of AAV capsids used in the study.

NAMES-Uniprot Identifiers:
AAV2-P03135; AAV3(AAV3 B)-O56139; AAV5-Q9YIJ1; AAV8-Q808Y3; AAV9-Q6JC40; AAVrh10-Q5Y9B4

```
FEATURES
AAV2        MAADGYLPDWLEDTLSEGIRQWWKLKPGPPPPKPAERHKDDSRGLVLPGYKYLGPFNGLD     60
AAV3        MAADGYLPDWLEDnLSEGIReWWaLKPGvPqPKanqqHqDnrRGLVLPGYKYLGPgNGLD     60
AAV5        MsfvdhpPDWLEevg.EGlReflgLeaGPPkPKPnqqHqDqaRGLVLPGYnYLGPgNGLD     59
AAV8        MAADGYLPDWLEDnLSEGIReWWdLKPGaPkPKanqqkqDDgRGLVLPGYKYLGPFNGLD     60
AAV9        MAADGYLPDWLEDnLSEGIReWWaLKPGaPqPKanqqHqDnaRGLVLPGYKYLGPgNGLD     60
AAVrh10     MAADGYLPDWLEDnLSEGIReWWdLKPGaPkPKanqqkqDDgRGLVLPGYKYLGPFNGLD     60
Consensus   maadgylpdWled lsegireWW lkpg p pk nqq qd  rglvlpgykylgp ngld

AAV2        KGEPVNEADAAALEHDKAYDRQLDSGDNPYLKYNHADAEFQERLKEDTSFGGNLGRAVFQ    120
AAV3        KGEPVNEADAAALEHDKAYDqQLkaGDNPYLKYNHADAEFQERLqEDTSFGGNLGRAVFQ    120
AAV5        rGEPVNrADevArEHDisYneQLeaGDNPYLKYNHADAEFQEkLadDTSFGGNLGkAVFQ    119
AAV8        KGEPVNaADAAALEHDKAYDqQLkaGDNPYLrYNHADAEFQERLqEDTSFGGNLGRAVFQ    120
AAV9        KGEPVNaADAAALEHDKAYDqQLkaGDNPYLKYNHADAEFQERLKEDTSFGGNLGRAVFQ    120
AAVrh10     KGEPVNaADAAALEHDKAYDqQLkaGDNPYLrYNHADAEFQERLqEDTSFGGNLGRAVFQ    120
Consensus   kgepvn adaaalehdkayd ql agdnpyl ynhadaefqerl edtsfggnlgravfq

AAV2        AKKRVLEPLGLVEEPVKTAPGKKRPVEHSPV.EPDSSSGTGKAGQQPARKRLNFGQTGDA    179
AAV3        AKKRiLEPLGLVEEaaKTAPGKKRPVdqSPq.EPDSSSGvGKsGkQPARKRLNFGQTGDs    179
AAV5        AKKRVLEPfGLVEEgaKTAPtgKRiddHfPk.........rkKArteedsKpstssdaeag    171
AAV8        AKKRVLEPLGLVEEgaKTAPGKKRPVEqSPq.EPDSSSGiGKtGQQPAkKRLNFGQTGDs    179
AAV9        AKKRlLEPLGLVEEaaKTAPGKKRPVEqSPq.EPDSSaGiGKsGaQPAkKRLNFGQTGDt    179
AAVrh10     AKKRVLEPLGLVEEaaKTAPGKKRPVEpSPqrsPDSStGiGKkGQQPAkKRLNFGQTGes    180
Consensus   akkr leplglvee aktapgkkrpv  sp   pdss g gk g qpa krlnfgqtg

AAV2        DSVPDPQPLGQPPAAPSGLGTNTMATGSGAPMADNNEGADGVGNSSGNWHCDSTWMGDRV    239
AAV3        eSVPDPQPLGePPAAPtsLGsNTMAsGgGAPMADNNEGADGVGNSSGNWHCDSqWlGDRV    239
AAV5        pSg..sQqLqiPaqpaSsLGadTMsaGgGgPlgDNNqGADGVGNaSGdWHCDSTWMGDRV    229
AAV8        eSVPDPQPLGePPAAPSGLGpNTMAsGgGAPMADNNEGADGVGNSSGNWHCDSTWlGDRV    239
AAV9        eSVPDPQPiGePPAAPSGvGslTMAsGgGAPvADNNEGADGVGsSSGNWHCDSqWlGDRV    239
AAVrh10     eSVPDPQPiGePPAgPSGLGsgTMAaGgGAPMADNNEGADGVGsSSGNWHCDSTWlGDRV    240
Consensus    svpdpqp g ppa ps lg  tma gggap adnnegadgvg ssgnWhcds W gdrv

AAV2        ITTSTRTWALPTYNNHLYKQIS.SQSGAS.NDNHYFGYSTPWGYFDFNRFHCHFSPRDWQ    297
AAV3        ITTSTRTWALPTYNNHLYKQIS.SQSGAS.NDNHYFGYSTPWGYFDFNRFHCHFSPRDWQ    297
AAV5        vTkSTRTWvLPsYNNHqYreIksgsvdgS.NaNaYFGYSTPWGYFDFNRFHsHWSPRDWQ    288
AAV8        ITTSTRTWALPTYNNHLYKQISngtSGgStNDNtYFGYSTPWGYFDFNRFHCHFSPRDWQ    299
AAV9        ITTSTRTWALPTYNNHLYKQISnStSGgSsNDNaYFGYSTPWGYFDFNRFHCHFSPRDWQ    299
AAVrh10     ITTSTRTWALPTYNNHLYKQISngtSGgStNDNtYFGYSTPWGYFDFNRFHCHFSPRDWQ    300
Consensus   ittstrtWalptynnhlykqis   sg s ndn yfgystpWgyfdfnrfhchfsprdWq

AAV2        RLINNNWGFRPKRLNFKLFNIQVKEVTQNDGTTTIANNLTSTVQVFTDSEYQLPYVLGSA    357
AAV3        RLINNNWGFRPKkLsFKLFNIQVKEVTQNDGTTTIANNLTSTVQVFTDSEYQLPYVLGSA    357
AAV5        RLINNyWGFRPrsLrvKiFNIQVKEVTvqDsTTTIANNLTSTVQVFTDddYQLPYVvGng    348
AAV8        RLINNNWGFRPKRLNFKLFNIQVKEVTtNeGTkTIANNLTSTVQVFTDSEYQLPYVLGSA    359
AAV9        RLINNNWGFRPKRLNFKLFNIQVKEVTdNnGvkTIANNLTSTVQVFTDSdYQLPYVLGSA    359
AAVrh10     RLINNNWGFRPKRLsFKLFNIQVKEVTQNeGTkTIANNLTSTiQVFTDSEYQLPYVLGSA    360
Consensus   rlinnnWgfrpk l fklfniqvkevt n gt tiannltstvqvftds yqlpyvlgsa

AAV2        HQGCLPPFPADVFMVPQYGYLTLN..NGSQAVGRSSFYCLEYFPSQMLRTGNNFTFSYTF    415
AAV3        HQGCLPPFPADVFMVPQYGYLTLN..NGSQAVGRSSFYCLEYFPSQMLRTGNNFqFSYTF    415
AAV5        teGCLPaFPpqVFtlPQYGYaTLNrdNtenpteRSSFfCLEYFPSkMLRTGNNFeFtYnF    408
AAV8        HQGCLPPFPADVFMVPQYGYLTLN..NGSQAlGRSSFYCLEYFPSQMLRTGNNFqFSYTF    417
AAV9        HeGCLPPFPADVFMiPQYGYLTLN..dGSQAVGRSSFYCLEYFPSQMLRTGNNFqFSYeF    417
AAVrh10     HQGCLPPFPADVFMiPQYGYLTLN..NGSQAVGRSSFYCLEYFPSQMLRTGNNFeFSYTF    418
Consensus   h gclppfpadvfm pqygyltln  ngsqa grssfycleyfpsqmlrtgnnf fsy f

AAV2        EDVPFHSSYAHSQSLDRLMNPLIDQYLYYLSRTN.TPSGTTTQSRLQFSQAGASDIRDQS    474
AAV3        EDVPFHSSYAHSQSLDRLMNPLIDQYLYYLnRTqgTtSGTTnQSRLlFSQAGpqsmslQa    475
AAV5        EeVPFHSSfApSQnLfkLaNPLvDQYLYrfvsTNnTgg.......vQFnknlAgryanty    461
```

```
AAV8        EDVPFHSSYAHSQSLDRLMNPLIDQYLYYLvRTq.Ttg.TggtqtLaFSQAGpSsmanQa    475
AAV9        EnVPFHSSYAHSQSLDRLMNPLIDQYLYYLSkTi.ngS.gqnQqtLkFSvAGpSnmavQg    475
AAVrh10     EDVPFHSSYAHSQSLDRLMNPLIDQYLYYLSRTq.stgGTqgtqqLlFSQAGpanmsaQa    477
Consensus   e vpfhssyahsqsldrlmnplidqylyyl  t           l fs ag      q

AAV2        RNWLPGPCYRQQRVSKTSADNNNSEYSWTGATKYHLNGRDSLVNPGPAMASHKDDEEKFF    534
AAV3        RNWLPGPCYRQQRlSKTanDNNNSnfpWTaAsKYHLNGRDSLVNPGPAMASHKDDEEKFF    535
AAV5        kNWfPGPmgRtQgWnlgSgvNraSvsafattnrmeLeGasyqVpPqPngmtnnlqgsnty    521
AAV8        RNWvPGPCYRQQRVStTtnqNNNSnfaWTGAaKfkLNGRDSLmNPGvAMASHKDDddrFF    535
AAV9        RNyiPGPsYRQQRVStTvtqNNNSEfaWpGAssWaLNGRnSLmNPGPAMASHKegEdrFF    535
AAVrh10     kNWLPGPCYRQQRVStTlsqNNNSnfaWTGATKYHLNGRDSLVNPGvAMAtHKDDEErFF    537
Consensus    nW pgp yrqqr s t   nnns   W  a    lngr sl npg ama hk     ff

AAV2        PQSGVLIFGKQGS...EKTNVDIEKVMITDEEEIRTTNPVATEQYGSVSTNLQRGNRQAA    591
AAV3        PmhGnLIFGKeGt...tasNaeldnVMITDEEEIRTTNPVATEQYGtVanNLQssNtapt    592
AAV5        alentmIFnsQpanpgttatylegnmlITsEsEtqpvNrVAynvgGqmaTNnQssttapA    581
AAV8        PsSGVLIFGKQGa...gndgVDysqVlITDEEEIkaTNPVATEeYGaVaiNnQaaNtQAq    592
AAV9        PlSGsLIFGKQGt...grdNVDadKVMITnEEEIkTTNPVATEsYGqVaTNhQsaqaQAq    592
AAVrh10     PsSGVLmFGKQGa...grdNVDyssVMlTsEEEIkTTNPVATEQYGvVadNLQqaNtgpi    594
Consensus   p  g lifgkqg            v it eeei  tnpvate yg va n q

AAV2        TADVNTQGVLPGMVWQDRDVYLQGPIWAKIPHTDGHFHPSPLMGGFGLKHPPPQILIKNT    651
AAV3        TrtVNdQGaLPGMVWQDRDVYLQGPIWAKIPHTDGHFHPSPLMGGFGLKHPPPQImIKNT    652
AAV5        TgtyNlQeivPGsVWmeRDVYLQGPIWAKIPeTgaHFHPSPaMGGFGLKHPPPmmLIKNT    641
AAV8        TglVhnQGViPGMVWQnRDVYLQGPIWAKIPHTDGnFHPSPLMGGFGLKHPPPQILIKNT    652
AAV9        TgWVqnQGiLPGMVWQDRDVYLQGPIWAKIPHTDGnFHPSPLMGGFGmKHPPPQILIKNT    652
AAVrh10     vgnVNsQGaLPGMVWQnRDVYLQGPIWAKIPHTDGnFHPSPLMGGFGLKHPPPQILIKNT    654
Consensus   t  v  qg  pgmvWq rdvylqgpiWakiphtdg fhpsplmggfglkhpppqiliknt

AAV2        PVPANPSTTFSAAKFASFITQYSTGQVSVEIEWELQKENSKRWNPEIQYTSNYNKSVNVD    711
AAV3        PVPANPpTTFSpAKFASFITQYSTGQVSVEIEWELQKENSKRWNPEIQYTSNYNKSVNVD    712
AAV5        PVPgN.iTsFSdvpvsSFITQYSTGQVtVEmEWELkKENSKRWNPEIQYTnNYNdpqfVD    700
AAV8        PVPAdPplTFnqAKlnSFITQYSTGQVSVEIEWELQKENSKRWNPEIQYTSNYyKStNVD    712
AAV9        PVPAdPpTaFnkdKlnSFITQYSTGQVSVEIEWELQKENSKRWNPEIQYTSNYyKSnNVe    712
AAVrh10     PVPAdPpTTFSqAKlASFITQYSTGQVSVEIEWELQKENSKRWNPEIQYTSNYyKStNVD    714
Consensus   pvpa p t f   k  sfitqystgqvsveieWelqkenskrWnpeiqytsny ks nvd

AAV2        FTVDTNGVYSEPRPIGTRYLTRNL                                        735
AAV3        FTVDTNGVYSEPRPIGTRYLTRNL                                        736
AAV5        FapDstGeYrttRPIGTRYLTRpL                                        724
AAV8        FaVnTeGVYSEPRPIGTRYLTRNL                                        736
AAV9        FaVnTeGVYSEPRPIGTRYLTRNL                                        736
AAVrh10     FaVnTeGtYSEPRPIGTRYLTRNL                                        738
Consensus   f v t g yseprpigtryltrnl
```

Chapter III Methods for AAV capsid titer determination

III.1 Introduction

As already described in Chapter I, AAV concentration is a CQA and refers either to infectious, genome, or capsid titer. Chapter III will focus on capsid titer, because it is the most useful measure from a process development perspective, allowing for comparability. Of course, the genome and infection titers are also of importance during the development process but the capsid titer is a measure for all capsids, independent of the packaged genome. Moreover, quantification of total capsids is crucial for the development and optimization of downstream recovery and purification processes because these mainly depend on the load of product. Furthermore, the capsid titer is of special interest after full-empty separation by AEX or gradient ultracentrifugation, as a ratio between capsid and vector genome titer indicates successful separation (95, 305).

The most common techniques for measuring capsid titer are ELISA, AUC, and TEM. While these methods are widely used and established, they have their downsides. To streamline the development process of AAV DP, alternative methods are needed that are less labor intensive, have higher accuracy, are faster to perform, and/or can easily be used as in-process controls. Thus, this Chapter investigates potential alternatives. In total, seven different methods for quantifying capsid titers are compared and the additional information provided by each method is discussed.

In the research process towards improved capsid titer determination, it was uncovered that substantial loss of capsids takes place within the downstream process. Having identified filtration as a main issue, its improvement will be discussed shortly at the end of the chapter.

III.2 Material and methods

III.2.1 AAV material

Recombinant AAV vectors with genomes carrying inverted terminal repeats, derived from AAV2 and packaged with wildtype AAV8, were produced and purified in adherent HEK293T cells (The Leibniz Institute DSMZ-German Collection of Microorganisms and Cell Cultures GmbH, Braunschweig, Germany) as previously described (293, 294). The packaged self-complementary (sc) genome comprised a CMV promoter driving expression of eGFP (306). All purifications using liquid chromatography were performed with an ÄKTA purifier from Cytiva (Marlborough, MA, USA). For sample loading, a Superloop

or sample pump were used. All runs were performed at room temperature (25 °C), and the detection was done with a UV detector (UL-9, fixed wavelength) at 280 nm implemented in the ÄKTA system. The evaluation was conducted with Unicorn Software (7.3) (Cytiva, Marlborough, MA, USA).

For affinity chromatography (AC), a Poros capture select AAVx column (1 mL; Thermo Fisher Scientific, Dreieich, Germany) was used. AAV samples, in 10 mM sodium phosphate buffer and 150 mM NaCl at pH 7.4, were loaded at a flow rate of 0.3 mL/min on the column and eluted with 100 mM citric acid (VWR, Geldenaaksenbaan, Belgium), pH 3.0 at a flow rate of 0.7 mL/min. AAV were neutralized by elution into 200 µL 1 M Tris, pH 8.7 (95).

Full-empty separation was achieved with a CIMmultus PrimaS (AAV) column (1 mL, 2-µm pores, BIA separations, Ajdovščina, Slovenia). Buffer A contained 10 mM Tris, 10 mM bis-tris-propane (Sigma-Aldrich Chemie GmbH, Steinheim, Germany), 2 mM $MgCl_2$, and 0.1% poloxamer 188 (Kolliphor P 188, BASF, Ludwigshafen, Germany) at pH 8.0, while buffer B had the same composition at pH 10.0.

III.2.2 Enzyme-linked immunosorbent assay – ELISA

To determine the capsid titer of AAV8, the quantitative and serotype specific ELISA (Progen, Germany) were performed according to the manufacturer's instructions (57, 113).

III.2.3 Size exclusion chromatography – SEC

A Waters 2695 system (Waters GmbH, Eschborn, Germany) and Wyatt SEC protein column 50 (WTC-050S5, 5 µm, 7.8x300 mm) (Wyatt Technology, Santa Barbara, USA) were used for SEC measurements. AAV elution was detected with a fluorescence detector (Dionex RF2000, Sunnyvale, CA, USA) at an excitation wavelength of 280 nm and an emission wavelength of 330 nm. The running buffer consisted of 10 mM sodium phosphate and 150 mM NaCl at pH 7.4, with a flow rate of 0.5 mL/min. The chromatograms were integrated with Chromeleon V6.8 (Thermo Fisher, Dreieich, Germany). The AAV8 sample with the capsid titer determined by ELISA was used to calibrate the SEC in a range from $3*10^{10}$ to $1*10^{12}$ cp.

III.2.4 Anion exchange chromatography – AEX

For the analytical separation of full and empty AAV, a Waters 2695 system (Waters GmbH, Eschborn, Germany) was combined with a Protein-Pak Hi Res Q column (5 µm, 4.6×100 mm; Waters GmbH, Eschborn, Germany). For this purpose, 70 mM bis-tris-propane (Sigma-Aldrich, St. Louis, MO, USA) and 2 mM $MgCl_2$, pH 9.0, were used as buffer A. Buffer B was created by adding 1M tetramethylammoniumchlorid (Sigma-Aldrich, St. Louis, MO, USA) to buffer A. To separate the full and empty AAV, a gradient from 10% to 30% B for 20 min was performed at a flow rate of 0.3 mL/min. AAV elution was detected using a fluorescence detector (FI) (Dionex RF2000, Sunnyvale, CA, USA) at excitation and emission wavelengths of 280 nm and 330 nm, respectively. The chromatograms were integrated with Chromeleon V6.8 (Thermo Fisher Scientific, Dreieich, Germany).

III.2.5 Asymmetrical flow field flow fractionation (AF4) and multiangle light scattering (MALS)

For AF4 measurements, an Agilent 1100 system comprising an UV Detector, a RI detector (Agilent Technologies, Santa Clara, USA), and a MALS detector (Dawn Heleos II, Wyatt Technology, Santa Barbara, USA) was used. For flow control, an Eclipse Dualtec (Wyatt Technology, Santa Barbara, USA) with a small chancel containing a regenerated cellulose membrane (cut off 10 kDa) and a spacer 350 µm S were used.

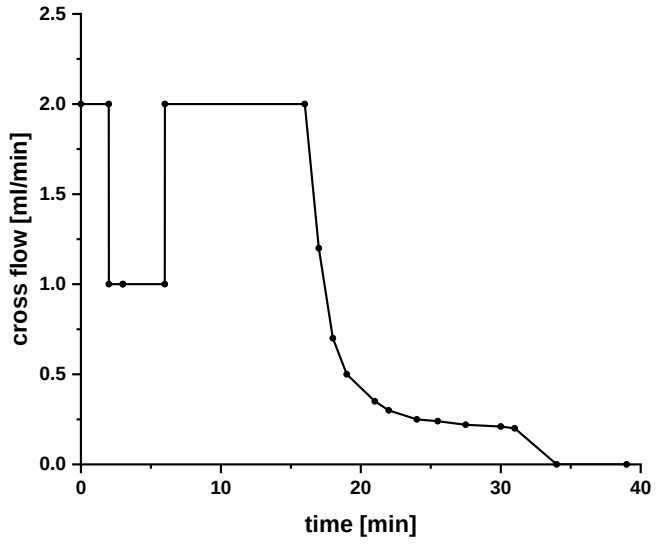

Figure III.1 Crossflow profile of the AF4 measurement: 2 mL/min for 2 min (elution),1 mL/min for 4 min (focusing), 2 mL/min for 10 min; exponential gradient from 2 to 0.2 mL/min over 15 min; linear gradient from 0.2 to 0 mL/min over 3 min; 0 mL/min for 5 min.

The measurements were performed with the following method: detector flow set to 1mL/min during the whole measurement, while the crossflow profile is configured according to Figure III.1. The used buffer consists of 10 mM sodium phosphate, 150 mm NaCl, 200 ppm sodium azide at pH 7.0. The chromatograms were integrated and data analysis of the MALS data was performed with Astra 7.3.2 (Wyatt Technology, Santa Barbara, USA).

III.2.6 Dynamic light scattering (DLS) and static light scattering (SLS)

DLS and SLS measurements were performed on a Wyatt DynaPro III (Wyatt Technologies, Santa Barbara, USA), using Corning 3540 384-well plates (Corning, New York, USA) with 20 µL sample volume. The plate was centrifuged at 2000 rpm for 2 minutes, using a Heraeus Megafuge 40 centrifuge equipped with an M-20 well plate rotor (Thermo Fisher, Dreieich, Germany). For SLS analysis, the particle shape was set to a sphere and the refractive index at 830 nm was set to 1.43 for empty AAV, 1.48 for full AAV, and 1.45 for a mixture of full and empty AAV (307). Each measurement consists of 10 acquisitions within an acquisition time of 5 seconds. Data were collected as replicates. The autocorrelation function of each measurement was analyzed using cumulant analysis with the Dynamics V7.10 software (Wyatt Technology, Santa Barbara, USA).

III.2.7 Sodium dodecyl sulfate polyacrylamide gel electrophoresis (SDS-PAGE)

For SDS-PAGE, samples were loaded on a NuPAGE™ 6–12% Tris-HCl gel (Thermo Fisher, Dreieich, Germany) after the addition of Laemmli 4× (Bio-Rad, Hercules, CA, USA) and denaturation at 95 °C for 5 minutes. After electrophoresis at 200 V for 50 minutes in MOPS SDS Running buffer (1x) (Thermo Fisher, Dreieich, Germany), the gel was silver stained with a SilverXpress Silver Staining Kit (Thermo Fisher, Dreieich, Germany) and pictures were taken by ChemiDog (Bio-Rad, Feldkirchen, Germany) (66). The BSA (Sigma-Aldrich, St. Louis, MO, USA) for the concentration series ranges from 2 ng to 660 ng. The amount of the viral protein 3 (VP3) of the capsid in gram was calculated from the calibration curve and divided by the mass of VP3 per capsid ($4.9868*10^{-18}$ g), resulting in the number of capsids (65, 74).

III.2.8 Stunner

The Stunner instrument from Unchained Labs (Boston, USA) combines UV/Vis spectrometry and DLS and SLS measurements. Through this, it can provide information on

the number of vg and cp, as well as additional information on sample aggregation. For the measurements 2 µL per sample were pipetted as duplicates on the stunner plate. Data analyses were conducted by the AAV quant tool of the Stunner software. Excitation coefficients were calculated with the software, based on DNA length and serotype information.

III.2.9 UV spectrometry

The AAV8 samples with pAAV2.1-sc-CMV-GFP plasmid (367683 MW) were denatured with 0.1% SDS and heated up to 95 °C for 5 minutes and equilibrated to RT. The UV measurement was performed with a NanoDrop2000c (Thermo Fisher, Dreieich, Germany) with a sample volume of 1 µL.

The vector genome titer was determined by equation:

$$vg/mL = \frac{4{,}47 \ * 10^{19} \ (A_{260} \ - 0{,}59 \ A_{280})}{MW_{DNA}}$$

The ratio of full and empty capsids was calculated by equation:

$$cp/_{vg} = MW_{DNA} * \frac{1{,}76 * 10^{-6}(1{,}8 - \frac{A_{260}}{A_{280}})}{\frac{A_{260}}{A_{280}} \ - 0{,}59}$$

The capsid titer was calculated by multiplication of the vector genome titer with the ratio of cp to vg (65).

III.2.10 Filtration

The filtration experiment was performed with 10^{12} cp/mL AAV in PBS with and without 0.001% poloxamer 188 (PX 188). One milliliter of the suspension was filled into a 1 mL BD Plastipak syringe (Becton Dickinson, Franklin Lakes, USA) and filtered through one of the three used filter materials - regenerated cellulose (RC4, Sartorius, Göttingen, Germany), polyethersulfon (Supor, Pall Corporation, New York, USA), polyvinylidendifluorid (Durapore, Merck, Darmstadt, Germany) - with a pore size of 0.2 µm and a diameter of 25 mm. Samples were taken before and after filtration. For comparison, some of the samples were not filtered but put into the syringe and out again. Analysis was performed with SEC and a fluorescence detector.

III.3 Results and discussion

III.3.1 Capsid determination by different methods

The capsid titers of four different samples were measured and calculated by seven different methods: SEC, AEX, AF4-MALS, SLS, UV spectrometry, Stunner, and SDS-PAGE. To evaluate the methods, the capsid titer of one sample was determined with the standard method: capsid ELISA. The same sample was used for calibration of the SEC and AEX. The sample, depicted in Figure III.3A, had a capsid titer determined by ELISA of around 10^{13} cp/mL. Only small differences between the measurement methods were detected, with the highest variability found for Stunner.

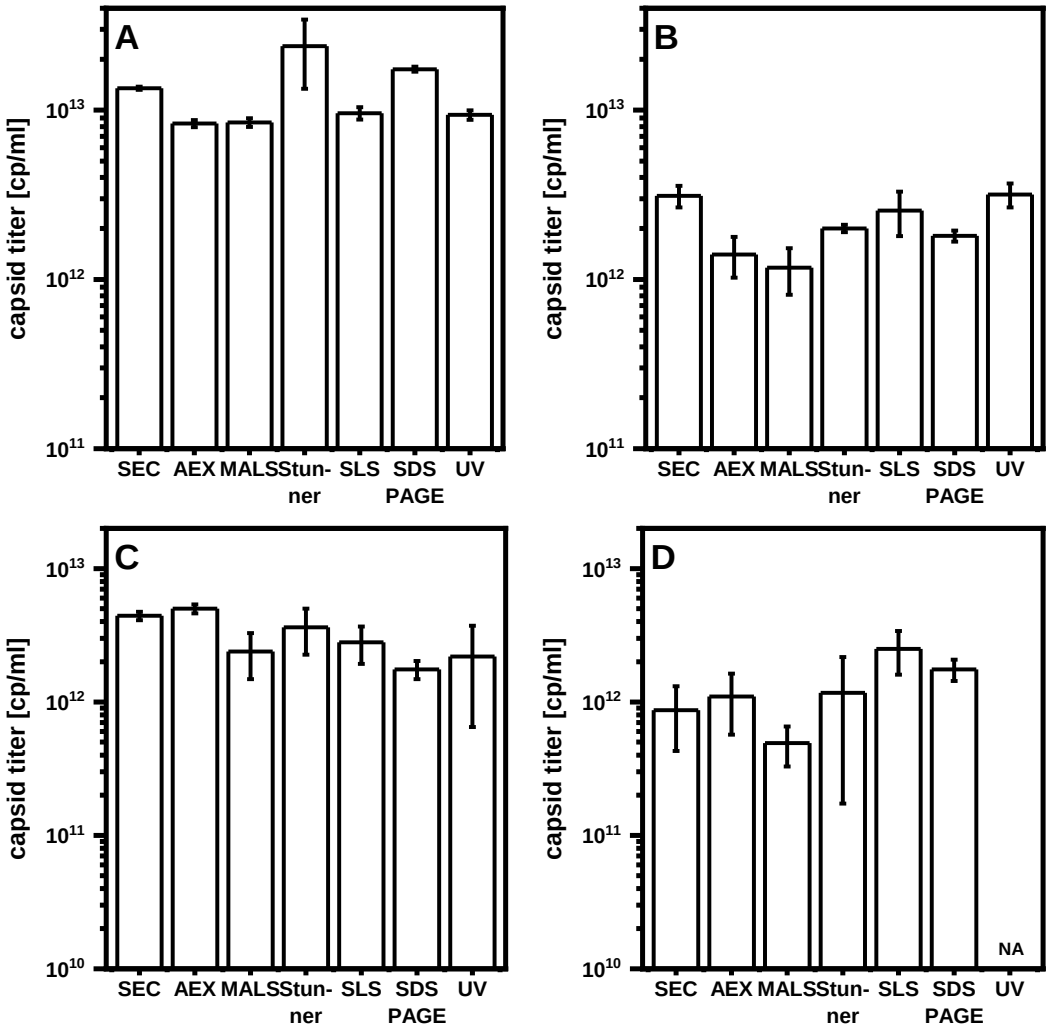

Figure III.3 Capsid titer determined by different measurements of four different sampels (A) Full/empty mix after AC 10^{13}cp/mL, (B) Full/empty mix after AC 10^{12}cp/mL, (C) mainly empty capsids after AEX $4*10^{12}$ cp/mL, (D) mainly full capsids after AEX $9*10^{11}$ cp/mL.

Figure III.3B shows the capsid titer calculations for a sample containing 10^{12} cp/mL. Again, only minor differences between the different methods were observed. within line with the results from Figure III.2A, AEX and AF4-MALS detection of AAV capsid results in a slightly lower titer in respect to the SEC result. SLS and SDS-PAGE range in between.

For the sample containing only empty capsids (Figure III**.**3C), SEC and AEX identify a similar number of capsids, whereas the measurements performed with AF4-MALS, Stunner, UV spectrometry, SLS, and SDS-PAGE detected a slightly lower number of capsids. The standard deviation (SD) for the UV spectrometry increased considerably. One explanation is that because of the missing DNA the UV absorption decreases and with this uncertainty is rising.

Table III.1 Comparison of the different capsid determination methods. ELISA, UV, FI, SDS-PAGE, DLS/SLS and Stunner.

Method	Number of Capsids [cp]	Injection Volume [µL]	Time [min]	Detection Principle
ELISA	$10^7 – 10^9$	100	300	Fluorescence calibrated by kit control
SEC	$>10^{10}$ (FI) $>10^{11}$(UV)	2-100	30	Calibration, FI/UV
AEX	$>10^{10}$ (FI) $>10^{11}$(UV)	2-100	60	Calibration, FI/UV
AF4-MALS	$>10^{11}$	2-100	60	UV, RI; Light scattering
SDS-Page	$>10^{10}$	4-20	240	Calibration BSA amount VP3 silver-staining
DLS/SLS	$6*10^9 – 10^{14}$	5-100	2	Light scattering
Stunner	$>2*10^9$	2	2	Light scattering and UV
UV spectrometry	$>1*10^9$	1	30	UV

The last sample contained mostly full AAV (Figure III**.**3D). Again, SEC and AEX detected a similar quantity of capsids, whereas AF4-MALS resulted in lower and SLS and SDS-PAGE in higher values. Stunner measurement gave a comparable number of capsids but with a higher SD. From the UV spectrometry measurement, no reliable data were obtained. There are two possible reasons for this: (1) the overall low titer or (2) some coeluted free

DNA in the sample, as shown in Chapter IV for the AUC results of the purification strategies.

To sum up the findings, the higher the capsid concentration in a sample the easier the determination of the capsid amount is, as illustrated in Figure III.3A and 2C. When the titer is only in the range of 10^{11} cp/mL, it becomes harder to obtain valid data with all available methods, as can be seen by the higher SD in Figure III.3B and 2D. For the chromatography-based methods it is possible to increase the injected amount of the sample to finally reach the amount of capsid needed for a good measurement. Other methods, like Stunner, have a fixed amount of sample for the measurement, meaning that it is not possible to adapt the sample volume, resulting in a considerably higher SD.

For capsid titer determination, the capsid titer of one standard sample was determined by ELISA and was later used to calibrate SEC and AEX. Because ELISA is rather time-consuming and expensive, alternative methods have been explored. The major advantage of ELISA is the high sensitivity, which demands a relatively low number of capsids for measurement. The limit of detection (LOD) of capsids depends on the detection method used for chromatography. If a UV detector is used, the minimum amount of capsids has to be > 10^{11} cp and for a fluorescence detector (FI) > 10^{10} cp is sufficient (cf. Table III.1) (26, 96, 207).

The other measurements have different advantages: From SEC additional information about impurities like soluble aggregates and fragments can be obtained and if used together with a MALS detector, the full-empty ratio of the capsids can be derived. With AEX chromatography, the ratio between full and empty capsids can be quantified, as well as the amount of other impurities which are resulting in an additional peak in the chromatogram when using UV or FI detection. AF4 informs about soluble and non-soluble aggregates, because the AAV suspension can be injected without previous centrifugation or filtration. This is possible because the separation takes place in a channel with a membrane and separation is achieved by the diffusion coefficients of each particle using a detector flow along the membrane and a vertical crossflow (308-311). By adding a MALS detector into a HPLC system, it is even possible to measure the diameter, molecular weight, full-empty ratio, and particle number in one measurement without a calibration curve. Yet, to evaluate the MALS data another concentration detector is necessary and for this purpose only a UV or RI detector can be used, limiting the detection to 10^{11} cp and above. All three

chromatography systems mentioned above can be combined with a MALS detector (83, 93, 312). The only necessity for all chromatography-based methods is 100% recovery, which can be certainly achieved as long as a solid method development is ensured.

In contrast to the HPLC based methods, light scattering methods (DLS/SLS) allow batch measurements. These batch measurements can be performed for example by a Wyatt plate reader III (Wyatt Technology, Santa Barbara, USA) or by Stunner (Unchained Lab, Boston, USA). For valid and correct data, the samples should be monodisperse for the measurements. The measurement itself takes only a few minutes and only needs a few microliters of sample. If the measurement is done by Stunner, a full UV/Vis spectrum is incorporated in addition to DLS/SLS data and from there information about impurities like free DNA and proteins can be deduced. From DLS/SLS, information on aggregation and size can be derived and, through combination of these results with the UV/Vis spectrum, a full-empty ratio of the AAV as well as capsid and vg titer can be calculated.

Information about vg and cp amount can also be derived from UV spectrometry alone. To this end, denaturation is needed to reduce the significant light scatter resulting from intact particles. Overall, it is a fast and easy measurement without the need for any special equipment. However, the measurement requires a highly purified sample, because it can be affected by residual protein or DNA impurities as well as by density gradient components or excipients that absorb in the UV range, such as iodixanol or Tween 80.

The last method to determine the capsid titer tested, was the SDS-PAGE calibrated with a BSA calibration curve. This technique is more time-consuming compared to the others, but the required equipment can be found in nearly every laboratory. A new calibration curve must be created for each gel. Especially with this method, it is important to have a rough estimate of the capsid titer so that the measured samples lie within the calibration curve. However, the duration of the experiment is particularly long and the number of samples that can be run in parallel is very limited. This is due to the limited number of available gel pockets and the need to run several BSA concentrations for the calibration curve on the same gel. However, an advantage of the SDS-PAGE is that it also detects impurities and thus provides further information about the corresponding sample.

III.3.2 Prevention of capsid loss due to filtration

During the comparison experiments, it was discovered that substantial amounts of capsids are lost during the downstream purification process. Adsorption problems due to the injection and filtration process have already been documented to be a problem in AAV manufacturing (313). In this context, filtration of AAV samples is of particular relevance. For instance, the medium from the cell culture must be filtered to remove dead cells and cell debris. Also, before loading the sample on a chromatography column, a 0.45-µm filtration is required to reduce the bioburden and the final purified AAV sample is sterile filtrated (0.22-µm) to achieve sterility of the sample. During these filtration steps, loss of AAV can occur, but the loss can be reduced significantly by using the proper membrane material as well as by adding a surfactant to the sample to reduce adsorption of AAV to the syringe and/or filter.

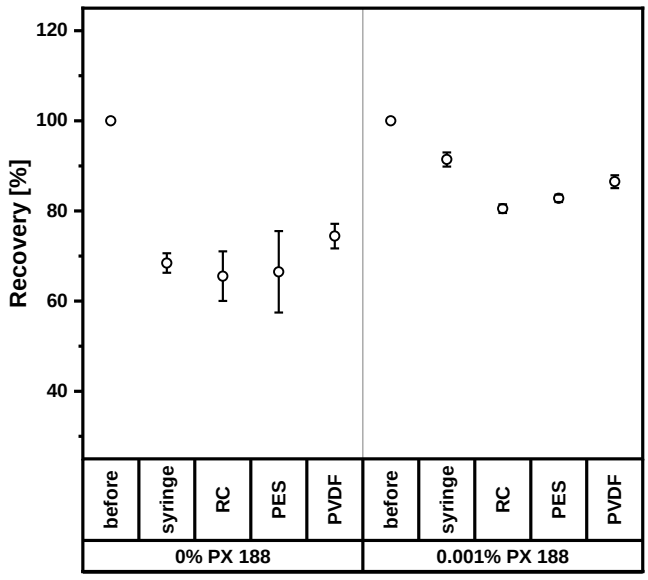

Figure III.4 depicts the loss of AAV capsid determined by SEC due to filtration of $1*10^{12}$ cp/mL AAV in PBS with and without poloxamer 188 (PX 188) with a regenerated cellulose (RC), polyether sulfone (PES) or polyvinyldifluoride (PVDF) membrane.

To optimize filtration of AAV samples, three different filtration membranes were tested with an AAV suspension of 10^{12} cp/mL buffered in PBS. In addition, for one series 0.001% poloxamer 188 was added. As evident from Figure III.4, an initial loss (32%) was detected directly after 1 mL of the AAV sample was filled and immediately withdrawn from the syringe without performing

the actual filtration. This suggests adsorption of AAV to the syringe material. For the actual filtration, loss of AAV was observed in all cases, with no clear difference between the three membranes for the samples without poloxamer 188. Recovery after filtration ranged between 65% and 74%, with a slight tendency in favor of the PVDF membrane. Using 0.001% poloxamer 188 in the filtration sample reduced the loss of AAV through the syringe and membranes and decreased the SD. The loss of AAV ranged from 14% for the PVDF membrane over 18% for PES, to 20% for RC (Figure III.4). In any case, recovery of AAV after filtration was clearly higher with poloxamer 188. Especially the adsorption to the syringe could be drastically reduced by poloxamer 188 in the formulation buffer (9% compared to 32% without surfactant). This phenomenon matches the results of Patrício et al. (313) who tested the yield of rAAV2 with and without poloxamer 188 after getting in contact with all devices which are needed for a subretinal injection and also observed significatly reduced AAV vector loss if the formulation contained poloxamer.

The filtration experiment performed for this thesis used a medium high titer of 10^{12} cp/mL. It would be interesting to repeat the experiment with higher and lower AAV titers for further testing the influence of concentration on adsorption. Theoretically, when adsorption on the syringe and filter reaches saturation, a lower relative loss can be expected for high titers, as is required for therapeutic interventions (Luxturna: $5*10^{12}$ vg/mL and Zolgensma: $2*10^{13}$ vg/mL). To avoid high loss of AAV vector by filtration, the use of filters with smaller surface areas could be considered. However, a smaller filter area also decreases the flow per time and the pressure during filtration may be higher, leading to aggregation of capsids. It would also be of interest to test surfactants such as Tween 20 or Tween 80, as these have been used for other biopharmaceuticals (259, 314-316). Moreover, shear stress could be a problem during the filtration process leading to capsid damage (317-319).

III.4 Conclusion

In this Chapter capsid titer determination via SEC, AEX, AF4-MALS, SDS-PAGE, DLS/SLS, UV spectrometry, and Stunner, a combination of the latter two methods, was compared, because the more established methods like ELISA, AUC and TEM all come with some limitations, preventing a high-throughput application. The capsid titer determined by the seven methods was comparable for a capsid titer above $4*10^{12}$ cp/mL. Most of the explored alternatives reach their limit of detection (LOD) at 10^{11} cp/mL, at the

latest. The closer one gets to this limit, the less accurate the methods become, which is reflected in a higher SD. On the plus side, most of the methods provide additional information about aggregates, impurities, or full-empty ratio, that might be of interest. In particular, optical methods can not only speed up capsid titer determination without a loss of accuracy but could also offer additional valuable information about the AAV sample. Overall, Stunner provides in a short time the most comprehensive information about the sample with the lowest amount of material, but the sample must have a titer $>2*10^{12}$ cp/mL to obtain reliable data. However, such DP titers are well within the range of commonly used therapeutically useful titers.

After being able to measure the capsid titer easily by SEC, adsorption effects of AAV to the syringe and filter membrane during a sterile filtration process were studied. The finding that poloxamer 188 can drastically reduce the adsorption of AAV confirmed the previous literature regarding absorption to the syringe material. The further experiments confirmed this positive effect also with regard to adsorption to the filter membrane. Differences between filter materials were observed, as filtration with PVDF membranes was more beneficial in terms of absorbtion than RC or PES membranes.

III.5 Outlook

As the interest in gene therapy with AAV vectors is growing, there is an increasing need for robust and easy-to-use methods to determine the capsid titer. The new upcoming methods are easier to automate and require less work and time. Some of them are already established in the field of protein analytics and therefore well known to analytical laboratories.

It is possible to perform batch measurements using calibrated fluorescence detectors to get the total capsids number of purified AAV samples, as it was already done for HPLC based measurements (93). Instruments using fluorescence reading are fluorescence spectrometers or plate readers but also the Prometheus or Pantha systems (Nanotemper, Munich, Germany). To achieve more reliable data, a previous denaturation of AAV vectors can be helpful, as was done for the UV spectrometry measurement. Clearly lower LOQ and LOD are expected for fluorimetry compared to UV spectrometry.

Instead of a classical SDS-PAGE, CE-SDS (Maurice S. from Protein Simple, San Jose, CA, USA) or Bioanalyzer from Agilent Technologies (Santa Barbara, CA, USA) can be used to determine the sample purity and the total capsid amount. With these capillary- or chip-based SDS-PAGE methods, proteins up to 230 or 270 kDa, respectively, can be detected.

In experiments done in the context of the thesis, all three structural viral proteins (VPs) could be easily detected with these methods. All of them require only low volumes (4 up to 50 µL) and have a LOD of 10^{11} cp, which is comparable to conventional SDS-PAGE using Coomassie Blue staining. Caution should be exercised, as some matrix effects are known for samples with high salt concentrations or extreme pH (320, 321).

The main advantage of Bioanalyzer and CE-SDS is the time aspect: both take approximately 2 hours for the measurement, including sample preparation and running time, which is half of the time of classical SDS-PAGE. They are fast, reliable, can be automated, and offer protein and peptide characterization as well as quality control, and impurity detection.

Like SDS-PAGE, capillary isoelectric focusing (cIEF) has already been automated (PA 800 Plus Pharmaceutical Analysis system; SCIEX, Brea, CA, USA) and can be used for capsid and vector genome titer determination, because - like in AEX - it is possible to separate empty and full capsids by charge (207, 305). For the measurement, 3 µL containing 10^{11}cp are sufficient because a UV detector measuring at 280 nm is used (322). The ratio of full/partially filled/empty capsids can be calculated based on the corrected peak areas[1] of the separated capsid peaks in the cIEF electropherograms. Depending on the salt amount in the AAV sample, a buffer exchange might be necessary, which requires some extra time and could lead to loss of AAV. All in all, the method requires less than 1 h per sample and delivers additional insight into other impurities in the sample. Because of the small size of the AAV, use of methods already implemented for detection of subvisible particles like nanoparticle tracking analysis (NTA) requires labeling to make the AAV visible. For NTA the AAV were labeled with small gold nanoparticles (97). The resulting gold-labeled AAV particles scatter enough light to be visualized and tracked by the optical system, enabling the use of NTA to measure the size and concentration of AAV as well as aggregation state and formulation stability (97). Also, by using Virus Counter® (Sartorius Stedim Biotech GmbH, Göttingen, Germany) labeling of the AAV with a fluorescent dye is required. Sample preparation includes a 30 minutes labeling step and the method has been successfully applied to a variety of virus samples at different purification states (67). This technique is already in use for other viruses like lentiviruses for which it is also possible to determine the full-empty ratio in virus suspensions (98). The fluorescence signal can be

[1] With a correction factor, which must be determined for each serotype and plasmid vector, in order to not overestimate the full capsid due to the extra UV absorbance of the vector DNA

detected in the flowthrough of 195 µL for $5*10^5$ to 10^9 cp/mL. For the moment, this technique is only available for AAV2 and AAV3 because only for those two serotypes a Virotag is commercially available (99, 100).

Chapter IV Comparison of different liquid chromatography-based purification strategies for adeno-associated virus vectors

This chapter is published as: Rieser, R., Koch, J., Faccioli, G., Richter, K., Menzen, T., Biel, M., Winter, G. & Michalakis, S. (2021). Comparison of Different Liquid Chromatography-Based Purification Strategies for Adeno-Associated Virus Vectors. Pharmaceutics, 13(5), 748.

Author contributions: Conceptualization, S.M. and G.W.; data curation, R.R., J.K., G.F., T.M., K.R., and S.M.; formal analysis, R.R., T.M., and K.R.; funding acquisition, G.W., M.B., and S.M.; investigation, R.R., J.K., G.F., K.R., and T.M.; methodology, R.R., K.R., T.M., G.W., and S.M.; resources, G.W., T.M., K.R., M.B., and S.M.; supervision, G.W. and S.M.; visualization, R.R., K.R., T.M., and S.M.; writing—original draft, R.R. and S.M.; and writing—review and editing, T.M., K.R., and G.W. All authors have read and agreed to the published version of the manuscript.

Note from the authors:

The version included in this thesis is identical with the published article apart from minor changes. The reference, figure and table numbers were changed to fit into the coherent numbering of this document.

The published article can be accessed online via:

https://doi.org/10.3390/pharmaceutics13050748

IV.1 Abstract

Recombinant adeno-associated virus (rAAV) vectors have evolved as one of the most promising technologies for gene therapy due to their good safety profile, high transduction efficacy, and long-term gene expression in nondividing cells. rAAV-based gene therapy holds great promise for treating genetic disorders like inherited blindness, muscular atrophy, or bleeding disorders. There is a high demand for efficient and scalable production and purification methods for rAAV. This is particularly true for the downstream purification methods. The current standard methods are based on multiple steps of gradient ultracentrifugation, which allow for the purification and enrichment of full rAAV particles, but the scale up of this method is challenging. Here, we explored fast, scalable, and universal liquid chromatography-based strategies for the purification of rAAV. In contrast to the hydrophobic interaction chromatography (HIC), where a substantial amount of AAV

was lost, the cation exchange chromatography (CEX) was performed robustly for multiple tested serotypes and resulted in a mixture of full and empty rAAV with a good purity profile. For the used affinity chromatography (AC), a serotype dependence was observed. Anion exchange chromatography (AEX) worked well for the AAV8 serotype and achieved high levels of purification and a baseline separation of full and empty rAAV. Depending on the AAV serotype, a combination of CEX and AEX or AC and AEX is recommended and holds promise for future translational projects that require highly pure and full particle-enriched rAAV.

Keywords: adeno-associated virus; rAAV vector; column purification; empty capsids; ion exchange chromatography; affinity chromatography

IV.2 Introduction

Recombinant adeno-associated viral (rAAV) vectors have emerged as very promising gene delivery tools and have been already used in more than 190 clinical trials across different indications with very good safety characteristics (287-289, 323). A high number of immunologically distinct serotypes of AAV are currently in use; however, rAAV based on serotype 2 (AAV 2) have been most extensively evaluated in preclinical studies, as this was the first serotype to be fully characterized (324). Accordingly, there is a growing need for scalable commercial production and purification methods. The manufacturing processes for rAAV are composed of three phases: (i) upstream, which entails the production of the rAAV, (ii) downstream, which involves the purification of the AAV, and (iii) formulation/fill and finish processes, which ensure optimal stability and dosing at the desired therapeutic dose (325). Here, we focus on the downstream purification process.

In the past two decades, many protocols for the purification of rAAV vectors have been established (26, 74, 127, 175, 176, 191, 326, 327). Downstream purification processes are designed to remove process-related impurities such as host cell proteins, host cell DNA, and process additives, as well as product-related impurities, such as aggregated vectors and empty capsids that are generated during the upstream process (7). One way to purify rAAV vectors is cesium chloride (CsCl) or iodixanol gradient ultracentrifugation, and the material purified by such methods has been used in several clinical trials (328-330). The main advantage of these gradient ultracentrifugation protocols is the flexibility to be used with minimal adaptation to efficiently purify different AAV serotypes and the ability to separate full rAAV from empty particles. Nevertheless, gradient ultracentrifugation methods are

typically limited to product volumes of a few hundred microliters, are not readily scalable, and are difficult to run under GMP. In contrast, the liquid chromatography-based purification methods offer scalable alternative methods that enable the manufacturing of rAAV with high purity, potency, and consistency. However, chromatography resins and conditions are often uniquely developed and tailored for each serotype, and the efficient removal of vector-related impurities such as empty capsids is challenging (26). The impact of empty capsids on the potency and immunogenicity is discussed (42), and therefore, protocols for their efficient removal are desired and currently explored by several groups and companies. Here, we present data on the liquid chromatography column-based purification processes for AAV2/8, comparing affinity chromatography (AC) with hydrophobic interaction chromatography (HIC) and cation exchange chromatography (CEX), followed, in both cases, by anion exchange chromatography (AEX) to separate full from empty capsids. In AEX method development, we were able to achieve a baseline separation between genome-loaded and empty capsids.

The protocol of the AC and CEX could also be applied for the purification of AAV2 and resulted in a similar level of purification.

IV.3 Materials and methods

IV.3.1 AAV production

Recombinant AAV vectors with genomes carrying inverted terminal repeats derived from AAV2 and packaged with wildtype AAV2 or AAV8 or engineered AAV2 capsids (AAV2.NN and AAV2.GL) were produced and purified as previously described in adherent HEK293T cells (The Leibniz Institute DSMZ-German Collection of Microorganisms and Cell Cultures GmbH, Braunschweig, Germany) (293, 294). The packaged self-complementary (sc) genome comprised a CMV promoter driving expression of eGFP (331).

IV.3.2 Tangential flow filtration—TFF

For some rAAV vector batches, the cell culture supernatant was harvested, filtered, and concentrated by tangential flow filtration (TFF) performed with a KrosFlo® KRi2 universal using a 100-kDa mPES membrane from Repligen (Waltham, MA, USA) and buffered in 1× PBS (10 mM Na_2HPO_4, 1.8 mM KH_2PO_4, 4.27 mM KCl, and 137 mM NaCl, pH 7.4).

IV.3.3 PEG precipitation

For other rAAV vector batches, the cell culture supernatant was harvested three days and, for AAV8, also six days after transfection and filtered with a 0.45-µm filter. Subsequently, polyethylene glycol (PEG) 8000 (Merck, Darmstadt, Germany) was added to the supernatant to a final concentration of 8% (v/v). The mixture was centrifuged for 15 min at 1756× g at 4 °C. The supernatant was discarded, and the pellet was resuspended with 7.5 mL of PBS. To degrade free DNA, 2-µL Benzonase (Merck, Darmstadt, Germany; final concentration 50 U/mL) was added to the sample and incubated at 37 °C for 30 min and subsequently purified on the affinity column (AC), hydrophobic interaction chromatography (HIC) column, or directly by the cation exchange column (CEX).

IV.3.4 Cell pellet

In case the rAAV vectors were to be harvested from the cell pellet, the cells were detached from the culture dishes with a cell scraper, for AAV2 three and for AAV8 six days after transfection, collected into a centrifuge beaker, and pelleted by centrifugation at 1756× g at 4 °C for 15 min. Subsequently, the supernatant was decanted, and the cell pellet was resuspended in 7.5 mL of 50 mM Tris(hydroxymethyl)aminomethane (Tris)-HCl and 150 mM NaCl, pH 8.5. The resuspended cells were frozen three times with liquid nitrogen and thawed to 37 °C. After the last cycle of thawing, 2 µL of Benzonase (Merck, Darmstadt, Germany; final concentration 50 U/mL) were added and incubated for 30 min at 37 °C, followed by centrifugation at 4 °C, 1756× g for 25 min to separate the pellet and supernatant. The supernatant was collected and subsequently purified on the affinity column (AC), hydrophobic interaction chromatography (HIC) column, or to the cation exchange column (CEX).

IV.3.5 rAAV vector purification

All purifications using liquid chromatography were performed with an ÄKTA purifier from Cytiva (Marlborough, MA, USA). For sample loading, a Superloop or sample pump were used. All runs were performed at room temperature (25 °C), and the detection was done with a UV detector (UL-9, fixed wavelength) at 280 nm implemented in the ÄKTA system. The evaluation was done with Unicorn Software (7.3) (Cytiva, Marlborough, MA, USA).

IV.3.5.1.1 Hydrophobic interaction chromatography—HIC

The CIMmultus OH monolith column (1 mL, 2-µm pores; BIA separations, Ajdovščina, Slovenia) was used for HIC. The sample was diluted 2-fold with 3 M K_2HPO_4 (Merck,

Darmstadt, Germany), 2% glucose (Sigma-Aldrich Chemie GmbH, Steinheim, Germany), pH 7.0, and then filtrated over a 0.45-µm mPES membrane filter. After equilibration with 1.5-M K_2HPO_4 and 1% glucose, pH 7.0, the sample was loaded onto the column with a flow rate of 2 mL/min. For elution, the flow rate was set to 3 mL/min, and the gradient was run in 20 column volumes (CV) from 0% to 100% 50 mM K_2HPO_4 and 1% glucose, pH 7.0. The columns were washed in the cleaning in place (CIP) mode with 1 M NaOH (VWR, Geldenaaksenbaan, Belgium) for reuse (332).

IV.3.5.1.2 Cation exchange chromatography—CEX

The CIMmultus SO_3 column (1 mL, 2-µm pores; BIA separations) was used for CEX chromatography. The pooled peak fractions from the HIC, the PEG precipitates, or the cell lysates were diluted 10-fold with 25-mM sodium acetate ($C_2H_3NaO_2$) (Grüssing, Filsum, Germany) and 50 mM sodium chloride (NaCl) (Bernd Kraft, Duisburg, Germany) to achieve a conductivity of 15 to 20 mS/cm. The pH was adjusted to 4.0. After column equilibration with 50 mM sodium acetate and 100 mM NaCl, pH 4.0, the loading of the diluted sample was done at a flow rate of 5 mL/min. Elution was run with a 3 mL/min flow rate and a gradient ranging from 0% to 100% 50 mM $C_2H_3NaO_2$ and 2-M NaCl, pH 4.0, within 20 CVs. The column was washed in the cleaning in place (CIP) mode with 1 M NaOH and 2 M NaCl after each run.

IV.3.5.1.3 Anion exchange chromatography—AEX—salt gradient

The final purification step to separate the full and empty rAAV particles was performed with the CIMmultus QA column (1 mL, 2-µm pores; BIA separations). The peak containing fractions from the CEX or AC elutions were pooled and diluted 30-fold with 20 mM Tris (Sigma-Aldrich Chemie GmbH, Steinheim, Germany) and 2 mM $MgCl_2$ (Applichem GmbH, Darmstadt, Germany) and adjusted to pH 9.0. Required starting conductivity for the AEX was around 3–5 mS/cm. After column equilibration with 20 mM Tris and 2 mM $MgCl_2$, pH 9.0, the loading of the diluted sample was done at a flow rate of 6 mL/min. Elution was performed at a 3 mL/min flow and a gradient ranging from 5% to 50% 20 mM Tris, 2 mM $MgCl_2$, and 500 mM NaCl, pH 9.0, within 60 CVs. The column was cleaned in the cleaning in place (CIP) mode with 1 M NaOH and 2 M NaCl after each run (193, 332).

IV.3.5.1.4 Anion exchange chromatography—AEX—pH gradient

The CIMmultus PrimaS (AAV) column (1 mL, 2-µm pores; BIA separations) was evaluated as an additional option for separating empty from full rAAV. Buffer A contained 10 mM Tris, 10 mM bis-tris-propane (Sigma-Aldrich Chemie GmbH, Steinheim, Germany), 2 mM $MgCl_2$, and 0.1% poloxamer 188 (Kolliphor P 188, BASF, Ludwigshafen, Germany) at pH 8.0, and buffer B had the same composition but at pH 10.0. To achieve a conductivity below 4 mS/cm, the samples from CEX or AC were diluted 30-fold with dilution buffer (buffer A diluted 2-fold with water), and the pH was adjusted to 8.0. Loading and elution were performed at a flow rate of 4 mL/min and a linear pH gradient ranging from 0% to 100% B within 100 CVs. In some cases, a step gradient was used.

IV.3.5.1.5 Affinity chromatography—AC

For affinity chromatography (AC), a Poros capture select AAVx column (1 mL; Thermo Fisher Scientific, Dreieich, Germany) was used. AAV samples in PBS at pH 7.4 were loaded at a flow rate of 0.3 mL/min on the column and eluted with 100 mM citric acid (VWR, Geldenaaksenbaan, Belgium), pH 3.0, at a flow rate of 0.7 mL/min. AAV were neutralized by elution into 1 M Tris, pH 8.7. The used column was purified by cleaning in place with 100 mM phosphoric acid (Merck, Darmstadt, Germany), pH 2.0, and 6 M guanidine HCl (Sigma-Aldrich Chemie GmbH, Steinheim, Germany).

IV.3.6 Vector genome titer determination by qPCR

The vector titer was measured by real-time quantitative polymerase chain reaction (qPCR) and carried out with the QuantStudio 5 system (Thermo Fisher scientific, Dreieich, Germany). AAV2-free ITR qPCR was performed as described by D'Costa et al (110).

IV.3.7 Determination of HEK 293T DNA

Determination of HEK cell DNA was done on a QuantStudio 5 system (Thermo Fisher Scientific, Dreieich, Germany) with a SYBR Green qPCR assay designed to amplify a 94-bp Alu sequence using the following primers: 5′-GAGGCGGGCGGATCA-3′ (forward) and 5′-CCCGGCTAATTTTTGTATTTTTAG-3′ (reverse) (163).

IV.3.8 Sodium dodecyl sulfate polyacrylamide gel electrophoresis—SDS-PAGE

Samples were loaded on a 6–12% Tris-HCl gel after the addition of Laemmli 4× (Bio-Rad, Hercules, CA, USA) and denaturation at 95 °C for 5 min. After electrophoresis for 40 min at 200 V in denaturing conditions, the gel was silver-stained and pictures were taken by ChemiDog (Bio-Rad, Feldkirchen, Germany) (66).

IV.3.9 Sedimentation velocity analytical ultracentrifugation—SV-AUC

Sedimentation velocity analytical ultracentrifugation (SV-AUC) was performed on an Optima AUC instrument (Beckman Coulter, Brea, CA, USA). rAAV samples were loaded into AUC cells with standard 2-sector centerpieces (Beckman Coulter, Brea, CA, USA) into both sectors. Sedimentation of particles was monitored at 16,336× g at the wavelengths of 230 nm, 260 nm, and 280 nm in an AN Ti-50 rotor (Beckman Coulter, Brea, CA, USA). Data analysis was then performed in UltraScan III (AUC Solutions, Katy, TX, USA) using the intensity signal of each sample cell. Data were processed to contain the relevant scan range and optimal solutions for the time-invariant and radial-invariant noises, which were determined together with the optimal meniscus position. Final fitting was performed with the PCSA-SL-MC model and the statistical evaluation based on 100 Monte-Carlo simulations. Peak integration was performed to derive the relative contents of the empty (~65 S) and filled capsids (~105 S) and of the formulation components, such as small proteins, DNA fragments, and smaller unidentified species. For determination of the full/empty ratio, the same factors for 260 nm and 280 nm were used as in the analytical AEX experiments, and for 230 nm, a correction factor of 1.6 was used.

IV.3.10 Analytical anion exchange chromatography

For the analytical separation of full and empty rAAV, a Waters 2695 system (Eschborn, Germany) and a Protein-Pak Hi Res Q column (5 µm, 4.6 × 100 mm; Waters GmbH, Eschborn, Germany) were used. Therefore, 70 mM bis-tris-propane (Sigma-Aldrich, St. Louis, MO, USA) and 2 mM $MgCl_2$, pH 9.0, were used as buffer A. Adding 1-M tetramethylammoniumchlorid (Sigma-Aldrich, St. Louis, MO, USA) to buffer A created buffer B. At a flow rate of 0.3 mL/min, a gradient from 10% to 30% B in 20 min was performed to separate the full and empty AAV. rAAV elution was detected at 280 nm and 260 nm with a UV detector (Waters 2487) and with a fluorescence detector (Dionex RF2000, Sunnyvale, CA, USA) at excitation and emission wavelengths of 280 nm 330 nm, respectively. The chromatograms were integrated with Chromeleon V6.8 (Thermo Fisher Scientific, Dreieich, Germany). For the correct determination of a fraction of empty rAAV, the following equation, according to Reference (96), was used:

$$\%\, Empty\ capsids = 100 \times \frac{Area_{empty}}{(Area_{empty} + \frac{Area_{full}}{RF_{F/E}})}$$

$RF_{F/E}$ fluorescence detection: 0.85, UV 260 nm: 7.69, and UV 280 nm:

IV.4 Results

IV.4.1 Evaluation of two different liquid chromatography-based purification strategies for rAAV2/8 vectors

We evaluated different purification strategies based on the liquid chromatography columns (Figure IV.1). For the initial testing, we decided to work with AAV8-pseudotyped AAV2 (rAAV2/8) vectors carrying a self-complementary (sc) genome with a CMV_eGFP gene expression cassette. The harvested rAAV vectors from the same batch were split into two parts, which were subsequently purified with different purification strategies. Purification process HIC-CEX-AEX was a three-step process consisting of hydrophobic interaction chromatography (HIC), followed by cation exchange chromatography (CEX) and, finally, anion exchange chromatography (AEX). Figure IV.2 summarizes the results obtained with HIC-CEX-AEX and AC-AEX for rAAV2/8. In the HIC-CEX-AEX process, the combination of HIC and CEX successfully removed most of the DNA and protein impurities (Figure IV.2A,B), and the final AEX step was able to separate, at least to some extent, the full and empty rAAV (Figure IV.2C).

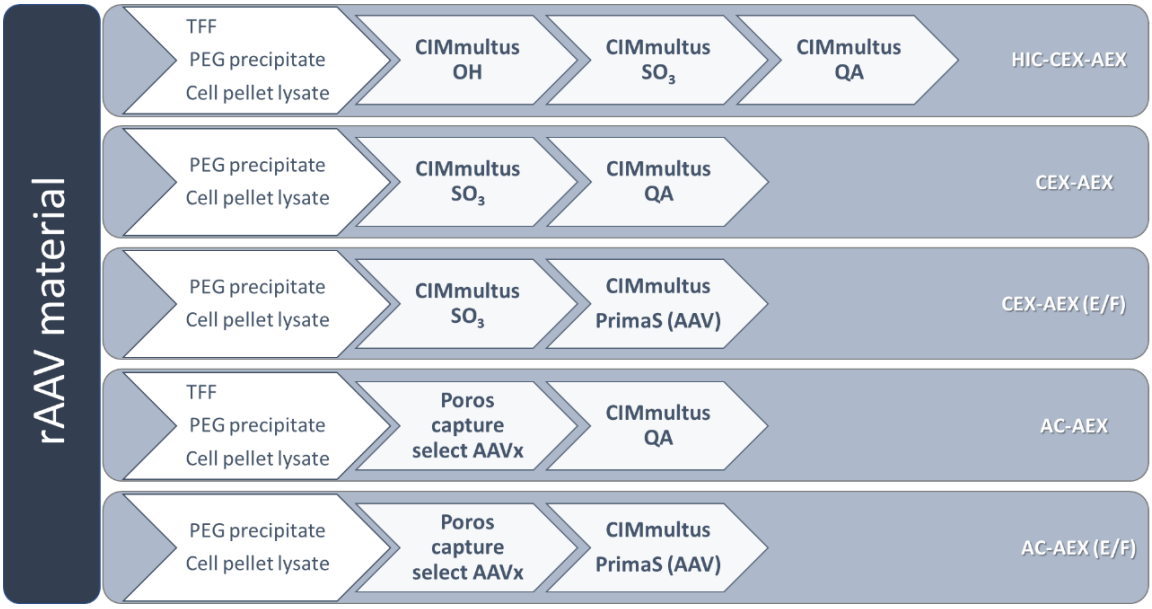

Figure IV.1 Overview of the five tested purification strategies to purify and to separate the empty and full recombinant adeno-associated virus (rAAV). For each experiment, only one harvesting method mentioned in the first arrow was performed. The abbreviations (in white) on the right side are also used throughout the text and refer here to the shown purification processes. AC, affinity chromatography; AEX, anion exchange chromatography; CEX, cation exchange chromatography; HIC, hydrophobic interaction chromatography; PEG, polyethylene glycol; TFF, tangential flow filtration.

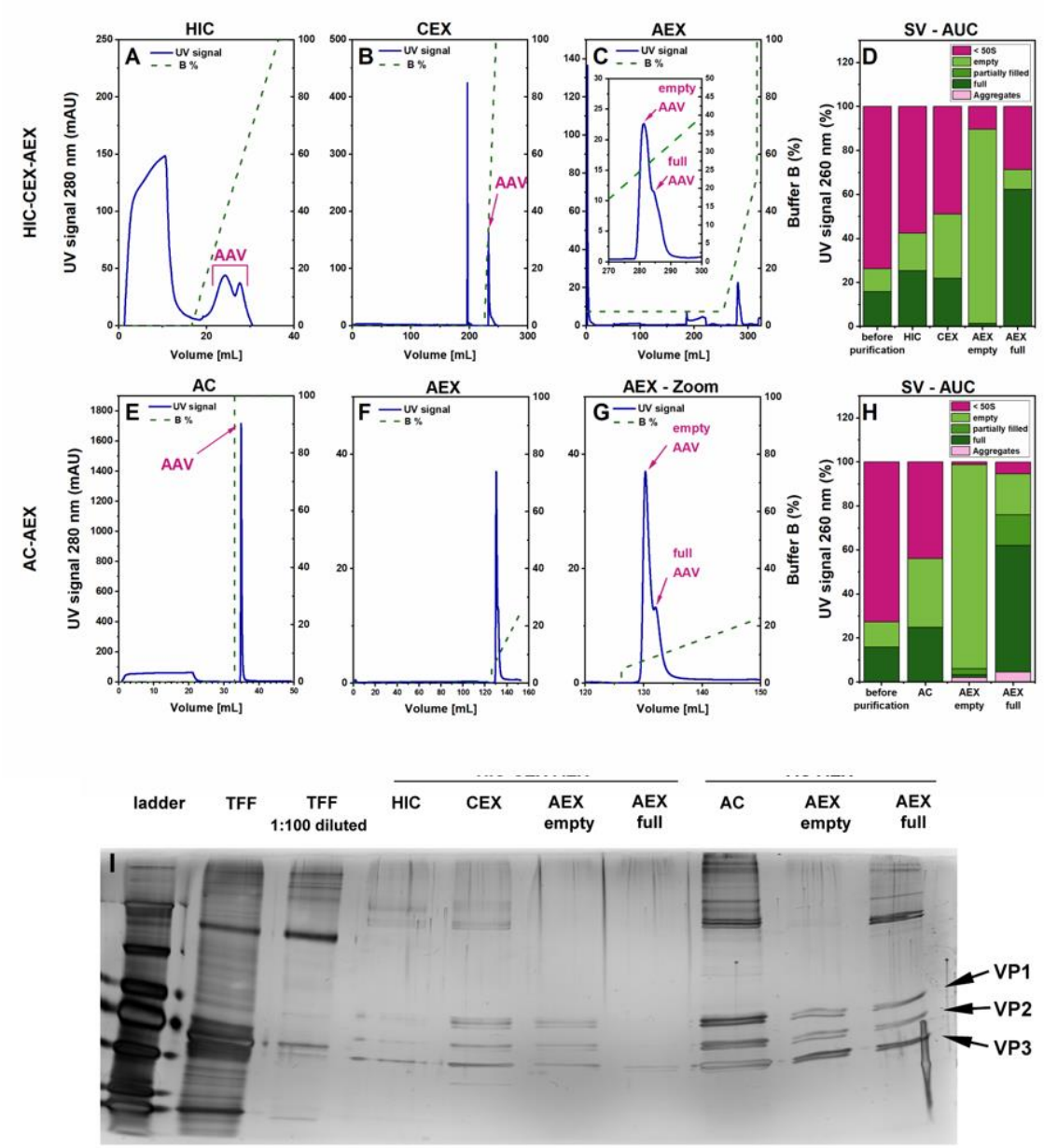

Figure IV.2 Comparison of HIC-CEX-AEX and AC-AEX for purification of the rAAV2/8 vectors. Each chromatogram shows the respective ultra-violet (UV) signal in blue (scale on the left Y-axis) and the concentration of buffer B depicted as a dashed green line (scale on the right). (A–C) Chromatograms obtained with HIC-CEX-AEX in three subsequent steps on a HIC (A), a CEX (B), and an AEX (C) column. (D) SV-AUC analysis of rAAV2/8 of the indicated samples from different purification states. (E,F) Chromatograms obtained with AC-AEX in two subsequent steps on an AC (E) and an AEX (F) column. (G) Magnification view of the AEX chromatogram shown in F (focusing on the 120–150-mL range) to better visualize the peaks of the empty and full rAAV. (H) SV-AUC analysis after AC and AEX. (I) Silver-stained sodium dodecyl sulfate polyacrylamide gel electrophoresis (SDS-PAGE) of the rAAV material after TFF, and the intermediate steps from the purification downstream processes HIC-CEX-AEX and AC-AEX. AC, affinity chromatography; AEX, anion exchange chromatography; CEX, cation exchange chromatography; HIC, hydrophobic interaction chromatography; PEG, polyethylene glycol; rAAV, recombinant adeno-associated virus; TFF, tangential flow filtration; VP, viral protein.

In contrast, AC-AEX is a two-step process and starts with affinity chromatography (AC) on a Poros capture select AAVx column, which can selectively capture AAV capsids (12, 176, 333, 334), while most of the DNA and protein impurities are not retained on the column (Figure IV.2E). In the second step, the same AEX as in HIC-CEX-AEX was used (Figure IV.2F,G).

To better characterize the purification process, we compared the eluates containing rAAV from each purification step with the starting material using sedimentation velocity analytical ultracentrifugation (SV-AUC). The SV-AUC results for HIC-CEX-AEX and AC-AEX are depicted in Figure IV.2D,H, respectively. In both cases, a relative increase of the rAAV-containing fractions was observed after each purification step, indicative of an improvement in the purity. A separation of full rAAV from empty capsids could also be observed with HIC-CEX-AEX and AC-AEX. The highest purity was achieved for the empty capsid fraction, which seemed to be devoid of impurities and full capsids. While the full capsid fraction showed a clear enrichment, this fraction in HIC-CEX-AEX and AC-AEX still contained some empty capsids and other impurities (Figure IV.2D,H). Some degree of aggregation was observed after the AEX in AC-AEX.

The SDS-PAGE results also clearly showed the purity improvement along the HIC-CEX-AEX and AC-AEX purification processes, starting with a high number of additional bands indicative of impurities for the sample after TFF. Directly after the first purification step, a clear improvement was detected, and the three protein bands of VP1, VP2, and VP3 could be seen. For AC-AEX, the overall concentration of the rAAV vectors at the end seemed higher than for HIC-CEX-AEX. Some additional bands in the sample containing the full rAAV were detected between 130 and 250 kDa, which might be the vector DNA.

IV.4.2 Different initial steps for the raw material

Next, we explored how HIC-CEX-AEX and AC-AEX performed with differently harvested rAAV vector materials. First, we used pooled cell culture supernatants and cell pellet lysates filtered, concentrated, and buffer-exchanged by TFF, which also possibly removed some impurities (335). Second, we precipitated the rAAV vectors with PEG from the cell culture supernatant only. Third, we pelleted the producer cells and purified the rAAV vectors from the cell pellet lysate. As shown in Figure IV.3, we were able to consistently

purify the rAAV vectors with HIC-CEX-AEX and AC-AEX and from all three starting materials.

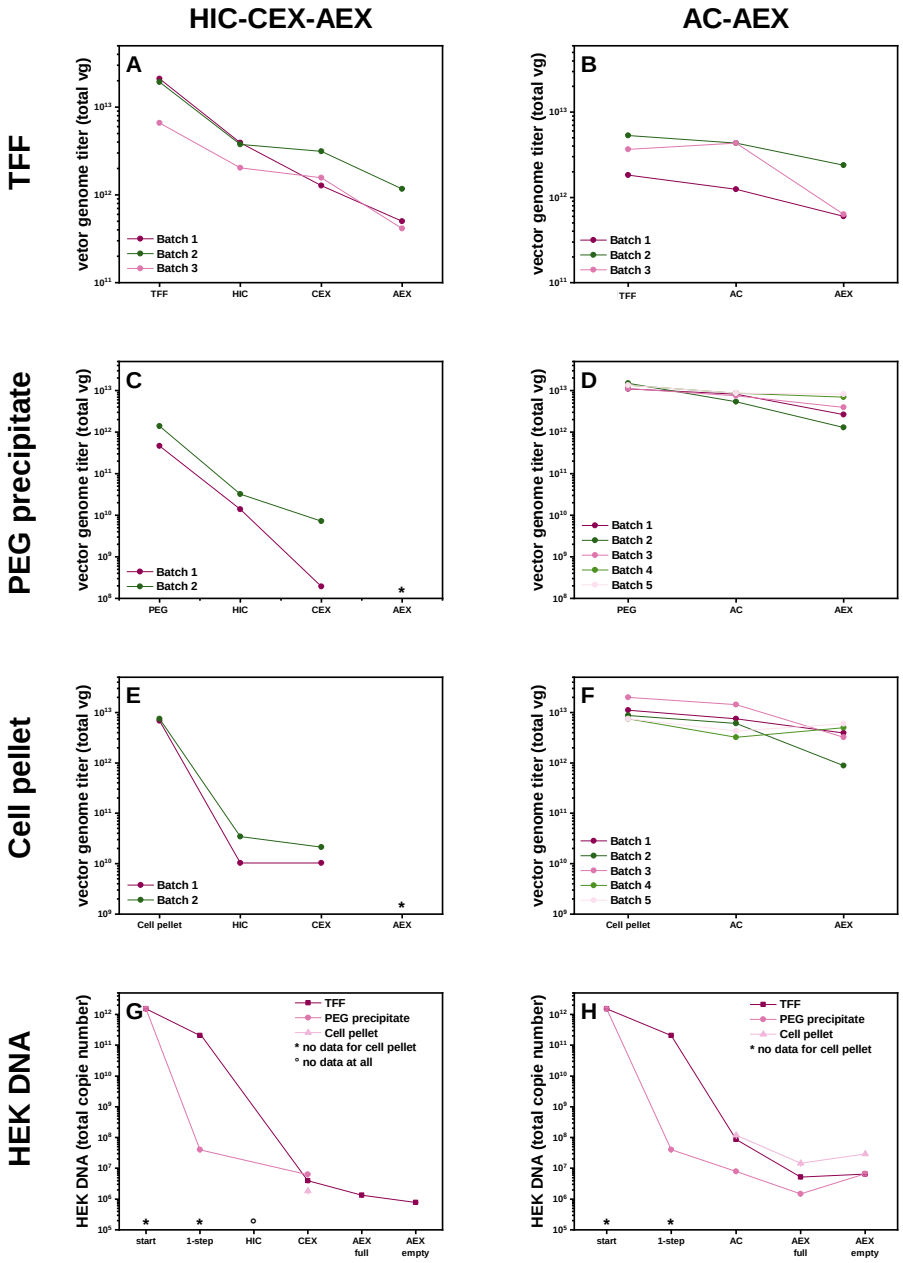

Figure IV.3 Effect of different harvesting methods on the rAAV2/8 vector production yield and pureness of the human embryonic kidney (HEK) 293T cell DNA**.** (A–F) Graphs showing the yield (total vector genomes, vg) for the rAAV2/8 vectors obtained with the two strategies, with materials harvested from (A,B) the cell culture supernatant and cell pellet lysate filtered, concentrated, and buffer-exchanged by tangential flow filtration (TFF) (n = 3). (C,D) Culture supernatant by polyethylene glycol (PEG) precipitation (C), followed by HIC-CEX (n = 2) and (D) followed by AC-AEX (n = 5) or (E,F) cell pellet lysate (E) followed by HIC-CEX (n = 2) and (F) followed by AC-AEX (n = 5). (G,H) Graphs showing the removal efficiency of the strategies for HEK cell DNA at all the purification steps. AC, affinity chromatography; AEX, anion exchange chromatography; CEX, cation exchange chromatography; HIC, hydrophobic interaction chromatography; PEG, polyethylene glycol; rAAV, recombinant adeno-associated virus.

According to the vector genome (vg) titers, there was some loss of rAAV vectors during the different steps of the downstream process AC-AEX, ending up with a maximum remaining yield of 44% ($4*10^{12}$ vg) after AEX of the initial vg amount ($1*10^{13}$ vg). The corresponding values for the different purification steps are summarized in Table IV.1.

Table IV.1 Remaining percentage of the original vg amount of rAAV after the distinct process steps.

Purification Strategy	Purification Step	TFF (%)	SD (%)	PEG Precipitate (%)	SD (%)	Cell Pellet Lysate (%)	SD (%)
HIC-CEX-AEX	HIC	23	6	3	-	0.3	-
	CEX	15	7	0.3	-	0.2	-
	AEX	5	2	ND	ND	ND	ND
CEX-AEX	CEX	ND	ND	ND	ND	65	13
	AEX	ND	ND	ND	ND	59	24
AC-AEX	AC	89	21	69	24	59	12
	AEX	32	11	44	21	37	23

ND: not done.

For the HIC-CEX-AEX protocol, we observed a significant drop of the vg titer after the HIC step (Figure IV.3B,D,F). After the HIC step, we could recover 23% of the rAAV when starting with material coming from the TFF. In contrast, the recovery was only 3% from the PEG precipitates and only 0.3% when starting with cell pellet lysates. For the samples from the TFF, we performed the subsequent AEX step and could recover 5% of the originally harvested rAAV in the full fraction. The data are summarized in Table IV.1. Due to the low yield, we decided not to perform the AEX step with the corresponding samples from the PEG precipitates or the cell pellet lysates.

The determination of the HEK cell DNA showed a clear reduction in HEK cell DNA for the HIC-CEX-AEX and AC-AEX processes. For the starting material of the cell pellet lysate, and for all the samples of the HIC step, it was not possible to determine the amount of HEK cell DNA in the sample because of the matrix effects in the qPCR. We figured out that the first very effective step in the purification process for the supernatant material was PEG precipitation. As expected, the TFF also reduced the amount of DNA and protein impurities but less than the PEG precipitation. In the case of the TFF treatment, the AC, as well as the CEX, were able to reduce the amount of HEK cell DNA. The AEX step further

improved the amount of the residual HEK cell DNA in the full rAAV and even more for the empty capsid fraction.

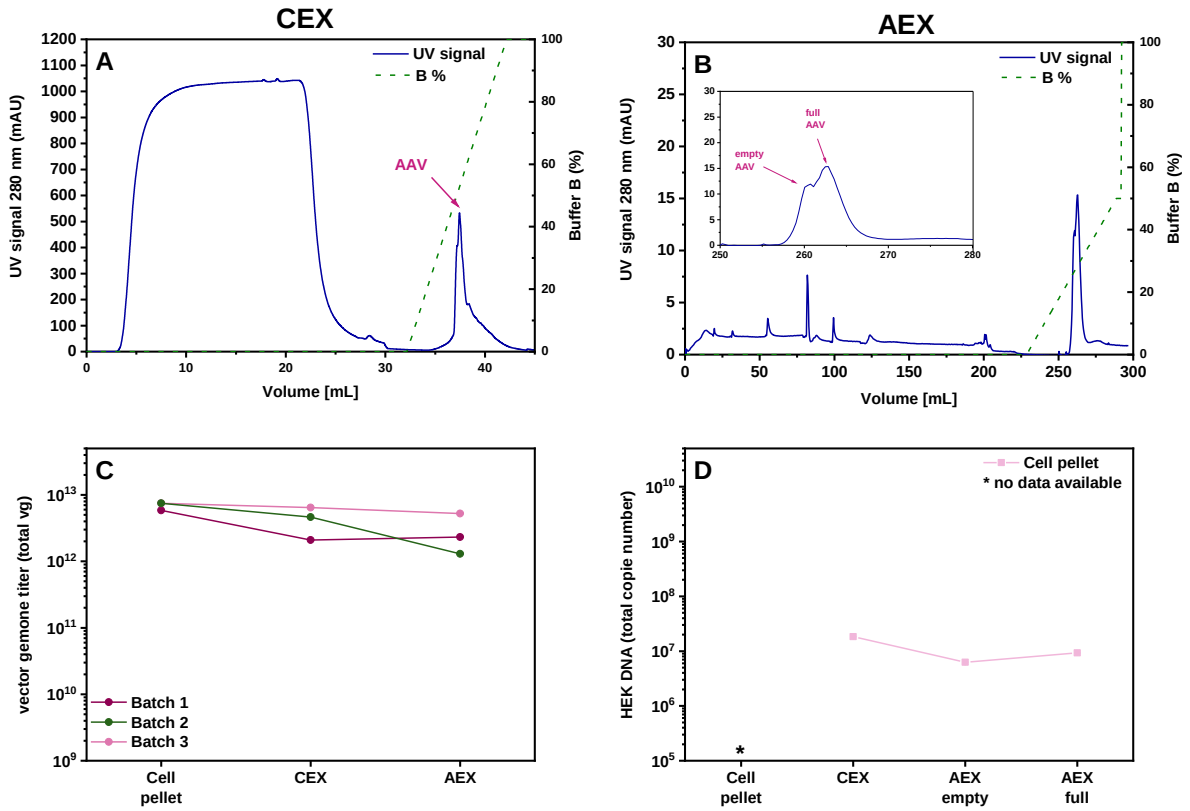

Figure IV.4 Purification of the rAAV2/8 vectors using the CEX-AEX process. (A–C) Chromatograms obtained with cell pellet materials in only two steps on the CEX (A) and AEX (B) columns. (A) CEX with a linear buffer B gradient. (B) AEX with a linear buffer B gradient. Magnification view of the AEX chromatogram shown in B. Each chromatogram shows the respective UV signal in blue (scale on the left Y-axis) and the concentration of buffer B depicted as a dashed green line (scale on the right). (C) Graph showing the yield (total vector genomes, vg) for the rAAV2/8 vectors obtained in CEX-AEX with the material harvested by lysis of the cell pellet. The residual HEK cell DNA amount is shown in (D). Due to matrix effects in the qPCR, the starting amount cannot be shown here. AAV, recombinant adeno-associated virus; AC, affinity chromatography; AEX, anion exchange chromatography; CEX, cation exchange chromatography.

Given the high loss observed during the HIC step of HIC-CEX-AEX, we decided to test whether it is possible to skip this step and directly load the sample onto the CEX. As shown in the corresponding chromatogram in Figure IV.4A, omission of the HIC step did not impair proper purification at the CEX column. The same plateau in the UV signal during the sample loading, as in the HIC, was seen in the CEX when the cell pellet lysate material was directly loaded onto the CEX. The amount of rAAV eluted from the column was 65% for the cell pellet lysate (Table IV.1). Absolute yield in vg titer for the cell pellet is shown

in Figure IV.4C. Further purification of the sample on the AEX column resulted in a recovery of 59% of the rAAV from the cell pellet lysate (Figure IV.4B). Thus, this simplified CEX-AEX process performed better than the original downstream process HIC-CEX-AEX. The residual amount of HEK cell DNA was comparable with the amount in the samples purified by AC-AEX (Figure IV.4D).

IV.4.3 Anion exchange chromatography using a pH gradient

All tested protocols have so far used the same AEX column (QA column, BIA Separations), which, in principle, allowed for the separation of full rAAV from empty capsids. However, an optimal (i.e., baseline) separation of the corresponding chromatography peaks could not be achieved. We therefore explored another preparative AEX column (CIMmultus PrimaS (AAV), BIA separations) for full/empty separation. With this column, a linear pH gradient was used for AAV separation, ranging from pH 8.0 to 10.0. The results obtained with this strategy CEX-AEX(E/F) are depicted in Figure IV.5. A clear separation of the full and empty rAAV peaks could be achieved (Figure IV.5B). Still, up to 28% of the empty capsids were found in the fractions containing the full rAAV (Table IV.2). The residual amount of empty capsids was determined by analytical AEX (Figure IV.S1). We therefore tested a step gradient instead of a linear buffer B gradient. In particular, each step of the B gradient was designed to start at the amount of buffer B that corresponded to the peak maxima previously observed in the linear gradient experiment (Figure IV.5B).

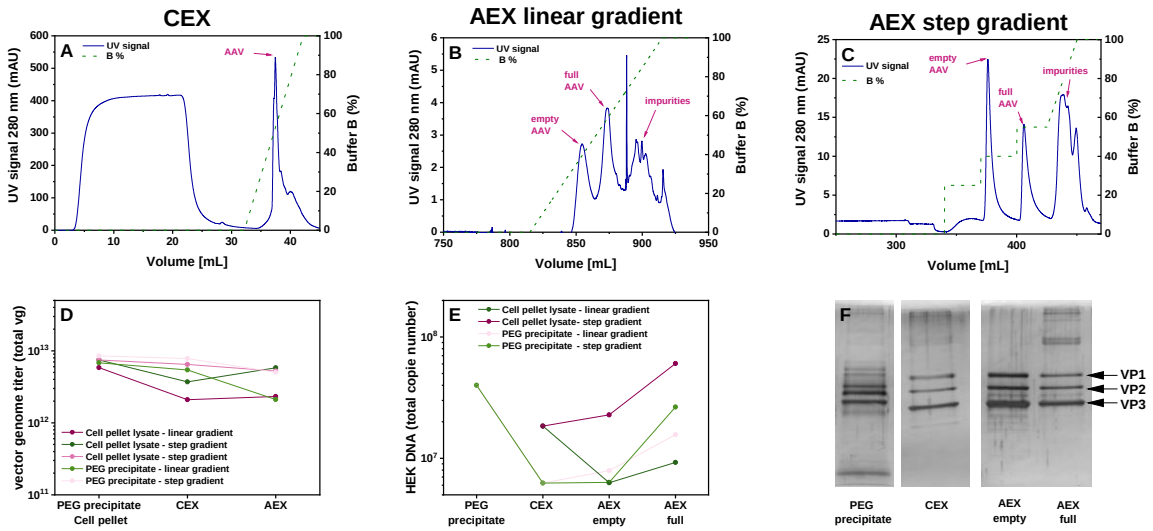

Figure IV.5 Purification of the rAAV2/8 vectors using CEX-AEX(E/F). (A–C) Chromatograms obtained with a PEG-precipitated material and a CEX-AEX(E/F) process in only two steps on a CEX (A) and a novel CIMmultus PrimaS (AAV) (B,C) column. (A) CEX with a linear buffer B gradient. (B) CIMmultus PrimaS (AAV) with a linear buffer B gradient. (C) CIMmultus PrimaS (AAV) with a step gradient of 25%, 40%, and 55% buffer B. Each chromatogram shows the respective UV signal in blue (scale on the left Y-axis) and the concentration of buffer B depicted as a dashed green line (scale on the right). (D) Graph showing the yield (total vector genomes, vg) for the rAAV2/8 vectors obtained in the CEX-AEX(E/F) downstream process with material harvested by PEG precipitation (n = 2) from the cell culture supernatant and cell pellet lysate (n = 3). (E) Residual human embryonic kidney (HEK) cell DNA amount determined by real-time quantitative polymerase chain reaction (qPCR). (F) Silver-stained sodium dodecyl sulfate polyacrylamide gel electrophoresis (SDS-PAGE) of the material from each step of the purification CEX-AEX(E/F) downstream process. AEX, anion exchange chromatography; CEX, cation exchange chromatography; PEG, polyethylene glycol; rAAV, recombinant adeno-associated virus; TFF, tangential flow filtration; VP, viral protein.

Table IV.2 Amount of empty capsids in the fractions containing full rAAV determined by analytical AEX.

Purification Strategy	Number of Preparations	Residual Amount of Empty Capsids in Full rAAV Fractions (%)	
		Entire Peak	Peak Maximum
CEX-AEX(E/F) linear	1	27	21
	2	31	23
CEX-AEX(E/F) steps	1	17	8
	2	17	12
	3	20	9
AC-AEX(E/F) linear	1	23	15
	2	40	28
AC-AEX(E/F) steps	1	20	13

As shown in Figure IV.5C, this step gradient protocol resulted in baseline separated peaks for the empty capsids and full rAAV, respectively. While the separation was improved, as calculated from the analytical AEX, around 19% of the empty capsids were still present in the fractions corresponding to the peak of the full rAAV. The overall yield of around 70% of the rAAV from the starting vg amount after CIMmultus PrimaS (AAV) for the CEX-AEX(E/F) process was quite promising (Table IV.3) and resulted in high genomic titers (Figure IV.5D).

Table IV.3 Remaining percentage of the original vg amount of rAAV after each different purification step.

Purification Strategy	Number of Preparations	Purification Step	Yield (%)
CEX-AEX(E/F) linear	1: Cell pellet	CEX	64
		AEX	70
	2: PEG pellet	CEX	80
		AEX	31
CEX-AEX(E/F) steps	1: Cell pellet	CEX	86
		AEX	70
	2: Cell pellet	CEX	55
		AEX	78
	3: PEG pellet	CEX	92
		AEX	63

Next, we assessed the purity profile and found quite a low amount of HEK cell DNA (Figure IV.5E) and rather low levels of non-VP bands in the SDS-PAGE (Figure IV.5F). The PEG precipitate as the starting material showed some additional bands around the actual VP1–3 bands, which disappeared after the subsequent purification steps and resulted in marked VP1, VP2, and VP3 bands.

IV.4.4 Comparison of yields of full rAAV harvested from cell pellet and supernatant

Comparison of the AEX chromatograms from the experiments with different starting materials revealed a difference in the ratio of empty and full rAAV vectors obtained from the PEG precipitate (Figure IV.5C) and cell pellet lysate (Figure IV.4B). We therefore investigated this further. As shown in Figure IV.6A, the fraction of full over empty rAAV is higher using cell pellet lysate as the starting material. To analyze this in more detail, we investigated five individual batches and consistently found the ratio of full/empty capsids to be constant in the different conditions and always lower when starting from the PEG precipitate material. Thus, the cell pellet lysate material consistently yielded a higher amount of full rAAV.

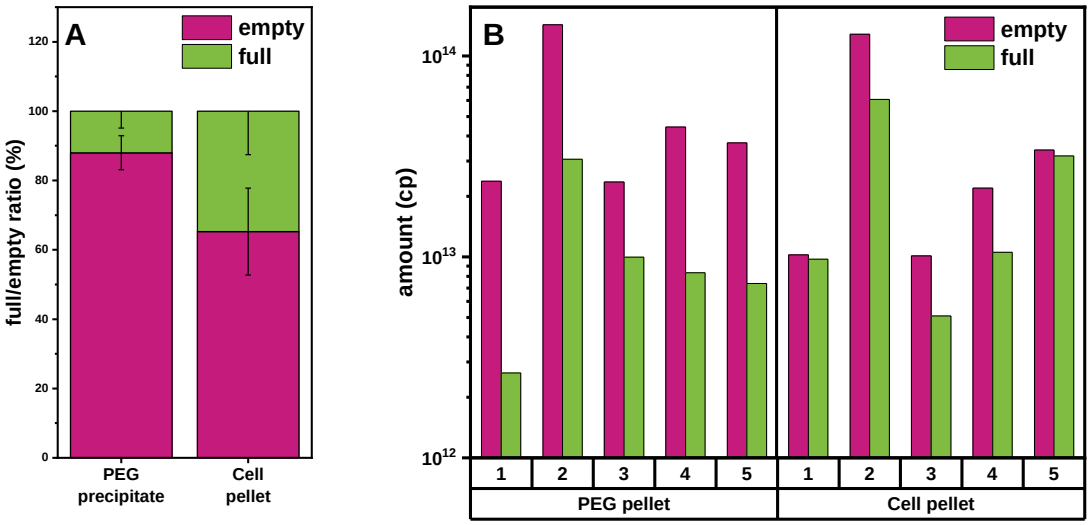

Figure IV.6 Assessment of the full/empty ratios from the PEG precipitate or cell lysate using analytical AEX chromatography. (A) Graph showing the full rAAV (light green) and empty capsid (purple) titer ratio determined using analytical AEX combined with a fluorescence detector. (B) Graph depicting the total amount of empty or full capsid values of 5 individual batches obtained from the PEG precipitate or from the cell pellet lysate. PEG, polyethylene glycol.

IV.4.5 Evaluation of AC and CEX purification protocols for four different serotypes

So far, the purification methods were evaluated with rAAV2/8 only. We next decided to test the purification of rAAV2/2 and engineered variants thereof only by AC and CEX. The results for "wildtype" rAAV2/2 and engineered rAAV2/2.NN and rAAV2/2.GL are illustrated in Figure IV.7.

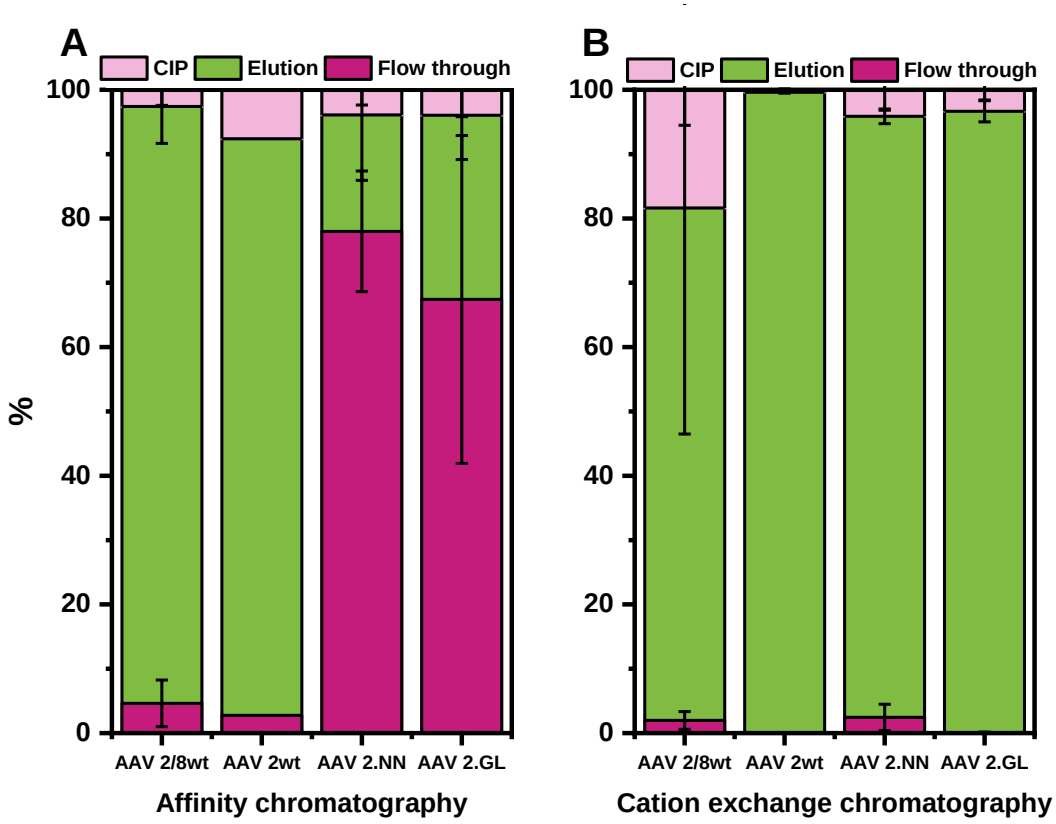

Figure IV.7 Comparison of AC and CEX for rAAV2/8, rAAV2/2, rAAV2/2.GL, and rAAV2/2.NN. Chromatography with AC (A) and CEX (B). Purple depicts the flow through and, thus, loss of rAAV during the loading process onto the column (flowthrough), light green shows the yield of rAAV in the elution, and pink illustrates the loss of rAAV during the cleaning in place (CIP) process. Minimum, n = 3 (except for AC rAAV2/2, n = 2)). rAAV, recombinant adeno-associated virus.

For all serotypes, a minimum of three runs with each column were done. The only exception was for the AC purification of rAAV2/2, for which we performed only two runs. The AC performed very well for rAAV2/8 and rAAV2/2, which could be quantitatively captured on the column. This was not the case for the two engineered rAAV2 variants, which were also bound to the AC column but with a much lower affinity (Figure IV.7A).

In contrast to the AC, the CEX showed very good results for all four tested types of rAAV, with yields of the remaining rAAV from the initial vg amount ranging from 93% to 99%

in the elution (Figure IV.7B). rAAV2/8 seemed to bind strongly to the CEX resin, and consequently, up to 20% of the total vector amount was lost, since it could only be eluted from the column during the cleaning in place mode.

IV.5 Discussion

Here, we explored different liquid chromatography-based methods for the purification of rAAV material harvested from the cell culture supernatant or from cell pellet lysate. For the initial evaluation, we opted to work with rAAV pseudotyped with the broadly used and easy-to-produce AAV8 serotype.

The HIC-CEX-AEX process included three subsequent chromatographic steps on the HIC, CEX, and AEX columns and consistently produced rAAV2/8 materials at high yields with good purity from the cell culture supernatant, which was initially buffer-exchanged via the TFF. However, there was substantial loss of the rAAV vector when using a cell culture supernatant PEG precipitate or cell pellet lysate (Table IV.1). A closer inspection of the yield after the different chromatography steps showed that the loss of material mainly happened during the HIC step. The exact reasons for this observation remain unclear. It is tempting to speculate that the initial TFF step helped remove the impurities that negatively impacted the HIC step. Thus, if not combined with an initial TFF step, the HIC-CEX-AEX process resulted in a low yield at the end of the purification process and had to be changed. Indeed, the removal of this initial HIC step in the CEX-AEX process resulted in increased yields from both starting materials, which performed less efficiently in the HIC-CEX-AEX process. Importantly, the CEX column tested in this study showed promising results for all the tested (naturally occurring and engineered) rAAV. Only for rAAV2/8, a substantial amount of rAAV remained on the column and, eventually, were lost, since they could only be eluted in the cleaning step.

Further improvements in the procedure, e.g., by adjusting the buffer pH from 4.0 to pH 4.5 or pH 5.0 to reduce binding to the column, might help to increase the fraction of rAAV2/8 that can be recovered in the elution part of the chromatography. It should be noted that longer times at a low pH could damage the capsid, as shown in a recent study (336). Thus, increasing the pH to optimize binding to the CEX column could also be beneficial for rAAV stability but was beyond the scope of the current work.

In the AC-AEX process, we explored the POROS AAVx affinity column as an alternative to the CEX. In a recent study (333), it was demonstrated that the AAVx column has a high

static-binding recovery (>95%) for a broad range of natural and synthetic serotypes. For rAAV pseudotyped with the naturally occurring AAV serotypes AAV8 or AAV2, we could confirm this observation and achieved a similar recovery for both of them. However, for purification of the two recently described engineered AAV2 variants (331), an affinity to and, thus, recovery from the AC column was substantially reduced, and a high amount of rAAV was lost in the flowthrough fraction. These AAV2 variants termed AAV2.GL and AAV2.NN carry peptide insertions in the surface-exposed hypervariable loop IV of the AAV capsid, which seems to impact the ability of this capsid to efficiently bind to the affinity matrix. While the exact composition of the affinity matrix was not disclosed by the manufacturer of the AC column, it seems like structural, or sequence epitopes made up by the hypervariable loop IV do substantially contribute to the binding affinity.

In addition to the desired vector genome-loaded “full” rAAV, all rAAV production methods yield varying amounts of genome-free “capsid-only” empty particles as byproducts. Therefore, the HIC-CEX-AEX and AC-AEX processes included a final AEX step, in order to separate the full rAAV from the empty capsids. The packaging of DNA is thought to induce small changes in the capsid structure and changes in the overall charge of the particles. Indeed, the IEP for empty capsids was reported to be around 6.3 and, for full rAAV, around 5.9 (25, 186, 188, 191). In combination with the running buffers with a pH higher than the IEP, this can be exploited for the separation of these two species by AEX chromatography.

Initially, we used the CIMmultus QA column for AEX chromatography in the HIC-CEX-AEX and AC-AEX downstream processes. This column did not achieve a baseline separation of the full and empty peaks but still resulted in an enrichment of the full rAAV. Subsequently, we tested the CIMmultus PrimaS (AAV) column and found a better separation of the full and empty chromatography peaks. In particular, when we applied a step protocol for buffer B, we achieved an almost baseline separation of the full rAAV and the empty capsid peaks. Other studies have also achieved full/empty separation for different AAV serotypes by AEX (9, 26, 188, 193, 207, 305, 337). For determination of the degree of separation of full rAAV from empty capsids, we used analytical AEX. To confirm the analytical AEX results, we used SV-AUC as the orthogonal method. Although the SV-AUC analysis at 230 nm provided more sensitivity compared to 260 and 280 nm, only the intermediate and highly concentrated rAAV preparations with absorbance in excess of 0.15 OD units were compared. The AUC consistently worked with the empty capsid fractions

and confirmed a very high purity of 99% (compared to 100%, as determined by analytical AEX). The value of the empty capsids that coeluted in the full rAAV fraction was quantified as 17% by SV-AUC, whereas AEX determined the value slightly lower at 12% being empty capsids. The SV-AUC measurements on the full and mixed rAAV fractions also revealed levels of partially filled and aggregated rAAV, which was not observable by AEX.

Apart from the empty capsids, other impurities are also of relevance. In this regard, we found that rAAV material from the cell pellet lysate ended up having slightly higher amounts of HEK cell DNA compared to rAAV harvested from the cell culture supernatant, either by PEG precipitation or by TFF. The initial step of the buffer exchange via TFF directly removes some process-related impurities, but PEG precipitation was even more effective in removing process-related impurities. However, as seen in the silver-stained SDS-PAGE, both steps did not fully remove the impurities and still resulted in additional bands. Better purification was achieved after HIC, CEX, or AC. An additional AEX step not only helped removing the empty AAV capsids but also further lowered the amount of HEK cell DNA. Interestingly, the AEX step removed the HEK cell DNA from the empty capsid fractions even more efficiently than from the full rAAV fractions. The exact reason for this remains unclear, but it might be related to the fact that full rAAV elutes later in the gradient of the AEX column. Since DNA binds strongly to the AEX column, DNA contaminations elute late in the gradient (325), which coincides more with the elution of the full rAAV.

Another point to consider when working with the different starting material are potential differences in the post-translational modification (PTM) pattern of the AAV capsid harvested, e.g., from the supernatant or the cell pellet. Such differences might impact on the production process or the properties of the product. Indeed, various PTMs of the AAV capsid have been identified (338, 339), and the potential effects on the rAAV vectors function discussed (10). Whether and how the PTM pattern impacts the chromatographic purification of rAAV needs to be clarified in future studies.

So far, the gold standard for the purification of rAAV are gradient ultracentrifugation-based protocols using cesium chloride (75) or iodixanol gradients (340). In addition to the removal of impurities, such protocols, in particular when performed with two (or more) subsequent ultracentrifugation steps, are able to efficiently separate full rAAV vectors from

empty AAV capsids. The drawbacks of the ultracentrifugation-based protocols are poor scalability and its dependence on the operator, which can lead to high batch-to-batch variability. Therefore, the use of ultracentrifugation-based processes for the large-scale commercial production of rAAV is challenging. Nevertheless, these methods are frequently used in basic research applications and preclinical in vivo studies (341) and can be considered with some optimizations for the GMP processes for indications of the local application of a vector that do not require a large scale for the manufacturing of high amounts of rAAV vectors.

Other than gradient ultracentrifugation-based protocols, all the chromatography-based steps we tested are readily scalable. AC is highly selective and recovers for rAAV2/8 60%–80% of the initial vg amount, but AC does not discriminate between full and empty, and the vg yield depends on the serotype—especially, the vectors produced with engineered AAV capsids are problematic with this type of column. In contrast to AC, the CEX worked with all the tested rAAV and has comparable yields of around 70–80%. On the other hand, CEX cannot discriminate assembled capsids from protein impurities that show a similar pI and, thus, usually require a subsequent step using an alternative matrix with distinct pH and salt conditions. However, both AC and CEX do not remove the inherent byproduct of empty capsids and, which requires an additional AEX step, which, under optimal conditions, can achieve baseline separation of full and empty rAAV. Of note, by combining the CEX with an AEX column, the aforementioned issue could be solved and protein impurities removed.

Table IV.4 Comparison of the ultracentrifugation based und liquid chromatography-based purification of the rAAV.

Purification Strategy	Yield for AAV2/8	Working Time (hours)	Scalability	GMP Readiness	Full/Empty Separation	Remaining Impurities
Ultracentrifuga-tion	good	8–10	poor	moderate	after 2 runs good	iodixanol/cesium chloride
AC	good to very good	2–3	good	good	poor	DNA
CEX	good to very good	0.5–1	good	good	poor	proteins, DNA
AEX	good	2–3	good	good	good	small amounts of DNA

IV.6 Conclusion

In conclusion, we presented a comparison of the different chromatographic purification methods, which allow for the efficient removal of the process-related impurities and separation of the full rAAV from the empty capsids at promising yields. The different protocols showed varying performances for the different serotypes. Our results, thus, can provide guidance for future refinement and the adjustment of chromatographic protocols to a specific type of capsid. Depending on the AAV serotype, a combination of CEX and AEX or AC and AEX is recommend. Full and empty rAAV separation worked particularly well and achieved a high level of purification for the commonly used AAV8 serotype. Our findings hold promise for future translational projects that require highly purified and full particle-enriched rAAV preparations.

IV.7 Acknowledgments

The authors would like to thank BIA separations for providing the CIMmultus PrimaS (AAV) column for beta testing.

IV.8 Supplement

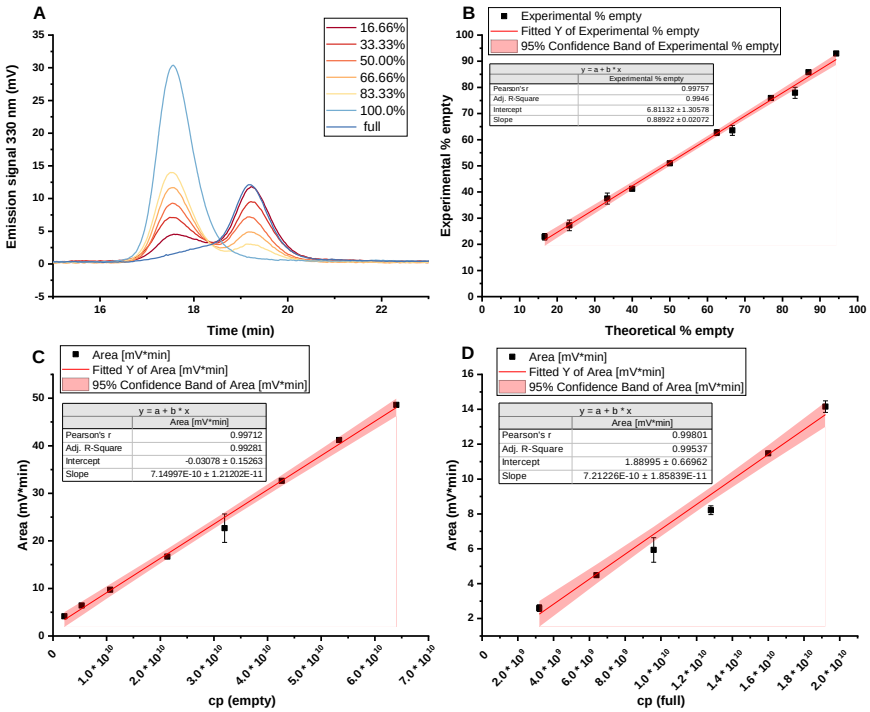

Figure IV.S1 Calibration data of the Protein-Pak Hi Res Q, 5 µm, 4.6 × 100 mm. (A) Depiction of the raw data of the chromatograms showing the amount of empty capsids in percent. (B) Experimentally determined percentage values of empty capsids plotted against the theoretical percentage. (C,D) Calibrations of empty capsid (C) and full rAAV (D) titers.

Chapter V Further studies on different purity levels and purification strategies of AAV2, AAV2.NN and AAV8

V.1 Introduction

In Chapter IV some methods were presented that are able to control the purity of an AAV sample. Yet, to describe the quality and purity of the sample more effectively and accurately, further experiments are necessary. To do so, this chapter focusses on additional sources of impurities and examines the influence of purification strategies on transduction efficiency of AAV. One example are host cell proteins that should also be considered as possible contaminants. Their presence can be verified by iDSF: With additional proteins besides the AAV capsids within a sample, several T_m can be expected (213).

Of course, the ratio of full to empty capsids is a CQA in assessing the purity of an AAV sample. In Chapter IV, this has already been controlled by means of AEX. In addition, this chapter controls the presence of empty capsids by mass photometry (MP) (206). The backscattered light is correlated with the molar mass of the particle, so that a distinction between full and empty capsids is easily possible. However, not only AAV scatter light back but also other proteins or DNA fragments that are still in the solution. A distinction of DNA and protein impurities based on their molar mass only is not possible.

Another common impurity in AAV samples is DNA of the pTransgene plasmid. This DNA is contained as a backbone in the plasmid and contains the bacterial origin of replication (ori) and a kanamycin or ampicillin resistance gene. Since the backbone is also located between ITR, it is possible that reverse packaging may occur, resulting in the pTransgene plasmid backbone being packaged instead of the gene of interest. Since these incorrectly packaged AAV are also capable of transfecting cells, this can lead to genotoxicity, so it is important to test for incorrectly packaged AAV. For this purpose, qPCR was performed on the ori sequence to evaluate the presence and possible gateways for incorrectly packaged AAV.

During purification, there may be damaged capsids that are no longer able to transfect cells and can even be immunogenic. Therefore, to investigate the proportion of damaged capsids, a dot plot was performed using mouse monoclonal antibody B1, which recognizes a binding site inside the capsid and only generates a signal when the capsid is damaged (54). That way, it is possible to identify the purification strategy that attacks the AAV capsids least,

potentially contributing to better transduction efficiency and reducing the risk of immunogenicity.

The ultimate determining factor for successful gene therapy is the ability of AAV to transduce target cells. An activity assay is the corresponding method to assess transduction efficiency. Both empty and damaged capsids do not contribute to transduction efficiency in the activity assay. However, some chemical changes on the capsid surface, such as deamidation or oxidation, may occur due to instabilities caused by different pH and/ or salt conditions during the purification process (10). Therefore, the activity was evaluated after different purification strategies, as well as in different steps of the AAV purification process.

V.2 Material and methods

V.2.1 Purification of AAV material

Downstream processing of AAV2wt and AAV2.NN using an iodixanol gradient followed by an AEX chromatography was performed as described in the dissertation of Susanne Koch (2013) (342).

V.2.2 Intrinsic differential scanning fluorimetry (iDSF)

The applied methods and parameters were already described in detail in Chapter II.

V.2.3 Mass photometry (MP)

The MP experiments were performed at room temperature (RT) using the OneMP instrument (Refeyn, UK). The 24×50 mm microscope coverslips (Fisher Scientific, Waltham, MA, USA) were prepared by cleaning with water and isopropanol, as well as drying under a stream of clean nitrogen, as explained previously (206). A piece of clean, precut 2×2-well CultureWell™ gasket (Sigma Aldrich, St. Louis, MO, USA) was attached to the coverslip. Before analysis the system was calibrated with NativeMark™ Unstained Protein Standard (Thermo Fisher, Dreieich, Germany) to correlate the scattered light to the corresponding molar mass.The AAV samples were diluted in 10 mM phosphate buffer to a concentration of about 10^{11} – 10^{12} cp/mL. 18 µL of the filtered phosphate buffer were loaded into a well of the CultureWell™ gasket, and, after MP focusing, 2 µL of rAAV solution were added into the same well. Immediately after the solution was mixed by pipetting, a 2-minute video was recorded using the AcquireMP (Refeyn, UK) software.

V.2.4 Vector plasmid backbone quantification

For the detection of vector plasmid backbone, the ori sequence (110 bp) was amplified using a SYBR Green qPCR assay, also used for the ITR qPCR (Chapter IV), and the following primers: 5'-CTGGCGTTTTTCCATAGGCTC-3' (forward) and 5'-GGGGGAAACGCCTGGTATCT-3' (reverse). The qPCR was performed with a StepOne plus (Thermo Fisher, Dreieich, Germany).

V.2.5 Dot blot with B1 antibody

The Dot blot assay was done using blotting membranes Amersham Hybond 0.2 PVDF (VWR, LT: NP0151, Radnor, PA, USA) that need to be equilibrated in three different solutions before the sample spotting. First, in Methanol (MeOH) 100% for 1 minute, followed by water for 3 minutes and at the end in TBST buffer consisting of 50 mM Tris (VWR International, Radnor, PA, USA), 0.5 M NaCl (Bernd Kraft, Duisburg, Germany) and 0.05% Tween-20 (Carl Roth, Karlsruhe, Germany) at pH 7.4 for 5 minutes. On the equilibrated membrane, 1 µL sample was spotted. After the spotting, the membrane was incubated at RT for 1 hour to dry. Then, a blocking step with 5% of dry milk (Sigma-Aldrich, St. Louis, MO, USA) in TBST was performed for 1 hour on a rotator. After discarding the block solution, the membrane was incubated with primary antibody B1 (Progen, Heidelberg, Germany) (1:250). After 1 hour reaction time at RT on a rotator, the membrane was washed three times with TBST, each time for 5 minutes. The secondary antibody anti mouse HRP (Progen, Heidelberg, Germany), diluted 1:2000 with TBST, was applied and followed again by three steps of washing. In the end, the membrane was washed in water. The binding detection was evaluated with ChemiDoc MP (Biorad, Hercules, CA, USA) taking 20 pictures in 300 s, using Image Lab as software.

V.2.6 Activity assay

The activity assay was performed in HeLa cells. 12/24-well plates (Greiner AG, Kremsmünster, Austria) were used and every well contained 50.000 cells at the beginning. 24 hours after splitting, the medium was removed, and 0.5 mL new medium were added to each well. Subsequently, for AAV2.NN 1000 vg per cell and for AAV8 100.000 vg per cell were added to the well. During the transduction, the cells were stored at 37 °C and 5% CO_2 for 48 hours. After two days, the cells were trypsinized and the number of green-fluorescent cells were measured by Countess (Thermo Fisher, Dreieich, Germany).

V.3 Results and discussion

V.3.1 Unfolding of AAV in different purification steps

The aim of this experiment was to find out whether the stability and purity of the capsids is affected by after different purification steps and whether this can be determined by intrinsic fluorescence. Therefore, samples of the AAV8 vector-producing cell culture supernatant were collected after TFF concentration and buffer exchange, HIC, CEX, AC, and AEX and then analyzed using iDSF (NT Prometheus NT.48).

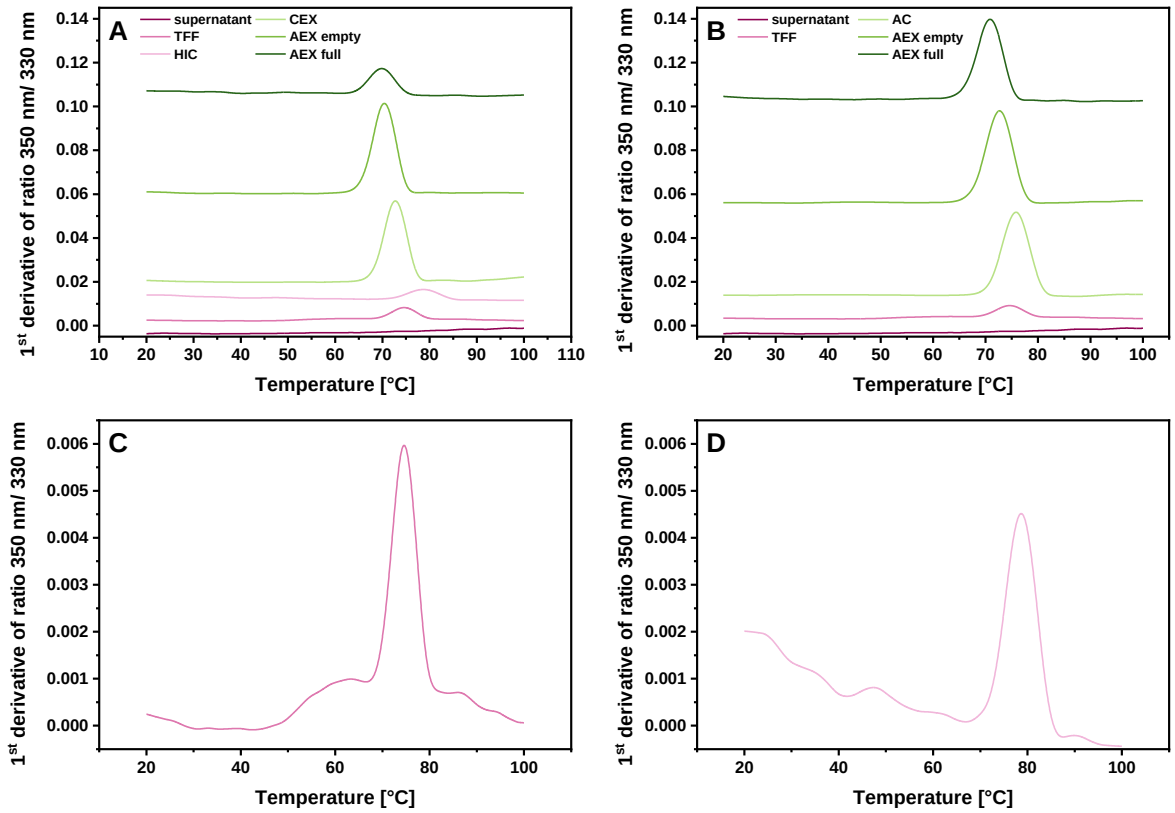

Figure V.1 iDSF measurements of intrinsic fluorescence signal of AAV8. 10 µL of AAV8 vector at different purification step,s heated at a rate of 1 °C per minute from 30 °C to 100 °C. (A) Shows the first derivative of the ratio 350 nm / 330 nm of samples from the supernatant ($2*10^{11}$ vg/mL), after concentration and buffer exchange by TFF ($3*10^{12}$ vg/mL), after HIC ($3*10^{11}$ vg/mL), after CEX ($6*10^{12}$ cp/mL) and finally for the separated empty ($1*10^{12}$ cp/mL) and full ($4*10^{11}$ cp/mL) AAV capsids. (B) shows the equivalent curves for the purification strategy using AC ($6*10^{12}$ cp/mL, empty $2*10^{12}$ cp/mL, full $9*10^{11}$ cp/mL)) instead of CEX. (C and D) show the magnification of the curves of TFF (C) and HIC (D).

For the supernatant no melting of the AAV capsids could be detected by intrinsic fluorescence because the AAV8 concentration is too low to be detected by this method. For the sample after concentration and buffer exchange the melting point of AAV8 was detected in the expected range plus some additional fluorescent signal at 60°C (Figure V.1C) (3, 55, 56). After the HIC purification step, an intrinsic fluorescence signal

for AAV capsid melting was detected, but shifted to higher temperatures, compared to the previous step (Figure V.1D). The reason for this phenomenon could be the comparably high ionic strength of the buffer, which can lead to higher T_m values, as shown in previous experiments (Chapter II). A clear AAV8 capsid unfolding was detected for further purified samples of the production process after purification with AC, CEX, as well as the empty and full samples after AEX (Figure V.1A and B). The detected peak maximum of the intrinsic fluorescence measurements shifted from purification step to purification step, which can be related to (1) the number of capsids in each sample, where higher capsid amounts result in a higher melting temperature, or (2) buffers with higher osmolarity that can also cause higher T_m value (Chapter II). (1) is the case for samples after AEX, as both AAV samples are in the same buffer and therefore only the number of capsids differs. The sample with empty capsids has 1-2*10^{12} cp/mL showing a higher T_m value, whereas the sample containing full capsid only has 4-9*10^{11} cp/mL and therefore a lower T_m. (2) becomes obvious by looking at the sample from HIC. This sample only contain 3*10^{11} vg/mL but nevertheless the capsid unfolding takes place at a temperature around 80°C. The characteristic of this sample is the high osmolarity of ~ 1 M K_2HPO_4 because all other samples have an osmolarity ranging from 20 mM up to 150 mM. So high osmolarity causes higher T_m values.

For the rather impure samples after TFF and HIC some additional intrinsic fluorescence signal was observed. This led us to the conclusion that a rather high number of other proteins must be present in these samples. This conclusion was confirmed by the AUC analysis. While the AUC analysis showed some impurities below 50 S for the samples after CEX and AC as well, the amounts of these protein impurities seem to be too low to be detected by intrinsic fluorescence measurements (for AUC data see Chapter IV).

Intrinsic fluorescence measurement can be used to determine the protein impurities of an AAV sample. However, iDSF is not as sensitive as an AUC measurement, as it can only detect substantial quantities of protein impurities, without the ability to quantify these impurities. Thus, it cannot be considered the optimal method for detection of impurities in AAV samples. For comparable T_m values of different serotypes, the AAV sample must be dissolved in the same buffer at the same concentration.

V.3.2 Analysis of different purified AAV samples by mass photometry

Some methods, including AUC, TEM, and AEX, offer the opportunity to determine the ratio of full and empty capsids. Yet, the determination is not straight forward and each of these methods has its own advantages and disadvantages.

MP measures the mass on the single particle level, by detecting the light scattered by the individual particles as they are touched on a glass surface. The interferometric contrast of scattered and reflected light can be related to the mass of the particles through a calibration procedure applied both to proteins (204) and nucleic acids (205). Therefore, quantification of full and empty capsids is easily possible with MP (202, 203).

This simple method establishment only requires titration of the adequate concentration of capsids, which are then loaded on the coverslip to avoid overloading. If overloading occurs during the measurement, the binding of single particles cannot be detected anymore.

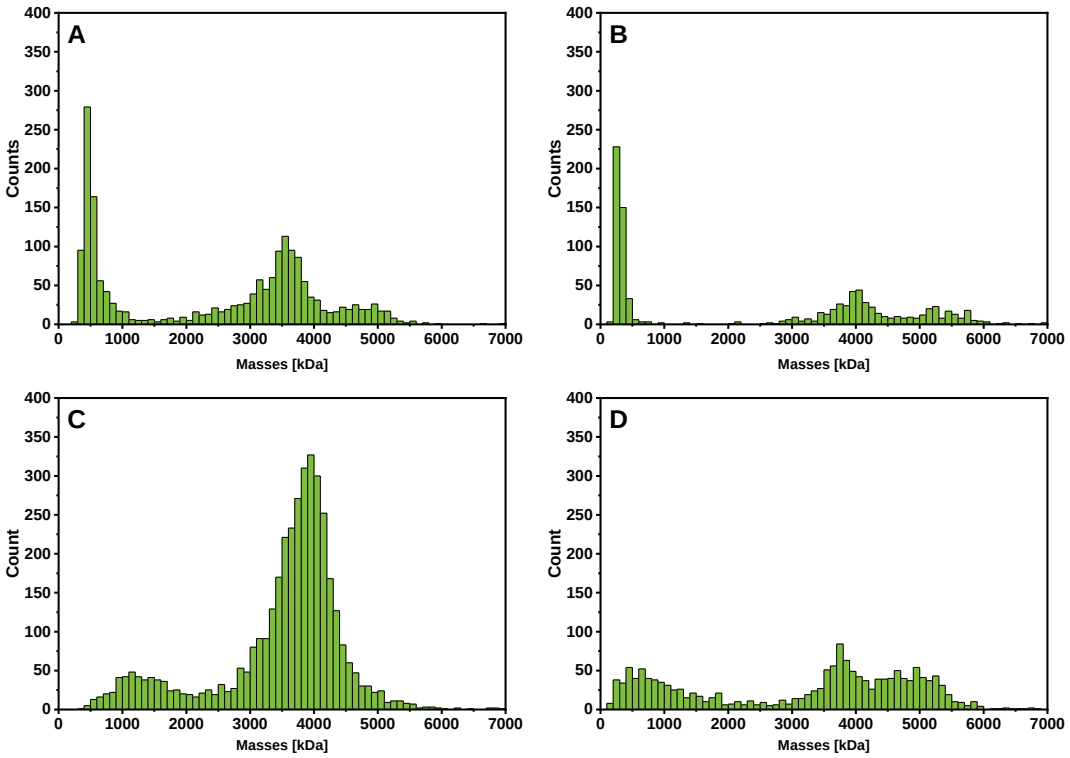

Figure V.2 The histograms of the mass photometry measurements. (A-D) show the sample after different purification steps / fractions. (A) AC (B) CEX (C) empty AAV and (D) full AAV separated by AEX.

After AC (Figure V.2A) and CEX (Figure V.2B) a mixture of full (5.1 MDa) and empty (3.8 MDa) capsids was detected by mass photometry. In addition, some impurities with a mass below 1000 kDa were observed for those two AAV samples. Especially for the sample purified by AC the number of empty capsids is higher in respect to the filled ones. The

fraction of the empty capsids generated by AEX separation seems to be well purified (Figure V.2C). Only a single clear peak at 3800 kDa and some counts between 1000 and 2000 kDa could be detected by mass photometry. For the sample from the peak of full AAV (Figure V.2D) a mixture of full and empty capsids is detected but the empty capsids as well as smaller impurities below 2000 kDa are lower compared to the previous step of AC processing.

In conclusion, full and empty AAV can be easily detected and distinguished from each other with MP. Also smaller impurities, like proteins or DNA can be detected and the proportion compared to the AAV is representativ. This is also true for the ratio of full and empty caspids. However, the absolute concentration of AAV cannot be reliably measured in the form of a cp titer. Because the number of counted capsids should be about the same in the AC and CEX sample because the samples were diluted to the same capsid titer before performing the measurement. But this is not the case for the data shown in Figure V.2A and B. A higher number of capsids was obtained for the sample after AC purification (Figure V.2A). Lastly, AAV aggregates lie outside the detection range from 30 kDa up to 6 MDa and can therefore not be investigated with this method.

V.3.3 Impurities –AAV capsid containing pTransgene plasmid

Previous studies reported that encapsulated plasmid DNA impurities are primarily derived from the backbone of the pTransgene plasmid (156, 158). Therefore, it is desired to monitor the level of encapsulated pTransgene plasmid by controlling the impurities in AAV samples. The most common method to determine residual plasmid DNA levels is qPCR using primers and probes specific for a sequence located in the plasmid backbone, e.g., the bacterial ori sequence.

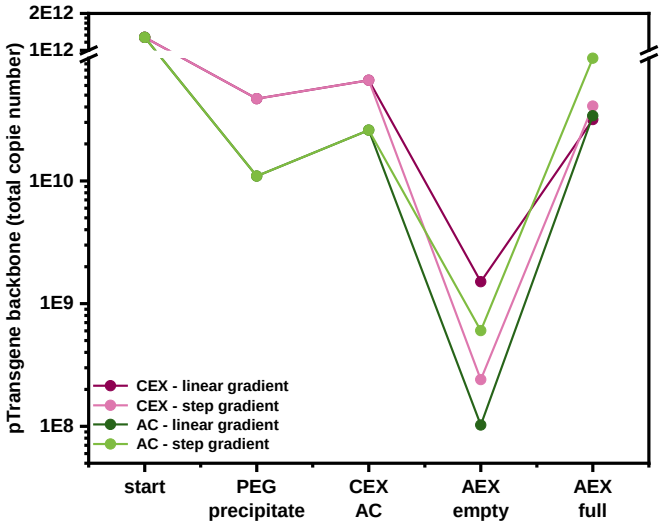

Figure V.3 Reduction of plasmid backbone DNA content by chromatography-based purification measured by qPCR amplifying ori sequence.

The number of capsids containing the pTransgene plasmid backbone can be reduced during purification. This is especially true for the first purification step (Figure V.3, PEG precipitate) and the peak of empty capsids after AEX (Figure V.3, AEX empty). The number of capsids containing the backbone of the pTransgene plasmid increases in the peak of full capsids (Figure V.3, AEX full), because their IEP is in the same range as the IEP of correctly packaged AAV. Thus, it is not possible to separate the capsids loaded with the backbone of the pTransgene plasmid from the correctly packed capsids by AEX.

However, the number of capsids containing the pTransgene plasmid backbone can be reduced by optimizing the pTransgene plasmid design. The most effective way is to artificially generate a heavier plasmid backbone that must be larger than 5 kb-the maximum AAV genome size that can be packed into an AAV capsid (15, 16, 157).

Overall, a reduction in the pTransgene plasmid backbone is possible during purification. However, the free pTransgene plasmid backbone is mainly removed during PEG

precipitation. The pTransgene plasmid backbone packaged in the AAV capsid can be poorly separated from the full AAV because both species have a very similar IEP. Therefore, a lower amount of AAV-containing pTransgene plasmid backbone in the fraction of full AAV can only be achieved by artificial enlargement of the pTransgene.

V.3.4 Detection of capsid damage during different purification strategies

To obtain information about capsid damage that occurred during the purification process a dot blot assay using the B1 monoclonal antibody was performed.

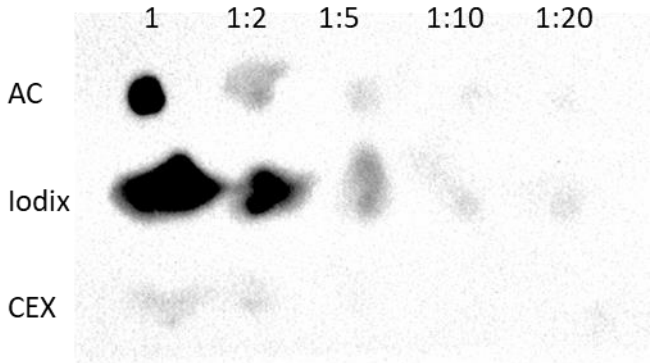

Figure V.4 Dot blot treated with B1 monoclonal antibody for detection of capsid damage of AAV2wt by different purification strategies. Samples were diluted to a titer of $1*10^9$ vg/µL and 1 µL each dot was used. From $1*10^9$ vg/µL the following dilutions were done (1:2, 1:5, 1:10 and 1:20).

The B1 antibody is specific to target the inside of an AAV capsid and can therefore be used to detect capsid damage (54). A clear B1 antibody signal indicates many damaged capsids in the sample. It can be easily seen from Figure V.4 that purification using the iodixanol gradient results in the highest capsid damage. Also, some capsid damage could be observed for the purification strategy using the AC. In this purification strategy the viruses stay at pH 3 for approximately 90 minutes, compared to only 30 minutes at pH 4 in the CEX, which consequently results in a higher yield of undamaged capsids.

These data suggest that CEX put the AAV capsids under less stress compared to iodixanol gradient and is therefore the gentler purification option for AAV2wt. This shows another advantage of purifying AAV by HPLC, which is discussed in more detail in Chapter IV. Compared to conventional purification by ultracentrifugation using iodixanol, both HPLC-based purification strategies show less damaged AAV capsids. Furthermore, this result holds further insights about the stability or instability of the AAV capsids at low pH values, which in turn plays a crucial role not only in purification but also in formulation development.

V.3.5 Activity in HeLa cells of AAV from different purification methods

To compare the potency of AAV vectors produced with the different purification methods, an activity assay is necessary. The activity of the AAV was tested by transduction of HeLa cells with vectors carrying a CMV-eGFP expression cassette and measurement of the fraction of green-fluorescent cells after 48 hours.

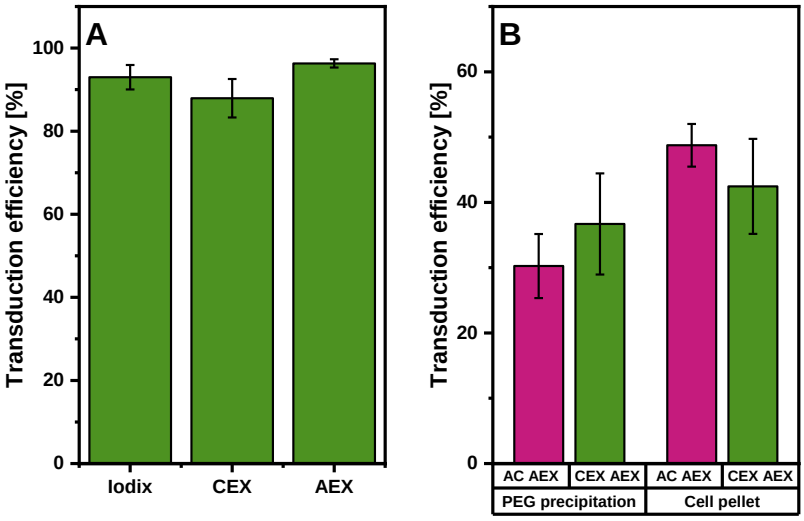

Figure V.5 Transduction efficiency of eGFP-expressing AAV vectors purified with different strategies. (A) shows the transduction efficiency of AAV2.NN after purification via iodixanol gradient, CEX and samples from CEX also purified by AEX (MOI 1000). In (B) the difference between the transduction efficiency of AAV8 after full-empty separation via AEX, coming from the PEG precipitation or from the cell pellet lysate is depicted (PEG n=2, cell pellet n=3).

No difference in transduction efficiency was observed for AAV2.NN vectors purified by using different purification strategies (Figure V.5A). The minor differences between the sample purified by CEX (88%), the AEX (96%), and iodixanol gradient (93%) should not be overinterpreted. These small differences can very well arise from the sample buffers: PBS for iodixanol gradient, acetate buffer for CEX, and Tris buffer for AEX. It is documented, that the buffer composition can affect the transduction efficiency of AAV vectors and Tris buffer indeed facilitated transduction (3).

In Figure V.5B the transduction levels for AAV8 after AEX are depicted, separated in AAV vectors coming from the PEG precipitation or cell pellet and using AC or CEX as previous purification step. No significant difference in transduction efficiency could be obtained between the two purification strategies. In contrast, a trend for higher transduction efficiency was observed for AAV from the cell pellet (AC-AEX 49%; CEX-AEX 43%) compared with the ones from PEG precipitation (AC-AEX 30%; CEX-AEX 37%). One

reason might be differences in the post-translational modification (PTM) pattern of the AAV capsid harvested, e.g., from the supernatant or the cell pellet. Such differences might impact the properties of the product. Indeed, various PTM of the AAV capsid have been identified for AAV batches form different host cells, as well as AAV batches from the supernatant or cell pellet lysate (338, 339). The potential effects on the AAV vector function are discussed by Giles et al. (10).

V.4 Conclusion

This Chapter demonstrated that different purification strategies resulted in different purity and stability of the AAV sample, whereas the transduction efficiency is only slightly affected. iDSF measurements can give additional information about the presents of protein impurities in an AAV sample by performing the serotype control using iDSF. However, iDSF is not as sensitive as an AUC measurement: While AUC detects protein and DNA impurities, even for the samples after purifications using AC and CEX, neither DNA impurities, nor impurities after AC/ CEX purification are detectable using iDSF. Thus, iDSF should not be considered the optimal method to detect impurities in AAV samples.

The capsid damage can be detected by a dot blot using the B1 antibody. This experiment showed that the purification via CEX seems to be the gentlest purification method for AAV2wt, as it substantially reduces capsid damage. Interestingly, the transduction efficiency of the same AAV vector produced with identical upstream process, but different downstream purification methods (AEX, CEX, or iodixanol gradient) was comparable. Only a slight difference in the transduction efficiency was observed for AAV vectors purified from the supernatant or the cell pellet, with the latter showing slightly higher activity, implying the downstream process has only a low impact on the transduction efficiency, even though it impacts the yield. MP proved to be an easy and straight forward method to distinguish between full and empty capsids and to calculate a ratio of the two species. However, for the moment it is not possible to determine the absolute number of full and empty capsids.

With the liquid chromatography-based purification methods, impurities in AAV samples can be reduced, but it is still not possible to discriminate between AAV species with the correct AAV genome and AAV vectors containing the reverse packaged pTransgene plasmid backbone. Thus, to avoid reverse packaging, the pTransgene backbone size must be increased to size which exceeds the maximum size of 5 kb that can be packaged by an AAV capsid.

Chapter VI Systemic studies on stabilization of AAV formulations by lyophilization

This chapter is published as: Rieser, R., Menzen, T., Biel, M., Michalakis, S & Winter, G. (2022) Systematic studies on stabilization of AAV vector formulations by lyophilization, *Journal of pharmaceutical science.*

Author contributions:

R.R. performed all experiments, evaluated the data and wrote the paper. R.R., T.M. and G.W. conceived the presented idea and planned the experiments. T.M., S.M. and G.W. conceptual guidance and corrected the manuscript. S.M. and M.B. provided the AAV and cell culture for the activity experiments.

Note from the authors:

The version included in this thesis is identical with the published article apart from minor changes. The reference, figure and table numbers were changed to fit into the coherent numbering of this document.

The published article can be accessed online via:

https://doi.org/10.1016/j.xphs.2022.03.004

VI.1 Abstract

Adeno-associated virus (AAV) vectors have evolved as one of the most promising delivery systems for gene therapy. The current standard for AAV vector storage is deep-freezing below -60°C. While this allows for long-term vector storage without loss of activity, it is inconvenient and involves high costs and logistical challenges. Therefore, there is a need for AAV formulations, such as freeze-dried formulations, that allow for long-term storage at 2-8°C. A major challenge in developing a lyophilization process for complex biological structures like an AAV vector is to minimize the stress on the capsid during the lyophilization cycle. Here, we evaluated different conditions for freeze-drying of AAV8 vectors and found that undesirable instability can be significantly reduced if secondary drying is performed at lower temperatures, kept as short as possible, and the residual moisture is kept between 1.5 and 2%. In a next step, we explored formulations with different salt concentration or excipient compositions and found that a combination of 10 mM phosphate buffer, 5.67% (150 mM) trehalose, 5% hydroxyectoine and 0.1% poloxamer with a residual moisture of approx. 1.5% provided stable long-term storage at

2-8 °C and for at least 4 weeks at 25°C. These results pave the way for future optimizations of freeze-drying processes for AAV vector-based gene therapy products.

Keywords: Adeno associated virus(es) (AAV), gene therapy, gene vector, freeze-drying, lyophilization, formulation development, stability, excipients

Abbreviations: AAV - Adeno associated virus(es); Cp - capsid particle; DNA - Deoxyribonucleic acid; DP - drug product; FT - freeze-thaw; ITR - inverted terminal repeats; SEC - Size exclusion chromatography; SD - standard deviation; T_g - glass transition temperature; T_g' - glass transition temperature of the freeze concentrate: T_c - collapse temperature; Vg - vector genome

VI.2 Introduction

Adeno-associated virus(es) (AAV) vectors have evolved as one of the most promising delivery systems for gene therapy due to their good safety profile, high efficacy, and long-term gene expression in non-dividing cells. AAV are non-enveloped, non-pathogenic DNA viruses that belong to the *Dependoparvoviruses* of the *Parvoviridae* and have a size of 25-28 nm. AAV consist of a mixture of three capsid-forming viral proteins (VP1, VP2 and VP3) and an approx. 4.7 kb single-stranded DNA genome containing two genes, Rep and Cap, between two inverted terminal repeats (ITR) (17, 19, 290). For the use as a gene therapy vector commonly AAV2-derived ITR are used and the Rep and Cap sequence is replaced by a therapeutic gene expression cassette. A large variety of naturally occurring or engineered AAV variants with distinct capsid composition and tropism exist referred to as serotypes and used to produce pseudotyped recombinant AAV vectors (17, 343, 344).

Final AAV vector drug product (DP) is usually stored as frozen solution at temperature below -60 C, as it is done for the two FDA-approved AAV gene therapy DP Luxturna® (345) and Zolgensma®(346), AAV vector-based gene therapies for *RPE65*-linked retinal dystrophy and *SMN1*-linked spinal muscular atrophy, respectively. Storage at such low temperature allows for long term stability of the AAV DP without loss of activity, but it is inconvenient, expensive. In addition, it has been reported that the stability of AAV vectors is sensitive to freeze-thaw (FT) cycles due to induction of unfolding, aggregation as well as DNA leakage, leading to reduced activity (6, 254, 301, 347, 348) further increasing the logistical challenges along the supply chain. In addition, pH related structural changes and reduced activity of AAV vectors have been reported (63, 186), which is critical because

some buffers used in AAV formulations, such as phosphate buffered saline (PBS), exhibit a pH shift upon freezing due to selective crystallization of disodium phosphate (349, 350).

Certain critical quality attributes described in the literature can give us a reasonable understanding of the stability of an AAV vector formulation (38). For example, the particle size of AAV2 measured by DLS increased 2-fold after 5 days of storage at 4°C, 6-fold after 10 freeze-thaw cycles at -20°C, and 10-fold after 10 freeze-thaw cycles at -80°C due to aggregation (6). For AAV1, AAV2, AAV5 and AAV8 reduction of activity was observed in liquid formulations with increasing storage time, higher storage temperature and lower pH of the formulation. Differences between the serotypes could be observed for pH sensitivity and freeze-thaw (63, 348). There are two recent publications by Bee et al. (254) and Xu et al. (348) both showing that classical cryoprotectants such as sugars like sucrose and trehalose are able to stabilize AAV vectors during freeze-thawing. However, very few systematic efforts to optimize the stability of liquid viral vector formulations and stability have been published (217, 263).

Lyophilization is a well-established process for stabilization of sensitive biopharmaceuticals, as such it may provide sufficient stability for AAV DP, potentially without the need for cold chains during transport and handling. Another benefit of lyophilization is minimized chemical degradation, as the water is largely removed and the solid cake decreases molecule mobility through the glass vitrification effect (351). However, previous studies identified issues that make lyophilization of AAV challenging. (i) Even though AAV vectors have a low mass fraction of the total mass of a typical freeze-drying formulation (<1%) even at extremely high concentrations (of up to 10^{14} vector genomes (vg)/mL) (7, 208), they have been reported to lower the glass transition temperature of the freezing concentrate (T_g') of sugar solutions (210). In the primary drying step, the water is removed due to sublimation by increasing the shelf temperature and reducing the chamber pressure. To avoid cake collapse, the primary drying temperature has to stay below the collapse temperature (T_c). T_c strongly correlates with T_g', requiring a lower primary drying temperature and thus resulting in a longer primary drying time. (ii) Wright et al. 2005 showed that a minimum ionic strength is needed to prevent AAV2 aggregation, typically between 150 and 200 mM (6). However, as the salt concentration increases, T_g' and T_c decrease, thereby further increasing the difficulty and requiring very slow drying cycles.

With these challenges in mind, we investigated the impact of the lyophilization cycle itself on stability of AAV vectors with a special focus on secondary drying. Furthermore, we evaluated various excipients for their ability to prevent aggregation and to stabilize the AAV vector lyophilizate for storage at 25°C.

We found that the undesirable instability of the AAV capsid during the lyophilization cycle can be significantly reduced if secondary drying is performed at lower temperatures and as short as possible, and the residual moisture is kept between 1.5 and 2%. Among the excipients tested, the group of extremolytes showed a very good improvement of the AAV capsid stability.

VI.3 Materials and methods

VI.3.1 Materials

VI.3.1.1 AAV vectors

Recombinant AAV vectors with genomes carrying inverted terminal repeats derived from AAV2 and packaged with wildtype AAV8 were produced as previously described in adherent HEK293T cells (The Leibniz Institute DSMZ-German Collection of Microorganisms and Cell Cultures GmbH, Braunschweig, Germany) (293, 294). The packaged self-complementary genome comprised a human cytomegalovirus promoter driving expression of eGFP (306). The purification using liquid chromatography was performed with an ÄKTA purifier from Cytiva (Marlborough, MA, USA). For sample loading, a Superloop or sample pump were used. All runs were performed at room temperature (25°C), and the detection was done with a UV detector (UL-9, fixed wavelength) at 280 nm implemented in the ÄKTA system. The evaluation was done with Unicorn Software (7.3) (Cytiva, Marlborough, MA, USA).

For affinity chromatography, a Poros capture select AAVx column (1 mL; Thermo Fisher Scientific, Dreieich, Germany) was used. AAV vector samples in 10 mM sodium phosphate, 150 mM sodium chloride at pH 7.4 were loaded at a flow rate of 0.3 mL/min on the column and eluted with 100 mM citric acid solution (VWR, Geldenaaksenbaan, Belgium), pH 3.0, at a flow rate of 0.7 mL/min. AAV vectors were neutralized by elution of 1 mL into 200 µL 1 M Tris, pH 8.7 (95).

VI.3.1.2 Excipients

Trehalose and di-sodium hydrogen phosphate were provided by VWR chemicals (Pennsylvania, USA), glycerol, HEPES, arginine-HCl and base, Tris-HCl, Tris-Base, tricin, hydroxyectoin and ectoin from Sigma Aldrich (Missouri, USA), glucosylglycerol from bitop AG (Dortmund, Germany), potassium phosphate and sodium di-hydrogen phosphate from Grüssing (Filsum, Germany), histidine-HCl, potassium chloride, sodium chloride from Merck KGaA (Darmstadt, Germany), HES (Hydroxyethyl starch (200/0,5) from BOC Sciences (London, UK), poloxamer 188 from BASF (Ludwigshafen, Germany), PEG 400 from Caelo (Hilden, Germany), dextran 5 (5.000 MW) from Pharmacosmos A/S (Holbaek, Denmark). Arginine phosphate was generated by titration of arginine base (Sigma Aldrich, Missouri, USA) with ortho phosphoric acid (Merck KGaA, Darmstadt, Germany), until pH 7.4 was reached.

VI.3.2 Methods

VI.3.2.1 Preparation of formulations

All AAV vector material used for lyophilization was buffer exchanged to 10 mM potassium phosphate buffer (pH 7.4) with a Slide-a-lyzer 10 kDa Mini 0,5 – 2 mL (Thermo Fisher, Dreieich, Germany). After dialysis, concentration of the AAV vector suspension was measured with the main peak recovery in size exclusion chromatography (SEC) using the linear calibration curve of the fluorescence detector (Figure VI.S1). Then, stock solutions of each excipient and surfactant were prepared in the same buffer and mixed with dialyzed AAV vector suspension for each formulation. pH was adjusted to the targeted pH using a MP 220 pH meter (Mettler-Toledo GmbH, Gießen, Germany), and all stocks were filtered using a 0.22 µm Millex-GV, 33 mm, PVFD membrane filter (Merck KGaA, Darmstadt, Germany).

A tabular overview of the used formulations can be found in Table VI.1. The lyophilization process was performed with a Christ 2D6 two chamber freeze-dryer (Martin Christ Gefriertrocknungsanlagen GmbH, Osterode am Harz, Germany). 150 µL of the AAV vector suspension containing $1.0*10^{12}$ vector genome (vg)/mL and $1.0*10^{13}$ capsids (cp)/mL were filled with a Mulitpipette E3 (Eppendorf AG, Hamburg, Germany) in 2R-tubing vials (MGlas AG, Münnerstadt, Germany) and were semi-stoppered with lyophilization stoppers (West Pharmaceuticals Service Inc., Eschweiler, Germany).

VI.3.2.1.1 Vector genome titer determination by qPCR

The vector titer was measured by real-time PCR, carried out with the Step one Plus device (Thermo Fisher scientific, Germany). AAV2 free ITR qPCR was realized as described by D'Costa et al. (114).

VI.3.2.1.2 Size exclusion chromatography (SEC)

A Waters 2695 system (Eschborn, Germany) and Wyatt SEC protein column 50 (WTC-050S5, 5µm, 7.8x300 mm) (Wyatt Technology, Santa Barbara, USA) were used for the size exclusion chromatography. AAV vector elution was detected at 280 nm and 260 nm with a UV detector (Waters 2487) and at excitation wavelength 280 nm and emission wavelength 330 nm with a fluorescence detector (Dionex RF2000, Sunnyvale, CA, USA). The monomer peak area was calibrated by using an AAV8 sample of which the capsid amount had previously been determined by ELISA (Figure VI.S1). The running buffer consisted of 10 mM sodium phosphate and 150 mM sodium chloride at pH 7.4 with a flow rate of 0.5 mL/min. The chromatograms were integrated with Chromeleon V6.8 (Thermo Fisher, Dreieich, Germany).

VI.3.2.1.3 SYBR Gold fluorescence assay to determine free DNA release

Free DNA was determined by fluorescence of SYBR® Gold (Invitrogen, Eugene, OR, USA) that shows enhanced fluorescence intensity after binding to DNA (219). The fluorescence intensity was read with excitation at 485 nm and emission at 535 nm using a Tecan spark plate reader (Tecan Trading AG, Männedorf, Switzerland). The free DNA percentage was calculated by dividing the free DNA amount in the samples by the total DNA released from the AAV capsids in samples disrupted by exposure to 85°C for 20 min in the presence of 0.1% poloxamer 188. Each formulation was measured in triplicates.

VI.3.2.1.4 Activity assay

The activity assay was performed in HeLa cells. 12-well plates (Greiner AG, Kremsmünster, Austria) were used and every well contained 50.000 cells at the beginning. 24 h after splitting, the medium was removed, and 0.5 mL new medium were added to each well. Subsequently, 10 µL formulation were added to the wells. During the transduction, the cells were stored at 37°C and 5% CO_2 for 48 h. After two days, the cells were trypsinized and the number of green-fluorescent cells were measured by Countess (Thermo Fisher, Dreieich, Germany). For each formulation and time point biological duplicates were performed, and two measurements with the Countess were performed for every well.

VI.3.2.1.5 Dynamic light scattering (DLS)

Dynamic light scattering measurements were performed on a Wyatt DynaPro III using Corning 3540 384 well plates. Two wells with 20 µL were filled for each sample. The plate was centrifuged at 2000 rpm for 2 min using a Heraeus Megafuge 40 centrifuge, equipped with an M-20 well plate rotor (Thermo Fisher Scientific, Wilmington, USA). Each measurement contained 10 acquisitions within an acquisition time of 5 seconds. The DLS results were shown as z-average diameter and results from three vials of each formulation were averaged. The autocorrelation function of each measurement was analyzed using cumulant analysis with the Dynamics V7.10 software (Wyatt Technology, Santa Barbara, USA)

VI.3.2.2 Lyophilization process and analytics

VI.3.2.2.1 Lyophilization cycle

A standard cycle was performed as follows: Shelf temperature was decreased from 20°C to -50°C with a ramp rate of 1°C/min and then equilibrated for 180 minutes. Then a vacuum of 0.08 mbar was applied, and shelf temperature was increased to -20°C using a ramp rate of 1°C/min. This temperature was held for 7 hours and then raised to 20°C using a ramp rate of 1°C/min. This temperature was held for another 8 hours. This standard cycle was modified for the experiments with secondary drying temperatures, where the temperature was set to 4°C, 10°C or 20°C; references to the respective cycle are given in the text. Correspondingly, the time of secondary drying varied from 12 minutes up to 8 hours, depending on the secondary drying temperature and the formulation.

An annealing cycle was performed as follows: Shelf temperature is decreased from 20 °C to -50 °C with a ramp rate of 1°C/min and equilibration for 180 minutes. An annealing step is included by heating to -20°C with a ramp rate of 1°C/min and equilibration for 180 minutes. The shelf was cooled again to a temperature of -50°C with a ramp rate of 1°C/min and equilibration for 180 minutes. A vacuum of 0.08 mbar is used, and shelf temperature was increased to -20°C using a ramp rate of 1°C/min. This temperature is held for 7 hours to allow for primary drying. For secondary drying, the temperature was increased to 20°C and held for 8 hours.

For all cycles, venting was performed with nitrogen at 600 mbar with subsequent vial closing.

VI.3.2.2.2 Reconstitution of the lyophilizates

To reconstitute the lyophilized cakes, high purified water (HPW) was added. The amount of HPW was calculated individually for each formulation to match the original liquid volume for each formulation. For this purpose, the solid content of the formulation was calculated to obtain the amount of water needed for reconstitution.

VI.3.2.2.3 Karl fischer titration

Karl Fischer titration was used to determine residual water content after lyophilization and after storage time. The 2R vials with the samples were placed into the 100°C hot oven of the coulometric Karl Fischer titrator (Aqua 40.00; Elektrochemie Halle, Halle an der Saale, Germany). The results were calculated as relative water content in percent (w/w).

VI.3.2.2.4 Differential scanning calorimetry

Differential scanning calorimetric analysis was performed on a DSC 214 Polyma (Netzsch-Gerätebau GmbH, Selb, Germany) or DSC 821e (Mettler Toledo, Gießen, Germany) under nitrogen atmosphere. For determination of T_g', 20 µL of the liquid formulation were pipetted into aluminum crucibles and sealed hermetically. The samples were cooled from 20°C to -60°C (-43°C only for Netzsch) and finally heated up to 180°C with a ramp rate of 5°C/min. For determination of T_g, 5 to 10 mg of each sample were weighted into aluminum crucibles in a compressed air-purged glove box. A temperature ramp rate of 10°C/min was applied from 0 to 150°C. The Proteus® Analysis 7.10 and Mettler STARe softwares were used for data analysis. The measurements were performed in triplicates.

VI.3.2.2.5 X-Ray-diffraction – XRD

Crystallinity of KCl was measured using a XRD 3000 TT diffractometer (GE Sensing & Inspection Technologies GmbH, Ahrensburg, Germany). A copper anode at 40 kV and 30 mA was used to generate CuKα radiation (λ= 0.15417 nm). The lyophilized cakes of three to four vials were pulverized and the powder was placed on a copper sample holder. Powder diffraction was measured ranging from 5° to 45° 2-θ in 0.05° measurement intervals at a hold time of 2 seconds for each measurement angle.

VI.4 Results

It is commonly known that freezing of solutions can result in a pH shift (352-354). pH sensitivity is a well-documented problem for proteins (213) and AAV vectors alike (63, 210). Taking this into account, all formulations used were buffered in 10 mM potassium phosphate pH 7.4 because potassium phosphate buffer causes a smaller pH shift than sodium phosphate.

A major challenge for lyophilization of AAV vector formulations is the concentration of 150 mM - 200 mM of salt usually needed in liquid formulations to prevent AAV vectors self-association and aggregation (6). This high salt content poses a challenge to produce a stable lyophilized formulation, as high amounts of salt lower T_g' (259) and can crystallize during storage, resulting in an unstable matrix.

One option to create a stable formulation over storage with this high amount of salt is forcing the crystallization of the salt, as is already done for other crystalline bulking agents like mannitol (355). To achieve full crystallization, the ratio of salt to sugar must exceed a certain threshold (355), as sugar can inhibit the crystallization of salts (356).

Thus, we aimed to find an optimal ratio between KCl and trehalose that allows the salt to crystallize with enough trehalose left to stabilize the AAV vectors. First, we tested the following ratios of KCl to trehalose (150 mM KCl to 150 mM (100, 75, 50 and 37.5) trehalose) in placebos. The mixture of 150 mM KCl and 2.84% (75 mM) trehalose resulted in good looking cakes with a solid content of 4.45% and T_g of 52°C (Figure VI.S2A). To avoid AAV vector loss due to adsorption to the packing material, 0.1% poloxamer 188 was added, yielding our starting formulation for lyophilization (F02) (348). To increase T_g, 5% of dextran 5 (357) was added to F02 resulting in F03. Formulation F01 containing 10 mM sodium phosphate buffer, 150 mM NaCl and 0.1% poloxamer 188, was used as a control formulation for liquid storage.

Table VI.1 Excipient combination for each formulation F01 -F11 and the corresponding T_g' and the activity after 4 weeks at 25°C of the lyophilizates.

Formulation number	AAV concentration [cp/mL]	Buffer	KCl [mM]	NaCl [mM]	Trehalose [%]	Dextran 5 [%]	HES [%]	Hydroxyectione [%]	Poloxamer 188 [%]	T_g' [°C]	Activity [%] of lyophilizates after 4 weeks at 25°C
F01	$1*10^{13}$	10 mM sodium phosphate		150					0.1	NA	NA
F02		10 mM potassium phosphate	150		2.84					NA	49
F03			150		2.84	5				-28.6	24
F04			150				10			-15.3	25
F05			150		5.67		10			-31.6	45
F06			150				10	5		-41.3	58
F07			150		5.67			5		-47.8	72
F08			150		5.67		10	5		-38.0	76
F09					5.67		10			-23.0	27
F10					5.67			5		-39.5	77
F11					5.67		10	5		-32.3	29

VI.4.1 The effect of storage temperature on AAV vector stability

In a six months stability study, F01 was tested in liquid form only, while F02 and F03 were tested in liquid and lyophilized forms, all stored in glass vials at 2-8°C and 25°C, respectively. F02 was lyophilized with the annealing lyophilization cycle and F03 with the standard cycle because dextran 5 is able to hold KCl in an amorphous matrix, as shown with X-Ray-Diffraction (XRD) (Figure VI.S2B).

For F02 initially after lyophilization full monomer recovery and activity was detected compared to the liquid formulation (Figure VI**.**1A and F). In contrast, for F03 lower monomer recovery was observed, as well as a higher concentration of aggregates (Figure VI**.1**A).

For F02 the residual moisture after lyophilization was around 0.7% and resulted in a T_g of 68°C. Both parameters changed only slightly over storage time. For formulation F03 the residual moisture after lyophilization was around 0.4% and T_g was around 117°C, but we observed moisture again, resulting in decreasing T_g over storage (Figure VI.1B). As shown in Figure VI**.**1A, no monomer loss detected over six months for F01, F02 and F03 liquid nor for F02 lyophilized samples. In contrast to these formulations, a clear loss was detected for F03 lyophilized samples and the concentration of soluble aggregates rose over storage time. The stable activity level (Figure VI.1E and F) over time correlates with the constantly low amount of free DNA (Figure VI.1C and D) for liquid storage at 2-8°C.

The lyophilized samples of F02 also performed well at 2-8°C, but the formulations stored at 25°C showed an increasing amount of free DNA over the course of storage (Figure VI**.1**D), and when comparing the results with the activity assay (Figure VI.1F), there was a clear loss of activity in the formulations stored at 25°C. The lyophilized AAV vectors lost about 40% of the activity after being stored at 25°C for six months. In contrast, the AAV vectors in the liquid formulation lost nearly all activity and showed an activity of only 10% after the six months storage at 25°C. For F03 the lyophilized and liquid samples stored at 25°C, activity was completely lost (Figure VI.S3).

These results indicate that stabilization of AAV vectors at 2-8°C is possible in liquid as well as in lyophilized formulations. F03, containing dextran 5, performed worse than F02, so high T_g does not seem to be indicative of a stable AAV vector lyophilizate. However, storage at 25°C proved to be the challenge. To achieve a higher AAV capsid stability and

to reduce the amount of free DNA, the formulation had to be adapted with new excipients or combinations of excipients.

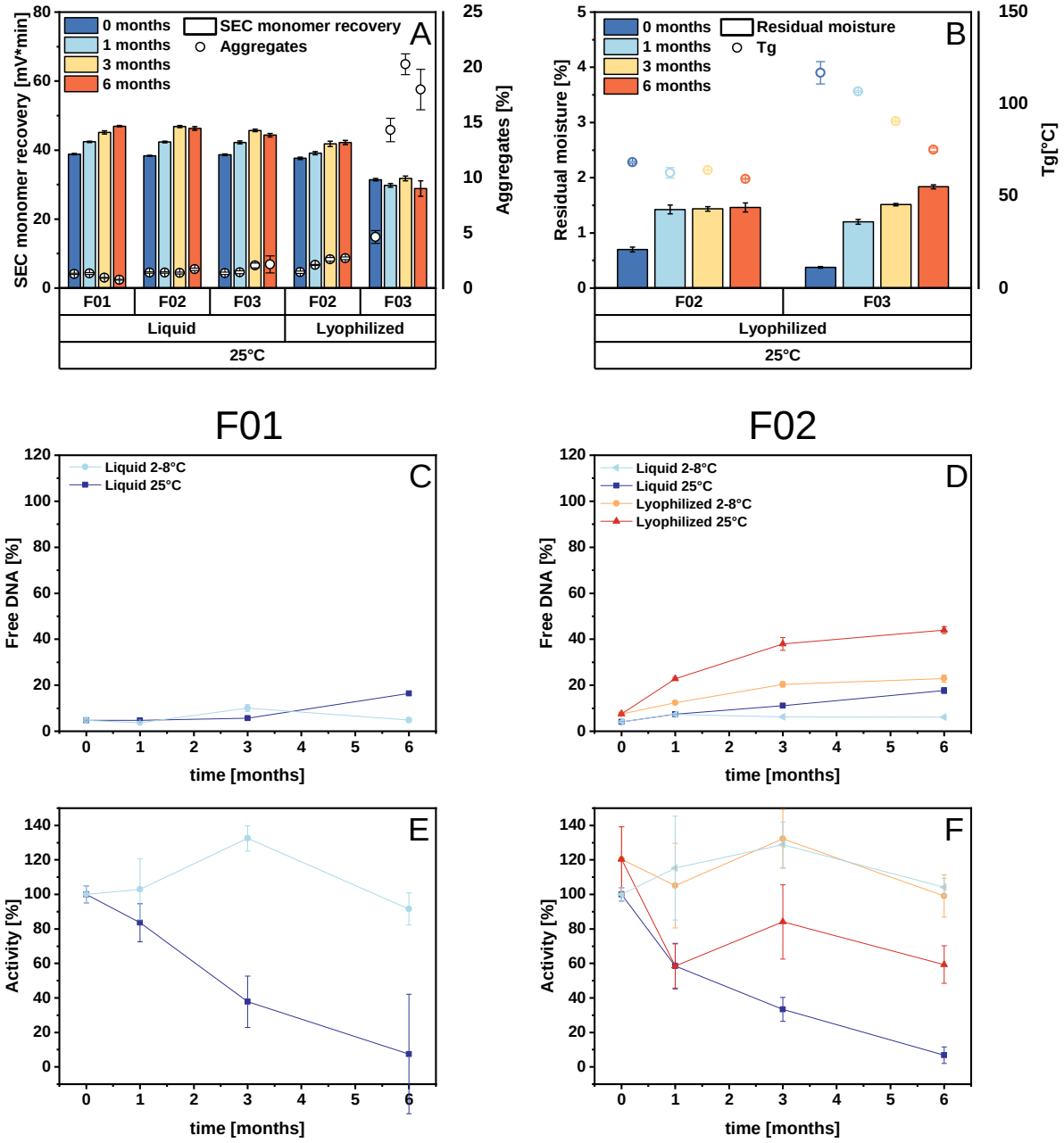

Figure VI.1 Results of the six months stability study of formulation F01, F02 and F03 stored liquid and lyophilized at 2-8°C and 25°C in glass vials. (A) The monomer recovery and percentage of soluble aggregates in SEC after storage at 25°C. (B) The residual moisture and T_g of F02 and F03 stored in solid state at 25°C. (C and D) The amount of free DNA in the samples during storage normalized to the 100% free DNA sample. (C) F01 liquid only. (D) F02 liquid and lyophilized. (E and F) Activity assay data after storage at 2-8°C or 25°C up to six months. The data were normalized to the activity of the corresponding liquid at the start of the study. (E) Activity data of liquid storage of F01. (F) Activity data of F02 liquid and lyophilized storage.

VI.4.2 Effect of HES and hydroxyectoine on undesired plasmid DNA release from the capsid

In a first step, we evaluated hydroxyethyl starch (HES) and hydroxyectoine. HES has been widely used as excipient to stabilize cells during lyophilization (358, 359). In addition, as a large polysaccharide, HES has strong water binding properties and increases the viscosity of a solution, resulting in less movement within the sample and less osmotic stress during drying (360, 361). Hydroxyectoine is also known for stabilization of proteins as well as DNA (362). Moreover, Hydroxyectoine is a tetrahydropyrimidine derivative and has a zwitterionic character that, dependent on the pH, contributes to the ionic strength of a formulation. The exact composition of the formulations used can be found in Table VI.1.

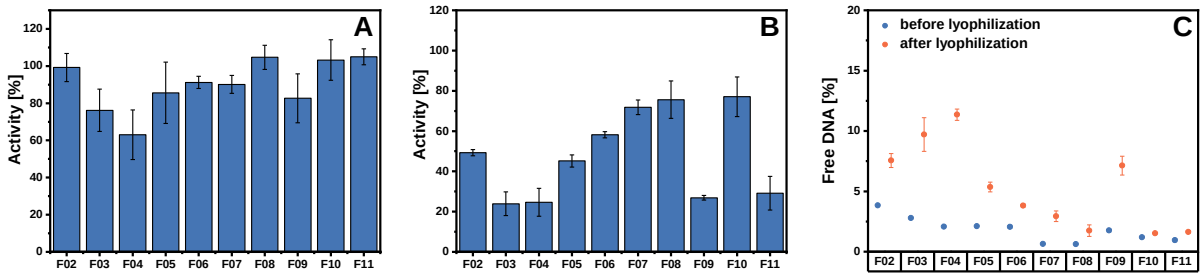

Figure VI.2 Data of liquid and lyophilized formulations showing the amount of free DNA and the activity before and after lyophilization. (A and B) show the activity data initially after lyophilization (A) and after four weeks at 25°C (B). The activity data are normalized to the activity of each formulation before lyophilization. (C) shows the differences of the free DNA amount before and after lyophilization of F02 – F11.

For this study, the formulations were stored as lyophilizates at 25°C for four weeks. Initially, after lyophilization, F03, F04 and F09 showed a clear loss in activity, whereas for F05, F06 and F07 only small losses of activity were detected. The formulations F02, F08, F10 and F11 performed best, with approx. 100% activity immediately after lyophilization (Figure VI.2A) compared to the corresponding liquid formulations before lyophilization.

After four weeks at 25°C, the activity of F03 and F04 dropped to only 20%. F05, which differs from F04 by the addition of 5.67% (150 mM) trehalose, showed improved stability of AAV vectors but retained only 45% activity after four weeks of storage. This correlates well with the corresponding SEC data (Figure VI.S4). Nonetheless, trehalose, a classical cryoprotectant and lyoprotectant, appears to be advantageous for stabilizing AAV vectors in lyophilizates. This is in line with the results of two other freeze-thaw studies which also showed a stabilizing effect of sucrose and trehalose against multiple freeze-thaw cycles

(254, 348). Addition of 5% hydroxectoine to F04 improved stability of the AAV vectors to 58% for F06. F07, F08 and F10 showed the best activity after storage with 71 – 77%. These three formulations also contained 5% hydroxyectoine. Comparing of F10 with F09 and F11 suggests that the presence of salt is not mandatory to stabilize the AAV vectors in lyophilizates. F10 did not contain salt and performed well after storage, while F09 and F11, both of which also contained no salt, performed poorly in stabilizing AAV vectors.

VI.4.3 Effect of processing steps on undesired DNA release from the capsid

In the previous experiments all formulations showed a higher amount of free DNA after lyophilization compared to the liquid state before lyophilization (Figure VI.2C).

To understand at which point in the lyophilization cycle the potential genome ejection or disassembly of the capsid occurred, we interrupted the lyophilization cycle at seven points. The first stop was set after freezing (at -50°C), the next three stops during the primary drying phase at -20°C and 0.08 mbar, and the last three stops in the secondary drying phase at 20°C (Figure VI.3A). This experiment was done with F08, because this formulation was among the best performing formulations concerning AAV vector stability after storage and had a high T_g of 91°C.

As expected, the residual moisture fell and T_g rose over process time. After primary drying, the residual moisture was 3.7% and T_g 34°C. After three hours in secondary drying the residual moisture dropped down to 0.6% and T_g rose to 79°C (Figure VI.3B).

In Figure VI.3E the amount of free DNA is depicted for all stops directly after lyophilization. Already after freeze-thaw, a very small increase in free DNA could be detected. The first large loss of packed DNA was detected during primary drying (plus 1.5%), and this amount remained stable throughout primary drying. During secondary drying at 20°C, a further increase of the amount of free DNA was observable over time.

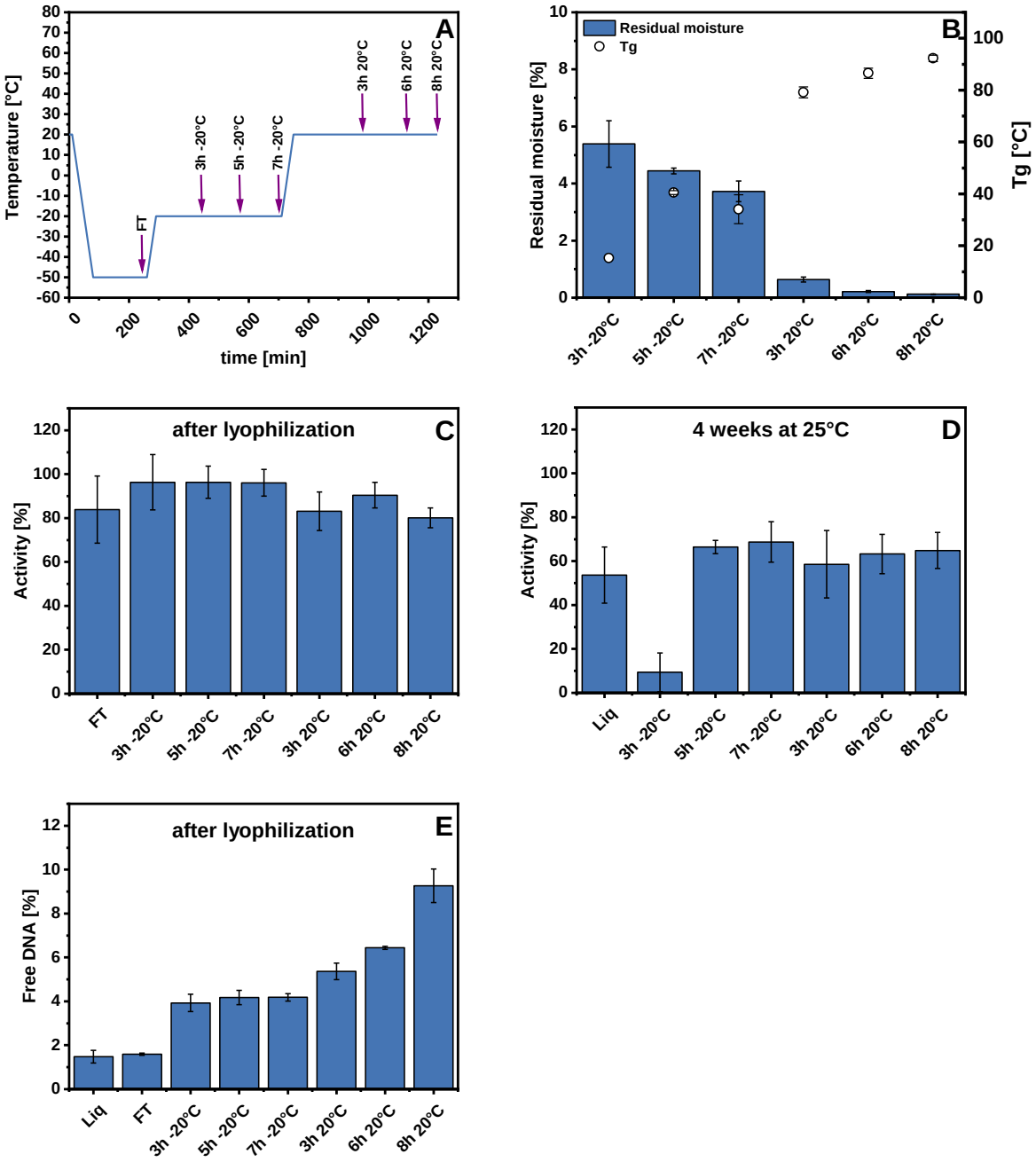

Figure VI.3 Data of liquid and lyophilized formulations showing residual moisture, the amount of free DNA and the activity at seven stops during the lyophilization cycle. In (A) the stops during the lyophilization cycle are marked with arrows. The data of residual moisture and T_g are shown in (B). The activity is depicted in (C) directly after lyophilization and in (D) after 4 weeks at 25°C and normalized to the activity before lyophilization. Error bars are standard deviation of two different vials and technical duplicates per well. (E) depicts the amount of free DNA directly after lyophilization, error bars are standard deviation of results from three different vials.

After lyophilization, all samples showed more or less the same activity (Figure VI.3C). After storage at 25°C for four weeks, the *in vitro* potency of all AAV vectors was reduced (Figure VI.3D). In particular, the sample that was in primary drying for only 3h lost almost

all of its activity, while all other lyophilized samples showed comparable activity levels. The liquid formulation also showed an activity of 53%. Thus, for formulation F08 the lyophilized form performed only slightly better than the one kept as liquid.

These data suggest that some genome ejection from the AAV capsid may occur at each step of the lyophilization cycle and that, particularly for the secondary drying, the amount of free DNA increases with the secondary drying time. Furthermore, storage stability at 25°C is only feasible if the residual moisture is below 4.4% and T_g is above 34°C.

VI.4.4 Effect of secondary drying temperature on undesired DNA release from the capsid

The previous experiment raised the question of whether the increasing amount of free DNA was caused by the elevated temperature during secondary drying (20°C) or by the reduced amount of water in the sample. Therefore, we repeated the freeze-drying with a fixed residual moisture content of 1.5-2% and varied the secondary drying temperature from 4°C (30 minutes) to 10°C (30 minutes) and 20°C (12 minutes).

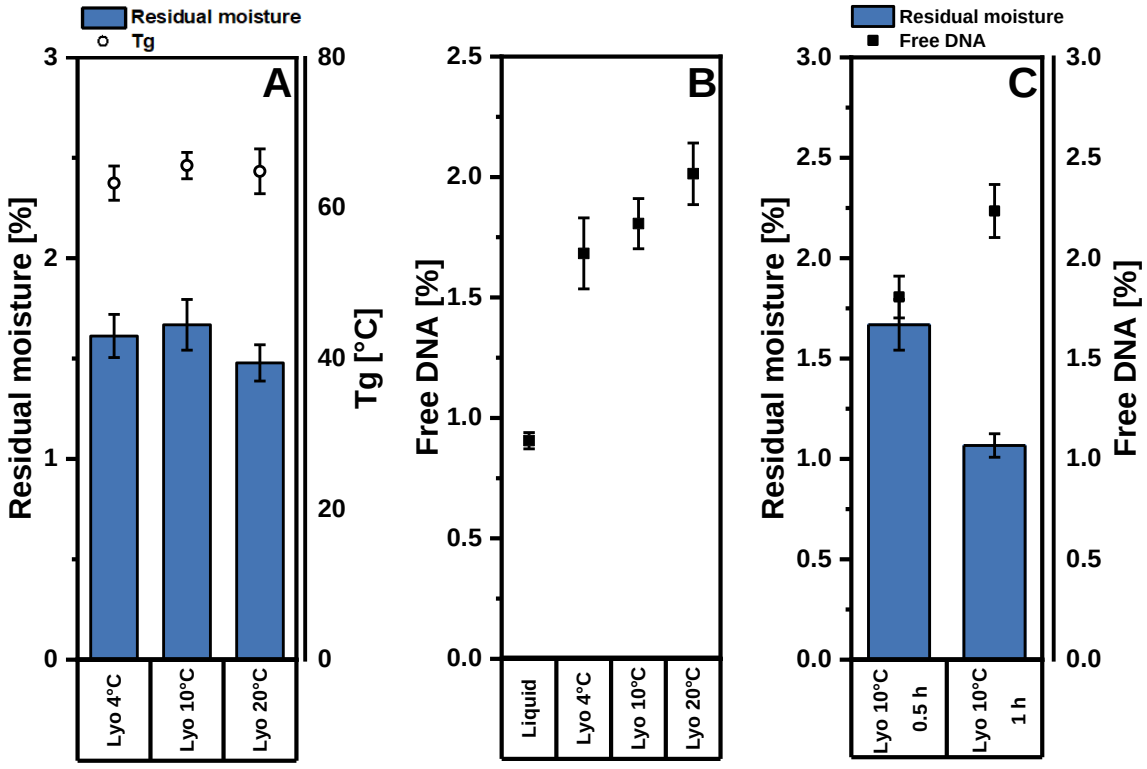

Figure VI.4 Formulation F08 dried at different secondary drying temperatures during lyophilization. (A) shows residual moisture and T_g of F08 at secondary drying temperatures of 4°C, 10°C and 20°C and (B) depict the free DNA of F08 for the secondary drying temperatures as well as the starting amount of free DNA in the formulation. (C) show the comparison of residual moisture and free DNA of F08 dried at 10°C in the secondary drying for 0,5 h and 1 h

We first confirmed that the values for both parameters, residual moisture and Tg, remained constant for the different samples of F08 post-dried at 4°C, 10°C and 20°C (Figure VI.4A). Next, we examined the amount of free DNA and found that it increased with rising secondary drying temperature (Figure VI.4B), while the drying time remained very short at all three temperatures.

As a control, F08 was dried at 10°C secondary drying temperature for 0.5h and 1h resulting in 1.7% and 1.1% residual moisture, respectively (Figure VI.4C). The samples with lower residual moisture had a 1% higher content of free DNA and low activity. In particular, the sample with 1.7% residual moisture reached 85% activity, while the sample with 1.1% residual moisture had only 64% activity immediately after lyophilization (data not shown). Both experiments indicate that "over-drying" is a problem in the lyophilization of AAV vectors. Although this is not a completely new finding (210, 218), it proves that sufficient water replacement was not achieved with the AAV vector formulations used for lyophilization so far. Therefore, it was necessary to search for better excipients to stabilize the AAV vectors while keeping the residual moisture above 1.5%.

VI.4.5 Effect of excipients on undesired DNA release from the capsid

Based on the above results, a new excipient screening was performed. A broad selection of excipients was screened for their stabilizing effect in lyophilization of AAV vector. In addition to sugars, amino acids, extremolytes, Good's buffers and plasticizers were included.

First, the effect of adding of the following amino acids to 150 mM trehalose plus 0.1% poloxamer 188: histidine-HCl, arginine-HCl and arginine-phosphate at a final concentration of 75 mM each was tested. The *in vitro* activity of the different freeze-dried AAV vectors over a storage period of four weeks at 25°C for the group of amino acids is depicted in Figure VI.5A. For both arginine containing formulations an initial drop of

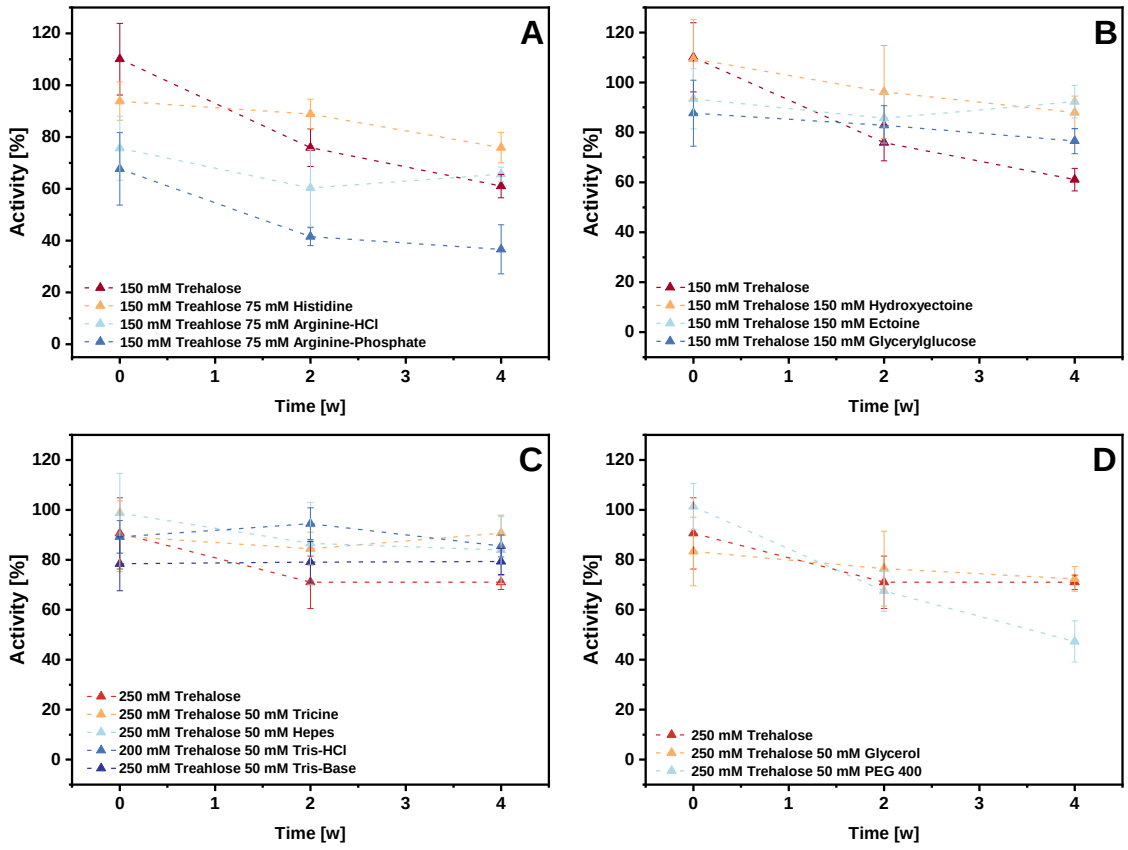

Figure VI.5 Formulation screen with different groups of excipients. For all excipients the activity directly after lyophilization and after two and four weeks at 25 °C, normalized to the activity before lyophilization, is shown (A-D), dark red 150 mM trehalose and light red 250 mM trehalose. (A) group of amino acids plus 150 mM trehalose, yellow 75 mM histidine, light blue 75 mM arginine-HCl and medium blue 75 mM arginine-phosphate. (B) Group of extremolytes plus 150 mM trehalose, yellow 150 mM hydroxyectoine, light blue 150 mM ectoine and medium blue 150 mM glycerylglucose. (C) Group of Good's buffers plus 200 – 250 mM trehalose, yellow 50 mM tricin, light blue 50 mM HEPES, medium blue 50 mM Tris-HCl and dark blue 50 mM Tris-base. (D) 250 mM trehalose plus, yellow 50 mM glycerol and light blue 50 mM PEG 400.

activity was detected. The activity of the arginine-phosphate formulation fell dramatically during storage. After four weeks the bioactivity for the formulation with arginine-HCl was similar to the activity of the formulation containing only 150 mM trehalose. The formulation with histidine showed the most stable activity during storage, outperforming this group with 75% activity after 4 weeks.

Next, the effect of addition of 150 mM of the extremolytes hydroxyectoine, ectoine, or glycerylglucose to the same formulation buffer (150 mM trehalose plus 0.1% poloxamer 188) was tested. Ectoin and glycerylglucose initially resulted in a slight drop in activity to 93% (ectoine) and 87% (glycerylglucose) at, which, however, remained constant over storage (Figure VI.5B). The formulation containing hydroxyectoine had a very good initial activity (109%), lost some activity over storage, ending up with 87% activity, comparable to ectoine and glycerylglucose. All three formulations containing an extremolyte in addition to trehalose outperformed trehalose alone.

Subsequently, the effect of 50 mM of the following Good's buffers was evaluated as additional excipients: tricine, HEPES, Tris-HCl, and Tris-base. To ensure isotonicity the trehalose concentration in the base formulation had to be adjusted to 250 or 200 mM, but poloxamer 188 remained at 0.1%. All formulations containing a Good's buffer showed constant activity over storage at 25°C (Figure VI.5C). All ended up in the range of 79-90% activity after four weeks and improved the stability of AAV vectors in lyophilized state compared to the formulation containing trehalose only.

The last group, plasticizers, was added because these excipients should have an impact on the residual moisture. Notably, glycerol and PEG 400 already showed promising results in stabilization of AAV during freeze-thawing (348). Nevertheless, this stabilizing effect was not found again during freeze-drying. Both, 50 mM of glycerol or PEG 400 added to 250 mM trehalose plus 0.1% poloxamer 188 showed no improvement over the formulation without plasticizer (Figure VI.5D). The idea of putting another H-bridge donor into the formulation to stabilize the AAV vectors failed, this formulation ended up with only 47% of activity after four weeks at 25°C.

VI.4.6 Effect of the amount of hydroxyectoine and trehalose on DNA release from the capsid

We next aimed to test the effect of different concentrations of an extremolyte and chose to focus on hydroxyectoine. For the hydroxyectoine concentration range study, 0.5 – 6% hydroxyectoine was added to 5.67% trehalose and 0.1% poloxamer 188. Both chosen readouts, the amount of free DNA, as well as the activity assay showed that a concentration of 5% hydroxyectoine is sufficient to provide a stable AAV vector lyophilizate (Figure .6A and C). For the formulations with less hydroxyectoine, the amount of free DNA increased over storage and the activity decreased to 60 - 74%. To determine the optimal concentration of trehalose, formulations with 2.84 - 11.35% trehalose plus 2.5% hydroxyectoine and 0.1% poloxamer 188 were prepared. The measurement of free DNA clearly showed that less DNA is released during freeze-drying and storage in the presence of higher concentrations of trehalose in the formulation (Figure VI.6B and D). However, taking into account the

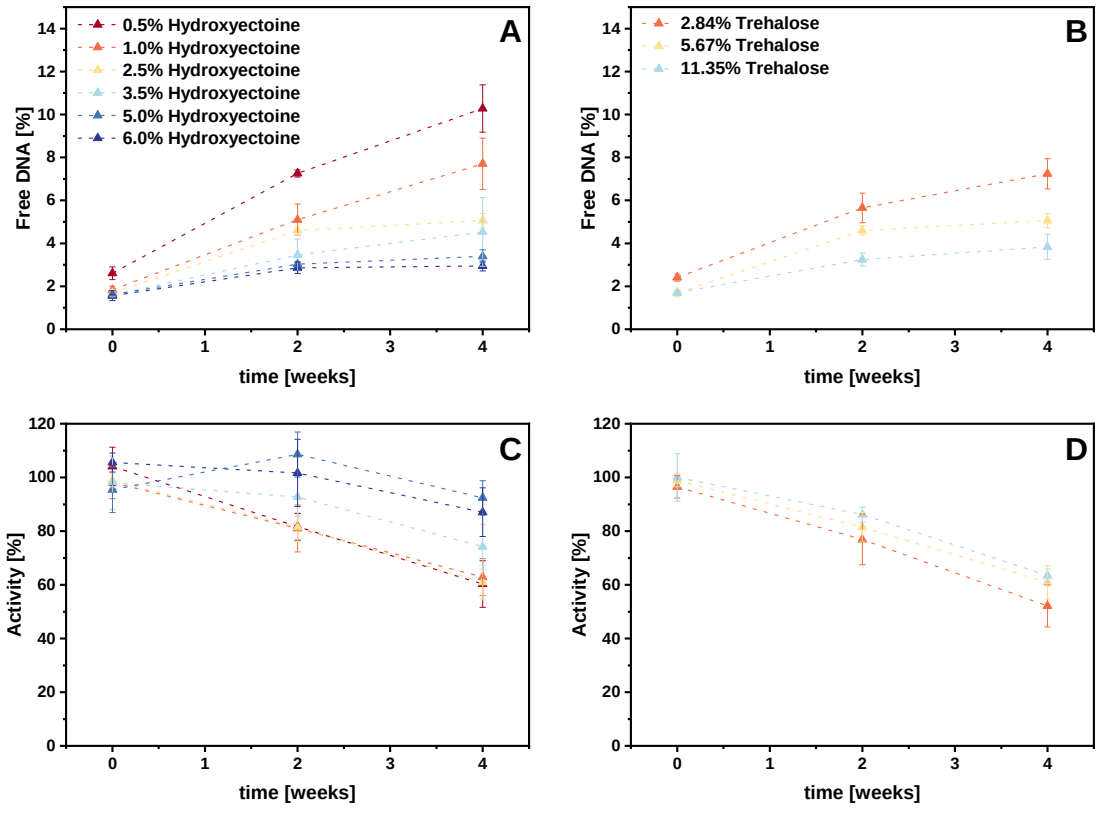

Figure VI.6 Free DNA amount and activity in freeze-dried formulations of concentration series of hydroxyectoine and trehalose. (A-B) show the amount of free DNA over storage time at 25°C (A) hydroxyectoine concentration series with 5.67% trehalose in each formulation (B) trehalose concentration series with 2.5% hydroxyectoine in all three formulations. (C-D) show the activity over storage time at 25°C (C) hydroxyectoine concentration series (D) trehalose concentration series.

activity data, the concentration optimum of trehalose seems to be reached already at a concentration of about 5.67% trehalose.

VI.4.7 Test of robustness for the lead formulation

To test the robustness of the formulation containing 5.67% trehalose, 5% hydroxyectoine and 0.1% poloxamer 188 at pH 7.4, three different lyophilization cycles with different secondary drying temperatures were performed (4°C for 8 hours, 10°C for 4 hours and 20°C for 2 hours) and compared to the liquid before lyophilization. Again, 1% more free DNA was detected after lyophilization (Figure VI.7A). However, with this formulation no differences between secondary drying at 4°C and 10°C was observed. This was confirmed by DLS, which shows the size distribution of the sample by measuring the dynamic light

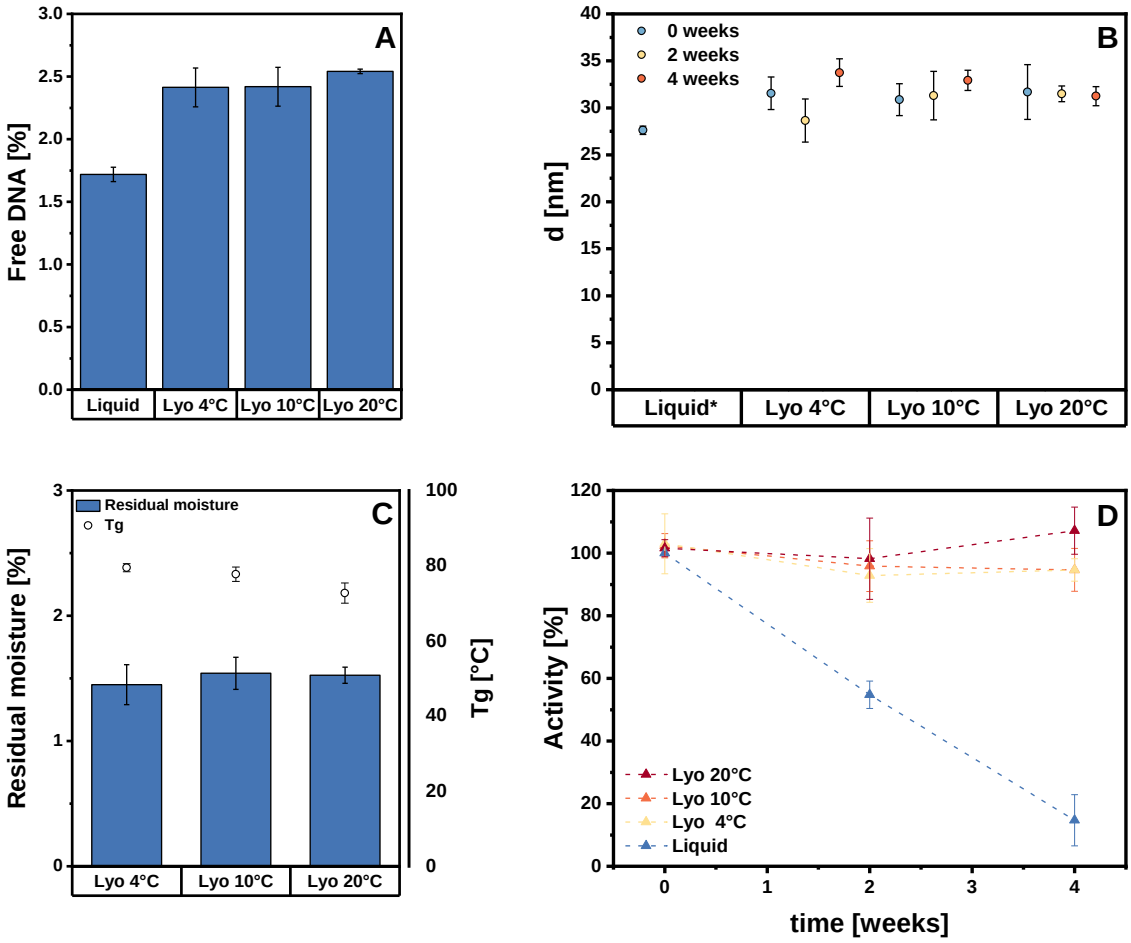

Figure VI.7 Formulation F10 dried at different secondary drying temperatures during lyophilization
(A) depict the free DNA of F10 for secondary drying temperatures as well as the starting amount of free DNA in the formulation. In (B) the DLS results are shown for all three lyophilization cycles and the storage of four weeks at 25°C. The residual moisture of 1.5% as well as the resulting glass transition temperature are depicted in (C). The activity of the formulation over the storage is shown in (D). *Due to the high polydispersity observed by DLS, a distinct diameter could not be determined for the liquid formulation.

scattering, and by the activity assay. Neither aggregation nor increased loss of activity could be observed (Figure VI.7B and D). In contrast, for the liquid formulation the activity fell down to 14% after four weeks storage at 25°C (Figure VI.7B).

VI.5 Discussion

In this study, we demonstrated that it is possible to lyophilize and stabilize AAV8-based AAV vectors for storage at 2-8°C and over at least four weeks at 25°C. Notably, we have also shown that this is possible without the minimum amount of 150 – 200 mM salt commonly thought to be necessary to prevent aggregation of AAV vectors for liquid formulations (6).

A first series of experiments demonstrated that it is possible to produce stable lyophilizates containing 150 mM KCl. However, while the liquid and lyophilized samples of formulations F01 and F02 stored at 2-8°C were stable over six months, all formulations stored at 25°C showed a dramatical loss of activity directly after the first month of storage. Although little loss of AAV capsid and vector could be detected by SEC and qPCR, the amount of free DNA increased dramatically over time, indicating that a high degree of genome ejection and little degradation of the capsid for F03 had occurred under these conditions. In contrast, the liquid storage showed an acceptable stability at 2-8°C, which eliminates the need for lyophilization when storage at this temperature is acceptable.

However, since we aimed for storage stability at 25°C, we decided to test excipients which are known to have stabilizing effects on cell membranes, proteins, and DNA (HES and hydroxyectoine). While we were able to improve the stability especially with hydroxyectoine (e.g. in formulations F08 and F10), we realized, that the lyophilization process itself leads to AAV capsid instability and DNA release and thereby having a negative impact on biological activity.

We therefore decided to carefully evaluate the lyophilization process and learned that every step during lyophilization leads to increased DNA release from the AAV particles. Particularly the secondary drying temperature and the drying time seem to have a major impact on the amount of ejected genomes. Secondary drying temperatures of 20°C or higher substantially increase the amount of free DNA the can be detected with the SYBR Gold dye. This correlates with the observation that drying, below a residual moisture of 1.5%, generates more free DNA. The importance of the amount of residual moisture has been discussed before by Zhang et al. 2021 (218). Yet, it is also known that at high moisture

content, chemical degradation such as deamidation can occur, leading to a loss of AAV vector activity (10, 95). Thus, it was necessary to find the optimal residual moisture content.

For the lyophilization cycle we discovered two critical parameters: the secondary drying temperature and the secondary drying time, which should be kept as low and as short as possible, respectively. The final freeze-dried formulation should ideally have a residual moisture of 1.5-2%.

With this in mind, amino acids, extremolytes, Good's buffers, glycerol and PEG 400 were investigated for a stabilizing effect on AAV vectors during lyophilization and storage. Similar excipients were also studied by Xu et al. (348) in terms of their ability to protect AAV from freeze-thaw stress. The authors reported that during freeze-thawing sucrose, glycerol and PEG are able to stabilize AAV8. In contrast, we found that arginine, glycerol and PEG 400 are not able to improve the stability of AAV8 in the lyophilized state beyond trehalose only. Whereas histidine, extremolytes and Good's buffers all led to an improved stability of AAV8 during storage.

From the promising group of excipients – the extremolytes - hydroxyectoine was selected because it is even more H-bond forming, i.e., hydrophilic compared to ectoine. Different ratios of hydroxyectoine and trehalose were tested and the optimum ratio was determined to be 5% of hydroxyectoine and 5.67% trehalose. This lead to the optimized formulation with 10 mM potassium phosphate buffer, 5.67% trehalose, 5% hydroxyectoine and 0.1% poloxamer 188 with a residual moisture of 1.5% and a T_g of 77°C, resulting in only (1%) increase of free DNA after lyophilization, and a robust residual activity of 94% (±6%) after four weeks at 25°C. Finally, we showed that at this setting, the effects of secondary drying temperature are negligible in a range of 4°C to 20°C, although we recommend staying below 20°C.

VI.6 Acknowledgments

The authors want to thank Johanna Koch and Kerstin Skokann for the production of the AAV vectors and bitop AG for providing glycerylglucose for our excipient screening.

VI.7 Supplement

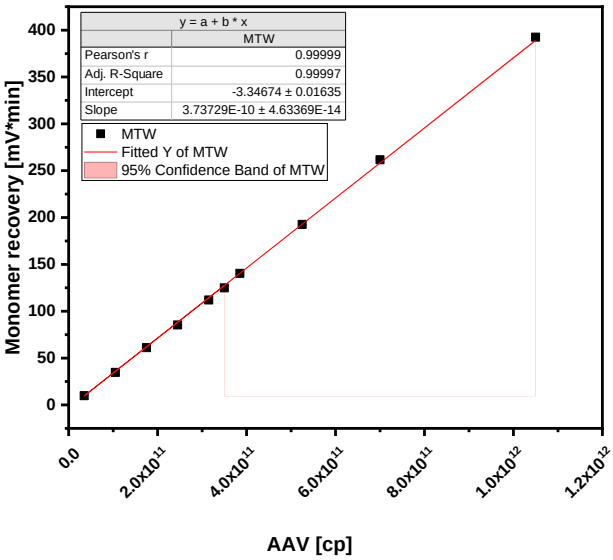

Figure VI.S1 SEC calibration. Monomer recovery plotted against capsid amount determined by capsid ELISA.

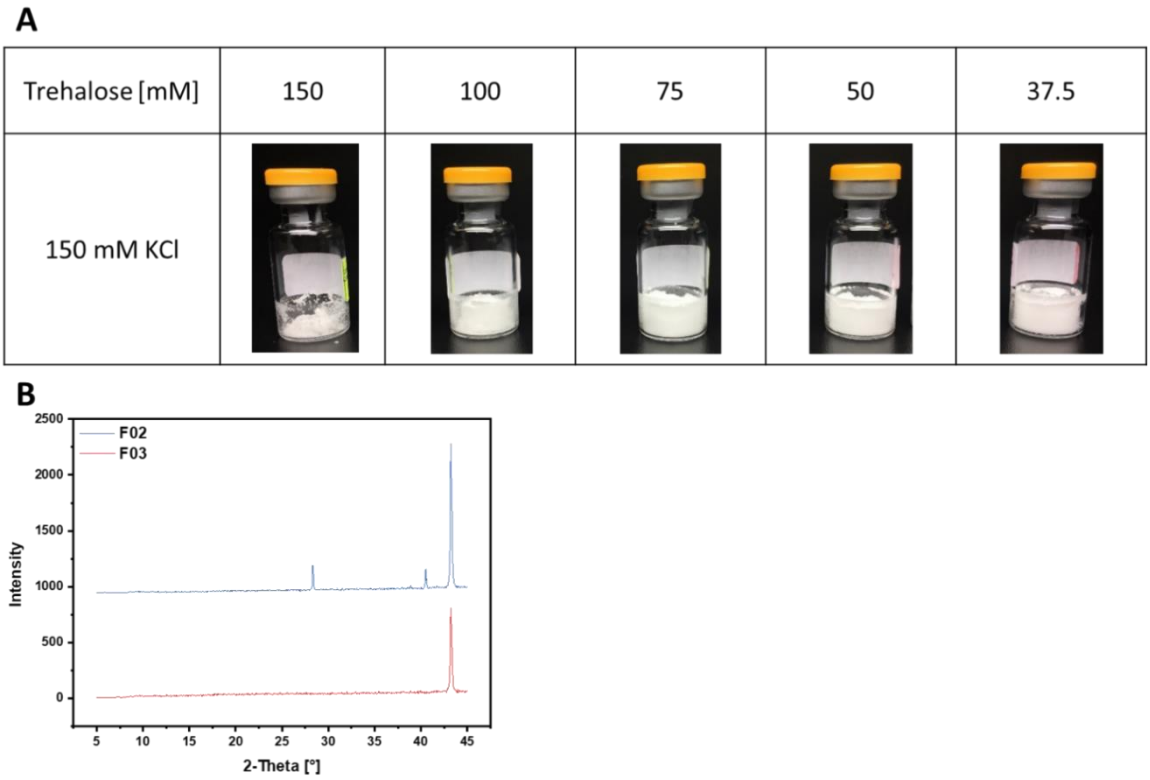

Figure VI.S2 Cake appearance with different KCl to trehalose ratios. In (A) pictures of 2R vials containing 1 mL lyophilized formulation with 150 mM KCl and the shown amount of Trehalose. (B) shows the XRD results for F02 and F03 initially after lyophilization.

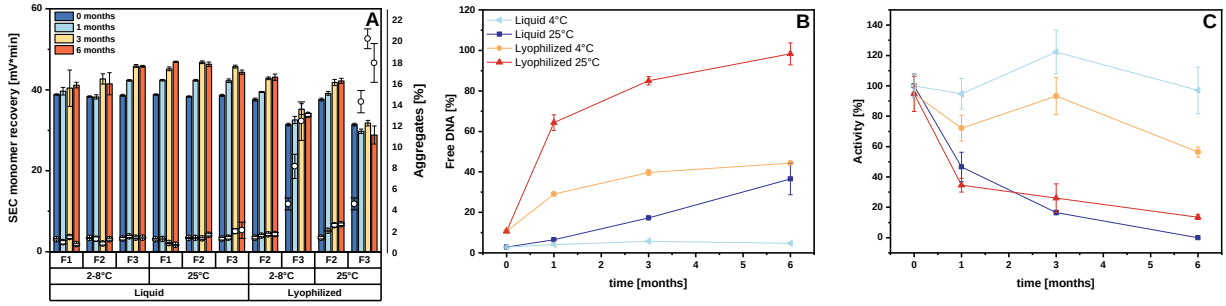

Figure VI.S3 Results of the six months stability study of formulation F01, F02 and F03 stored liquid and lyophilized at 2-8°C and 25°C in glass vials. (A) The monomer recovery and percentage of soluble aggregates in SEC after storage at 2-8°C and 25°C. Monomer recovery is shown as bar and the amount of aggregates is depicted as circle. (B) The amount of free DNA in F03 liquid and lyophilized during storage normalized to the 100% free DNA sample. (C) Activity assay data of F03 liquid and lyophilized after storage at 2-8°C or 25°C up to six months. The data were normalized to the activity of the corresponding liquid at the start of the study.

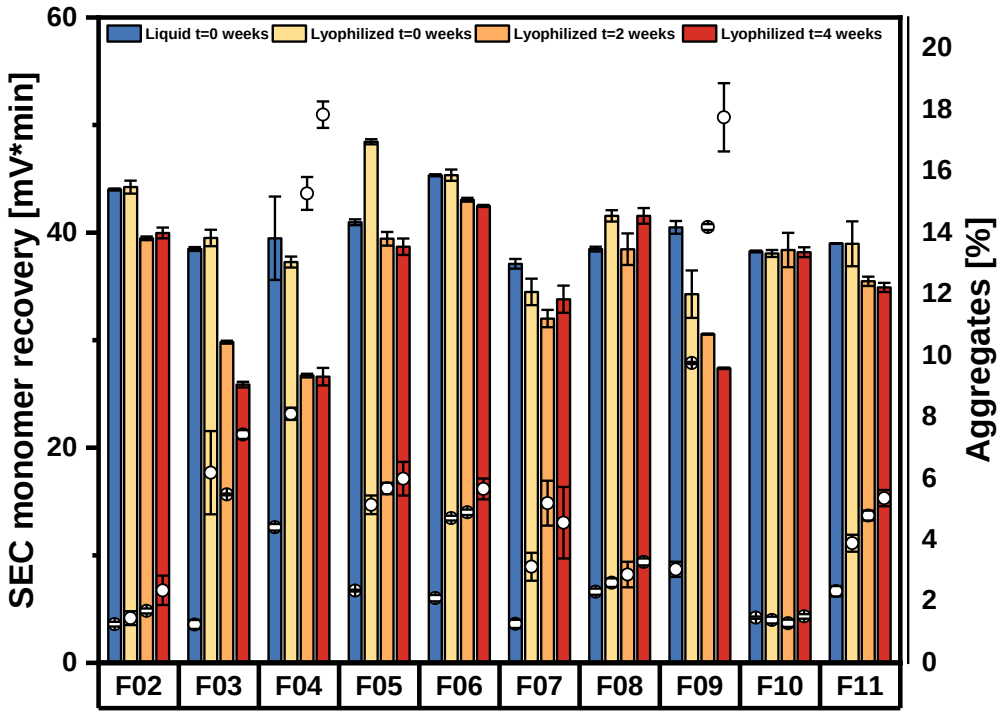

Figure VI.S4 Data of liquid and lyophilized formulations F02 – F11 showing SEC monomer recovery and aggregates before and after lyophilization as well as after 2 and 4 weeks storage at 25°C. Monomer recovery is shown as bar and the amount of aggregates is depicted as circle.

Chapter VII Summary of the thesis

Gene therapy using AAV represents a valuable additional tool for the treatment of inherited monogenetic diseases, especially when the consequences of this genetic disease are difficult or impossible to treat with conventional drugs. An important factor for successful gene therapy is the efficient insertion of the correct and intact DNA strand into the cell nucleus. The transfection of the target cells is one of the main downsides of other carrier systems. With AAV as transfection carrier, on the other hand, the two drugs on the market, Luxturna and Zolgensma, have proven to be effective therapeutics for *RPE65*-linked retinal dystrophy and *SMN1*-linked spinal muscular atrophy, respectively. The aim of this thesis was to improve the analytical characterization of AAV looking at serotype identity and capsid titer, to develop a serotype-independent purification method, that is easy to scale up to meet the ever-increasing production capacity, and, ultimately, to improve storage stability of AAV vector formulations using lyophilization. Accordingly, the chapters of the thesis build upon each other and reflect not only the research process but can also function as a guidance for an improved AAV DP development.

Chapter I discusses the analytical opportunities and challenges to control the central critical quality attributes (CQA) (i.e., identity, potency, purity, safety, and stability) for developing AAV drug product (DP) and lays out the motivation behind this thesis.

In Chapter II, an easy and fast serotype identification method is described using intrinsic fluorescence. It was proven that serotype identification is possible with iDSF in less than one hour with just 10 µL of an AAV sample containing $3*10^{11}$ cp/mL. Even though the state-of-the-art dot blot with antibody labeling only requires about 1 µL of $1*10^{9}$ cp/mL, the assay takes between 6-8 hours, scale up and automation is difficult and, if different serotypes are to be tested, different antibodies are required. The data from intrinsic differential scanning fluorimetry (iDSF) were compared with the melting points measured with the SYPROrange dye, as an established orthogonal method. With intrinsic fluorescence measurements melting point detection is even possible for formulations containing surfactants. Finally, the AAV serotype in the DP can be controlled by iDSF even in the presence of surfactants.

Having established improved identification of the AAV serotype, chapter III compares different methods for capsid titer determination. The evaluated detection methods range from fluorescence and UV detectors over light scattering analysis using MALS, DLS and/or SLS, UV spectrometry, to the established SDS-PAGE. All methods resulted in the same

range of capsid titer for the different samples. However, the analytical methods using UV detection showed a 10-fold higher LOD in respect to fluorescence detection. A special focus was given to the additional information that can be gathered through the respective methods like impurity and aggregate detection. In this work, it was shown that capsid titer can be reliably determined using a wide variety of methods. Thus, in future studies, researchers can choose their method based on the parameters mentioned here as additional information, being assured that the measurement of capsid titer is possible either way.

As the experimental data from this evaluation process revealed a substantial AAV loss during sterile filtration, chapter III also addresses the effect of poloxamer 188 and different membrane material on AAV loss. It was discovered that the presence of poloxamer 188 reduces the AAV adsorb to the syringe itself, as well as to the filtration membrane. Between the three filter materials a slight advantage of polyvinylidendifluorid (PVDF) over the regenerated cellulose (RC) and polyethersulfon (PES) was found.

In the following Chapter IV, different liquid chromatography-based purification strategies for AAV8 were tested and compared with a special focus on virus yield and residual impurities. The key finding is that PEG precipitation, combined with affinity chromatography (AC), results in the highest purity and yield of AAV8 but lacks separation of full and empty capsids. To validate this promising purification strategy, several variants of AAV2, AAV2.NN, and AAV2.GL, engineered variants of AAV2, were tested on the AC and cation exchange (CEX) chromatography. It became clear that binding to the AC column was disturbed by the changes at the AAV2 capsid present in AAV2.NN and AAV2.GL. Thus, considering all serotypes tested, the CEX column showed more promising results regarding yield. In a final purification step, it was demonstrated that full-empty separation and baseline separation is possible for AAV8 using a step gradient.

Next, Chapter V supplements the purification experiments with further studies on the purified samples. The analytical scope was extended towards the control for the residual p-Transgene backbone which was found to be encapsulated in AAV capsid and poses a safety risk for AAV DP. In addition, mass photometry (MP) was tested as a new approach for full-empty capsid determination, showing good results for discrimination of the two species and reliable ratios of full and empty capsids in one sample. The chapter closes with an evaluation of the impact of different purification strategies on capsid damage and transfection efficiency. A central outcome of these experiments is that the classical iodixanol purification strategy results in considerably higher capsid damage compared to

chromatography-based methods. Among those, the capsid damage was the lowest for CEX purification, because of the higher pH (4.0) and shorter running time compared to AC.
Ultimately, Chapter VI examines the storage stability of liquid and lyophilized formulations containing AAV. Based on the preliminary results, some critical obstacles for AAV lyophilization were identified. These hurdles are discussed in the chapter, as is the subsequent process optimization of the lyophilization cycle focusing on secondary drying temperature. In addition, the impact of different excipients including, buffers, amino acids, and extremolytes on formulation stability was tested. One lesson learned was that a minimum water content of 1.5% is necessary for a stable AAV lyophilizate. The chapter closes with a lyophilized formulation containing 10 mM potassium phosphate buffer, 5.67% trehalose, 5% hydroxyectoine and 0.1% poloxamer 188 that is stable at 25°C for at least four weeks and clearly outperforms the liquid formulation. It should be noted, however, that most AAV samples stored at 2-8°C in liquid were surprisingly stable over six months when sufficient salt amounts were included in the formulation - stabilizing the AAV son a par with the lyophilized formulations.
In summary, this thesis provides improved analytical methods for the detection of different CQA of an AAV DP. It also documents purification development for AAV8, that was also tested for AAV2 and engineered variants. It is important to note that the results of the AEX are highly specific for the AAV8 tested. Thus, chromatography conditions must be adjusted separately for each serotype. The results of the lyophilization experiments on AAV8 confirm a recently published study by Zhang et al. (218) on the stability of AAV lyophilizates and indicate that a minimum amount of residual water in the lyophilizate > 1.5% is necessary to generate a stable AAV lyophilizate. Pharmaceutical strategies were presented which can support scientists to further improve analytical and purification strategies and the challenging stabilization on AAV during storage.

There is still room for improvement: Especially in the area of AAV purification, and more precisely in the separation of full and empty capsids. It has already been shown several times that the separation of the two species using AEX is possible, but it has also been shown that the method must be adapted for each serotype. To simplify the purification process, it would be desirable to find a method and/or column for this final purification step that allows the simple and reliable separation of full and empty capsids for as many serotypes as possible.

Lastly, there is still limited knowledge on factors influencing AAV stability. In addition to the already tested factors such as pH, ionic strength and auxiliary substances, possible factors of interest might be buffers, surfactants, oxygen and antioxidants, further excipients, AAV concentration, and finally primary packaging materials.

References

1. Pfeifer A, Verma IM. Gene therapy: promises and problems. Annu Rev Genomics Hum Genet. 2001;2:177-211.
2. High KA. AAV-mediated gene transfer for hemophilia. Ann N Y Acad Sci. 2001;953:64-74.
3. Bennett A, Patel S, Mietzsch M, Jose A, Lins-Austin B, Yu JC, et al. Thermal Stability as a Determinant of AAV Serotype Identity. Mol Ther Methods Clin Dev. 2017;6:171-82.
4. Ayuso E, Mingozzi F, Bosch F. Production, purification and characterization of adeno-associated vectors. Curr Gene Ther. 2010;10(6):423-36.
5. Pharmacopoeia E. 5.1.7 Virussicherheit. Ph. Eur. 10.0.
6. Wright JF, Le T, Prado J, Bahr-Davidson J, Smith PH, Zhen Z, et al. Identification of factors that contribute to recombinant AAV2 particle aggregation and methods to prevent its occurrence during vector purification and formulation. Mol Ther. 2005;12(1):171-8.
7. Wright JF. Product-Related Impurities in Clinical-Grade Recombinant AAV Vectors: Characterization and Risk Assessment. Biomedicines. 2014;2(1):80-97.
8. Kohlbrenner E, Weber T. Production and Characterization of Vectors Based on the Cardiotropic AAV Serotype 9. Methods Mol Biol. 2017;1521:91-107.
9. Tomono T, Hirai Y, Okada H, Miyagawa Y, Adachi K, Sakamoto S, et al. Highly Efficient Ultracentrifugation-free Chromatographic Purification of Recombinant AAV Serotype 9. Mol Ther Methods Clin Dev. 2018;11:180-90.
10. Giles AR, Sims JJ, Turner KB, Govindasamy L, Alvira MR, Lock M, et al. Deamidation of Amino Acids on the Surface of Adeno-Associated Virus Capsids Leads to Charge Heterogeneity and Altered Vector Function. Mol Ther. 2018;26(12):2848-62.
11. Kotin RM, Snyder RO. Manufacturing Clinical Grade Recombinant Adeno-Associated Virus Using Invertebrate Cell Lines. Hum Gene Ther. 2017;28(4):350-60.
12. Naso MF, Tomkowicz B, Perry WL, 3rd, Strohl WR. Adeno-Associated Virus (AAV) as a Vector for Gene Therapy. BioDrugs. 2017;31(4):317-34.
13. Atchison RW, Casto BC, Hammon WM. Adenovirus-Associated Defective Virus Particles. Science. 1965;149(3685):754-6.
14. Hermonat PL, Muzyczka N. Use of adeno-associated virus as a mammalian DNA cloning vector: transduction of neomycin resistance into mammalian tissue culture cells. Proc Natl Acad Sci U S A. 1984;81(20):6466-70.
15. Dong B, Nakai H, Xiao W. Characterization of genome integrity for oversized recombinant AAV vector. Mol Ther. 2010;18(1):87-92.
16. Lai Y, Yue Y, Duan D. Evidence for the failure of adeno-associated virus serotype 5 to package a viral genome > or = 8.2 kb. Mol Ther. 2010;18(1):75-9.
17. El Andari J, Grimm D. Production, Processing, and Characterization of Synthetic AAV Gene Therapy Vectors. Biotechnol J. 2021;16(1):2000025.
18. Naumer M, Sonntag F, Schmidt K, Nieto K, Panke C, Davey NE, et al. Properties of the adeno-associated virus assembly-activating protein. J Virol. 2012;86(23):13038-48.
19. Grosse S, Penaud-Budloo M, Herrmann AK, Borner K, Fakhiri J, Laketa V, et al. Relevance of Assembly-Activating Protein for Adeno-associated Virus Vector Production and Capsid Protein Stability in Mammalian and Insect Cells. J Virol. 2017;91(20):01198-17.
20. Elmore ZC, Patrick Havlik L, Oh DK, Anderson L, Daaboul G, Devlin GW, et al. The membrane associated accessory protein is an adeno-associated viral egress factor. Nature communications. 2021;12(1):1-13.

21. Hefferon KL, Dugdale B. Independent expression of Rep and RepA and their roles in regulating bean yellow dwarf virus replication. Journal of General Virology. 2003;84(12):3465-72.

22. Rayaprolu V, Kruse S, Kant R, Venkatakrishnan B, Movahed N, Brooke D, et al. Comparative analysis of adeno-associated virus capsid stability and dynamics. J Virol. 2013;87(24):13150-60.

23. Salganik M, Hirsch ML, Samulski RJ. Adeno-associated Virus as a Mammalian DNA Vector. Microbiol Spectr. 2015;3(4):827-49.

24. Mingozzi F, High KA. Immune responses to AAV vectors: overcoming barriers to successful gene therapy. Blood. 2013;122(1):23-36.

25. Schnodt M, Buning H. Improving the Quality of Adeno-Associated Viral Vector Preparations: The Challenge of Product-Related Impurities. Hum Gene Ther Methods. 2017;28(3):101-8.

26. Qu G, Bahr-Davidson J, Prado J, Tai A, Cataniag F, McDonnell J, et al. Separation of adeno-associated virus type 2 empty particles from genome containing vectors by anion-exchange column chromatography. J Virol Methods. 2007;140(1-2):183-92.

27. Buller RM, Janik JE, Sebring ED, Rose JA. Herpes simplex virus types 1 and 2 completely help adenovirus-associated virus replication. J Virol. 1981;40(1):241-7.

28. Ogston P, Raj K, Beard P. Productive replication of adeno-associated virus can occur in human papillomavirus type 16 (HPV-16) episome-containing keratinocytes and is augmented by the HPV-16 E2 protein. J Virol. 2000;74(8):3494-504.

29. McPherson RA, Rosenthal LJ, Rose JA. Human cytomegalovirus completely helps adeno-associated virus replication. Virology. 1985;147(1):217-22.

30. Thomson BJ, Weindler FW, Gray D, Schwaab V, Heilbronn R. Human herpesvirus 6 (HHV-6) is a helper virus for adeno-associated virus type 2 (AAV-2) and the AAV-2 rep gene homologue in HHV-6 can mediate AAV-2 DNA replication and regulate gene expression. Virology. 1994;204(1):304-11.

31. Cheung AK, Hoggan MD, Hauswirth WW, Berns KI. Integration of the adeno-associated virus genome into cellular DNA in latently infected human Detroit 6 cells. J Virol. 1980;33(2):739-48.

32. Nakai H, Yant SR, Storm TA, Fuess S, Meuse L, Kay MA. Extrachromosomal recombinant adeno-associated virus vector genomes are primarily responsible for stable liver transduction in vivo. J Virol. 2001;75(15):6969-76.

33. Penaud-Budloo M, Le Guiner C, Nowrouzi A, Toromanoff A, Chérel Y, Chenuaud P, et al. Adeno-associated virus vector genomes persist as episomal chromatin in primate muscle. Journal of virology. 2008;82(16):7875-85.

34. Ramsey JP, Khatwani SL, Lin M, Boregowda R, Surosky R, Ramelmeier RA. Overview of Analytics Needed to Support a Robust Gene Therapy Manufacturing Process. Current Opinion in Biomedical Engineering. 2021:100339.

35. Zheng BY, Li XD, Wiklund F, Chowdhry S, Angstrom T, Hallmans G, et al. Detection of adeno-associated virus type 2 genome in cervical carcinoma. Br J Cancer. 2006;94(12):1913-7.

36. Grossman Z, Mendelson E, Brok-Simoni F, Mileguir F, Leitner Y, Rechavi G, et al. Detection of adeno-associated virus type 2 in human peripheral blood cells. J Gen Virol. 1992;73 (4):961-6.

37. Food U, Administration D. Guidance for industry: Q8 (R2) pharmaceutical development. Center for Drug Evaluation and Research. 2009.

38. Gimpel AL, Katsikis G, Sha S, Maloney AJ, Hong MS, Nguyen TNT, et al. Analytical methods for process and product characterization of recombinant adeno-associated virus-based gene therapies. Mol Ther Methods Clin Dev. 2021;20:740-54.

39. Rumachik NG, Malaker SA, Poweleit N, Maynard LH, Adams CM, Leib RD, et al. Methods Matter: Standard Production Platforms for Recombinant AAV Produce Chemically and Functionally Distinct Vectors. Mol Ther Methods Clin Dev. 2020;18:98-118.

40. Mary B, Maurya S, Arumugam S, Kumar V, Jayandharan GR. Post-translational modifications in capsid proteins of recombinant adeno-associated virus (AAV) 1-rh10 serotypes. The FEBS journal. 2019;286(24):4964-81.

41. Zhong L, Li B, Mah CS, Govindasamy L, Agbandje-McKenna M, Cooper M, et al. Next generation of adeno-associated virus 2 vectors: point mutations in tyrosines lead to high-efficiency transduction at lower doses. Proc Natl Acad Sci U S A. 2008;105(22):7827-32.

42. Wright JF. AAV empty capsids: for better or for worse? Mol Ther. 2014;22(1):1-2.

43. AN180608: Measuring the Concentration of Adeno-Associated Virus with Multi-Angle Dynamic Light Scattering (MADLS). Malvern Panalytical. 2020.

44. Zhang X, Wang, W., and Kenrick S. AN50007: Characterization of AAV-Based Viral Vectors by DynaPro DLS/SLS Instruments. Wyatt Technology Corporation.

45. Koza SM, Chen W. AN135047399: Size-Exclusion Chromatography Analysis of Adeno-Associated Virus (AAV) Preparations Using a 450 Å Diol-Bonded BEH Column and Fluorescence Detection. Waters Corporation. 2020.

46. Kieleczawa J. Fundamentals of Sequencing of Difficult Templates—An Overview. J Biomol Tech 2006;17(3):207-17.

47. Ruffing M, Zentgraf H, Kleinschmidt JA. Assembly of viruslike particles by recombinant structural proteins of adeno-associated virus type 2 in insect cells. J Virol. 1992;66(12):6922-30.

48. Warrington Jr KH, Gorbatyuk OS, Harrison JK, Opie SR, Zolotukhin S, Muzyczka N. Adeno-associated virus type 2 VP2 capsid protein is nonessential and can tolerate large peptide insertions at its N terminus. Journal of virology. 2004;78(12):6595-609.

49. Farr GA, Zhang L-g, Tattersall P. Parvoviral virions deploy a capsid-tethered lipolytic enzyme to breach the endosomal membrane during cell entry. Proceedings of the National Academy of Sciences. 2005;102(47):17148-53.

50. Stahnke S, Lux K, Uhrig S, Kreppel F, Hösel M, Coutelle O, et al. Intrinsic phospholipase A2 activity of adeno-associated virus is involved in endosomal escape of incoming particles. Virology. 2011;409(1):77-83.

51. Grieger JC, Snowdy S, Samulski RJ. Separate basic region motifs within the adeno-associated virus capsid proteins are essential for infectivity and assembly. Journal of virology. 2006;80(11):5199-210.

52. Wu P, Xiao W, Conlon T, Hughes J, Agbandje-McKenna M, Ferkol T, et al. Mutational analysis of the adeno-associated virus type 2 (AAV2) capsid gene and construction of AAV2 vectors with altered tropism. Journal of virology. 2000;74(18):8635-47.

53. Popa-Wagner R, Porwal M, Kann M, Reuss M, Weimer M, Florin L, et al. Impact of VP1-specific protein sequence motifs on adeno-associated virus type 2 intracellular trafficking and nuclear entry. Journal of virology. 2012;86(17):9163-74.

54. Wistuba A, Kern A, Weger S, Grimm D, Kleinschmidt JA. Subcellular compartmentalization of adeno-associated virus type 2 assembly. J Virol. 1997;71(2):1341-52.

55. Pacouret S, Bouzelha M, Shelke R, Andres-Mateos E, Xiao R, Maurer A, et al. AAV-ID: A Rapid and Robust Assay for Batch-to-Batch Consistency Evaluation of AAV Preparations. Mol Ther. 2017;25(6):1375-86.

56. Rieser R, Penaud-Budloo M, Bouzelha M, Rossi A, Menzen T, Biel M, et al. Intrinsic Differential Scanning Fluorimetry for Fast and Easy Identification of Adeno-Associated Virus Serotypes. J Pharm Sci. 2020;109(1):854-62.

57. Grimm D, Kern A, Pawlita M, Ferrari F, Samulski R, Kleinschmidt J. Titration of AAV-2 particles via a novel capsid ELISA: packaging of genomes can limit production of recombinant AAV-2. Gene Ther. 1999;6(7):1322-30.

58. Mietzsch M, Grasse S, Zurawski C, Weger S, Bennett A, Agbandje-McKenna M, et al. OneBac: platform for scalable and high-titer production of adeno-associated virus serotype 1-12 vectors for gene therapy. Hum Gene Ther. 2014;25(3):212-22.

59. Kuck D, Kern A, Kleinschmidt JA. Development of AAV serotype-specific ELISAs using novel monoclonal antibodies. J Virol Methods. 2007;140(1-2):17-24.

60. Wistuba A, Weger S, Kern A, Kleinschmidt JA. Intermediates of adeno-associated virus type 2 assembly: identification of soluble complexes containing Rep and Cap proteins. J Virol. 1995;69(9):5311-9.

61. Krell T, Manin C, Nicolai MC, Pierre-Justin C, Berard Y, Brass O, et al. Characterization of different strains of poliovirus and influenza virus by differential scanning calorimetry. Biotechnol Appl Biochem. 2005;41(Pt 3):241-6.

62. Johnson CM. Differential scanning calorimetry as a tool for protein folding and stability. Archives of biochemistry and biophysics. 2013;531(1-2):100-9.

63. Lins-Austin B, Patel S, Mietzsch M, Brooke D, Bennett A, Venkatakrishnan B, et al. Adeno-Associated Virus (AAV) Capsid Stability and Liposome Remodeling During Endo/Lysosomal pH Trafficking. Viruses 2020,12(6). 668.

64. Cole L, Fernandes D, Hussain MT, Kaszuba M, Stenson J, Markova N. Characterization of Recombinant Adeno-Associated Viruses (rAAVs) for Gene Therapy Using Orthogonal Techniques. Pharmaceutics. 2021;13(4):586.

65. Sommer JM, Smith PH, Parthasarathy S, Isaacs J, Vijay S, Kieran J, et al. Quantification of adeno-associated virus particles and empty capsids by optical density measurement. Mol Ther. 2003;7(1):122-8.

66. Kohlbrenner E, Henckaerts E, Rapti K, Gordon RE, Linden RM, Hajjar RJ, et al. Quantification of AAV particle titers by infrared fluorescence scanning of coomassie-stained sodium dodecyl sulfate-polyacrylamide gels. Hum Gene Ther Methods. 2012;23(3):198-203.

67. Rossi CA, Kearney BJ, Olschner SP, Williams PL, Robinson CG, Heinrich ML, et al. Evaluation of ViroCyt® Virus Counter for rapid filovirus quantitation. Viruses. 2015;7(3):857-72.

68. Lock M, Alvira M, Vandenberghe LH, Samanta A, Toelen J, Debyser Z, et al. Rapid, simple, and versatile manufacturing of recombinant adeno-associated viral vectors at scale. Hum Gene Ther. 2010;21(10):1259-71.

69. Ayuso E, Blouin V, Lock M, McGorray S, Leon X, Alvira MR, et al. Manufacturing and characterization of a recombinant adeno-associated virus type 8 reference standard material. Hum Gene Ther. 2014;25(11):977-87.

70. Girod A, Wobus CE, Zadori Z, Ried M, Leike K, Tijssen P, et al. The VP1 capsid protein of adeno-associated virus type 2 is carrying a phospholipase A2 domain required for virus infectivity. J Gen Virol. 2002;83(5):973-8.

71. Aucoin MG, Perrier M, Kamen AA. Critical assessment of current adeno-associated viral vector production and quantification methods. Biotechnol Adv. 2008;26(1):73-88.

72. Kohlbrenner E, Aslanidi G, Nash K, Shklyaev S, Campbell-Thompson M, Byrne BJ, et al. Successful production of pseudotyped rAAV vectors using a modified baculovirus expression system. Molecular therapy. 2005;12(6):1217-25.

73. Wörner TP, Bennett A, Habka S, Snijder J, Friese O, Powers T, et al. Adeno-associated virus capsid assembly is divergent and stochastic. Nature communications. 2021;12(1):1-9.

74. Ayuso E, Mingozzi F, Montane J, Leon X, Anguela XM, Haurigot V, et al. High AAV vector purity results in serotype- and tissue-independent enhancement of transduction efficiency. Gene Ther. 2010;17(4):503-10.

75. Burova E, Ioffe E. Chromatographic purification of recombinant adenoviral and adeno-associated viral vectors: methods and implications. Gene Ther. 2005;12 Suppl 1(1):5-17.

76. Chahal PS, Aucoin MG, Kamen A. Primary recovery and chromatographic purification of adeno-associated virus type 2 produced by baculovirus/insect cell system. J Virol Methods. 2007;139(1):61-70.

77. Doria M, Ferrara A, Auricchio A. AAV2/8 vectors purified from culture medium with a simple and rapid protocol transduce murine liver, muscle, and retina efficiently. Hum Gene Ther Methods. 2013;24(6):392-8.

78. Smith JK, Agbandje-McKenna M. Creating an arsenal of Adeno-associated virus (AAV) gene delivery stealth vehicles. PLoS Pathog. 2018;14(5):1006929.

79. Zolotukhin S, Byrne B, Mason E, Zolotukhin I, Potter M, Chesnut K, et al. Recombinant adeno-associated virus purification using novel methods improves infectious titer and yield. Gene therapy. 1999;6(6):973-85.

80. Allay JA, Sleep S, Long S, Tillman DM, Clark R, Carney G, et al. Good manufacturing practice production of self-complementary serotype 8 adeno-associated viral vector for a hemophilia B clinical trial. Hum Gene Ther. 2011;22(5):595-604.

81. Philo JS. A critical review of methods for size characterization of non-particulate protein aggregates. Curr Pharm Biotechnol. 2009;10(4):359-72.

82. AN: Take a peek inside your AAV capsid with Stunner. Unchained Labs. 2020.

83. McIntosh NL, Berguig GY, Karim OA, Cortesio CL, De Angelis R, Khan AA, et al. Comprehensive characterization and quantification of adeno associated vectors by size exclusion chromatography and multi angle light scattering. Sci Rep. 2021;11(1):3012.

84. Steppert P, Burgstaller D, Klausberger M, Tover A, Berger E, Jungbauer A. Quantification and characterization of virus-like particles by size-exclusion chromatography and nanoparticle tracking analysis. J Chromatogr A. 2017;1487:89-99.

85. Some D, Amartely H, Tsadok A, Lebendiker M. Characterization of Proteins by Size-Exclusion Chromatography Coupled to Multi-Angle Light Scattering (SEC-MALS). J Vis Exp. 2019;(148):59615.

86. Fraunhofer W. Asymmetrical flow field-flow-fractionation in pharmaceutical analytics: LMU; 2003.

87. Fraunhofer W, Winter G, Coester C. Asymmetrical flow field-flow fractionation and multiangle light scattering for analysis of gelatin nanoparticle drug carrier systems. Analytical chemistry. 2004;76(7):1909-20.

88. Deng C., AN2003: Quantifying AAV aggregation and quality attributes by FFF-MALS. Wyatt Technology.

89. Bousse T, Shore DA, Goldsmith CS, Hossain MJ, Jang Y, Davis CT, et al. Quantitation of influenza virus using field flow fractionation and multi-angle light scattering for quantifying influenza A particles. J Virol Methods. 2013;193(2):589-96.

90. Patel BA, Gospodarek A, Larkin M, Kenrick SA, Haverick MA, Tugcu N, et al. Multi-angle light scattering as a process analytical technology measuring real-time molecular weight for downstream process control. MAbs. 2018;10(7):945-50.

91. Amartely H, Avraham O, Friedler A, Livnah O, Lebendiker M. Coupling Multi Angle Light Scattering to Ion Exchange chromatography (IEX-MALS) for protein characterization. Sci Rep. 2018;8(1):6907.

92. Chen M, Purchel, A. AN1617: Quantifying quality attributes of AAV gene therapy vectors by SEC-UV-MALS-dRI. Wyatt Technology Corporation.

93. Gagnon P, Goricar B, Mencin N, Zvanut T, Peljhan S, Leskovec M, et al. Multiple-Monitor HPLC Assays for Rapid Process Development, In-Process Monitoring, and Validation of AAV Production and Purification. Pharmaceutics. 2021;13(1):113.

94. Wyatt PJ, Weida MJ. Method and apparatus for determining absolute number densities of particles in suspension. Google Patents; 2004.

95. Rieser R, Koch J, Faccioli G, Richter K, Menzen T, Biel M, et al. Comparison of Different Liquid Chromatography-Based Purification Strategies for Adeno-Associated Virus Vectors. Pharmaceutics 2021,13(5). 748.

96. Yang H, Koza SM, Chen W., AN135051172: Anion-Exchange Chromatography for Determining Empty and Full Capsid. Waters Corporation: Milford,USA. 2019.

97. AN160307: Characterization of gold-labeled Adeno-Associated Virus (AAV) and other small viruses by Nanoparticle Tracking Analysis (NTA). Malvern Panalytical. 2021.

98. Virus Counter Reagents: Rapid, Direct,Biologically relevant Virus Quantification. Sartorius Stedim Biotech GmbH. 2020.

99. Virus Counter®3100 Instrument Product Datasheet. Sartorius Stedim Biotech GmbH; 2020 [cited 2021 17.11]; Available from: https://www.sartorius.com/shop/medias/?context=bWFzdGVyfGRvY3VtZW50c3wzMTIwNjR8YXBwbGljYXRpb24vcGRmfGRvY3VtZW50cy9oYmYvaDgxLzkwNDA4MzIyNjYyNzAucGRmfDk5YWM5MDNhNTMzYzUyMWUwZDhmMzhiYzYyMDllYjAyMmYzZTRkZDc5ZTAzMmFkMmZhZWUyZTJjNWEwMGFjZmY.

100. Tyler Gates RM, Antje Schickert, Katherine D. Shives, Jeff Steaffens M. Rapid Quantification of Adeno-Associated Virus (AAV) and Lentiviral Vectors with the Virus Counter®Platform: Near-Real-Time Monitoring of Viral Vector Production. [cited 2021 17.11]; Available from: https://www.sartorius.com/shop/medias/?context=bWFzdGVyfGRvY3VtZW50c3w1OTAyNzh8YXBwbGljYXRpb24vcGRmfGRvY3VtZW50cy9oYTUvaGM3LzkwNDA2NDA5MzM5MTgucGRmfDhhY2VkMzk4ZjQ1MGU0ZDlhMmJjNmU3Yzg0ZjAxYzhkNmFiNTIxY2NhMjMzMzdmODEyZWI4YTRhYWNlZWFmZGQ.

101. Li H, Joseph T, Kang B, Rose A, Boenning K, Sanderson T. AN30: Rapid, automated, at-line AAV2 virus quantitation advances bioprocessing in gene therapy. ForteBio.

102. Lock M, Alvira MR, Chen SJ, Wilson JM. Absolute determination of single-stranded and self-complementary adeno-associated viral vector genome titers by droplet digital PCR. Hum Gene Ther Methods. 2014;25(2):115-25.

103. Clark KR, Liu X, McGrath JP, Johnson PR. Highly purified recombinant adeno-associated virus vectors are biologically active and free of detectable helper and wild-type viruses. Hum Gene Ther. 1999;10(6):1031-9.

104. Samulski RJ, Chang L-S, Shenk T. Helper-free stocks of recombinant adeno-associated viruses: normal integration does not require viral gene expression. Journal of virology. 1989;63(9):3822-8.

105. Aucoin MG, Perrier M, Kamen AA. Improving AAV vector yield in insect cells by modulating the temperature after infection. Biotechnol Bioeng. 2007;97(6):1501-9.

106. McCarty DM, Monahan PE, Samulski RJ. Self-complementary recombinant adeno-associated virus (scAAV) vectors promote efficient transduction independently of DNA synthesis. Gene Ther. 2001;8(16):1248-54.

107. Piedra J, Ontiveros M, Miravet S, Penalva C, Monfar M, Chillon M. Development of a rapid, robust, and universal picogreen-based method to titer adeno-associated vectors. Hum Gene Ther Methods. 2015;26(1):35-42.

108. Xu J, DeVries SH, Zhu Y. Quantification of Adeno-Associated Virus with Safe Nucleic Acid Dyes. Hum Gene Ther. 2020;31(19-20):1086-99.

109. Werling NJ, Satkunanathan S, Thorpe R, Zhao Y. Systematic Comparison and Validation of Quantitative Real-Time PCR Methods for the Quantitation of Adeno-Associated Viral Products. Hum Gene Ther Methods. 2015;26(3):82-92.

110. D'Costa S, Blouin V, Broucque F, Penaud-Budloo M, Francois A, Perez IC, et al. Practical utilization of recombinant AAV vector reference standards: focus on vector genomes titration by free ITR qPCR. Mol Ther Methods Clin Dev. 2016;5:16019.

111. Rohr U-P, Wulf M-A, Stahn S, Steidl U, Haas R, Kronenwett R. Fast and reliable titration of recombinant adeno-associated virus type-2 using quantitative real-time PCR. Journal of virological methods. 2002;106(1):81-8.

112. Veldwijk MR, Topaly J, Laufs S, Hengge UR, Wenz F, Zeller WJ, et al. Development and optimization of a real-time quantitative PCR-based method for the titration of AAV-2 vector stocks. Mol Ther. 2002;6(2):272-8.

113. Lock M, McGorray S, Auricchio A, Ayuso E, Beecham EJ, Blouin-Tavel V, et al. Characterization of a recombinant adeno-associated virus type 2 Reference Standard Material. Hum Gene Ther. 2010;21(10):1273-85.

114. D'Costa S, Blouin V, Broucque F, Penaud-Budloo M, Fçranois A, Perez IC, et al. Practical utilization of recombinant AAV vector reference standards: focus on vector genomes titration by free ITR qPCR. Molecular Therapy - Methods & Clinical Development 2016;3:16019.

115. Mayginnes JP, Reed SE, Berg HG, Staley EM, Pintel DJ, Tullis GE. Quantitation of encapsidated recombinant adeno-associated virus DNA in crude cell lysates and tissue culture medium by quantitative, real-time PCR. J Virol Methods. 2006;137(2):193-204.

116. Fagone P, Wright JF, Nathwani AC, Nienhuis AW, Davidoff AM, Gray JT. Systemic errors in quantitative polymerase chain reaction titration of self-complementary adeno-associated viral vectors and improved alternative methods. Human Gene Therapy, Part B: Methods. 2012;23(1):1-7.

117. Aurnhammer C, Haase M, Muether N, Hausl M, Rauschhuber C, Huber I, et al. Universal real-time PCR for the detection and quantification of adeno-associated virus serotype 2-derived inverted terminal repeat sequences. Hum Gene Ther Methods. 2012;23(1):18-28.

118. Moullier P, Snyder RO. International efforts for recombinant adeno-associated viral vector reference standards. Mol Ther. 2008;16(7):1185-8.

119. Sykes P, Neoh S, Brisco M, Hughes E, Condon J, Morley A. Quantitation of targets for PCR by use of limiting dilution. Biotechniques. 1992;13(3):444-9.

120. Whale AS, Cowen S, Foy CA, Huggett JF. Methods for applying accurate digital PCR analysis on low copy DNA samples. PLoS One. 2013;8(3):58177.

121. Bhat S, Herrmann J, Armishaw P, Corbisier P, Emslie KR. Single molecule detection in nanofluidic digital array enables accurate measurement of DNA copy number. Anal Bioanal Chem. 2009;394(2):457-67.

122. Corbisier P, Bhat S, Partis L, Xie VR, Emslie KR. Absolute quantification of genetically modified MON810 maize (Zea mays L.) by digital polymerase chain reaction. Anal Bioanal Chem. 2010;396(6):2143-50.

123. Dobnik D, Kogovsek P, Jakomin T, Kosir N, Tusek Znidaric M, Leskovec M, et al. Accurate Quantification and Characterization of Adeno-Associated Viral Vectors. Front Microbiol. 2019;10:1570.

124. Dreo T, Pirc M, Ramsak Z, Pavsic J, Milavec M, Zel J, et al. Optimising droplet digital PCR analysis approaches for detection and quantification of bacteria: a case study of fire blight and potato brown rot. Anal Bioanal Chem. 2014;406(26):6513-28.

125. Dobnik D, Spilsberg B, Bogožalec Košir A, Štebih D, Morisset D, Holst-Jensen A, et al. Multiplex droplet digital PCR protocols for quantification of GM maize events. Digital PCR: Springer; 2018: 69-98.

126. Pavšič J, Žel J, Milavec M. Digital PCR for direct quantification of viruses without DNA extraction. Analytical and bioanalytical chemistry. 2016;408(1):67-75.

127. Gao G, Qu G, Burnham MS, Huang J, Chirmule N, Joshi B, et al. Purification of recombinant adeno-associated virus vectors by column chromatography and its performance in vivo. Hum Gene Ther. 2000;11(15):2079-91.

128. Kube DM, Srivastava A. Quantitative DNA slot blot analysis: inhibition of DNA binding to membranes by magnesium ions. Nucleic Acids Res. 1997;25(16):3375-6.

129. Wu CJ, Huang WC, Chen LC, Shen CR, Kuo ML. Pseudotyped adeno-associated virus 2/9-delivered CCL11 shRNA alleviates lung inflammation in an allergen-sensitized mouse model. Hum Gene Ther. 2012;23(11):1156-65.

130. Nieto K, Stahl-Hennig C, Leuchs B, Muller M, Gissmann L, Kleinschmidt JA. Intranasal vaccination with AAV5 and 9 vectors against human papillomavirus type 16 in rhesus macaques. Hum Gene Ther. 2012;23(7):733-41.

131. Xiao PJ, Samulski RJ. Cytoplasmic trafficking, endosomal escape, and perinuclear accumulation of adeno-associated virus type 2 particles are facilitated by microtubule network. J Virol. 2012;86(19):10462-73.

132. Mussche S, Devreese B, Nagabhushan Kalburgi S, Bachaboina L, Fox JC, Shih HJ, et al. Restoration of cytoskeleton homeostasis after gigaxonin gene transfer for giant axonal neuropathy. Hum Gene Ther. 2013;24(2):209-19.

133. Ahn SJ, Costa J, Rettig Emanuel J. PicoGreen quantitation of DNA: effective evaluation of samples pre-or post-PCR. Nucleic acids research. 1996;24(13):2623-5.

134. Ayuso E. Manufacturing of recombinant adeno-associated viral vectors: new technologies are welcome. Mol Ther Methods Clin Dev. 2016;3:15049.

135. Ellis BL, Hirsch ML, Barker JC, Connelly JP, Steininger RJ, 3rd, Porteus MH. A survey of ex vivo/in vitro transduction efficiency of mammalian primary cells and cell lines with Nine natural adeno-associated virus (AAV1-9) and one engineered adeno-associated virus serotype. Virol J. 2013;10(1):74.

136. Gonzalez-Cordero A, Goh D, Kruczek K, Naeem A, Fernando M, Kleine Holthaus SM, et al. Assessment of AAV Vector Tropisms for Mouse and Human Pluripotent Stem Cell-Derived RPE and Photoreceptor Cells. Hum Gene Ther. 2018;29(10):1124-39.

137. Quinn PM, Buck TM, Mulder AA, Ohonin C, Alves CH, Vos RM, et al. Human iPSC-derived retinas recapitulate the fetal CRB1 CRB2 complex formation and demonstrate that photoreceptors and müller glia are targets of AAV5. Stem Cell Reports. 2019;12(5):906-19.

138. Drittanti L, Jenny C, Poulard K, Samba A, Manceau P, Soria N, et al. Optimised helper virus-free production of high-quality adeno-associated virus vectors. J Gene Med. 2001;3(1):59-71.

139. Francois A, Bouzelha M, Lecomte E, Broucque F, Penaud-Budloo M, Adjali O, et al. Accurate Titration of Infectious AAV Particles Requires Measurement of Biologically Active Vector Genomes and Suitable Controls. Mol Ther Methods Clin Dev. 2018;10:223-36.

140. Yakobson B, Koch T, Winocour E. Replication of adeno-associated virus in synchronized cells without the addition of a helper virus. Journal of Virology. 1987;61(4):972-81.

141. Zhen Z, Espinoza Y, Bleu T, Sommer JM, Wright JF. Infectious titer assay for adeno-associated virus vectors with sensitivity sufficient to detect single infectious events. Human gene therapy. 2004;15(7):709-15.

142. Farson D, Harding TC, Tao L, Liu J, Powell S, Vimal V, et al. Development and characterization of a cell line for large-scale, serum-free production of recombinant adeno-associated viral vectors. J Gene Med. 2004;6(12):1369-81.

143. Buck TM, Wijnholds J. Recombinant Adeno-Associated Viral Vectors (rAAV)-Vector Elements in Ocular Gene Therapy Clinical Trials and Transgene Expression and Bioactivity Assays. Int J Mol Sci. 2020;21(12):4197.

144. De BP, Chen A, Salami CO, Van de Graaf B, Rosenberg JB, Pagovich OE, et al. In vivo potency assay for adeno-associated virus–based gene therapy vectors using AAVrh. 10 as an example. Human gene therapy methods. 2018;29(3):146-55.

145. Aronson SJ, Bakker RS, Moenis S, van Dijk R, Bortolussi G, Collaud F, et al. A Quantitative In Vitro Potency Assay for Adeno-Associated Virus Vectors Encoding for the UGT1A1 Transgene. Mol Ther Methods Clin Dev. 2020;18:250-8.

146. Couto LB, Buchlis G, Farjo R, High K. Potency assay for AAV vector encoding retinal pigment epithelial 65 protein. Investigative Ophthalmology & Visual Science. 2016;57(12):759.

147. Chadeuf G, Favre D, Tessier J, Provost N, Nony P, Kleinschmidt J, et al. Efficient recombinant adeno-associated virus production by a stable rep-cap HeLa cell line correlates with adenovirus-induced amplification of the integrated rep-cap genome. J Gene Med. 2000;2(4):260-8.

148. Clark KR, Voulgaropoulou F, Fraley DM, Johnson PR. Cell lines for the production of recombinant adeno-associated virus. Hum Gene Ther. 1995;6(10):1329-41.

149. Salvetti A, Oreve S, Chadeuf G, Favre D, Cherel Y, Champion-Arnaud P, et al. Factors influencing recombinant adeno-associated virus production. Hum Gene Ther. 1998;9(5):695-706.

150. Snyder RO, Francis J. Adeno-associated viral vectors for clinical gene transfer studies. Curr Gene Ther. 2005;5(3):311-21.

151. Smith RH, Ding C, Kotin RM. Serum-free production and column purification of adeno-associated virus type 5. J Virol Methods. 2003;114(2):115-24.

152. Urabe M, Ding C, Kotin RM. Insect cells as a factory to produce adeno-associated virus type 2 vectors. Human gene therapy. 2002;13(16):1935-43.

153. Maecker HT, Ghanekar SA, Suni MA, He XS, Picker LJ, Maino VC. Factors affecting the efficiency of CD8+ T cell cross-priming with exogenous antigens. J Immunol. 2001;166(12):7268-75.

154. Wang X-S, Khuntirat B, Qing K, Ponnazhagan S, Kube DM, Zhou S, et al. Characterization of wild-type adeno-associated virus type 2-like particles generated during recombinant viral vector production and strategies for their elimination. Journal of virology. 1998;72(7):5472-80.

155. Gao GP, Qu G, Faust LZ, Engdahl RK, Xiao W, Hughes JV, et al. High-titer adeno-associated viral vectors from a Rep/Cap cell line and hybrid shuttle virus. Hum Gene Ther. 1998;9(16):2353-62.

156. Chadeuf G, Ciron C, Moullier P, Salvetti A. Evidence for encapsidation of prokaryotic sequences during recombinant adeno-associated virus production and their in vivo persistence after vector delivery. Mol Ther. 2005;12(4):744-53.

157. Hauck B, Murphy SL, Smith PH, Qu G, Liu X, Zelenaia O, et al. Undetectable transcription of cap in a clinical AAV vector: implications for preformed capsid in immune responses. Mol Ther. 2009;17(1):144-52.

158. Smith P, Wright, JF, Qu, G, Patarroyo-White, S, Parker, A and Sommer, JM. Packaging of Host Cell and Plasmid DNA into Recombinant Adeno-Associated Virus Particles Produced by Triple Transfection. Molecular Therapy. 2003;7(5).

159. Wang Z, Troilo P, Wang X, Griffiths T, Pacchione S, Barnum A, et al. Detection of integration of plasmid DNA into host genomic DNA following intramuscular injection and electroporation. Gene therapy. 2004;11(8):711-21.

160. Ledwith BJ, Manam S, Troilo PJ, Barnum AB, Pauley CJ, Griffiths II TG, et al. Plasmid DNA vaccines: investigation of integration into host cellular DNA following intramuscular injection in mice. Intervirology. 2000;43(4-6):258-72.

161. Sheng L, Cai F, Zhu Y, Pal A, Athanasiou M, Orrison B, et al. Oncogenicity of DNA in vivo: tumor induction with expression plasmids for activated H-ras and c-myc. Biologicals. 2008;36(3):184-97.

162. Wright JF. Quality Control Testing, Characterization and Critical Quality Attributes of Adeno-Associated Virus Vectors Used for Human Gene Therapy. Biotechnology Journal. 2021;16(1):2000022.

163. Wang Y, Cooper R, Kiladjian A, Bergelson S, Feschenko M. A Digestion-free Method for Quantification of Residual Host Cell DNA in rAAV Gene Therapy Products. Mol Ther Methods Clin Dev. 2019;13:526-31.

164. Kim I, Yang D, Tang X, Carroll JL. Reference gene validation for qPCR in rat carotid body during postnatal development. BMC Res Notes. 2011;4(1):440.

165. Document FB. FDA Briefing Document: Cell lines derived from human tumors for vaccine manufacture. Available online:. [11.11.2021]; Available from: https://wayback.archive-it.org/7993/20161022170706/http://www.fda.gov/AdvisoryCommittees/CommitteesMeetingMaterials/BloodVaccinesandOtherBiologics/VaccinesandRelatedBiologicalProductsAdvisoryCommittee/ucm383914.htm.

166. Grachev V, Magrath D, Griffiths E, Petricciani J. WHO requirements for the use of animal cells as in vitro substrates for the production of biologicals (requirements for biological substances No. 50). Biologicals. 1998;26(3):175-93.

167. Tenenbaum L, Hamdane M, Pouzet M, Avalosse B, Stathopoulos A, Jurysta F, et al. Cellular contaminants of adeno-associated virus vector stocks can enhance transduction. Gene therapy. 1999;6(6):1045-53.

168. Denard J, Beley C, Kotin R, Lai-Kuen R, Blot S, Leh H, et al. Human galectin 3 binding protein interacts with recombinant adeno-associated virus type 6. Journal of virology. 2012;86(12):6620-31.

169. Mingozzi F, Anguela XM, Pavani G, Chen Y, Davidson RJ, Hui DJ, et al. Overcoming preexisting humoral immunity to AAV using capsid decoys. Science translational medicine. 2013;5(194):194ra92-ra92.

170. Gao K, Li M, Zhong L, Su Q, Li J, Li S, et al. Empty Virions In AAV8 Vector Preparations Reduce Transduction Efficiency And May Cause Total Viral Particle Dose-Limiting Side-Effects. Mol Ther Methods Clin Dev. 2014;1(9):20139.

171. Li T, Gao T, Chen H, Pekker P, Menyhart A, Guttman A. Rapid Determination of Full and Empty Adeno-Associated Virus Capsid Ratio by Capillary Isoelectric Focusing. Current Molecular Medicine. 2020, 20(10):814-820.

172. Pierson EE, Keifer DZ, Asokan A, Jarrold MF. Resolving Adeno-Associated Viral Particle Diversity With Charge Detection Mass Spectrometry. Anal Chem. 2016;88(13):6718-25.

173. Wu D, Hwang P, Li T, Piszczek G. Rapid Characterization of AAV gene therapy vectors by Mass Photometry. Gene Ther. 2022,1-7.

174. Fu X, Chen WC, Argento C, Clarner P, Bhatt V, Dickerson R, et al. Analytical Strategies for Quantification of Adeno-Associated Virus Empty Capsids to Support Process Development. Hum Gene Ther Methods. 2019;30(4):144-52.

175. Burnham B, Nass S, Kong E, Mattingly M, Woodcock D, Song A, et al. Analytical Ultracentrifugation as an Approach to Characterize Recombinant Adeno-Associated Viral Vectors. Hum Gene Ther Methods. 2015;26(6):228-42.

176. Nass SA, Mattingly MA, Woodcock DA, Burnham BL, Ardinger JA, Osmond SE, et al. Universal Method for the Purification of Recombinant AAV Vectors of Differing Serotypes. Mol Ther Methods Clin Dev. 2018;9:33-46.

177. den Engelsman J, Garidel P, Smulders R, Koll H, Smith B, Bassarab S, et al. Strategies for the assessment of protein aggregates in pharmaceutical biotech product development. Pharm Res. 2011;28(4):920-33.

178. Carpenter JF, Randolph TW, Jiskoot W, Crommelin DJ, Middaugh CR, Winter G. Potential inaccurate quantitation and sizing of protein aggregates by size exclusion chromatography: essential need to use orthogonal methods to assure the quality of therapeutic protein products. Journal of pharmaceutical sciences. 2010;99(5):2200-8.

179. Zhou ZH. Seeing engineered loops in a gene delivery vehicle by cryoEM. Structure. 2012;20(8):1286-8.

180. Chen H. Comparative observation of the recombinant adeno-associated virus 2 using transmission electron microscopy and atomic force microscopy. Microscopy and Microanalysis. 2007;13(5):384-9.

181. Subramanian S, Maurer AC, Bator CM, Makhov AM, Conway JF, Turner KB, et al. Filling Adeno-Associated Virus Capsids: Estimating Success by Cryo-Electron Microscopy. Hum Gene Ther. 2019;30(12):1449-60.

182. Grieger JC, Soltys SM, Samulski RJ. Production of Recombinant Adeno-associated Virus Vectors Using Suspension HEK293 Cells and Continuous Harvest of Vector From the Culture Media for GMP FIX and FLT1 Clinical Vector. Mol Ther. 2016;24(2):287-97.

183. Grimm D, Kern A, Rittner K, Kleinschmidt JA. Novel tools for production and purification of recombinant adenoassociated virus vectors. Hum Gene Ther. 1998;9(18):2745-60.

184. Horowitz ED, Rahman KS, Bower BD, Dismuke DJ, Falvo MR, Griffith JD, et al. Biophysical and ultrastructural characterization of adeno-associated virus capsid uncoating and genome release. J Virol. 2013;87(6):2994-3002.

185. Hutanu A, Boelsterli D, Schmidli C, Montealegre C, Dang Thai MHN, Bobaly B, et al. Stronger together: Analytical techniques for recombinant adeno associated virus. Electrophoresis. 2021.

186. Venkatakrishnan B, Yarbrough J, Domsic J, Bennett A, Bothner B, Kozyreva OG, et al. Structure and dynamics of adeno-associated virus serotype 1 VP1-unique N-terminal domain and its role in capsid trafficking. J Virol. 2013;87(9):4974-84.

187. Potter M, Lins B, Mietzsch M, Heilbronn R, Van Vliet K, Chipman P, et al. A simplified purification protocol for recombinant adeno-associated virus vectors. Mol Ther Methods Clin Dev. 2014;1:14034.

188. Urabe M, Xin KQ, Obara Y, Nakakura T, Mizukami H, Kume A, et al. Removal of empty capsids from type 1 adeno-associated virus vector stocks by anion-exchange chromatography potentiates transgene expression. Mol Ther. 2006;13(4):823-8.

189. Khatwani SL, Pavlova A, Pirot Z. Anion-exchange HPLC assay for separation and quantification of empty and full capsids in multiple adeno-associated virus serotypes. Mol Ther Methods Clin Dev. 2021;21:548-58.

190. Zolotukhin S, Potter M, Zolotukhin I, Sakai Y, Loiler S, Fraites TJ, Jr., et al. Production and purification of serotype 1, 2, and 5 recombinant adeno-associated viral vectors. Methods. 2002;28(2):158-67.

191. Qu W, Wang M, Wu Y, Xu R. Scalable downstream strategies for purification of recombinant adeno-associated virus vectors in light of the properties. Curr Pharm Biotechnol. 2015;16(8):684-95.

192. Brument N, Morenweiser R, Blouin V, Toublanc E, Raimbaud I, Cherel Y, et al. A versatile and scalable two-step ion-exchange chromatography process for the purification of recombinant adeno-associated virus serotypes-2 and -5. Mol Ther. 2002;6(5):678-86.

193. Lock M, Alvira MR, Wilson JM. Analysis of particle content of recombinant adeno-associated virus serotype 8 vectors by ion-exchange chromatography. Hum Gene Ther Methods. 2012;23(1):56-64.

194. Oksanen HM, Domanska A, Bamford DH. Monolithic ion exchange chromatographic methods for virus purification. Virology. 2012;434(2):271-7.

195. Vaya I, Gustavsson T, Miannay FA, Douki T, Markovitsi D. Fluorescence of natural DNA: from the femtosecond to the nanosecond time scales. J Am Chem Soc. 2010;132(34):11834-5.

196. Lakowicz JR, Shen B, Gryczynski Z, D'Auria S, Gryczynski I. Intrinsic fluorescence from DNA can be enhanced by metallic particles. Biochemical and Biophysical Research Communications. 2001;286(5):875-9.

197. Righetti PG, Sebastiano R, Citterio A. Capillary electrophoresis and isoelectric focusing in peptide and protein analysis. Proteomics. 2013;13(2):325-40.

198. Strasser L, Morgan TE, Guapo F, Fussl F, Forsey D, Anderson I, et al. A Native Mass Spectrometry-Based Assay for Rapid Assessment of the Empty:Full Capsid Ratio in Adeno-Associated Virus Gene Therapy Products. Anal Chem. 2021;93(38):12817-21.

199. Fuerstenau SD, Benner WH, Thomas JJ, Brugidou C, Bothner B, Siuzdak G. Mass spectrometry of an intact virus. Angewandte Chemie. 2001;113(3):559-62.

200. Solutions M. ImmerseTM Cambridge. 2020; Available from: https://megadaltonsolutions.com/applications/.

201. Snijder J, van de Waterbeemd M, Damoc E, Denisov E, Grinfeld D, Bennett A, et al. Defining the stoichiometry and cargo load of viral and bacterial nanoparticles by Orbitrap mass spectrometry. J Am Chem Soc. 2014;136(20):7295-9.

202. AN: Mass photometry of AAVs. Refeyn. 2021 [01.12.2021]; Available from: https://b1cd404c-33b3-4241-83b5-3b96f79f7fca.filesusr.com/ugd/8a9b7f_3aa8e451082b4bdca9d84dea73a2cdff.pdf.

203. Cole D, Young G, Weigel A, Sebesta A, Kukura P. Label-Free Single-Molecule Imaging with Numerical-Aperture-Shaped Interferometric Scattering Microscopy. ACS Photonics. 2017;4(2):211-6.

204. Young G, Hundt N, Cole D, Fineberg A, Andrecka J, Tyler A, et al. Quantitative mass imaging of single biological macromolecules. Science. 2018;360(6387):423-7.

205. Li Y, Struwe WB, Kukura P. Single molecule mass photometry of nucleic acids. Nucleic Acids Res. 2020;48(17):97.

206. Di Wu GP. Rapid determination of antibody-antigen affinity by mass photometry. Journal of visualized experiments: JoVE 2021;168:61784.

207. Wang C, Mulagapati SHR, Chen Z, Du J, Zhao X, Xi G, et al. Developing an Anion Exchange Chromatography Assay for Determining Empty and Full Capsid Contents in AAV6.2. Mol Ther Methods Clin Dev. 2019;15:257-63.

208. Rodrigues GA, Shalaev E, Karami TK, Cunningham J, Slater NK, Rivers HM. Pharmaceutical development of AAV-based gene therapy products for the eye. Pharmaceutical research. 2019;36(2):1-20.

209. Chi EY, Krishnan S, Randolph TW, Carpenter JF. Physical stability of proteins in aqueous solution: mechanism and driving forces in nonnative protein aggregation. Pharm Res. 2003;20(9):1325-36.

210. Croyle MA, Cheng X, Wilson JM. Development of formulations that enhance physical stability of viral vectors for gene therapy. Gene Ther. 2001;8(17):1281-90.

211. Wright JF, Qu G, Tang C, Sommer JM. Recombinant adeno-associated virus: formulation challenges and strategies for a gene therapy vector. Curr Opin Drug Discov Devel. 2003;6(2):174-8.

212. Xie Q, Hare J, Turnigan J, Chapman MS. Large-scale production, purification and crystallization of wild-type adeno-associated virus-2. J Virol Methods. 2004;122(1):17-27.

213. Krieg D, Svilenov H, Gitter JH, Winter G. Overcoming challenges in co-formulation of proteins with contradicting stability profiles-EPO plus G-CSF. European Journal of Pharmaceutical Sciences. 2020;141:105073.

214. Menzen T, Friess W. Temperature-ramped studies on the aggregation, unfolding, and interaction of a therapeutic monoclonal antibody. J Pharm Sci. 2014;103(2):445-55.

215. Menzen T, Friess W. High-throughput melting-temperature analysis of a monoclonal antibody by differential scanning fluorimetry in the presence of surfactants. J Pharm Sci. 2013;102(2):415-28.

216. Kelly SM, Price NC. The use of circular dichroism in the investigation of protein structure and function. Current protein and peptide science. 2000;1(4):349-84.

217. Srivastava A, Mallela KMG, Deorkar N, Brophy G. Manufacturing Challenges and Rational Formulation Development for AAV Viral Vectors. J Pharm Sci. 2021;110(7):2609-24.

218. Zhang YZ, DePaz RA, Bee JS, Marshall T. Development of a stable lyophilized adeno-associated virus gene therapy formulation. International Journal of Pharmaceutics 2021,606. 120912.

219. Bee JS, O'Berry K, Zhang YZ, Phillippi MK, Kaushal A, DePaz RA, et al. Quantitation of Trace Levels of DNA Released from Disrupted Adeno-Associated Virus Gene Therapy Vectors. J Pharm Sci. 2021;110(9):3183-7.

220. Manning MC, Liu J, Li T, Holcomb RE. Rational design of liquid formulations of proteins. Advances in protein chemistry and structural biology. 2018;112:1-59.

221. Chi EY, Krishnan S, Kendrick BS, Chang BS, Carpenter JF, Randolph TW. Roles of conformational stability and colloidal stability in the aggregation of recombinant human granulocyte colony-stimulating factor. Protein Science. 2003;12(5):903-13.

222. Blaffert J, Haeri HH, Blech M, Hinderberger D, Garidel P. Spectroscopic methods for assessing the molecular origins of macroscopic solution properties of highly concentrated liquid protein solutions. Analytical biochemistry. 2018;561:70-88.

223. Gao G, Lebherz C, Weiner DJ, Grant R, Calcedo R, McCullough B, et al. Erythropoietin gene therapy leads to autoimmune anemia in macaques. Blood. 2004;103(9):3300-2.

224. Flotte TR. Immune responses to recombinant adeno-associated virus vectors: putting preclinical findings into perspective. Human gene therapy. 2004;15(7):716-7.

225. Geoghegan JC, Fleming R, Damschroder M, Bishop SM, Sathish HA, Esfandiary R. Mitigation of reversible self-association and viscosity in a human IgG1 monoclonal antibody by rational, structure-guided Fv engineering. MAbs. 2016;8(5):941-50.

226. Sarangapani PS, Weaver J, Parupudi A, Besong TM, Adams GG, Harding SE, et al. Both reversible self-association and structural changes underpin molecular viscoelasticity of mAb solutions. Journal of pharmaceutical sciences. 2016;105(12):3496-506.

227. Fiedler C, Fritscher E, Hasslacher M, Mittergradnegger D, Tabish T. Adeno-associated virus formulation. 2018 [WO/2018/128689]; Available from: https://patentscope.wipo.int/search/en/detail.jsf?docId=WO2018128689.

228. Wonganan P, Croyle MA. PEGylated Adenoviruses: From Mice to Monkeys. Viruses. 2010;2(2):468-502.

229. Wright J, Qu G. Compositions and methods to prevent AAV vector aggregation. 2011 [US 2011/0076744 A1.]; Available from: https://patents.google.com/patent/US20110076744A1/en. .

230. Pharmacopoeia E. 2.2.35 Osmolalität. Ph. Eur. 10.0.

231. Le DT, Radukic MT, Muller KM. Adeno-associated virus capsid protein expression in Escherichia coli and chemically defined capsid assembly. Sci Rep. 2019;9(1):18631.

232. Wang Q, Firrman J, Wu Z, Pokiniewski KA, Valencia CA, Wang H, et al. High-Density Recombinant Adeno-Associated Viral Particles are Competent Vectors for In Vivo Transduction. Hum Gene Ther. 2016;27(12):971-81.

233. Gabrielson JP, Arthur KK, Stoner MR, Winn BC, Kendrick BS, Razinkov V, et al. Precision of protein aggregation measurements by sedimentation velocity analytical ultracentrifugation in biopharmaceutical applications. Analytical Biochemistry. 2010;396(2):231-41.

234. Kemter K, Scholz M. Method for obtaining efficient viral vector-based compositions for vaccination or gene therapy. Google Patents; 2021 [11166915].

235. Narhi LO, Schmit J, Bechtold-Peters K, Sharma D. Classification of protein aggregates. Journal of pharmaceutical sciences. 2012;101(2):493-8.

236. Turkki V, Alppila E, Ylä-Herttuala S, Lesch HP. Experimental evaluation of an interferometric light microscopy particle counter for titering and characterization of virus preparations. Viruses. 2021;13(5):939.

237. Vogel R, Savage J, Muzard J, Della Camera G, Vella G, Law A, et al. Measuring particle concentration of multimodal synthetic reference materials and extracellular vesicles with orthogonal techniques: Who is up to the challenge? Journal of Extracellular Vesicles. 2021;10(3):12052.

238. Gast M, Sobek H, Mizaikoff B. Nanoparticle tracking of adenovirus by light scattering and fluorescence detection. Human gene therapy methods. 2019;30(6):235-44.

239. Kramberger P, Ciringer M, Štrancar A, Peterka M. Evaluation of nanoparticle tracking analysis for total virus particle determination. Virology journal. 2012;9(1):1-10.

240. Trenkenschuh E, Richter M, Heinrich E, Koch M, Fuhrmann G, Friess W. Enhancing the Stabilization Potential of Lyophilization for Extracellular Vesicles. Adv Healthc Mater. 2021:2100538.

241. Akpinar F, Yin J. Characterization of vesicular stomatitis virus populations by tunable resistive pulse sensing. Journal of virological methods. 2015;218:71-6.

242. Yang L, Yamamoto T. Quantification of virus particles using nanopore-based resistive-pulse sensing techniques. Frontiers in microbiology. 2016;7:1500.

243. Roesch A, Zölls S, Stadler D, Helbig C, Wuchner K, Kersten G, et al. Particles in biopharmaceutical formulations, part 2: an update on analytical techniques and applications for therapeutic proteins, viruses, vaccines and cells. Journal of Pharmaceutical Sciences. 2021.

244. Härdter N, Menzen T, Winter G. Minimizing Oxidation of Freeze-Dried Monoclonal Antibodies in Polymeric Vials Using a Smart Packaging Approach. Pharmaceutics. 2021;13(10):1695.

245. AN8: AAV aggregate quantitation and identification with the Aura system. Halo Labs. 2021.

246. Bennicelli J, Wright JF, Komaromy A, Jacobs JB, Hauck B, Zelenaia O, et al. Reversal of blindness in animal models of leber congenital amaurosis using optimized AAV2-mediated gene transfer. Molecular Therapy. 2008;16(3):458-65.

247. Bunting S, Colosi PC, Pungor E. Adeno-associated virus factor VIII vectors, associated viral particles and therapeutic formulations comprising the same. Google Patents; 2019.

248. Wang W, Nema S, Teagarden D. Protein aggregation--pathways and influencing factors. Int J Pharm. 2010;390(2):89-99.

249. Rabe M, Verdes D, Seeger S. Understanding protein adsorption phenomena at solid surfaces. Advances in colloid and interface science. 2011;162(1-2):87-106.

250. Wang W, Singh S, Zeng DL, King K, Nema S. Antibody structure, instability, and formulation. J Pharm Sci. 2007;96(1):1-26.

251. Wang W. Instability, stabilization, and formulation of liquid protein pharmaceuticals. Int J Pharm. 1999;185(2):129-88.

252. Manning MC, Patel K, Borchardt RT. Stability of protein pharmaceuticals. Pharm Res. 1989;6(11):903-18.

253. Martos A, Koch W, Jiskoot W, Wuchner K, Winter G, Friess W, et al. Trends on analytical characterization of polysorbates and their degradation products in biopharmaceutical formulations. Journal of Pharmaceutical Sciences. 2017;106(7):1722-35.

254. Bee JS, Zhang YZ, Phillippi MK, Finkner S, Mezghebe T, Webber K, et al. Impact of Time out of Intended Storage and Freeze-Thaw Rates on the Stability of Adeno-Associated Virus 8 and 9. Journal of Pharmaceutical Sciences. 2022.

255. Kiese S, Papppenberger A, Friess W, Mahler H-C. Shaken, not stirred: mechanical stress testing of an IgG1 antibody. Journal of pharmaceutical sciences. 2008;97(10):4347-66.

256. Randolph TW, Schiltz E, Sederstrom D, Steinmann D, Mozziconacci O, Schöneich C, et al. Do not drop: mechanical shock in vials causes cavitation, protein aggregation, and particle formation. Journal of pharmaceutical sciences. 2015;104(2):602-11.

257. Koepf E, Eisele S, Schroeder R, Brezesinski G, Friess W. Notorious but not understood: how liquid-air interfacial stress triggers protein aggregation. International Journal of Pharmaceutics. 2018;537(1-2):202-12.

258. Manning MC, Chou DK, Murphy BM, Payne RW, Katayama DS. Stability of protein pharmaceuticals: an update. Pharm Res. 2010;27(4):544-75.

259. Carpenter JF, Chang BS, Garzon-Rodriguez W, Randolph TW. Rational design of stable lyophilized protein formulations: theory and practice. Pharm Biotechnol. 2002;13:109-33.

260. Aloor A, Zhang J, Gashash EA, Parameswaran A, Chrzanowski M, Ma C, et al. Site-specific N-glycosylation on the AAV8 capsid protein. Viruses 2018,10(11). 644.

261. Zhang Y, Wang Y, Sosic Z, Zang L, Bergelson S, Zhang W. Identification of adeno-associated virus capsid proteins using ZipChip CE/MS. Anal Biochem. 2018;555:22-5.

262. Evans RK, Nawrocki DK, Isopi LA, Williams DM, Casimiro DR, Chin S, et al. Development of stable liquid formulations for adenovirus-based vaccines. Journal of pharmaceutical sciences. 2004;93(10):2458-75.

263. Reinauer EB, Grosso SS, Henz SR, Rabas JA, Rodenstein C, Altrichter J, et al. Algorithm-Based Liquid Formulation Development Including a DoE Concept Predicts Long-Term Viral Vector Stability. J Pharm Sci. 2020;109(1):818-29.

264. Pelliccia M, Andreozzi P, Paulose J, D'Alicarnasso M, Cagno V, Donalisio M, et al. Additives for vaccine storage to improve thermal stability of adenoviruses from hours to months. Nature communications. 2016;7(1):1-7.

265. Stewart M, Ward S, Drew J. Use of adenovirus as a model system to illustrate a simple method using standard equipment and inexpensive excipients to remove live virus dependence on the cold-chain. Vaccine. 2014;32(24):2931-8.

266. Zheng JY, Janis LJ. Influence of pH, buffer species, and storage temperature on physicochemical stability of a humanized monoclonal antibody LA298. Int J Pharm. 2006;308(1-2):46-51.

267. Fekete S, Guillarme D. Reversed-phase liquid chromatography for the analysis of therapeutic proteins and recombinant monoclonal antibodies. LCGC Europe. 2012;25(10):540-50.

268. Jin X, Liu L, Nass S, O'Riordan C, Pastor E, Zhang XK. Direct Liquid Chromatography/Mass Spectrometry Analysis for Complete Characterization of Recombinant Adeno-Associated Virus Capsid Proteins. Hum Gene Ther Methods. 2017;28(5):255-67.

269. Fekete S, Veuthey JL, Beck A, Guillarme D. Hydrophobic interaction chromatography for the characterization of monoclonal antibodies and related products. J Pharm Biomed Anal. 2016;130:3-18.

270. Liu AP, Patel SK, Xing T, Yan Y, Wang S, Li N. Characterization of Adeno-Associated Virus Capsid Proteins Using Hydrophilic Interaction Chromatography Coupled with Mass Spectrometry. Journal of Pharmaceutical and Biomedical Analysis. 2020;189:113481.

271. Verma A, Ngundi MM, Burns DL. Mechanistic Analysis of the Effect of Deamidation on the Immunogenicity of Anthrax Protective Antigen. Clin Vaccine Immunol. 2016;23(5):396-402.

272. Catak S, Monard G, Aviyente V, Ruiz-Lopez MF. Deamidation of asparagine residues: direct hydrolysis versus succinimide-mediated deamidation mechanisms. J Phys Chem A. 2009;113(6):1111-20.

273. Robinson NE, Robinson AB. Prediction of protein deamidation rates from primary and three-dimensional structure. Proc Natl Acad Sci U S A. 2001;98(8):4367-72.

274. Robinson AB, Rudd CJ. Deamidation of Glutaminyl and Asparaginyl Residues in Peptides and Proteins. In: Horecker BL, Stadtman ER, editors. Current Topics in Cellular Regulation: Academic Press; 1974:247-95.

275. Kim J, Kim YJ, Cao M, De Mel N, Miller K, Bee JS, et al. Analytical characterization of coformulated antibodies as combination therapy. MAbs. 2020;12(1):1738691.

276. Cao M, De Mel N, Shannon A, Prophet M, Wang C, Xu W, et al. Charge variants characterization and release assay development for co-formulated antibodies as a combination therapy. MAbs. 2019;11(3):489-99.

277. Wang YJ, Shahrokh Z, Vemuri S, Eberlein G, Beylin I, Busch M. Characterization, stability, and formulations of basic fibroblast growth factor. Formulation, Characterization, and Stability of Protein Drugs: Case Histories. 2002:141-80.

278. Shahrokh Z, Eberlein G, Buckley D, Paranandi MV, Aswad DW, Stratton P, et al. Major degradation products of basic fibroblast growth factor: Detection of succinimide and iso-aspartate in place of aspartate 15. Pharmaceutical research. 1994;11(7):936-44.

279. Xie Q, Bu W, Bhatia S, Hare J, Somasundaram T, Azzi A, et al. The atomic structure of adeno-associated virus (AAV-2), a vector for human gene therapy. Proc Natl Acad Sci U S A. 2002;99(16):10405-10.

280. Pulicherla N, Kota P, Dokholyan NV, Asokan A. Intra-and inter-subunit disulfide bond formation is nonessential in adeno-associated viral capsids. PLoS One. 2012;7(2):32163.

281. Cacia J, Keck R, Presta LG, Frenz J. Isomerization of an aspartic acid residue in the complementarity-determining regions of a recombinant antibody to human IgE: identification and effect on binding affinity. Biochemistry. 1996;35(6):1897-903.

282. Wright JF. Manufacturing and characterizing AAV-based vectors for use in clinical studies. Gene Ther. 2008;15(11):840-8.

283. Wright JF, Zelenaia O. Vector Characterization Methods for Quality Control Testing of Recombinant Adeno-Associated Viruses. In: Merten O-W, Al-Rubeai M, editors. Viral Vectors for Gene Therapy: Methods and Protocols. Totowa, NJ: Humana Press; 2011:247-78.

284. Ramamoorth M, Narvekar A. Non viral vectors in gene therapy- an overview. J Clin Diagn Res. 2015;9(1):GE01.

285. Bloquel C, Bourges JL, Touchard E, Berdugo M, BenEzra D, Behar-Cohen F. Non-viral ocular gene therapy: potential ocular therapeutic avenues. Adv Drug Deliv Rev. 2006;58(11):1224-42.

286. Auricchio A, Smith AJ, Ali RR. The Future Looks Brighter After 25 Years of Retinal Gene Therapy. Hum Gene Ther. 2017;28(11):982-7.

287. Boye SE, Boye SL, Lewin AS, Hauswirth WW. A comprehensive review of retinal gene therapy. Molecular therapy : the journal of the American Society of Gene Therapy. 2013;21(3):509-19.

288. Schön C, Biel M, Michalakis S. Retinal gene delivery by adeno-associated virus (AAV) vectors: Strategies and applications. European journal of pharmaceutics and biopharmaceutics. 2015;95:343-352.

289. Trapani I, Puppo A, Auricchio A. Vector platforms for gene therapy of inherited retinopathies. Progress in retinal and eye research. 2014;43:108-128.

290. Sonntag F, Schmidt K, Kleinschmidt JA. A viral assembly factor promotes AAV2 capsid formation in the nucleolus. Proc Natl Acad Sci U S A. 2010;107(22):10220-5.

291. Niesen FH, Berglund H, Vedadi M. The use of differential scanning fluorimetry to detect ligand interactions that promote protein stability. Nat Protoc. 2007;2(9):2212-21.

292. Carreira A, Menendez M, Reguera J, Almendral JM, Mateu MG. In vitro disassembly of a parvovirus capsid and effect on capsid stability of heterologous peptide insertions in surface loops. J Biol Chem. 2004;279(8):6517-25.

293. Becirovic E, Bohm S, Nguyen ON, Riedmayr LM, Hammelmann V, Schon C, et al. AAV Vectors for FRET-Based Analysis of Protein-Protein Interactions in Photoreceptor Outer Segments. Frontiers in neuroscience 2016,10. 356.

294. Schon C, Becirovic E, Biel M, Michalakis S. Design and Development of AAV-based Gene Supplementation Therapies for Achromatopsia and Retinitis Pigmentosa. Methods Mol Biol. 2018;1715:33-46.

295. Penaud-Budloo M, Lecomte E, Guy-Duche A, Saleun S, Roulet A, Lopez-Roques C, et al. Accurate Identification and Quantification of DNA Species by Next-Generation Sequencing in Adeno-Associated Viral Vectors Produced in Insect Cells. Hum Gene Ther Methods. 2017;28(3):148-62.

296. Svilenov H, Winter G. The ReFOLD assay for protein formulation studies and prediction of protein aggregation during long-term storage. Eur J Pharm Biopharm. 2019;137:131-9.

297. D. Breitsprecher NG, A. Hawe, T. Menzen. ANNT-PR-066: Thermal unfolding of anti-bodies comparison of NanoDSF andMDSC for thermal stability assessment duringbiopharmaceutical formulation development. NanoTemperTechnol GmbH. 2016.

298. Rumachik NG, Malaker SA, Poweleit N, Maynard LH, Adams CM, Leib RD, et al. Methods Matter -- Standard Production Platforms For Recombinant AAV Can Produce Chemically And Functionally Distinct Vectors. Molecular Therapy-Methods & Clinical Development. 2020; 18:98-118.

299. Rodrigues GA, Shalaev E, Karami TK, Cunningham J, Slater NKH, Rivers HM. Pharmaceutical Development of AAV-Based Gene Therapy Products for the Eye. Pharm Res. 2018;36(2):29.

300. Wanner R, Breitsprecher D, Duhr S, Baaske P, Winter G. Thermo-Optical Protein Characterization for Straightforward Preformulation Development. J Pharm Sci. 2017;106(10):2955-8.

301. Howard DB, Harvey BK. Assaying the Stability and Inactivation of AAV Serotype 1 Vectors. Hum Gene Ther Methods. 2017;28(1):39-48.

302. Khan TA, Mahler HC, Kishore RS. Key interactions of surfactants in therapeutic protein formulations: A review. Eur J Pharm Biopharm. 2015;97(Pt A):60-7.

303. Bam NB, Cleland JL, Yang J, Manning MC, Carpenter JF, Kelley RF, et al. Tween protects recombinant human growth hormone against agitation-induced damage via hydrophobic interactions. J Pharm Sci. 1998;87(12):1554-9.

304. Grieger JC, Choi VW, Samulski RJ. Production and characterization of adeno-associated viral vectors. Nat Protoc. 2006;1(3):1412-28.

305. Dickerson R, Argento C, Pieracci J, Bakhshayeshi M. Separating Empty and Full Recombinant Adeno-Associated Virus Particles Using Isocratic Anion Exchange Chromatography. Biotechnology Journal 2021,16(1). 2000015.

306. Pavlou M, Schön C, Occelli LM, Rossi A, Meumann N, Boyd RF, et al. Novel AAV capsids for intravitreal gene therapy of photoreceptor disorders. EMBO molecular medicine 2021,13(4). 13392.

307. Senapathy P, Carter BJ. Molecular cloning of adeno-associated virus variant genomes and generation of infectious virus by recombination in mammalian cells. J Biol Chem. 1984;259(7):4661-6.

308. Lang R, Winter G, Vogt L, Zurcher A, Dorigo B, Schimmele B. Rational design of a stable, freeze-dried virus-like particle-based vaccine formulation. Drug Dev Ind Pharm. 2009;35(1):83-97.

309. Citkowicz A, Petry H, Harkins RN, Ast O, Cashion L, Goldmann C, et al. Characterization of virus-like particle assembly for DNA delivery using asymmetrical flow field-flow fractionation and light scattering. Anal Biochem. 2008;376(2):163-72.

310. Eskelin K, Lampi M, Meier F, Moldenhauer E, Bamford DH, Oksanen HM. Asymmetric flow field flow fractionation methods for virus purification. J Chromatogr A. 2016;1469:108-19.

311. Fraunhofer W, Winter G, Coester C. Asymmetrical flow field-flow fractionation and multiangle light scattering for analysis of gelatin nanoparticle drug carrier systems. Anal Chem. 2004;76(7):1909-20.

312. Gentiluomo L, Svilenov HL, Augustijn D, El Bialy I, Greco ML, Kulakova A, et al. Advancing Therapeutic Protein Discovery and Development through Comprehensive Computational and Biophysical Characterization. Mol Pharm. 2020;17(2):426-40.

313. Patricio MI, Cox CI, Blue C, Barnard AR, Martinez-Fernandez de la Camara C, MacLaren RE. Inclusion of PF68 Surfactant Improves Stability of rAAV Titer when Passed through a Surgical Device Used in Retinal Gene Therapy. Mol Ther Methods Clin Dev. 2020;17:99-106.

314. Carpenter JF, Pikal MJ, Chang BS, Randolph TW. Rational design of stable lyophilized protein formulations: some practical advice. Pharm Res. 1997;14(8):969-75.

315. Maa YF, Nguyen PA, Andya JD, Dasovich N, Sweeney TD, Shire SJ, et al. Effect of spray drying and subsequent processing conditions on residual moisture content and physical/biochemical stability of protein inhalation powders. Pharm Res. 1998;15(5):768-75.

316. Adler M, Lee G. Stability and surface activity of lactate dehydrogenase in spray-dried trehalose. J Pharm Sci. 1999;88(2):199-208.

317. Manning MC, Chou DK, Murphy BM, Payne RW, Katayama DS. Stability of protein pharmaceuticals: an update. Pharmaceutical research. 2010;27(4):544-75.

318. Harano Y, Yoshidome T, Kinoshita M. Molecular mechanism of pressure denaturation of proteins. J Chem Phys. 2008;129(14):145103.

319. Krywka C, Sternemann C, Paulus M, Tolan M, Royer C, Winter R. Effect of osmolytes on pressure-induced unfolding of proteins: a high-pressure SAXS study. Chemphyschem. 2008;9(18):2809-15.

320. Zhang C-X, Meagher MM. Highly sensitive SDS capillary gel electrophoresis with sample stacking requiring only nanograms of adeno-associated virus capsid proteins. Clinical Applications of Capillary Electrophoresis: Springer; 2019:263-70.

321. Li T, Malik M, Yowanto H, Mollah S. ANRUO-MKT-02-9761-A: Purity Analysis of Adeno-Associated Virus (AAV) Capsid Proteins using CE-SDS Method. SCIEX Brea, CA. 2019.

322. Li T, Gao T, Chen H, Pekker P, Menyhart A, Guttman A. Rapid Determination of Full and Empty Adeno-Associated Virus Capsid Ratio by Capillary Isoelectric Focusing. Curr Mol Med. 2020;20(10):814-20.

323. Ali RR, Auricchio A, Smith AJ. The future looks brighter after 25 years of retinal gene therapy. Hum Gene Ther. 2017;28(11):982-987.

324. Samulski RJ, Srivastava A, Berns KI, Muzyczka N. Rescue of adeno-associated virus from recombinant plasmids: Gene correction within the terminal repeats of AAV. Cell. 1983;33(1):135-43.

325. Adams B, Bak H, Tustian AD. Moving from the bench towards a large scale, industrial platform process for adeno-associated viral vector purification. Biotechnol Bioeng. 2020;117(10):3199-3211.

326. Davidoff AM, Ng CY, Sleep S, Gray J, Azam S, Zhao Y, et al. Purification of recombinant adeno-associated virus type 8 vectors by ion exchange chromatography generates clinical grade vector stock. J Virol Methods. 2004;121(2):209-15.

327. Kaludov N, Handelman B, Chiorini JA. Scalable purification of adeno-associated virus type 2, 4, or 5 using ion-exchange chromatography. Hum Gene Ther. 2002;13(10):1235-43.

328. Flotte TR, Brantly ML, Spencer LT, Byrne BJ, Spencer CT, Baker DJ, et al. Phase I trial of intramuscular injection of a recombinant adeno-associated virus alpha 1-antitrypsin (rAAV2-CB-hAAT) gene vector to AAT-deficient adults. Hum Gene Ther. 2004;15(1):93-128.

329. Flotte TR, Zeitlin PL, Reynolds TC, Heald AE, Pedersen P, Beck S, et al. Phase I trial of intranasal and endobronchial administration of a recombinant adeno-associated virus serotype 2 (rAAV2)-CFTR vector in adult cystic fibrosis patients: a two-part clinical study. Human gene therapy. 2003;14(11):1079-88.

330. Bowles DE, McPhee SWJ, Li C, Gray SJ, Samulski JJ, Camp AS, et al. Phase 1 Gene Therapy for Duchenne Muscular Dystrophy Using a Translational Optimized AAV Vector. Molecular Therapy. 2012;20(2):443-55.

331. Pavlou M, Schön C, Occelli LM, Rossi A, Meumann N, Boyd RF, et al. Novel AAV capsids for intravitreal gene therapy of photoreceptor disorders. EMBO Molecular Medicine. 2021;13392.

332. Leskovec M, Primec, S., Gagnon, P., & Štrancar, A. . An Industrial Purification Platform for AAV. https://wwwbiaseparationscom/en/library/posters/988/an-industrialpurification-platform-for-aav. 2018.

333. Terova O, Soltys S, Hermans P, De Rooij J, Detmers F. Overcoming Downstream Purification Challenges for Viral Vector Manufacturing: Enabling Advancement of Gene Therapies in the Clinic. Cell and Gene Therapy Insights. 2018;4(2):101-11.

334. Mietzsch M, Jose A, Chipman P, Bhattacharya N, Daneshparvar N, McKenna R, et al. Completion of the AAV Structural Atlas: Serotype Capsid Structures Reveals Clade-Specific Features. Viruses. 2021;13(1):101.

335. Hebben M. Downstream bioprocessing of AAV vectors: industrial challenges & regulatory requirements. Cell and Gene Therapy Insights. 2018;4(2):131-46.

336. Lins-Austin B, Patel S, Mietzsch M, Brooke D, Bennett A, Venkatakrishnan B, et al. Adeno-associated virus (AAV) Capsid stability and liposome remodeling during Endo/Lysosomal pH trafficking. Viruses. 2020;12(6):668.

337. Joshi PR, Barnier A, Moço PD, Schrag J, Chahal PS, Kamen A. Development of a Scalable and Robust Anion-Exchange Chromatographic Method for Enriched Recombinant Adeno-Associated Virus Preparations in Genome Containing Vector Capsids of Serotypes-5, 6, 8, and 9. Molecular Therapy-Methods & Clinical Development. 2021:118.

338. Mary B, Maurya S, Arumugam S, Kumar V, Jayandharan GR. Post-translational modifications in capsid proteins of recombinant adeno-associated virus (AAV) 1-rh10 serotypes. FEBS J. 2019;286(24):4964-81.

339. Zhong L, Li B, Jayandharan G, Mah CS, Govindasamy L, Agbandje-McKenna M, et al. Tyrosine-phosphorylation of AAV2 vectors and its consequences on viral intracellular trafficking and transgene expression. Virology. 2008;381(2):194-202.

340. Crosson SM, Dib P, Smith JK, Zolotukhin S. Helper-free Production of Laboratory Grade AAV and Purification by Iodixanol Density Gradient Centrifugation. Mol Ther Methods Clin Dev. 2018;10:1-7.

341. Merten OW, Geny-Fiamma C, Douar AM. Current issues in adeno-associated viral vector production. Gene Ther. 2005;12 Suppl 1(1):51-61.

342. Koch S. Therapie des präklinischen CNGB1-defizienten Mausmodells der Retinitis pigmentosa mittels rekombinanter AAV-Vektoren: Ludwig-Maximilians-Universität München; 2013.

343. Mendell JR, Al-Zaidy SA, Rodino-Klapac LR, Goodspeed K, Gray SJ, Kay CN, et al. Current clinical applications of in vivo gene therapy with AAVs. Molecular Therapy. 2021;29(2):464-88.

344. Xu X, Chen W, Zhu W, Chen J, Ma B, Ding J, et al. Adeno-associated virus (AAV)-based gene therapy for glioblastoma. Cancer Cell International. 2021;21(1):1-10.

345. Luxturna(R), information P. https://www.fda.gov/vaccines-blood-biologics/cellular-gene-therapy-products/luxturna. 2018 [cited 2021 11/24].

346. Zolgensma(R), information P. https://www.fda.gov/vaccines-blood-biologics/zolgensma. 2019 [cited 2021 11/24].

347. Rexroad J, Evans RK, Middaugh CR. Effect of pH and ionic strength on the physical stability of adenovirus type 5. J Pharm Sci. 2006;95(2):237-47.

348. Xu AY, Jiang B, Samai P, Tank S-M, Shameem M, Liu D. Genome DNA Leakage of Adeno–Associated Virus Under Freeze–Thaw Stress. International Journal of Pharmaceutics. 2022:121464.

349. Pikal-Cleland KA, Rodriguez-Hornedo N, Amidon GL, Carpenter JF. Protein denaturation during freezing and thawing in phosphate buffer systems: monomeric and tetrameric beta-galactosidase. Arch Biochem Biophys. 2000;384(2):398-406.

350. Wu C, Shamblin S, Varshney D, Shalaev E. Advance understanding of buffer behavior during lyophilization. Lyophilized Biologics and Vaccines: Springer; 2015:25-41.

351. Hancock BC, Shamblin SL, Zografi G. Molecular mobility of amorphous pharmaceutical solids below their glass transition temperatures. Pharmaceutical research. 1995;12(6):799-806.

352. Gómez G. Crystallization-relatedpH changes during freezing of sodium phosphate buffer solutions: University of Michigan; 1995.

353. Gomez G, Pikal MJ, Rodriguez-Hornedo N. Effect of initial buffer composition on pH changes during far-from-equilibrium freezing of sodium phosphate buffer solutions. Pharm Res. 2001;18(1):90-7.

354. Kolhe P, Amend E, Singh SK. Impact of freezing on pH of buffered solutions and consequences for monoclonal antibody aggregation. Biotechnol Prog. 2010;26(3):727-33.

355. Johnson RE, Kirchhoff CF, Gaud HT. Mannitol-sucrose mixtures--versatile formulations for protein lyophilization. J Pharm Sci. 2002;91(4):914-22.

356. Thorat AA, Suryanarayanan R. Characterization of Phosphate Buffered Saline (PBS) in Frozen State and after Freeze-Drying. Pharm Res. 2019;36(7):98.

357. Haeuser C, Goldbach P, Huwyler J, Friess W, Allmendinger A. Impact of dextran on thermal properties, product quality attributes, and monoclonal antibody stability in freeze-dried formulations. Eur J Pharm Biopharm. 2020;147:45-56.

358. Stolzing A, Naaldijk Y, Fedorova V, Sethe S. Hydroxyethylstarch in cryopreservation–mechanisms, benefits and problems. Transfusion and Apheresis Science. 2012;46(2):137-47.

359. Crowe JH, Oliver AE, Hoekstra FA, Crowe LM. Stabilization of dry membranes by mixtures of hydroxyethyl starch and glucose: the role of vitrification. Cryobiology. 1997;35(1):20-30.

360. Sun WQ, Wagner CT, Connor J. The glass transition behaviors of hydroxyethyl starch solutions. Cell Preservation Technology. 2004;2(1):55-65.

361. Rockinger U, Müller C, Bracher F, Funk M, Winter G. DMSO as new, counterintuitive excipient for freeze-drying human keratinocytes. European Journal of Pharmaceutical Sciences 2021,160. 105746.

362. Pastor JM, Salvador M, Argandona M, Bernal V, Reina-Bueno M, Csonka LN, et al. Ectoines in cell stress protection: uses and biotechnological production. Biotechnol Adv. 2010;28(6):782-801.

Appendix 1: Publications associated with this thesis

Rieser, R., Penaud-Budloo, M., Bouzelha, M., Rossi, A., Menzen, T., Biel, M., Büning, H., Ayuso,E. & Michalakis, S. (2020). Intrinsic differential scanning fluorimetry for fast and easy identification of adeno-associated virus serotypes. *Journal of pharmaceutical sciences, 109*(1), 854-862: https://doi.org/10.1016/j.xphs.2019.10.031

Rieser, R., Koch, J., Faccioli, G., Richter, K., Menzen, T., Biel, M., Winter, G. & Michalakis, S. (2021). Comparison of Different Liquid Chromatography-Based Purification Strategies for Adeno-Associated Virus Vectors. Pharmaceutics, 13(5), 748. https://doi.org/10.3390/pharmaceutics13050748

Rieser, R., Menzen, T., Biel, M., Michalakis, S & Winter, G. (2022) Systematic studies on stabilization of AAV vector formulations by lyophilization, *Journal of pharmaceutical sciences*, https://doi.org/10.1016/j.xphs.2022.03.004

Appendix 2: Presentations associated with this thesis

Oral presentations:

Rieser R, Klaus Richter, Tim Menzen, Stylianos Michalakis Winter, G. Downstream processing of AAV – Purification, Characterization and Formulation. 13th PEGS Europe, Protein and Antibody Engineering Summit, 2nd-4th of November 2021, Barcelona, Spain

Ruth Rieser, Klaus Richter, Tim Menzen, Stylianos Michalakis, Gerhard Winter
Comparison of different chromatography-based purification strategies for AAV vectors
12th World Meeting on Pharmaceutics, Biopharmaceutics and Pharmaceutical Technology, 11th-14th of May 2021

Poster presentations:

R. Rieser, Tim Menzen, S. Michalakis, G. Winter

Effect of salt and sugar on the storage stability of liquid and freeze-dried adeno-associated virus formulations, 27th ESGTC, 22nd-25th of October 2019, Barcelona

R. Rieser, H. Büning, E. Ayuso, S. Michalakis, G. Winter
Intrinsic differential scanning fluorimetry for fast and easy identification of AAV serotype, International Research Conference on Protein Stability, and Interactions, 1-3rd of April 2019 Heidelberg

Appendix 3: Curriculum vitae

Personal data:

Name:	Ruth Katharina Rieser
Date of birth:	16.05.1993
Place of birth:	Weingarten
Nationality:	German

Working experience:

since 01/2022	Pharmacist, Altdorf Apotheke Weingarten
01/2018 - 09/2021	PhD student, Pharmaceutical Technology and Biopharmaceutics, Ludwig-Maximilians-Universität München

Education:

12/2017	Pharmaceutical state examination and license as pharmacist
05/2017 - 10/2017	Pharmacist Trainee in local pharmacy, Internationale Ludwigsapotheke, München
11/2016 - 04/2017	Pharmacist Trainee in the Department Formulation Research and Development, Roche, Basel
10/2012 - 10/2016	Studies of Pharmacy, Ruprecht Karls Universität Heidelberg
06/2012	Abitur, Spohn-Gymnasium Ravensburg